Synthesis of Rare Earth Complexes Involving Pyrazolate Ligands

A thesis submitted for the degree of

Doctor of Philosophy

by

Nazli Eslamirad

B.Sc., M.Sc. (Master of Engineering)

Supervisors:

Prof. Peter C. Junk

Dr. Murray Davies

College of Science and Engineering

James Cook University (JCU)

April 2018

Dedicated to my loving parents

and

My husband, Mehdi

Table of Contents

Abstract

This thesis explores the synthesis and characterisation of rare earth complexes involving pyrazolate ligands. Redox transmetallation/protolysis and high temperature metal-based routes were employed to synthesis the complexes. Besides, some chemistry of Li, Zn and Al pyrazolate complexes is also discussed when metalation of the pyrazole using nBuli and metal alkyls produced a range of compounds. Below are the ligands that were used for each chapter.

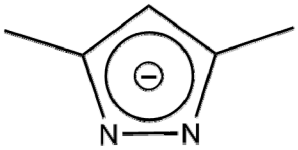

3,5- dimethylpyrazolate (Me_2pz)

Chapters: *2,3,4*

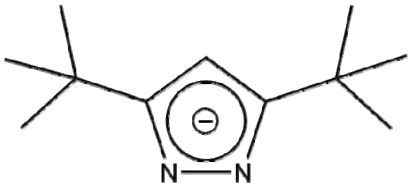

3,5- Di-*tert*-Butylpyrazolate (tBu_2pz)

Chapters: *2,3,4*

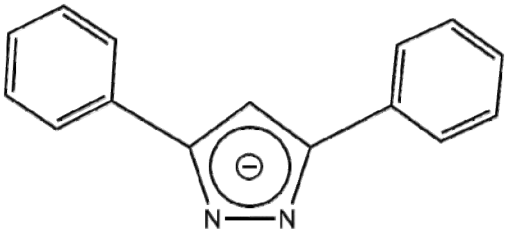

3,5-Diphenylpyrazolate (Ph_2pz)

Chapters: *2,3,4*

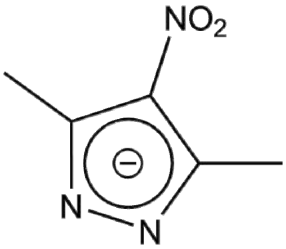

4-nitropyrazolate (Me_2pzNO_2)

Chapters: *4*

Ligands used throughout chapters two to four

Chapter **2** describes a series of rare earth pyrazolate complexes which were prepared by redox transmetallation/protolysis (RTP) using the rare earth metals (Sc, Y, La, Ce, Sm, Tb, Er and Lu), bispentafluorophenyl mercury ($Hg(C_6F_5)_2$), a pyrazole and using different solvents such as THF, DME and Et_2O. A variety of trivalent rare earth pyrazolate complexes were synthesised and characterised in this chapter: dinuclear $[Ln(Me_2pz)_3(thf)]_2$, oxide cage complexes and complexes formed by C-F activation. Investigations into the high reactivity of 3,5-dimethylpyrazolate resulted in the isolation of several novel structures such as

$[Sc_3O(Me_2pz)_7(Me_2pzH)_2]$, $[Sc(Me_2pz)_2(Me_2pz(SiMe_2O))]_2$, $[Y_3O(Me_2pz)_9Na_2(Et_2O)_2]$ and $[Y_3O(Me_2pz)_9Na_2(Me_2PzH)_2]$. This chapter also describes the synthesis of $[La_4(Me_2pz)_9(\mu_2\text{-}F)_2(\mu_4\text{-}F)(thf)_4].3THF$ with a significant feature of having three different pyrazolate bonding modes: η^2, $\mu\text{-}\eta^1\text{:}\,\eta^1$ and $\mu\text{-}\eta^2\text{:}\,\eta^1$ in the one structure. The complexes were characterised using NMR spectroscopy, IR and microanalysis.

Chapter **3** investigates new metal-based solvent-free elevated temperature reactions involving rare earth metals (Y, La, Ce, Pr, Dy and Ho) and three pyrazole pro-ligands (Me_2pzH, tBu$_2$pzH and Ph_2pzH). This chapter suggests a simple route to isolate predominantly homoleptic but also some heteroleptic rare earth pyrazolate complexes. Another surprising ligation of lanthanoid pyrazolates is observed in homoleptic $[La(Me_2pz)_3]_n$. η^5 Bonding in this compound gives the Me_2pz ligands a "cyclopentadienyl (Cp)" type coordination that has a few examples in rare earth pyrazolate chemistry.

Finally, chapter **4** presents small contribution to main group chemistry involving pyrazolates, while presenting the synthesis and structural characterisation of the newly synthesised complexes $[(Li_4(Me_2pz)_4(Et_2)_4]$, $[Li_6(Me_2pz)_6(tmeda)_2]$, $[Li_2(C_2N_3H_6O_2)_2(thf)_2]_n$, $\{[Zn(t$Bu$_2pz)_2(t$Bu$_2pzH)_2].1/2THF\}$ and $\{AlMe_2(Ph_2pz)]_2.1/2THF\}$. The hexameric pyrazolate complex using nBuLi is being reported for the first time in this study. Also, polymeric complex $[Li_2(C_5N_3H_6O_2)_2thf_2]_n$ is now being reported for the first time. These compounds should have utility as reagents in metathesis chemistry or in protolysis reactions where, for example the alkyl group, in the Al complex can be substituted.

Declaration

To the best of this author's knowledge, this thesis does not contain any material that has been accepted for the award of any other degree or diploma at any university or other institution, except where due reference is made in the text.

Nazli Eslamirad

College of Science and Engineering

James Cook University

April 2018

Acknowledgments

Firstly, I would like to thank my supervisor Prof. Peter C. Junk for his invaluable help and support during my Ph.D. Peter, thanks for the opportunity you offered me, with all the difficulties, to travel somewhere far from home and experience a new life. I am grateful for all your patience and trust in me over these last few years.

I would also like to thank Prof. Glen B. Deacon for his valuable advice and support he has given me throughout my study. Many thanks to my secondary supervisor Dr Murray Davies for providing me with necessary chemicals whenever I asked for, and helping me with sealing my tubes for high temperature reactions in his lab. To thank Dr. Jun Wang for helping with the X-ray crystallography and introducing me to the techniques of working with air-sensitive chemistry in Lab.

Many thanks to all group members (past and present), your support and friendship have been greatly appreciated over the years, in particular, thanks to Elius, Areej, Bill, Aymeric and Safaa. To the lovely friends in office: Dr. Ioana Bowden, Dr Simon Ho and lovely Hannah. I would like to thank my sweet friends Hadis Khakbaz and Shakiba Neshat.

Many thanks to the chemical staff in the discipline of chemistry at James Cook University, in particular: I would like to thank Dr. Bruce Bowden and Dr. Mark Robertson for aid with NMR experiments, to Dr. Winnie Lee, for assistance with running IR whenever I needed. Also, thanks to Dr. Elizabeth Tynan for helping with editing.

I would like to thank James Cook University for supporting me and Australian Research Council (ARC) for funding our research project.

Finally, I like to thank all my family in Iran especially my uncle Ebi, Aunt Simin and dear Shahrzad and Roozbeh for being so kind and supportive. I especially want to thank my lovely parents who helped me to feel confident to leave home and find a new home on the other side of the word. You were always there for me and continually supported me in all aspects of my life and I can never thank you enough for everything you have done for me. To my wonderful husband and friend, Mehdi, for always being by my side. Thank you for your endless love and support.

ABBREVIATIONS

3,5-dimethylpyrazole = Me_2pzH

3,5-diohenylpyrazole = Ph_2pzH

3,5-di-tert-butylpyrazole = tBu$_2$pzH

RE = Rare earth (La-Lu, Sc, Y)

RTP = Redox transmetallation/protolysis

Ln = Lanthanoid metal

THF = tetrahydrofuran (solvent)

thf = tetrahydrofuran (coordinated)

DME = 1,2-dimethoxyethane (solvent)

dme = 1,2-dimethoxyethane (coordinated)

TMEDA = tetramethylethylenediamine (solvent)

tmeda = tetramethylethylenediamine (coordinated)

Å = Angstrom unit, 10^{-10} m

CN = coordination number

Et_2O = diethyl ether

MeCN/NCMe = acetonitrile

EDTA = ethylenediaminetetraacetic acid

pz = deprotonated pyrazolate ion

dbmH = dibenzoylmethane

Chapter 1

Introduction to rare earths and their pyrazolate complexes

1. Introduction

1.1 Rare earth elements

1.1.1 General

Important properties of rare earth materials such as chemical, metallurgical, magnetic, electromagnetic and nuclear properties have been extensively studied.[1, 2] The rare earth elements comprise of the group three elements scandium (Sc, Z = 21), yttrium (Y, Z = 39) and lanthanum (La, Z = 57), in addition to fourteen lanthanoid metals ranging from cerium (Ce, Z = 58) to lutetium (Lu, Z = 71). Discovering rare earth materials took many years. It had been started in 1787 by Karl Arrhenius. Minerals bastnasite ($LnFCO_3$), monazite ($(Ln,Th)PO_4$) and lateritic ion-absorbing clays are the principal sources of rare earth elements. According to experience over the years it can be noted that despite these elements being relatively highly abundant, mining and extraction of them are more difficult than transition metals. Therefore, the process of extracting rare earth elements is expensive. During the late 1950s and early 1960s efficient separation techniques such as ion exchange, fractional crystallization and liquid extraction were developed to minimize cost and difficulty.[1, 3, 4]

It has been reported that during World War II, it was found that the addition of RE metals to steel could significantly improve its properties such as strength, increasing resistance to corrosion and increasing hot workability. Since then, RE metals have become widely applied in steel manufacturing.[5] It has been reported that by addition of suitable amount of cerium the morphology and distribution of the eutectic boride in low carbon Fe-B cast steel were improved and the overall mechanical properties were increased accordingly.[6] Among rare earth materials, the oxides of elements such as ytterbium, cerium, lanthanum, lutetium, samarium and scandium have a variety of commercial, industrial and scientific applications. As an example, cerium oxides have been extensively used in exhaust emission catalysis, with the other catalyst, $LaFePdO_3$, dubbed as an ‘intelligent catalyst’ due to its self-regenerative capability.[7, 8] Also, scandium oxide has proved to be a damage-resistant high-index material in laser coatings for use at 248 nm.[9] Excellent coatings for super luminescent light-emitting diodes were obtained using Sc_2O_3.[10, 11] In addition, material scientists use these rare earth oxides in applications like jet engines, superconducting microwave filters, high-capacity rechargeable electrodes, catalysts for self-cleaning ovens, fluid catalysts for oil refineries, chemical oxidizing agents, infrared lasers, welding glass screens, magnetic resonance imaging

contrast agents and X-ray machines.[1]

1.1.2 Isolation of rare earth metals

Apart from cerium which has an accessible tetravalent oxidation state that allows it to be separated as $Ce^{IV}O_2$ and europium which has a stable divalent oxidation state that can be separated as $Eu^{II}SO_4$ from other metals, the separation of other rare earth metals is much more difficult [2]. A significant aspect of rare earth metals is the lanthanoid contraction. An increase in effective nuclear charge across the series happens since *f* electrons inadequately screen each other from the nuclear charge which leads to a decrease in radii. This phenomenon results in stabilities of complexes with a specific ligand that increase from La^{3+} to Lu^{3+}. The practical application of this feature is in solvent extraction, which is the most efficient method to separate the rare earth elements. By using two immiscible solvents (non-polar hydrocarbon mixtures and aqueous nitrate solutions) and using extracting agents (such as: $(^{n}BuO)_3PO$ or $(Me(CH_2)_3(CH(Et)CH_2O)_2POOH)$),[12] the complexes can be separated based on different affinities between the two layers. Moreover, an ion-exchange process is employed in the final purification step in order to obtain higher levels of purity [2].

1.1.3 Applications of rare earth materials

Nowadays, rare earths are being used in different applications like metallurgy, the production of glass and ceramics and catalysis. Another outstanding usage of rare earths is as mischmetal (alloy of rare earths). A summary of their applications is shown in Table 1-1: [1, 13-16]

Table 1-1. Applications of Rare Earth Materials in Industry

Areas Of Application	Brief Details
Nonferrous metal	Alloying with aluminium and silicon in order to make pistons
Nonferrous metal	Alloying with zinc to make corrosion resistant coatings
Glass	Colouring and decolouring glass
Petroleum refining	Catalysts of rare earth chlorides
Medicine	Enhancing magnetic resonance image (MRI) by injection of gadolinium salts into patient
Clean energy technology	Magnets in wind turbines and electric vehicle motors
Cast Iron	In order to modify the graphite morphology from flakes to nodular, cerium mischmetal (Mischmetal contains a combination of rare-earth metals predominantly cerium and lanthanum) can be used
Commercial	High capacity batteries, high intensity flood lights for stadiums

1.2 Characteristics and Chemistry of Rare Earth Materials

As noted above the term “rare earths” is constituted by the group of elements numbered 57-71 [La-Lu] and Sc (21) and Y (39) from group 3, that exhibit some features in their chemistry that differentiate them from the *d*-block metals. As the 4f electrons penetrate the [Xe] core and are shielded by the outer 5*s* and 5*p* orbitals, the 4*f* orbitals overlap with coordinated ligands is poor. So, ligand-metal bonding in rare earth complexes is typically ionic and non-directional which sets these elements aside from transition metals.[17]

The primary oxidation state of all the rare earth metals in aqueous solution is “+3” which dominates chemistry of the lanthanoid elements. Oxidation state of “+4” for elements like cerium, praseodymium and terbium (Pr^{IV} and Tb^{IV} only for oxides and fluoride) and “+2” for europium, ytterbium and samarium are few exceptions.[2, 13] Later, the +2 oxidation state has been observed for the rest all of the rare earth elements.[18-21]

Electronic configurations of the atoms and their derived ions can help to describe the reasons of similarity and differences of chemical and physical properties. In these elements, the continuous filling of the 4*f* orbitals (La^{3+}: [Xe] $4f^0$ – Lu^{3+}: [Xe] $4f^{14}$) along with an increase in the effective nuclear charge causes a decrease in ionic radii named the lanthanoid contraction. The lanthanoid contraction is due to the poor shielding of an electron by others in the 4*f* sub-shell. As the 4*f* shells are filled with increasing atomic number, the effective nuclear charge also increases, resulting in the reduction of in size of the entire $4f^n$ shell. Since the 4*f* subshell is higher in energy than 5*d*, by progressing along the 4*f* series, they become more stable. Moreover, the “lanthanoid contraction” causes structural changes in homologous compounds. The most notable effect of this concept is a decrease in both the ionic radii and atomic radii as the series La-Lu is traversed. Table 1-2 shows the atomic number, symbol, electronic configuration, and abundance of each rare earth metal in the earth’s crust.[13, 22]

Generally speaking, although lanthanoids have been studied for many years, their chemical properties are not well understood but by comparing electronegativity of bonded atoms, some chemical bond properties such as bond covalency etc. can be studied. Coordination numbers such as 7, 8, 9, 10, 11, and 12 are the most important ones in various lanthanoid complexes because of high charge and large size of ions.[2, 23, 24] However, coordination numbers as low as two have been reported by using very sterically demanding ligands.

Table 1-2. The Rare Earth Elements [13, 22]

Atomic Number	Name	Symbol	Electronic Configuration		Abundance In Earth's Crust (ppm)
			Ln^0	Known Oxidation State **Common;** unusual	
21	Scandium	Sc	$3d^14s^2$	**III;** 0, I,II	0.26
39	Yttrium	Y	$4d^15s^2$	**III**; 0, II	0.29
57	Lanthanum	La	$5d^16s^2$	**III;** 0, II	34
58	Cerium	Ce	$4f^15d^16s^2$	**III, IV**; II	60
59	Praseodymium	Pr	$4f^36s^2$	**III**, **IV**; 0, II	8.7
60	Neodymium	Nd	$4f^46s^2$	**III**; 0, II	33
61	Promethium	Pm	$4f^56s^2$	**III**	Negligible/radioactive
62	Samarium	Sm	$4f^66s^2$	**II**, **III**; 0	6
63	Europium	Eu	$4f^76s^2$	**II**, **III**	1.8
64	Gadolinium	Gd	$4f^75d^16s^2$	**III**; 0, II	5.2
65	Terbium	Tb	$4f^96s^2$	**III, IV**; 0, II	0.94
66	Dysprosium	Dy	$4f^{10}6s^2$	**III**; 0, II	6.2
67	Holmium	Ho	$4f^{11}6s^2$	**III**; 0, II	1.2
68	Erbium	Er	$4f^{12}6s^2$	**III**; 0, II	3
69	Thulium	Tm	$4f^{13}6s^2$	**III**; II	0.45
70	Ytterbium	Yb	$4f^{14}6s^2$	**II, III**	2.8
71	Lutetium	Lu	$4f^{14}5d^16s^2$	**III**; 0, II	5.6

1.3 Coordination Chemistry

Many years ago, very little was known about rare earth complexes. Later, it has been shown that rare earth coordination chemistry has many characteristic properties compared with *d*-block metals complexes. There are three main issues that will be mentioned in this section: the valence state, chemical bonding and the coordination number.

1.3.1 The valence state

Compounds containing rare earths in oxidation states +2 and +4 are known in addition to rare earth elements displaying the oxidation state +3. Samarium, ytterbium and europium can form Ln^{2+} ions, while Ce and Tb are known to occur as Ln^{4+} ions.[25-33] With the formation of energetically stable vacant $4f^0$ (Ce^{4+}), half-filled $4f^7$(Eu^{2+}, Tb^{4+}) and completely filled $4f^{14}$

(Yb^{2+}) subshells, the stability increases. Therefore, the increased stability can be the reason of the existence of +2 and +4 oxidation state.[25-27, 30] However, this theory does not explain the inaccessibility of Sm^{+} and Tm^{+}, which would have energetically favoured configurations of 4 f^{7} and $4f^{14}$ respectively, or the existence of Sm^{2+} ($4f^{6}$) and Tm^{2+} ($4f^{13}$). Enthalpies of sublimation and ionisation or lattice energies can best interpret the existence of other oxidation states.[25] Reduction potentials indicates that amongst rare earth elements, Eu^{2+} is the most stable, followed by Yb^{2+}, Sm^{2+} and Tm^{2+} (Table 1-3).

Table 1-3. Standard reduction potentials E^{o}_{red} of rare earths.

Electro-pair	E^{o} (V)	Electro-pair	E^{o} (V)
Ce^{4+}/Ce^{3+}	+1.74	Eu^{3+}/Eu^{2+}	-0.35
Tb^{4+}/Tb^{3+}	+3.1±0.2	Yb^{3+}/Yb^{2+}	-1.15
Pr^{4+}/Pr^{3+}	+3.2±0.2	Sm^{3+}/Sm^{2+}	-1.55
Nd^{4+}/Nd^{3+}	+5.0±0.4	Tm^{3+}/Tm^{2+}	-2.3±0.2
Dy^{4+}/Dy^{3+}	+5.2±0.4		

1.3.1.1 Divalent Rare Earths

Although the divalent oxidation state was dominated recently by only Sm, Eu and Yb (classic divalent lanthanoids) attempts to expand organometallic complexes have led to the synthesis of more lanthanoid (II) complexes. Oxidative reactions involving lanthanoid metal, metathesis reactions of a divalent lanthanoid halide, and reductive reactions involving trivalent lanthanoid complexes are three ways to synthesise divalent organolanthanoid complexes.[34] Previously, the reductive divalent chemistry of the lanthanoids was limited to three ions, Eu^{2+}, Yb^{2+}, and Sm^{2+}.[19] According to the successful synthesis of lanthanoid divalent diiodides, LnI_2 (Ln= Tm, Dy, Nd), a new area has opened up in divalent lanthanoid chemistry.[35] Later, the number of fully characterised divalent lanthanoids has doubled. Therefore, now divalent organometallics are known for all rare earths (except the radioactive Pm).[19, 36]

1.3.1.2 Tetravalent Rare Earths

Among the elements which can make tetravalent compounds, only Ce^{4+} ($4f^{0}$) is stable in both solution and solid phases whereas Tb^{4+} ($4f^{7}$) and Pr^{4+}($4f^{1}$) can only exist as oxide and fluoride salts.[3] Moreover, tetravalent cerium has been found to have numerous applications in organic synthesis since it is a strong one electron oxidant. CAN (Ceric ammonium nitrate) is

the most widely used reagent.[37] Werner et. al. also reported a series of cerium (IV) complexes and the first cerium (IV) formamidinate complex.[38]

1.3.2 Chemical bonding

Rare earths are considered to be strong Lewis acids, or "hard acids" since there is a high electropositive charge on the rare earth ion (Table 1-4).[2, 39] Therefore, bonding with hard Lewis bases, primarily oxide/oxygen containing ligands or fluoride, is the preference. Moreover, since the 4*f* electrons penetrate the [Xe] core and are shielded by the outer 5*s* and 5*p* orbitals, overlap of the 4*f* orbitals with coordinating ligands is poor. Therefore, ligand-metal bonding in rare-earth complexes is typically ionic and non-directional.

Table 1-4. Redox potentials (V) of rare earth elements.

Z	Name	E^0 (V) for $RE^{3+} + e^- = RE^{2+}$	E^0 (V) for $RE^{3+} + 3e^- = RE$	E^0 (V) for $RE^{4+} + e^- = RE^{3+}$
21	Scandium	-	−1.88	-
39	Yttrium	-	−2.37	-
57	Lanthanum	-3.1*	−2.37	-
58	Cerium	-3.2*	−2.34	1.70
59	Praseodymium	-2.7*	−2.35	3.4*
60	Neodymium	-2.6†	−2.32	4.6*
61	Promethium	-2.6*	−2.29	4.9*
62	Samarium	-1.55	−2.30	5.28
63	Europium	-0.34	−1.99	6.4*
64	Gadolinium	-3.9*	−2.29	7.9*
65	Terbium	-3.7*	−2.30	3.3*
66	Dysprosium	-2.5†	−2.29	5.0*
67	Holmium	-2.9*	−2.33	6.2*
68	Erbium	-3.1*	−2.31	6.1*
69	Thulium	-2.3†	−2.31	6.1*
70	Ytterbium	-1.05	−2.22	7.1*
71	Lutetium	-	−2.30	8.5*

Table was adapted from ref, [2] and [39] * = estimated, † = in THF

1.3.3 The coordination numbers

With the deep lying 4*f* orbitals not exhibiting large directional control and larger ionic radius of lanthanoids (Table 1-5) it can be concluded that lanthanoid ions can accommodate more than six coordination sites in their coordination sphere due to their much larger size.[2] Regardless of the oxidation state of Ln, Ln^{n+} cations are relatively large in comparison with ions that give ionic compounds (Table 1-5).[22] Compared with transition metals, lanthanoids have two distinct characteristics in terms of their coordination number: large coordination numbers of eight or nine are the most common and coordination numbers can be variable from 3 to 12.[34]

Table 1-5. Ionic radii of lanthanoids and non-lanthanoids.

Ionic charge	**Lanthanoids**	**Radius (Å)**	**Non-lanthanoids**			
			Ion	**Radius (Å)**	**Ions**	**Radius (Å)**
+2 and +3	Sm^{2+}	1.11	Fe^{2+}	0.83		
	Eu^{2+}	1.09	Zn^{2+}	0.83		
	Yb^{2+}	0.93	Cd^{2+}	1.03		
	Sc^{3+}	0.75	Al^{3+}	0.51		
	Y^{3+}	1.01	Cr^{3+}	0.63		
	La^{3+}	1.061	Rh^{3+}	0.69		
	Pr^{3+}	1.13	U^{3+}	1.03		
	Nd^{3+}	1.11	Pu^{3+}	1.00		
	Pm^{3+}	1.09	Rh^{3+}	0.69		
	Gd^{3+}	0.938	Pb^{2+}	1.32		
	Dy^{3+}	1.03	Ca^{2+}	0.99		
	Ho^{3+}	1.02	Sr^{2+}	1.12		
	Er^{3+}	1.00				
	Tm^{3+}	0.99				
	Lu^{3+}	0.848				
+4	Ce^{4+}	0.92	Zr^{4+}	0.79	Th^{4+}	0.99
	Tb^{4+}	0.84	Mo^{4+}	0.68	Am^{4+}	0.89

1.4 Organometallic complexes of rare earths

According to availability of rare earth metals and in order to increase their compound applications, developments in organolanthanoid chemistry has increased rapidly. There are some important features about organometallic compounds of lanthanoid (particularly in comparison to the chemistry of transition metals):

(a) According to the inability of *f* orbitals to overlap with the ligand molecular orbitals, organolanthanoids are dominated by ionic bonding rather than covalent interactions.

(b) Oxidative-addition reactions are not favoured since the trivalent state of lanthanoids is very stable and other oxidation states are not easily accessible.

(c) Sterically demanding ligands are needed to form discrete monomeric compounds because of the large ionic radii, and therefore coordination numbers of lanthanoids, leading to aggregation.

(d) Coordinatively unsaturated species can be produced and be used as catalysts since lanthanoids can possess coordination numbers as high as 12.

Mostly organometallic complexes of lanthanoids have one π donor/ π acceptor type of ligand (cyclopentadienyl, cyclooctatetraenes) along with other ligands like alkyls, hydrides, halides, etc. [4] Moreover, suitable solvents which are compatible with organometallic rare earth complexes are restricted to aromatic non-protic solvents or aliphatic hydrocarbons and ether. It should be noted that the mentioned solvents must be dried completely before use due to the very high air- and moisture sensitivity of these compounds.

1.5 Synthesis of organoderivative rare earth compounds

Since this thesis involves the synthesis of rare earth complexes with pyrazolate ligands (Figure 1-1), the common synthetic routes to rare earth metal-organic compounds are introduced.

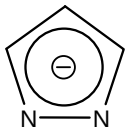

Figure 1-1. Pyrazolate ligand.

1.5.1 Metathesis

Metathesis (salt elimination) reactions include the treatment of a rare earth halide with an alkali metal form of the ligand (Equation 1-1).[40, 41]

Equation 1-1. $LnX_n + nML \rightarrow [LnL_n] + n\ MX$

M= alkali metal
L= anionic ligand
X= halide
n = 2, 3

In metathesis reactions the choice of the lanthanoid halide and alkali metal salt as reagents is often critical. The low solubility of solvent free LnX_3 is one of the issues. Also, incorporation of MX in the final products can be problematic as well. In many cases low yields or unwanted side products (e.g. LnL_3X^-) can hamper the isolation of desired products in metathesis reactions.[42, 43]

1.5.2 Protolysis

According to Equation 1-2 protolysis reactions involve treatment of a lanthanoid precursor (LnR_n) with protic agents (LH).[44, 45] Since the reactants are highly soluble in common solvents, it can be performed without using any coordinating/donor solvents.

Equation 1-2. $Ln(R)_n + n\ HL \rightarrow [LnL_n] + n\ HR$

R= usually $N(SiMe_3)_2$, $N(SiHMe_2)_2$ or C_6F_5
L = ligand, n = 2, 3

Although protolysis is a highly versatile route for synthesis heteroleptic and homoleptic lanthanoid complexes, there are some drawbacks with this reaction. Firstly, most reagents are highly air- and/or moisture-sensitive, leading to the possibility of decomposition. Secondly, the precursor lanthanoid amides or alkyls need to prepared by metathesis leading to issues encountered above.[46]

1.5.3 Metal-based preparations

An alternative strategy to synthesise rare earth complexes (organoamides, aryloxides/alkoxides and organometallics) to the more commonly used protolysis and

metathesis reactions are free metal-based preparations. One prominent method is redox transmetallation using pyrazolates,[32, 47] thallium cyclopentadienyls,[28] diarylmercurials,[48-50] tin (II)[51] and triphenylbismuth (Equation 1-3).[52]

Equation 1-3. **m** $Ln + n\ ML_m \rightarrow m\ [LnL_n] + nM$

L = anionic ligand
n = 2, 3
m = 1- 4
M = Hg, Bi, Sn or $SnMe_3$

Redox transmetallation/protolysis (RTP) is an alternative free metal-based reaction which involves the treatment of a rare earth metal with a diarylmercurial such as diphenylmercury (weaker oxidant) or bis(pentafluorophenyl) mercury (stronger oxidant) and a protic ligand. When this reaction is performed, a vast array of new possibilities are available.[44, 53, 54]

Equation 1-4. $2Ln + n\ HgR_2 + 2n\ LH \rightarrow 2\ [\ LnL_n(solv)] + n\ Hg + 2n\ RH$

R= C_6F_5, Ph
L = Ligand of choice
n = 2,3

Typically donor solvents are used in this reaction such as tetrahydrofuran or 1,2-dimethoxyethane. However, this reaction has been successfully performed in a non-donor solvent (toluene) under reflux conditions.[55]

It should be noted that the protolysis is driven by acidities of the labile proton and alkoxides and aryloxides are highly reactive towards water, O_2 and CO_2 [45, 56].

Another metal-based preparation is the direct reaction of lanthanoid metals with protic reagents which is often done at elevated temperatures (Equation 1-5).[50, 55, 57, 58]

Equation 1-5 $Ln + n\ LH \xrightarrow{Hg} [\ Ln(L)_n] + n/2\ H_2$

L = Ligand
n = 2,3

Since rare earths are highly electropositive, mercury or mercuric chloride is usually

added to aid with surface cleaning of the likely oxide layer on the surface of metal which can hamper the metal-based reactions.[59, 60] Homoleptic complexes are commonly obtained using this method which is typically performed in an evacuated Carius tube at approximately 300 °C, either solvent free or in the presence of an inert flux, typically 1,2,4,5-tetramethylbenzene. [55, 61] For a successful reaction, both reactants and products should have a high thermal stability which is one of the main drawbacks of this method. Also formation of hydrogen gas and the use of mercury are other disadvantages of this methodology and reactions must be performed in Carius tubes that can contain the high pressure (up to 15 atm).[49, 62, 63] Occasionally single crystals of the resulting lanthanoid complexes are obtained directly from the tube. If not, the homoleptic product can be crystallised using a suitable non-donor solvent, such as toluene or hexane, to isolate the pure product.[64]

1.6 Ligands

Ligands are neutral molecules or ions that bind to a central atom or ion and play very important role in organometallic chemistry since they can change physical properties of complexes. The number of active sites in ligands is variable. The strength of different ligands in making bonds with metals is different with each other. Therefore, this difference leads to differences in splitting energy levels of the metal in the presence of a ligand.[56]

Moreover, there are two parameters that are important in predicting the influence of ligands. The first factor is the electronic effect that says if ligands have electron-donating substituents, they can be generally strong donors. Moreover the higher the basicity of the ligand, the stronger is the donor ability. The other factor is the steric effect that can determine the influence of the ligand on the selectivity and reactivity of the resulting organometallic compounds.[45, 65]

1.7 General pyrazole/pyrazolate chemistry

Traditionally, pyrazole derivatives have been used in the medical science.[66, 67] Moreover, these ligands have been used as chemical bleaching agents and luminescent/fluorescent substances,[68, 69] and antioxidants in motor fuels.[67] Since the coordination behaviour of pyrazoles and pyrazolate ions are widely versatile towards a great range of metals such as *d*-block, *f*-block as well as main group elements, they attracted interest as ligands for preparing compounds. In the pyrazole ring substitution of C3 and/or C5, adjacent to the nitrogen atoms, can affect the steric environment around the N donors and any metal

ions coordinated to them. Also pyrazolates are aromatic [70, 71] five-membered heterocycles. Since pyrazolatolanthanoids (II/III) display different structures, different synthesizing methods can be used such as salt metathesis reactions, transmetallation reactions, protolysis reactions, direct reactions between ligand acid and metal at elevated temperatures under solventless conditions and redox transmetallation/protolysis reactions.[72, 73]

Pyrazolates can coordinate to metals or metalloids through one or both nitrogen atoms, and through carbon atoms. They become anionic in a similar fashion to Cp (cyclopentadienyl) ligands when deprotonated (Figure 1-2).[73]

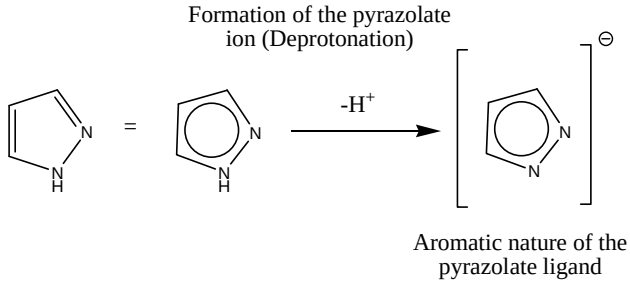

Figure 1-2. Deprotonation of pyrazole to form the pyrazolate ion.[73]

Most often pyrazolate (pz^-) ions behave as bridging ligands (μ) (Figure 1-3) for *d*-block chemistry but two other bonding modes are known as well.[57, 74-79] Now η^2 – coordination has been extended from f-block to transition metal and main group elements (Figure 1-3). Pyrazolate coordination is not restricted to the nitrogen atoms and binding through the carbon has been documented (Figure 1-3).[73, 80] The large size of Ln^{n+} permits coordination of neutral co-ligands that results in the isolation of most rare earth pyrazolates complexes. These complexes with the composition of $[Ln(R_mpz)_n(L)_x]$ are usually derived from synthesizing the lanthanoid complexes in a coordinating solvent (R are possible substituents, typically in the 3,5-positions and L are auxiliary neutral molecules (typically solvents); m= 0-3, n= 2 or 3).[57, 80-82]

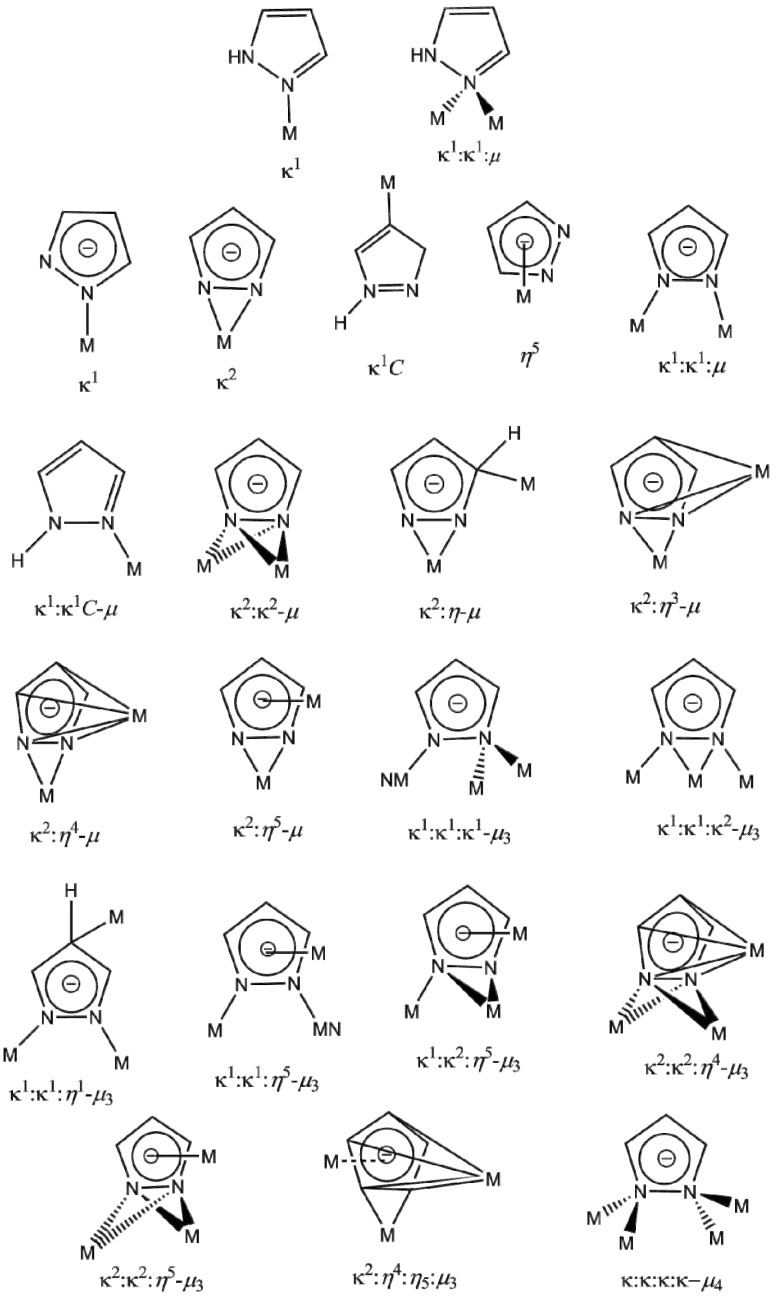

Figure 1-3. Known bonding modes of pyrazoles/pyrazolates.[83]

Moreover, R substituent groups on the carbon atoms can change the properties of pyrazolate ligands. Alkyl substituents make the pyrazolate more basic and aryl groups reduce their basicity.[70, 84, 85] Furthermore, the nucleophilicity of the nitrogen atoms, as well as the physical and chemical properties of the pyrazole/pyrazolate ligand can be affected by the variation of substituents position on the heterocycle.[86]

1.8 The current study

The work presented in this thesis discusses the formation and characterization of a variety of different pyrazolate complexes (Figure 1-4).

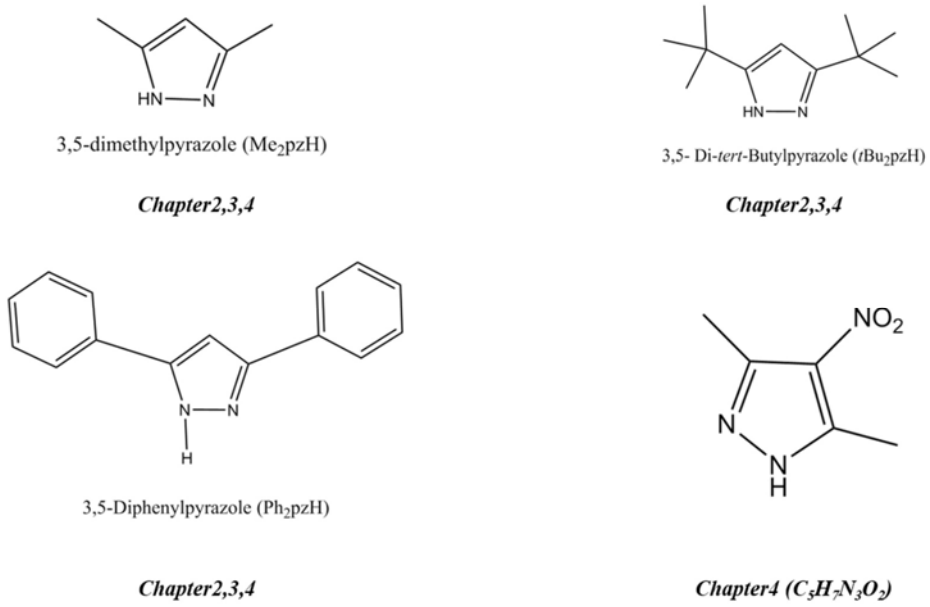

Figure 1-4. Pyrazole ligands used throughout this work.

The majority of rare-earth complexes known have been synthesized by redox transmetallation protolysis (RTP) in THF. ***Chapter two*** reports a series of new pyrazolate compounds having significant features using three different pyrazolate ligands (Me_2pzH, tBu_2pzH and Ph_2pzH). Initially complexes were generated by the RTP method using THF as solvent medium. Due to the failure in isolating pure product from THF, DME was used for the crystallization step. New compounds with crystal structures such as $[La_4(Me_2pz)_9(\mu_2\text{-}F)_2(\mu_4\text{-}F)(thf)_4].3THF$ with three different binding modes are reported in this chapter.

Chapter three introduces a solvent free synthesis of lanthanoid pyrazolate complexes by elevated-temperature reactions. X-ray analysis is the prime characterization technique for these complexes due to the difficulty of separating final product from the rest of the reagents in the tube; however, IR spectroscopy was also obtained.

Chapter four describes the synthesis and characterization of some alkali-metal

pyrazolate complexes. Since the interest for synthesizing pyrazolate complexes has been increased, some works have been done synthesising group I pyrazolate complexes that could be very useful reagents for metathesis reactions in the formation of other metal pyrazolate complexes. Therefore, in this chapter several unknown compounds using different pyrazoles as ligands have been isolated.

1.9 References

1. A. R. Jha, *Rare Earth Materials: Properties and Applications*, CRC Press, 2014.
2. S. Cotton, *Lanthanide and actinide chemistry*, John Wiley & Sons, 2007.
3. G. Meyer and L. R. Morss, *Synthesis of lanthanide and actinide compounds*, Springer, 1991.
4. V. R. Sastri, J. R. Perumareddi, V. R. Rao, G. V. S. Rayudu and J. C. Bünzli, *Modern aspects of rare earths and their complexes*, Elsevier, 2003.
5. K. A. Gschneidner, *Industrial Applications of Rare Earth Elements*, AMERICAN CHEMICAL SOCIETY, 1981.
6. H. Fu, Q. Xiao, J. Kuang, Z. Jiang and J.-d. Xing, *Materials Science and Engineering: A*, 2007, **466**, 160-165.
7. M. B. Katz, G. W. Graham, Y. Duan, H. Liu, C. Adamo, D. G. Schlom and X. Pan, *J. Am. Chem. Soc.*, 2011, **133**, 18090-18093.
8. H. Tanaka, I. Tan, M. Uenishi, M. Taniguchi, M. Kimura, Y. Nishihata and J. i. Mizuki, *J. Alloys Compd.*, 2006, **408**, 1071-1077.
9. F. Rainer, W. H. Lowdermilk, D. Milam, T. T. Hart, T. L. Lichtenstein and C. K. Carniglia, *Appl. Opt.*, 1982, **21**, 3685-3688.
10. Z. Xu, A. Daga and H. Chen, *Appl. Phys. Lett*, 2001, **79**, 3782.
11. I. Ladany, P. J. Zanzucchi, J. T. Andrews, J. Kane and E. DePiano, *Appl. Opt.*, 1986, **25**, 472-473.
12. *Rare earth-based corrosion inhibitors* Woodhead Publishing Limited is an imprint of Elsevier, Cambridge, UK ; Waltham, MA, USA, 2014.
13. M. Halka and B. Nordstrom, *Lanthanides and Actinides*, Facts on File, 2011.
14. E. C. Subbarao, *Science and technology of rare earth materials*, Elsevier, 1980.
15. T. J. Meyer, *Comprehensive Coordination Chemistry II: From Biology to Nanotechnology*, Elsevier Pergamon, 2004.
16. S. P. Sinha, *Complexes of the Rare Earths*, Elsevier Science, 2013.
17. D. Astruc, *Organometallic chemistry and catalysis*, Springer, 2007.
18. W. J. Evans, G. Zucchi and J. W. Ziller, *J. Am. Chem. Soc.*, 2003, **125**, 10-11.
19. W. J. Evans, *Inorg. Chem.*, 2007, **46**, 3435-3449.
20. F. Jaroschik, A. Momin, F. Nief, X.-F. Le Goff, G. B. Deacon and P. C. Junk, *Angew. Chem. Int. Ed.*, 2009, **48**, 1117-1121.
21. M. R. MacDonald, J. W. Ziller and W. J. Evans, *J. Am. Chem. Soc.*, 2011, **133**, 15914-15917.
22. J. C. Bailar, H. J. Emeleus, R. Nyholm and A. F. Trotman-Dickenson, *Comprehensive*

inorganic chemistry, 1973.

23. C. E. Housecroft and A. G. Sharpe, *Inorganic Chemistry*, Pearson Prentice Hall, 2005.
24. N. N. Greenwood and A. Earnshaw, *Chemistry of the Elements*, Elsevier Science, 2012.
25. F. A. Cotton, G. Wilkinson, C. A. Murillo and M. Bochmann, *Advanced Inorganic Chemistry*, Wiley, New York, sixth edn., 1996.
26. T. Moeller, *The Chemistry of the Lanthonides*, Reinhold, New York, 1963.
27. C. J. Schaverien, in *Adv. Organomet. Chem.*, eds. F. G. A. Stone and R. West, Academic Press, 1994, vol. **36**, pp. 283-362.
28. M. N. Bochkarev, L. N. Zakharov and G. S. Kalinina, *Organoderivatives of Rare Earth Elements*, Kluwer Academic Publishers, Dordrecht, 1995.
29. F. A. Hart, ed. G. Wilkinson, Pergamon, Oxford, 1987, vol. **3**, p. 1059.
30. W. J. Evans, *Polyhedron*, 1987, **6**, 803.
31. W. J. Evans, in *Adv. Organomet. Chem.*, eds. F. G. A. Stone and R. West, Academic Press, 1985, vol. **24**, pp. 131-177.
32. G. B. Deacon, E. E. Delbridge, B. W. Skelton and A. H. White, *Eur. J. Inorg. Chem.*, 1998, 543-545.
33. R. Anwander, D. Werner, G. B. Deacon and P. C. Junk, *Dalton Trans.*, 2017.
34. C.-H. Huang, *Rare earth coordination chemistry: Fundamentals and applications*, John Wiley & Sons, 2010.
35. W. J. Evans, *J. Organomet. Chem*, 2002, **647**, 2-11.
36. M. R. MacDonald, J. E. Bates, J. W. Ziller, F. Furche and W. J. Evans, *J. Am. Chem. Soc.*, 2013, **135**, 9857-9868.
37. Z. Duan, X. Xuan, T. Li, C. Yang and Y. Wu, *Tetrahedron Lett.*, 2006, **47**, 5433-5436.
38. D. Werner, G. B. Deacon, P. C. Junk and R. Anwander, *Chem. Eur. J.*, 2014, **20**, 4426-4438.
39. T. D. Tilley, R. A. Andersen and A. Zalkin, *Inorg. Chem.*, 1984, **23**, 2271-2276.
40. M. N. Bochkarev, L. N. Zakharov and G. S. Kalinina, *Organoderivatives of rare earth elements*, Kluwer Academic Publishers Dordrecht, 1995.
41. S. Cotton, in *Comprehensive Coordination Chemistry II*, ed. J. A. M. J. Meyer, Pergamon, Oxford, 2003, pp. 93-188.
42. K. Izod, S. T. Liddle and W. Clegg, *Inorg. Chem.*, 2004, **43**, 214-218.
43. R. C. Mehrotra, P. N. Kapoor and J. M. Batwara, *Coord. Chem. Rev.*, 1980, **31**, 67-91.
44. G. B. Deacon, C. M. Forsyth and S. Nickel, *J. Organomet. Chem*, 2002, **647**, 50-60.
45. R. Anwander, in *Lanthanides: Chemistry and Use in Organic Synthesis*, Springer, 1999, pp. 1-61.

46. L. Barton, *J. Am. Chem. Soc.*, 1997, **119**, 12028-12028.
47. G. B. Deacon, E. E. Delbridge, B. W. Skelton and A. H. White, *Eur. J. Inorg. Chem.*, 1999, 751-761.
48. G. Z. Suleimanov, V. I. Bregadze, N. A. Koval'chuk and I. P. Beletskaya, *J. Organomet. Chem.*, 1982, **235**, C17-C18.
49. G. B. Deacon and D. G. Vince, *J. Organomet. Chem.*, 1976, **112**, C1-C2.
50. G. Meyer, D. Naumann and L. Wesemann, *Inorganic Chemistry Highlights*, Wiley, 2002.
51. B. etinkaya, P. B. Hitchcock, M. F. Lappert and R. G. Smith, *J. Chem. Soc., Chem. Commun.*, 1992, 932-934.
52. L. N. Bochkarev, T. A. Stepantseva, L. N. Zakharov, G. K. Fukin, A. I. Yanovsky and Y. T. Struchkov, *J. Organomet. Chem*, 1995, **14**, 2127-2129.
53. H. Schumann, J. A. Meese-Marktscheffel and L. Esser, *Chem. Rev.*, 1995, **95**, 865-986.
54. G. B. Deacon, G. D. Fallon, C. M. Forsyth, S. C. Harris, P. C. Junk, B. W. Skelton and A. H. White, *Dalton Trans*, 2006, 802-812.
55. G. B. Deacon, T. Feng, C. M. Forsyth, A. Gitlits, D. C. R. Hockless, Q. Shen, B. W. Skelton and A. H. White, *J. Chem. Soc., Dalton Trans.*, 2000, 961-966.
56. S. Komiya, M. Hurano and S. Komiya, *Synthesis of Organometallic Compounds: A Practical Guide. 1997*.
57. G. B. Deacon, A. Gitlits, P. W. Roesky, M. R. Bürgstein, K. C. Lim, B. W. Skelton and A. H. White, *Chem. Eur. J.*, 2001, **7**, 127-138.
58. K. Müller-Buschbaum, *Z. Anorg. Allg. Chem.*, 2005, **631**, 811-828.
59. T. J. Boyle and L. A. M. Ottley, *Chem. Rev.*, 2008, **108**, 1896-1917.
60. J. N. Spencer and A. F. Voigt, *J. Phys. Chem.*, 1968, **72**, 464-470.
61. G. B. Deacon, C. M. Forsyth, P. C. Junk and A. Urbatsch, *Eur. J. Inorg. Chem.*, 2010, 2787-2797.
62. G. B. Deacon, C. M. Forsyth and S. Nickel, *J. Organomet. Chem*, **2002**, 647, 50-60.
63. G. B. Deacon, A. J. Koplick, W. D. Raverty and D. G. Vince, *J. Organomet. Chem.*, 1979, **182**, 121-141.
64. J. Townley, Ph.D Thesis, Monash University, 2010.
65. A. D. McNaught, A. Wilkinson and A. D. Jenkins, *IUPAC Compendium of Chemical Terminology: The Gold Book*, International Union of Pure and Applied Chemistry, 2006.
66. G. I. Kornis, in *Kirk-Othmer Encyclopedia of Chemical Technology*, John Wiley & Sons, Inc., 2000.
67. A. N. Kost and I. I. Grandberg, in *Adv. Heterocycl. Chem.*, eds. A. R. Katritzky and A. J.

Boulton, Academic Press, 1966, vol. **6**, pp. 347-429.

68. O. Neunhoeffer and D. Rosahl, *Chem. Ber.*, 1953, **86**, 226-231.
69. O. Neunhoeffer, G. Alsdorf and H. Ulrich, *Chem. Ber.*, 1959, **92**, 252-255.
70. S. Trofimenko, *Chem. Rev.*, 1972, **72**, 497-509.
71. B. Y. Simkin, V. I. Minkin and M. N. Glukhovtsev, in *Adv. Heterocycl. Chem.*, ed. R. K. Alan, Academic Press, 1993, vol. **56**, pp. 303-428.
72. G. B. Deacon, P. C. Junk and A. Urbatsch, *Dalton Trans.*, 2011, **40**, 1601-1609.
73. M. A. Halcrow, *Dalton Trans.*, 2009, 2059-2073.
74. G. B. Deacon, E. E. Delbridge, B. W. Skelton and A. H. White, *Angew. Chem. Int. Ed. Engl.*, 1998, **37**, 2251-2252.
75. G. B. Deacon, A. Gitlits, B. W. Skelton and A. H. White, *Chem. Commun.*, 1999, 1213-1214.
76. A. Steiner, G. T. Lawson, B. Walfort, D. Leusser and D. Stalke, *J. Chem. Soc., Dalton Trans.*, 2001, 219-221.
77. G. B. Deacon, E. E. Delbridge and C. M. Forsyth, *Angew. Chem. Int. Ed.*, 1999, **38**, 1766-1767.
78. L. R. Falvello, J. Fornies, A. Martin, R. Navarro, V. Sicilia and P. Villarroya, *Chem. Commun.*, 1998, 2429-2430.
79. J. R. Perera, M. J. Heeg, H. B. Schlegel and C. H. Winter, *J. Am. Chem. Soc*, 1999, **121**, 4536-4537.
80. G. B. Deacon, R. Harika, P. C. Junk, B. W. Skelton, D. Werner and A. H. White, *Eur. J. Inorg. Chem.*, 2014, 2412-2419.
81. G. B. Deacon, P. C. Junk and A. Urbatsch, *Eur. J. Inorg. Chem.*, 2011, 3592-3600.
82. J. E. Cosgriff, G. B. Deacon, B. M. Gatehouse, P. R. Lee and H. Schumann, *Z. Anorg. Allg. Chem.*, 1996, **622**, 1399-1403.
83. J. E. Cosgriff, G. B. Deacon and B. M. Gatehouse, *Aust. J. Chem.*, 1993, **46**, 1881-1896.
84. G. L. Monica and G. A. Ardizzoia, in *Prog. Inorg. Chem.*, John Wiley & Sons, Inc., 2007, pp. 151-238.
85. G. La Monica and G. A. Ardizzoia, *Prog. Inorg. Chem.*, 1997, **46**, 151-238.
86. G. B. Deacon, E. E. Delbridge, C. M. Forsyth, P. C. Junk, B. W. Skelton and A. H. White, *Aust. J. Chem.*, 1999, **52**, 733-740.

Chapter 2

Synthesis and structural characterisation of rare earth pyrazolate complexes using redox transmetallation/protolysis

---

2. Chapter 2

2.1 Introduction

Pyrazolate chemistry has attracted much attention over the years in both organic and inorganic chemistry. After the publication of two new comprehensive reviews by Trofimenko[1, 2] detailing the various properties of these ligands, this area of chemistry gained a great deal of attention. In the past 20 years, understanding of pyrazolate ligands has been enriched by the discovery of new bonding modes, for example, i)μ-η^2:η^5, [3] ii) μ^3-η^1:η^2:η^1,[4, 5] iii)μ- η^2:η^2,[6] iv)π- η^1 (*C*-bonded),[7, 8] v) η^5 (Figure 2-1).[9]

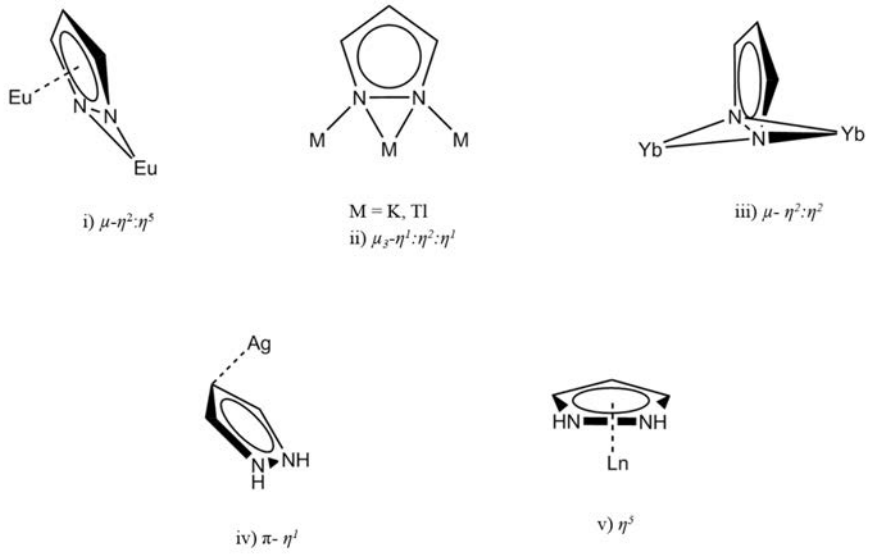

Figure 2-1. Some identified pyrazolate coordination modes.

Initially, the chemistry of many of the new coordination modes was observed in trivalent lanthanoid pyrazolates using bulky ligands (3,5-di-*tert*-butylpyrazole (*t*Bu$_2$pzH) and 3,5-diphenylpyrazole (Ph$_2$pzH). In addition, 3,5-dimethylpyrazole (Me$_2$pzH) which is a moderately bulky pyrazolate ligand (after deprotonation) has had an important role in main group complexes[10-12] and transition metals as well as in cyclopentadienyl-lanthanoid pyrazolates.[13, 14] Previously few known tris-(3,5-dimethylpyrazolate) lanthanoid complexes [Ln(Me$_2$pz)$_3$(L)$_n$] (L = neutral donor) were restricted to monomeric [Er(Me$_2$pz)$_3$(*t*Bupy)$_2$] (*t*Bu$_2$py = 4-*tert*-butylpyridine)[15], the first monodentate pyrazolate complex [Nd(η^2-Me$_2$pz)$_2$(κ^1(N)-Me$_2$pz))(Me$_2$pzH)][16] and dimeric [Ln$_2$(Me$_2$pz)$_4$(μ-Me$_2$pz)$_2$(μ-thf)$_2$].[17, 18] Also, some other structurally uncharacterized complexes have been known such as

[$Nd(Me_2pz)_3(py)$] (py = pyridine)[16] and [$Ln(Me_2pz)_3(thf)$] (Ln = La, Er).[19]

Rare earth complexes using 3,5-dimethylpyrazole (Me_2pzH) have been extended by Harika[20] by synthesizing isostructural [$Ho(Me_2pz)_3(thf)]_2$ and [$Nd(Me_2pz)_3(thf)]_2$.[3] Also [$Nd(Me_2pz)_3(py)_3$], a compound that remained structurally undefined, has been reported as well.[3]

Recently a variety of rare-earth 3,5-dimethylpyrazolate (Me_2pz) complexes of general formula [$Ln(Me_2pz)_3(thf)]_2$ (Ln = La, Ce, Pr, Dy, and Lu) were synthesised by Werner.[21] A change in bridging pyrazolates has been observed from μ_2-η^2:η^5 coordination in La-Pr, to η^1:η^1 bridging in Nd-Lu.[3] Also the lanthanum derivative [$La(Me_2pz)_3(thf)]_2$ and the praseodymium analogue, [$Pr(Me_2pz)_3(thf)]_2$, have been fully characterized along with the dysprosium analogue [$Dy(Me_2pz)_3(thf)]_2$.[21] Moreover, the first cerium (IV) pyrazolate species was obtained as well.[21] All the recent progress in synthesising pyrazolate rare earth complexes aroused our interest to focus this study on the Sc pyrazolate compounds as it is even smaller than lutetium, the last lanthanoid (the ionic radius of six-coordinate Sc^{3+}, La^{3+}, and Lu^{3+} are 0.745 Å , 1.032 Å , and 0.861 Å respectively)[22] along with other rare earth elements using pyrazolate ligands. In this study bulky 3,5-diphenylpyrazole (Ph_2pzH) and 3,5- di-*tert*-butylpyrazole (t-Bu_2pzH) and the less bulky 3,5-dimethylpyrazole (Me_2pzH) have been used.

2.1.1 Current study

This chapter discusses the synthesis and structural characterisation of a variety of rare earth pyrazolate complexes using three different pyrazoles: 3,5-dimethylpyrazole (Me_2pzH), 3,5-di-*tert*-butylpyrazole (t-Bu_2pzH) and 3,5- diphenylpyrazole (Ph_2pzH), in which the structures span the whole La-Lu array beside Sc and Y. There are further developments in this study: the scandium derivative is synthesised having different coordination κ^1, κ^2, κ^1:κ^1:μ along with the lanthanum complex with three different coordination modes. Also, formation of a silanoxide-Me_2pz ligand which has been observed previously as [$Yb(Me_2pz)(MeCp)_2(Me_2pzSiMe_2O)]_2$[23] and [$Ce_4O(Me_2pz)_9(Me_2pz(SiMe_2O))_2$][21], has now been reported and fully characterised with scandium as the rare earth metal. Notably, not many studies have been performed on scandium compounds, particularly with pyrazolate ligands. Previously, most of the reported compounds using t-Bu_2pzH were monomeric compounds. However, there have been three further developments in this study: the lanthanum derivative [$La(t\text{-}Bu_2pz)_3(thf)_2$], which was reported previously without a crystal structure, now has been

structurally characterised, along with the cerium and lutetium analogues. Also, a polymeric structure with samarium has been synthesised in this study, for which the neodymium analogue has been reported previously. By using 1,2-dimethoxyethane (DME) instead of tetrahydrofuran (THF) the new [Eu(*t*Bu$_2$pz)$_3$(dme)$_2$] has now been reported. Previously, different compounds have been reported by using 3,5-diphenylpyrazole (Ph$_2$pzH). Therefore, attempts have been made to synthesise the compounds using smaller rare earth metals, which have led to the formation of lanthanoid dibenzoylmethane compounds as by-products.

2.2 Results and discussion

Glossary of compounds and codes

Below is a summary of the pyrazolate complexes discussed throughout this chapter, along with their respective codes.

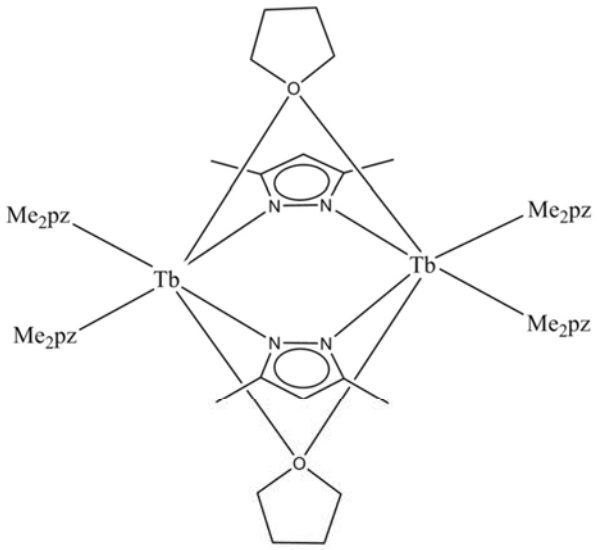

$[Tb(Me_2pz)_3(thf)]_2$ **(2.1)**

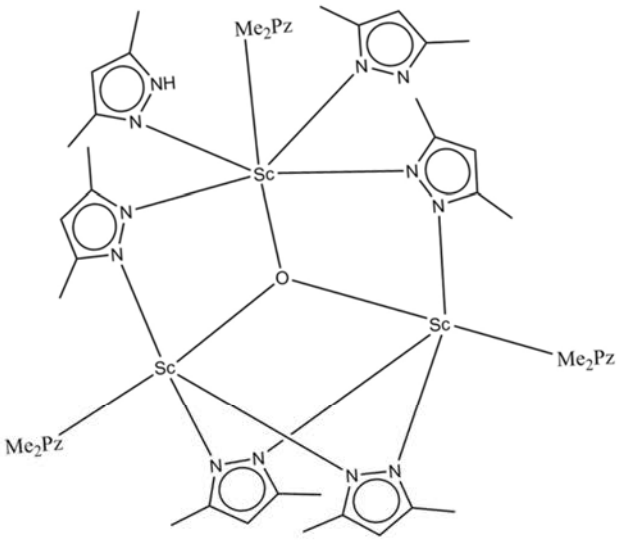

$[Sc_3O(Me_2pz)_7(Me_2pzH)_2]$**(2.2)**

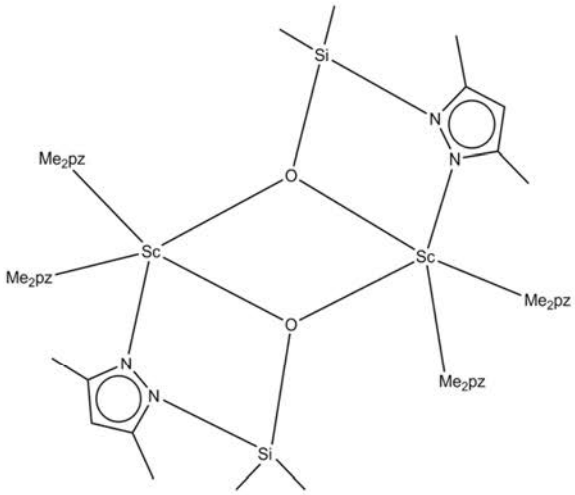

$[Sc_2(Me_2pz)_4(Me_2pz(SiMe_2O))_2]_2$ **(2.3)**

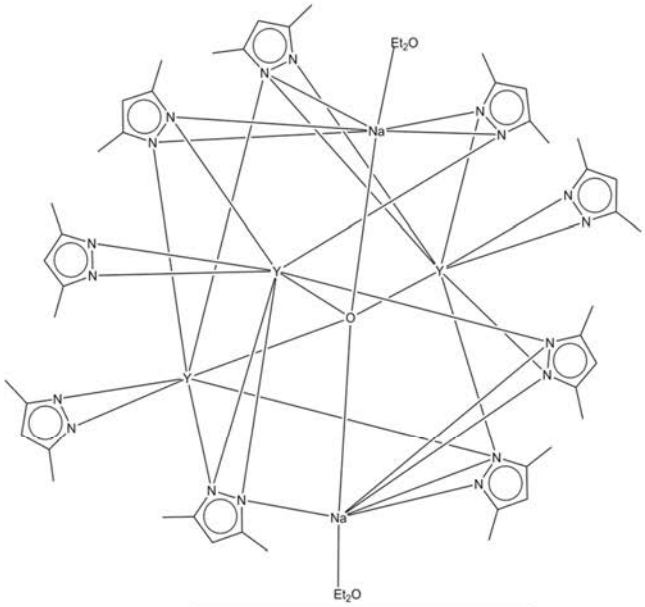

$[Na_2(Et_2O)_2OY_3(Me_2pz)_9]$ **(2.4)**

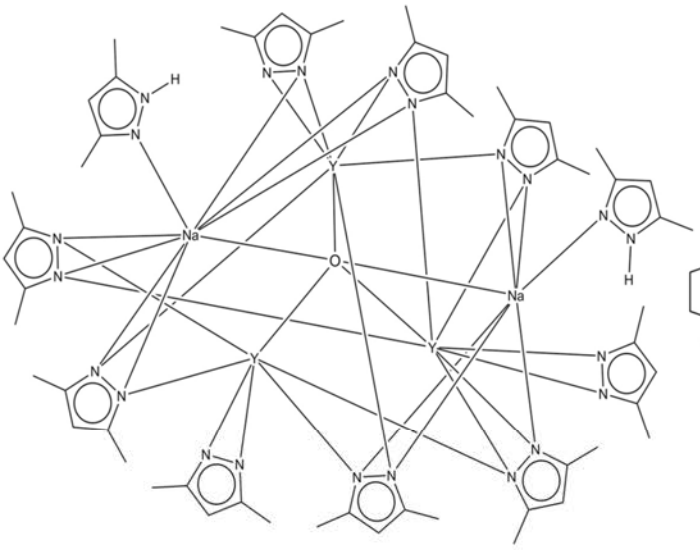

$[Y_3(Me_2pz)_9(Me_2pzH)_2Na_2O]$**(2.5)**

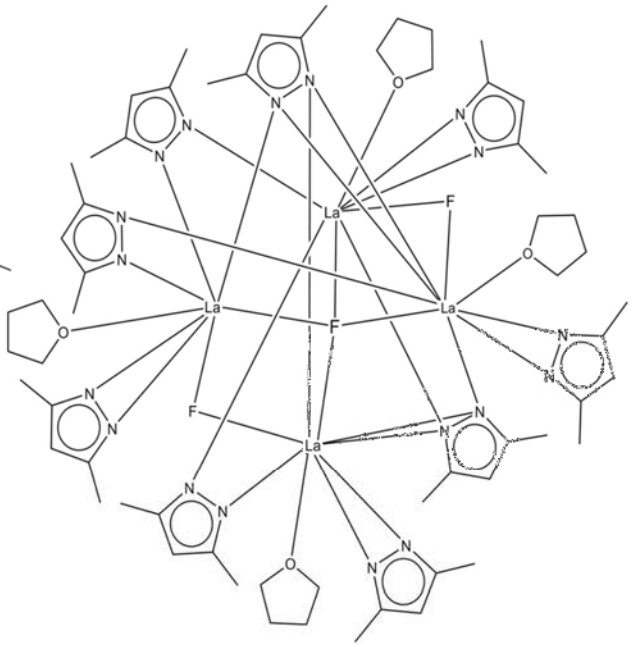

$[La_4(Me_2pz)_9(\mu_2\text{-}F)_2(\mu_4\text{-}F)(thf)_4].3THF$ (**2.6**)

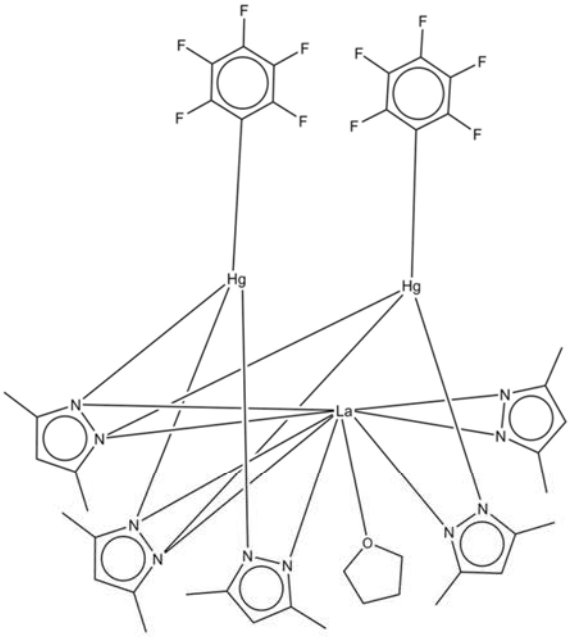

$[La(Me_2pz)_5Hg_2(C_6F_5)_2\ (thf)]$**(2.7)**

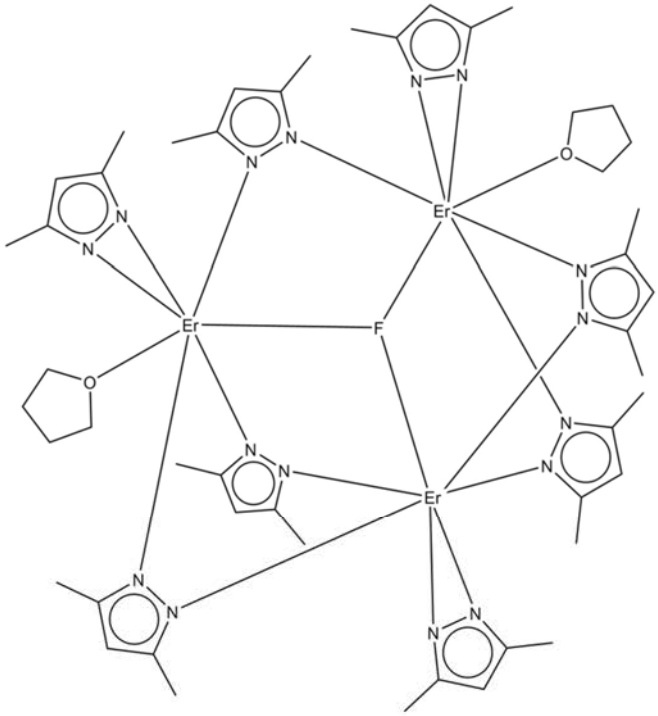

$[Er_3F(Me_2pz)_8(thf)_2]$**(2.8)**

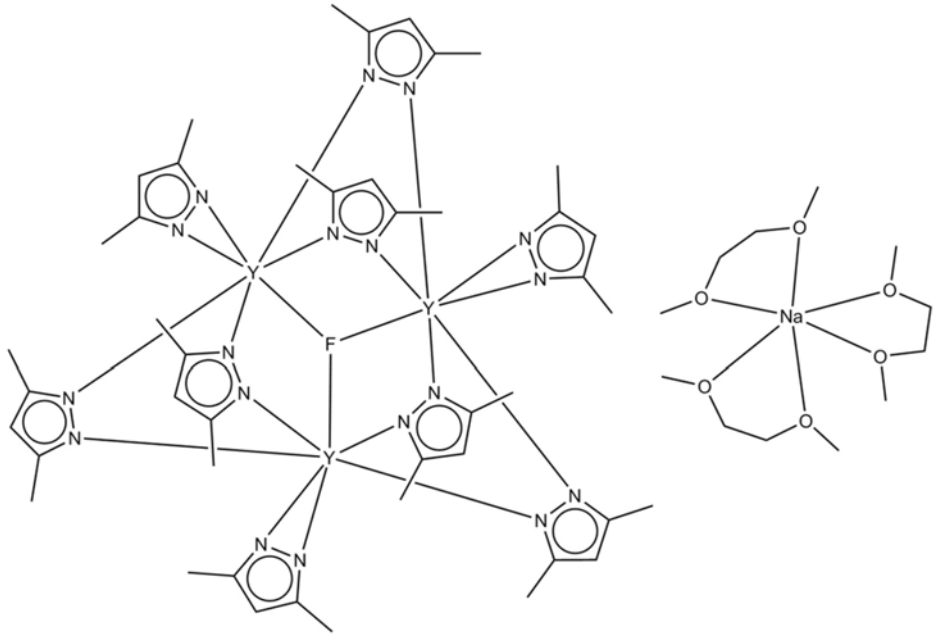

$[Na(dme)_3Y_3F(Me_2pz)_9].3/2DME$ **(2.9)**

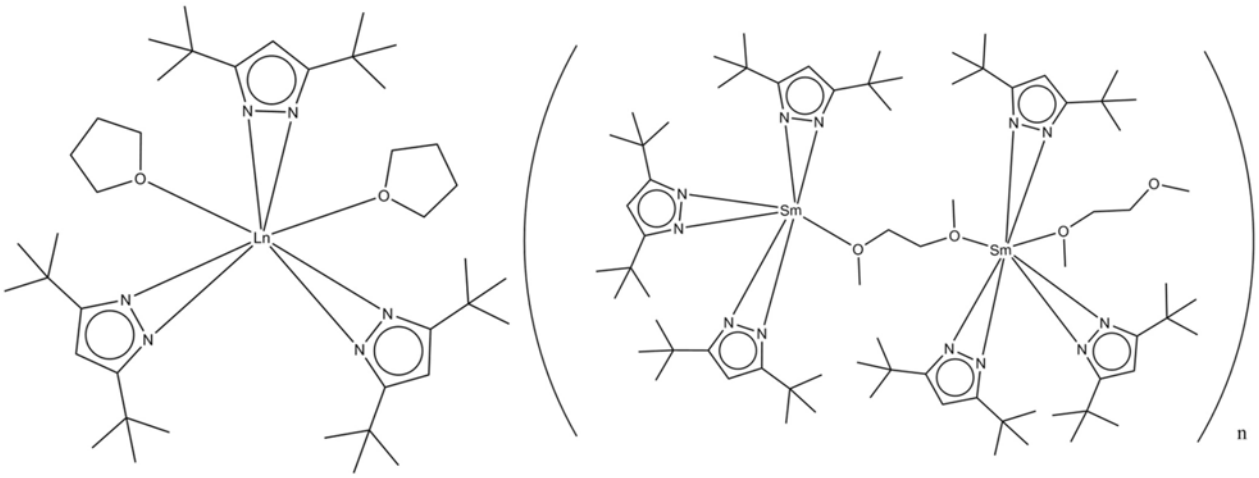

$[Ln(tBu_2pz)_3(thf)_2]$ **(2.10)**
Ln = La **(2.10a)**
Ln = Ce **(2.10b)**
Ln = Lu **(2.10c)**

$[Sm_2(tBu_2pz)_3(dme)_2]_n$ **(2.11)**

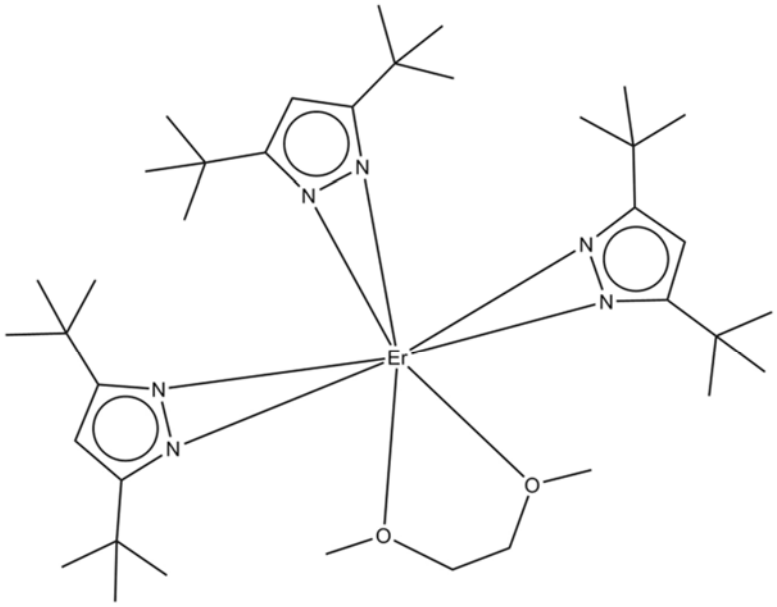

$[Er_2(tBu_2pz)_3(dme)]$ **(2.12)**

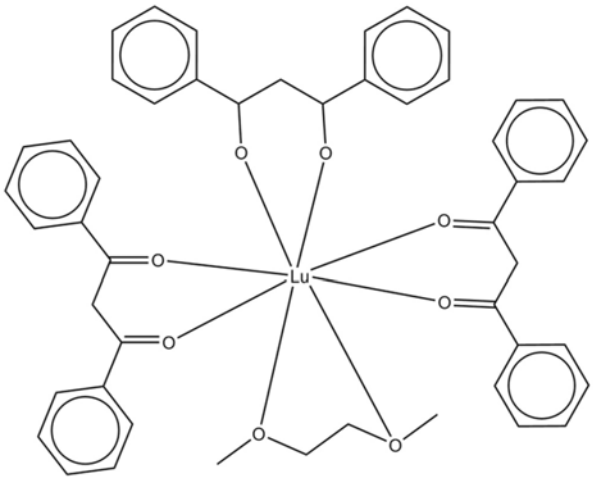

$[Lu(dbm)_3(dme)]$ **(2.13)**

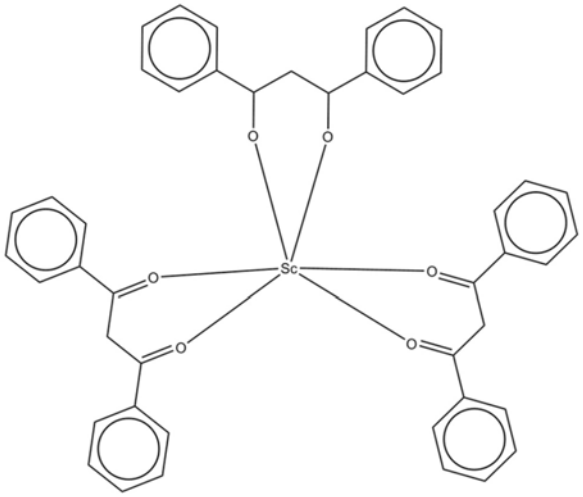

$[Sc(dbm)_3]$ **(2.14)**

2.2.1 Synthesis and characterisation of 3,5-dimethylpyrazolate complexes

Dinuclear $[Ln(Me_2pz)_3(thf)]_2$ complexes (Ln = Y, La, Ce, Pr, Nd, Ho, Lu) have been prepared by redox transmetallation/protolysis in THF previously.[20, 21] However, the formation of $[Ce_4O(Me_2pz)_9(Me_2pz(SiMe_2O))_2]$, $[Ce_4O(Me_2pz)_{11}]$, $[Ce(Me_2pz)_4(thf)(Me_2pzH)]$ and $[Yb(Me_2pz)(MeCp)(Me_2pzSiMe_2O)(thf)]_2$) in the previous researches were reported.[21, 23] Therefore, a series of transmetallation/protolysis reactions (RTP) using rare earth elements (RE) (RE = Sc, Y, La, Sm, Eu, Gd, Tb, Ho, Er and Yb), 3,5-dimethylpyrazole and $Hg(C_6F_5)_2$ were performed as a structural survey to make sure there were no surprises for the intervening elements. Such reactions often require activation of the metal surface. Therefore, the addition of one drop of mercury is sufficient to form a RE/Hg amalgam at the surface of the metal. Rare earth complexes of Sc, Y, La, Tb and Er were synthesised successfully by RTP reactions using Me_2pzH in this research (Equation 2-1).

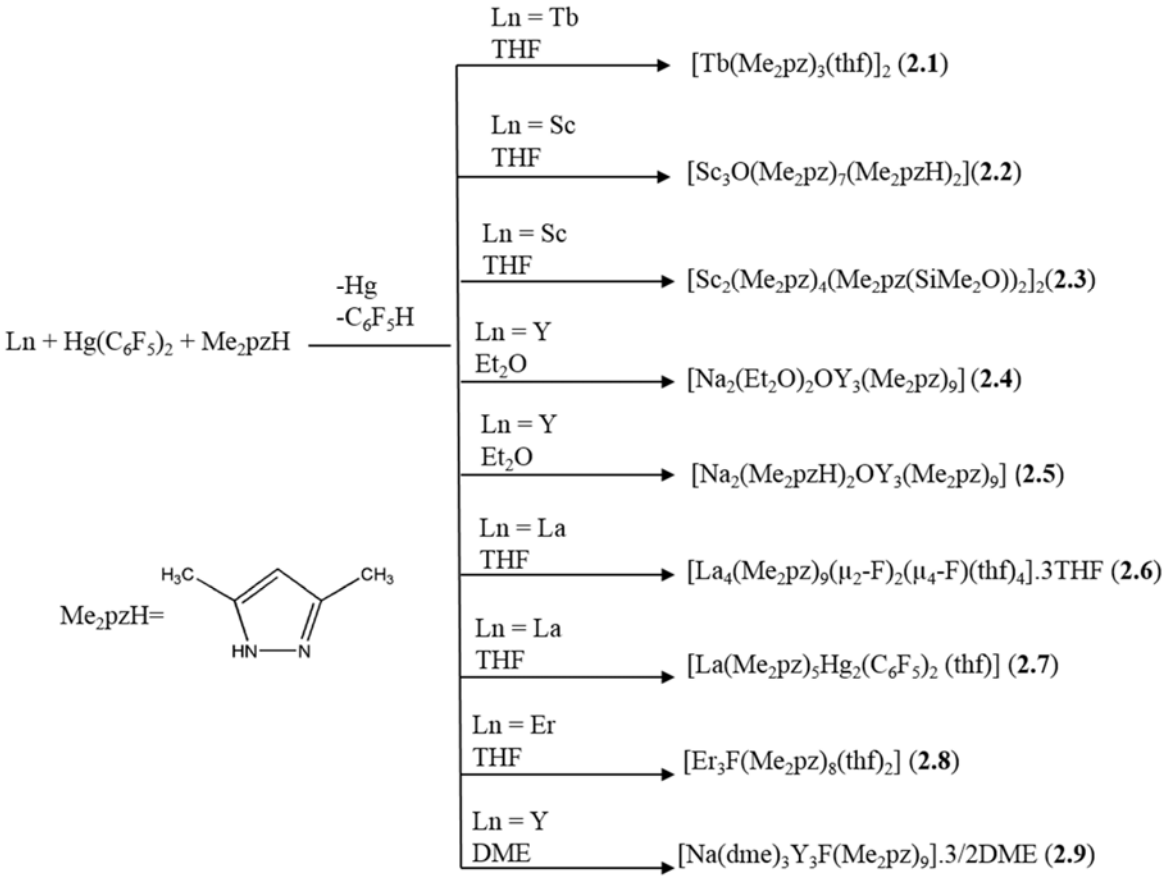

Equation 2-1. Synthesis of rare earth 3,5-dimethylpyrazolate complexes

Among the isolated compounds in this research, the only 3,5-dimethylpyrazolate complex that resembles the previously reported dinuclear $[Ln(Me_2pz)_3(thf)]_2$ complexes is $[Tb(Me_2pz)_3(thf)]_2$ (**2.1**). Compound **2.1** was obtained in good yield (73%). The ^1H NMR spectrum could not be interpreted due to line broadening and shifting because of the paramagnetic effect of Tb^{3+}. However, the elemental analysis confirmed the composition of the bulk material to be the same as found in the X-ray crystal structure (see later).

Challenges to structurally characterise the smaller rare earth 3,5-dimethylpyrazolate complexes (Sc, Y and Er) and larger rare earth 3,5-dimethylpyrazolate (La), resulted in the synthesis of some new compounds (oxide compounds and compounds as the result of C-F activation) with interesting features.

The complexes using lanthanum (**2.6**) and erbium (**2.8**) were obtained in good yields (44-76%) although the scandium and yttrium analogues were isolated as crystals in lower yields (23-55%). Single crystals suitable for X-ray crystallography were achieved through evaporation of the solvent to approximately 5 ml and then cooling very slowly for several days.

The reported compounds involving small rare earth elements have been found to contain two terminal η^2-pyrazolate ligands, two μ-κ^1-κ^1-Me_2pz ligands (the most common pyrazolate ligation for non-rare earth complexes) and two bridging thf donors, which is relatively uncommon in non-alkaline metal chemistry.[3] However, the Sc compound in this study revealed formation of a scandium oxide cage: $[Sc_3O(Me_2pz)_7(Me_2pzH)_2]$ (**2.2**). Oxygen is present in the structure possibly because of solvent or silicon grease as repeated attempts (with thoroughly dried solvents) to form non-oxygenated compounds repeatedly resulted in these cage compounds being isolated. These types of compounds have consistently appeared with this ligand system ($[Ce_4O(Me_2pz)_9(Me_2pz(SiMe_2O))_2]$, $[Ce_4O(Me_2pz)_{11}]$, $[Ce(Me_2pz)_4(thf)(Me_2pzH)]$ and $[Yb(Me_2pz)(MeCp)(Me_2pzSiMe_2O)(thf)]_2$)[21, 23] which suggests that compounds involving this system are very reactive and very likely to ring-open THF and extract oxygen or depolymerise/deoxygenate adventitious grease in the reaction mixture. The ^1H NMR spectrum (in C_6D_6) shows the presence of coordinated Me_2pzH with a resonance at δ = 10.86 ppm that does support the presence of Me_2pzH in crystal structure of $[Sc_3O(Me_2pz)_7(Me_2pzH)_2]$. The IR spectrum of the crystals of **2.2** contained an absorption at 3194 cm^{-1}, which can be attributed to the N-H stretch of the coordinated pyrazole.

The unintentional exposure of the scandium reaction mixture to silicon grease caused the formation of silanoxide substituted pyrazolate ligand, since silicon grease, $(Me_2SiO)_n$, was depolymerised and the monomer inserted into the Sc-N (pyrazolate) bond resulting in formation of complex **2.3** ($[Sc_2(Me_2pz)_4(Me_2pz(SiMe_2O))_2]_2$) (Equation 2-2).

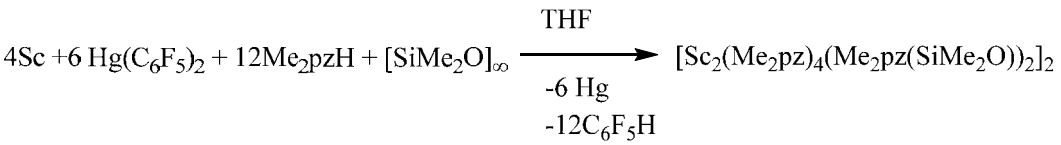

Equation 2-2. Synthesis of $[Sc_2(Me_2pz)_2(Me_2pz(SiMe_2O))_2]_2$

The presence of a resonance at δ = 0.29 ppm in the ^{1}H NMR spectrum can be attributed to methyl H atoms of $SiMe_2O$ and supports the results from the X-ray crystal structure. The reaction has been repeated using different solvents in addition to THF (DME and acetonitrile) and the product was isolated in low yield with a similar structure ($[Sc_2(Me_2pz)_4(Me_2pz(SiMe_2O))_2]_2$).

The reaction using yttrium and Me_2pzH in diethyl ether as solvent resulted in the formation of the $[Y_3O(Me_2pz)_9Na_2(Et_2O)_2]$ (**2.4**). In this reaction, the solvent was contaminated with Na_2O, as it was stored over sodium pieces under N_2 and the Na_2O was incorporated into material that crystallised from solution. Additionally, C-O bond cleavage of Et_2O occurred resulting in formation of the yttrium oxide cage complex. There are two kinds of bonding modes present in the structure **2.4**: μ_3- η^1:η^1 and η^2. Accordingly, the ^{1}H NMR spectrum of the product shows four resonances that reveals the presence of these two different environments for methyl group and backbone hydrogen of the ligands. The resonances at δ = 2.10 and 2.22 ppm are attributed to 54 H of 18 methyl groups of 3,5-dimethylpyrazolate ligand with two different environments around them. The resonances at δ = 5.68 and 6.29 ppm are attributed to the nine backbone hydrogens of 3,5-dimethylpyrazolate ligand with two different environments around them. Because of the coordination of two solvent molecules (Et_2O), two resonances at 1.02 ppm (attributed to hydrogens of CH_3 group) and 3.18 ppm (attributed to hydrogens of CH_2 group) are present in the ^{1}H NMR spectrum. By repeating the RTP reaction using Y and diethylether as solvent, $[Y_3O(Me_2pz)_9Na_2(Me_2PzH)_2]$ (**2.5**) was formed. In compound **2.5** the trinuclear yttrium cage surrounds a trapped Na_2O molecule, with each sodium ligated by a 3,5-dimethypyrazole. As mentioned for compound **2.4**, the solvent was contaminated with Na_2O, as it was stored over sodium pieces and the Na_2O was incorporated into material that crystallised from solution. There are three kinds of bonding modes present in the structure **2.5**: η^2, μ_3-η^1:η^1 and η^1. Accordingly, the ^{1}H NMR spectrum of the product shows five resonances that reveals the presence of these three different environments for methyl group and backbone hydrogen of the ligands. The resonances at δ = 1.95, 1.88 and 2.09 ppm are attributed to 12 H, 36 H and 18 H of 22 methyl groups of 3,5-dimethylpyrazolate ligand with three different environment around them. The resonances at δ = 5.71 and 6.29 ppm

are attributed to the eleven backbone hydrogens of 3,5-dimethylpyrazolate ligand with two different environments around them. The IR spectrum of the crystals of **2.5** contained a strong absorption at 3290 cm^{-1}, which can be attributed to the N-H stretch of the coordinated pyrazoles.

Considering the high fluorophilicity of rare earth ions, C-F activation can be observed when fluorocarbons are present in highly reactive metal-organic lanthanoid solutions. Previously, in related redox trasmetallation/protolysis (reactions involving DippFormH, Ln metal and $Hg(C_6F_5)_2$), isolation of $[Ln(DippForm)_2F(thf)]$ (Ln = La, Ce, Nd, Sm and Tm) were reported. Considering Equation 2-3, Equation 2-4 and Equation 2-5, it is established that reaction of lanthanoid elements and $Hg(C_6F_5)_2$ with the DippFormH in THF resulted in C-F activation and formation of $[Ln(DippForm)_2F(thf)]$ complexes, and [*o*-$HC_6F_4O(CH_2)_4$DippForm] in which the formamidinate is functionalised by a ring-opened THF that has trapped tetrafluorobenzyne.[24]

Equation 2-3. $2[LnL_2] + Hg(C_6F_5)_2 \longrightarrow 2[LnL_2(C_6F_5)] + Hg$

Equation 2-4. $[LnL_2(C_6F_5)] + LH \longrightarrow [LnL_3] + C_6F_5H$

Equation 2-5. $[LnL_2(C_6F_5)] \longrightarrow [LnL_2F] + o\text{-}C_6F_4$

Attempts to isolate a product using the RTP reaction between La, $Hg(C_6F_5)_2$ and ligand resulted in the formation of the complex $[La_4(Me_2pz)_9(\mu_2\text{-}F)_2(\mu_4\text{-}F)(thf)_4].3THF$ (**2.6**) which is the result of C-F activation of intermediate compounds (Equation 2-5). The ^1H NMR spectrum of compound **2.6** shows the presence of a resonance at ~2.09 ppm for 18 methyl groups and a resonance at ~5.86 ppm that is assigned to the nine backbone hydrogen atoms of the 3,5-dimethylpyrazolate ligands. The elemental analysis of the compound **2.6** shows the loss of three thf molecules that occurred during drying of the sample.

Previously a complex of $[La(Me_2pz)_3(thf)]_2$ by the RTP reaction with La, $Hg(C_6F_5)_2$ and Me_2pzH has been reported.[3] Since the compound isolated from the RTP reaction involving La was a C-F activation product, the preparation was attempted again to isolate $[La(Me_2pz)_3(thf)_2]_2$. However, the only compound isolated from this RTP reaction was the bimetallic complex $[Hg_2(Me_2pz)_5(C_6F_5)_2La]$ (**2.7**), where a C_6F_5 ligand is identified in the structure. Redox transmetallation/ protolysis can occur stepwise (Scheme 2-1).[25, 26] The LaL_3 can be isolated according to Scheme 2-1. Also, the reaction of $Hg(C_6F_5)_2$ with Me_2pzH was

attempted with no added lanthanoid and the formation of [(Me$_2$pz)Hg(C$_6$F$_5$)] was established by ^{1}H NMR and ^{19}F NMR. The ^{19}F NMR spectrum of the reaction of Hg(C$_6$F$_5$)$_2$ with Me$_2$pzH shows resonances at δ = -139.17 ppm, -153.72 ppm, -162.42 ppm, which shows the conversion of some Hg(C$_6$F$_5$)$_2$ to C$_6$F$_5$H. These resonances are distinct from the resonances of bispentafluorophenyl mercury at -119.64 ppm, -153.15 ppm, and 160.28 ppm.[27]

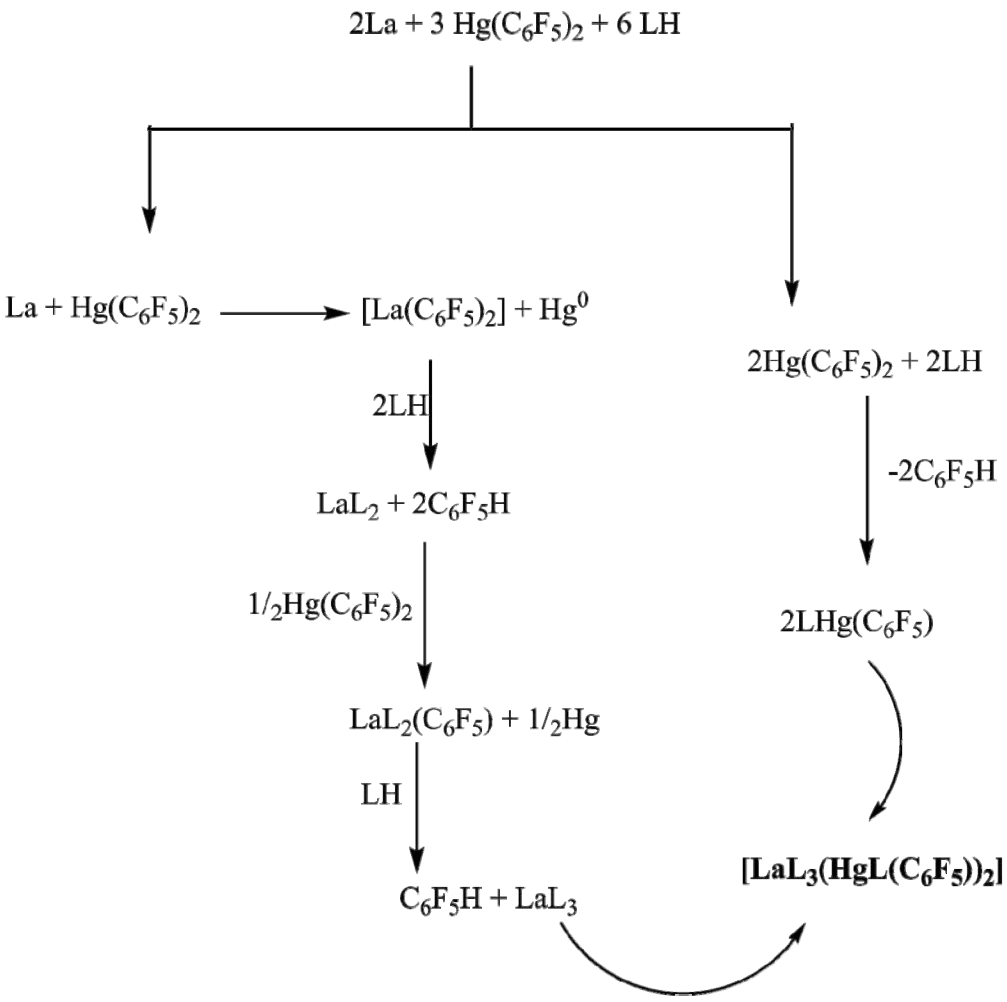

Scheme 2-1. Proposed path for RTP reaction with La, Hg(C$_6$F$_5$)$_2$ and Me$_2$pzH, resulting in the isolation of [Hg$_2$(Me$_2$pz)$_5$(C$_6$F$_5$)$_2$La] (**2.7**).

No NH resonance is observed at ~10 ppm in ^{1}H NMR that can confirm the formation of [(Me$_2$pz)Hg(C$_6$F$_5$)] along with the ^{19}F NMR. Also, the formation of [(Me$_2$pz)Hg(C$_6$F$_5$)] indicates that elimination of C$_6$F$_5$H had occurred due to the higher acidity of Me$_2$pzH (pK_a = 9) than C$_6$F$_5$H (pK_a = 25.6 in THF)[28]. So, it can be assumed that compound **2.7** is the result of co-crystallisation of present compounds LaL$_3$ and LHg(C$_6$F$_5$). Previously, some

mercury phosphanylamide compounds from the reaction of $Hg(C_6F_5)_2$ and $HN(PPh_2)_2$ in toluene with no added metal were reported.[29] The ^1H NMR spectrum of compound **2.7** shows the presence of resonance at ~ 2.01 ppm for 10 methyl groups (30 hydrogens) and resonance at ~5.75 ppm for the five backbone hydrogens of the 3,5-dimethylpyrazolate ligands.

Attempts to isolate a product using erbium, 3,5-dimethylpyrazolate in an RTP reaction with $Hg(C_5F_5)_2$ resulted in isolation of complex **2.8** ($[Er_3F(Me_2pz)_8(thf)_2]$). There is a synthetic complication with the RTP route for isolating compound **2.8**. It can be proposed that compound **2.8** is the result of co-crystallisation of $Er(Me_2pz)_3$ and $Er(Me_2pz)_2F$. Scheme 2-2 proposes that the intermediate complex $[Er(Me_2pz)_2(C_6F_5)]$ does not undergo a final protolysis step with Me_2pzH. Instead, the bound C_6F_5 undergoes C-F activation and due to the fluorophilicity of rare earth elements $[ErF(Me_2pz)_3]$ forms.[21] No ν (OH) absorptions in IR spectra were detected eliminating accidental hydrolysis and thus confirming no O-H is present. Also, the broad resonance at δ = -170.14 ppm in the ^{19}F NMR spectrum confirms the presence of fluoride in the structure.

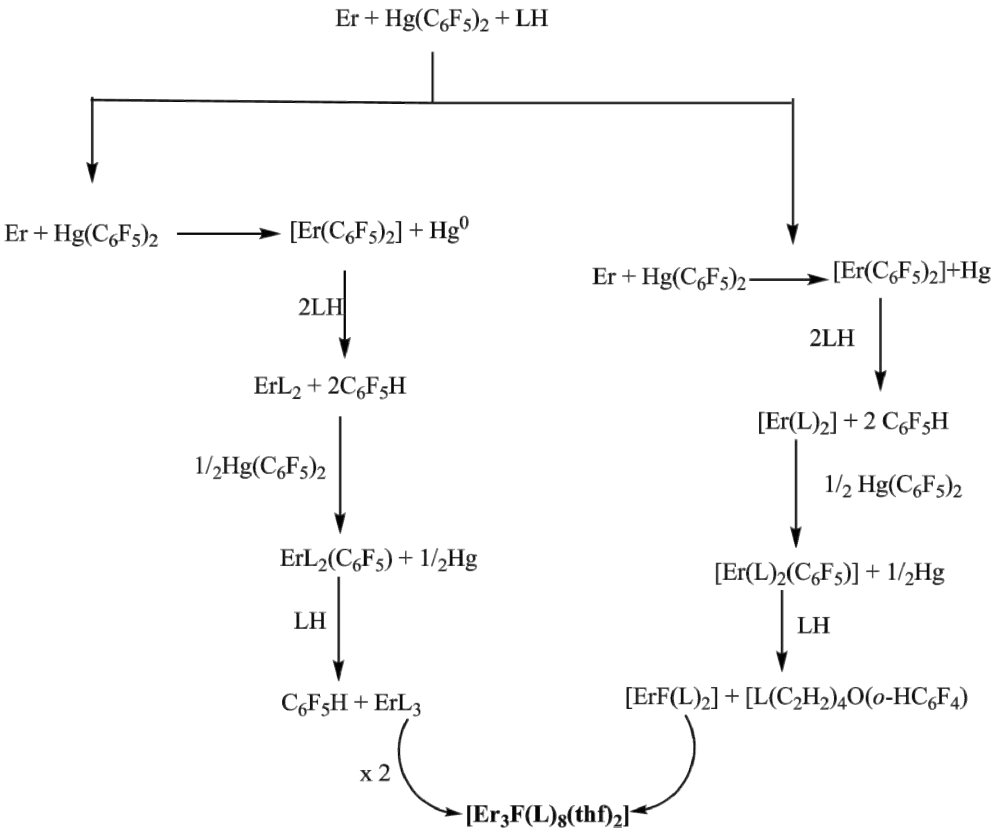

Scheme 2-2. Proposed pathway for the formation of $[Er_3F(Me_2pz)_8(thf)_2]$ (**2.8**) as the result of co-crystallisation of $Er(Me_2pz)_3$ and $Er(Me_2pz)_2F$.

The complex repeatedly returned a poor elemental analysis (consistently low in carbon %). The trend of low carbon has been suggested as incomplete combustion in the C, H analyser, which could result in the formation of metal carbides, and thus lower the percentage of carbon found.[30]

The RTP reaction involving Me_2pzH, yttrium and $Hg(C_6F_5)_2$ in DME resulted in the formation of complex **2.9** ($[Na(dme)_3Y_3F(Me_2pz)_9]$.3/2 DME) incorporating fluoride as a result of C-F activation. Since no elemental sodium was used in this reaction, the only source of sodium is the solvent since it was kept over sodium (to be sure that the solvent was dry) and therefore the presence of sodium containing compounds is possible. Compound **2.9** was isolated in very low yield, since the presence of Na-containing materials in the solvent could not be expected to be in high concentration. The presence of a resonance at δ = -168 ppm in the ^{19}F NMR spectrum supports the composition found in the X-ray crystal structure. The resonances at δ = 3.09 & 3.29 ppm in the ^{1}H NMR spectrum are attributed to DME in the complex. The C, H, N analysis of this compound ($[Na(dme)_3Y_3F(Me_2pz)_9]$.3/2DME) was problematic due to the very low yield and separation of the low yield of crystals from other microcrystalline bulk material.

2.2.1.1 X-ray structure determinations

2.2.1.1.1 Rare earth 3,5-dimethylpyrazolate complexes

The RTP reaction involving terbium, 3,5-dimethylpyrazole and $Hg(C_6F_5)_2$ in THF resulted in compound $[Tb(Me_2pz)_3(thf)]_2$ (**2.1**). The X-ray crystal structure of $[Tb(Me_2pz)_3(thf)]_2$ (**2.1**) is isomorphous with those of the previously reported $[Dy(Me_2pz)_3(thf)]_2$,[3] $[Lu(Me_2pz)_3(thf)]_2$[3], $[Nd(Me_2pz)_3(thf)]_2$[31] and $[Ho(Me_2pz)_3(thf)]_2$[20] analogues. Complex **2.1** crystallised in the triclinic space group $P\bar{1}$, with half the dimer within the asymmetric unit with the dimer residing over an inversion centre (Figure 2-2). The metal atoms contain two terminal η^2-pyrazolate ligands (the common feature with the other reported compounds)[3, 17, 32] and two bridging thf donors (a very uncommon thf binding mode in non-alkali metal chemistry) that resulted in an eight-coordinate Tb^{3+} ion.[12, 20] The geometry around Tb can best be described as a 4,4'-bicapped trigonal prism as it is for Dy ,Lu[21], Nd[31] and Ho[20].

The average Tb-N_{pz} and Tb-O_{thf} bond lengths in complex **2.1** (2.345 Å and 2.640 Å respectively) shows that these bond lengths fall between those of the larger Nd (Nd-N_{pz} = 2.45 Å, Nd-O_{thf} = 2.75 Å) and the smaller Lu (Lu-N_{pz} = 2.293 Å, Lu-O_{thf} = 2.607 Å) as expected

when considering the lanthanoid contraction. There is a decrease in average Ln-N_{pz} (Tb = 2.345 Å; Lu = 2.293 Å) that corresponds well with the differences in ionic radii.[32] Table 2-1 summarises the bond lengths of $[Ln(Me_2pz)_3(thf)]_2$ (Ln = Nd, Tb (**2.1**) and Lu).

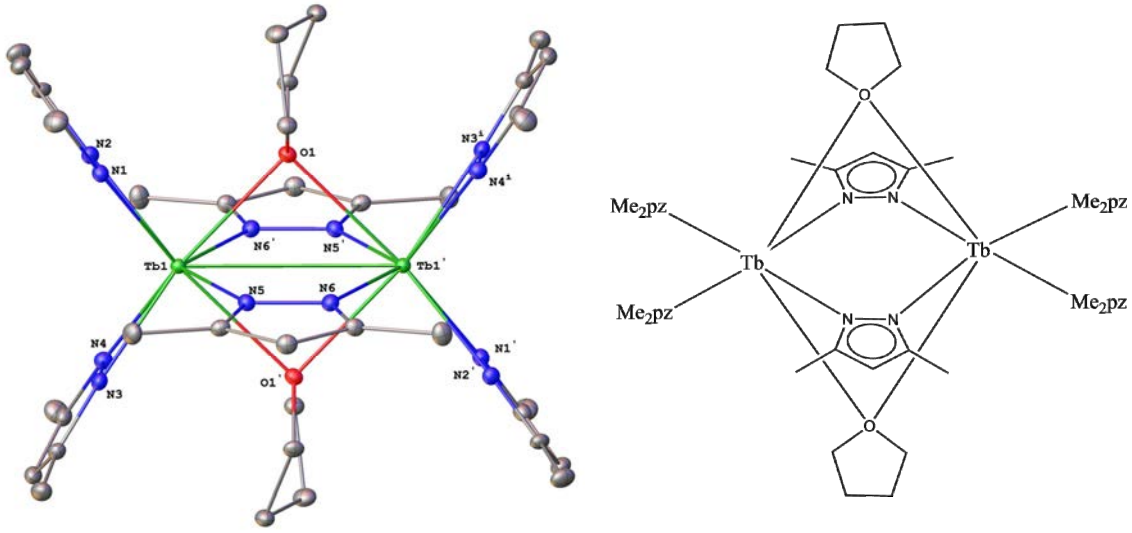

Figure 2-2. Molecular structure of $[Tb(Me_2pz)_3(thf)]_2$ (**2.1**). Ellipsoids shown at 50% probability, hydrogen atoms removed for clarity.

Table 2-1. Selected bond length (Å) for complexes $[Ln(Me_2pz)_3(thf)]_2$ (Ln = Nd, Tb (**2.1**) and Lu).

Bond	Nd	2.1	Lu
Ln1-N1	2.396 (3)	2.335(3)	2.281(7)
Ln1-N2	2.413(3)	2.334(3)	2.306(8)
Ln1-N3	2.418(3)	2.408(3)	2.316(6)
Ln1-N5	2.419(3)	2.327(3)	2.313(10)
Ln1-N6	2.510(3)	2.319(3)	2.304(7)
Ln1-O1	2.535(6)	2.635(2)	2.607(13)
Ln1-O1´	2.735(3)	2.691(2)	2.664(14)
Ionic radii Å (CN)	1.109(8)	1.040(8)	0.977(8)

Tb-N distances range from 2.332(3) Å to 2.408(3) and the average is 2.345 Å, which is comparable to the distance found previously in $[(C_5H_4Me)Tb(PzMe_2)(OSiMe_2PzMe_2)]_2$ eight-coordinate Tb^{3+} ion [33]. However, the Tb-O distance is 2.63 Å, which is longer than those previously reported.

2.2.1.1.2 Rare earth complexes incorporating oxo ligands

Complex **2.2** ($[Sc_3O(Me_2pz)_7(Me_2pzH)_2]$) crystallised in the monoclinic space group $P2_1/n$, with the whole molecule occupying the asymmetric unit (Figure 2-3). Three scandium atoms surround the central oxygen atom. Each scandium atom contains one terminal η^2-pyrazolate ligand. Also, two scandium atoms (Sc2 and Sc3) contain three μ-κ^1-κ^1-Me_2pz ligands (the most common pyrazolate ligation for non-rare-earth complexes).[3, 17]

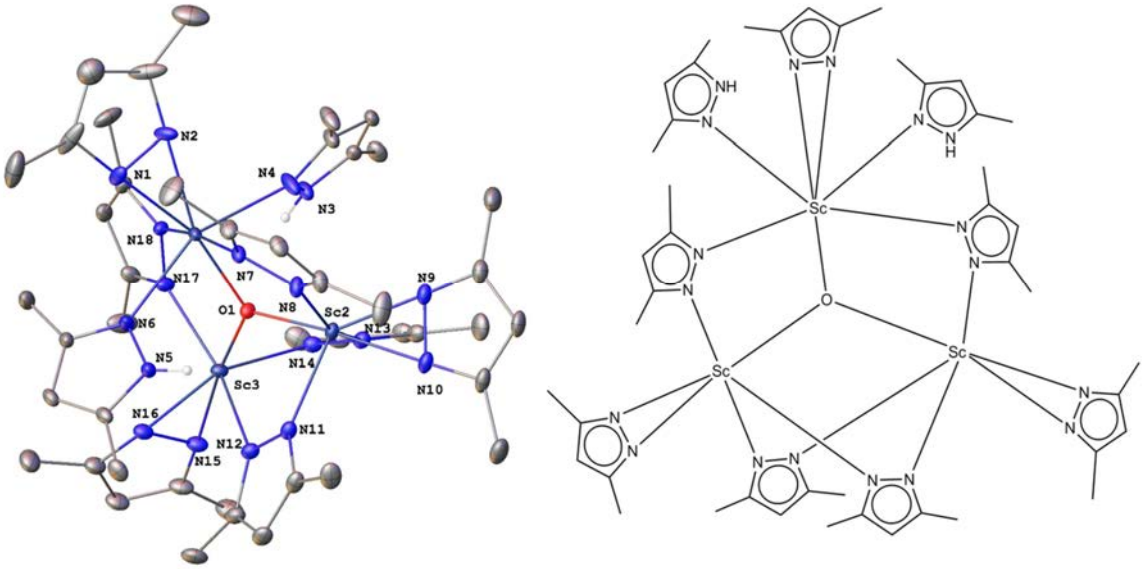

Figure 2-3. *Left:* molecular structure of $[Sc_3O(Me_2pz)_7(Me_2pzH)_2]$ (**2.2**). Ellipsoids shown at 50% probability. Hydrogen atoms removed for clarity. *Right*: Simplified diagram of **2.2**.

The crystal structure clearly shows that there are two coordinated pyrazoles ((N3, N4) and (N5, N6)), showing only κ(N) coordination. Therefore, compound **2.2** consists of two different Sc centres, in which two Sc^{3+} ions are six coordinate and the other Sc^{3+} ion is seven coordinate. The seven-coordinated scandium has one η^2-Me_2pz ligand, two μ-Me_2pz ligands and two η^1- Me_2pzH ligands while the six coordinate scandium has three μ-Me_2pz ligand and one η^2-Me_2pz ligand. The average chelating Sc-N bond length is 2.173Å and the

$\sum Sc - O - Sc$ ~360º indicating very close to trigonal planar geometry about the O atom (Table 2-2).A lanthanum oxide cage of formula $[La_4O(Me_2pz)_{10}(Me_2pzH)]$ [21] was reported by Werner but the scandium 3,5-dimethylpyrazolate compound involving an oxide ligand is reported for the first time. For the lanthanum compound the oxygen atom was shared between the four La atoms while for the smaller scandium ion, the oxygen atom is shared between the three Sc atoms, similar to the lutetium oxide cage, $[Lu_3O(Me_2pz)_9K_2(thf)_2]$.[21]

As has been determined by Werner[21] possible sources of oxide can either be silicon joint grease or solvent. There is a low possibility that air/H_2O can be the source of oxide as repeated chemistry involving the Me_2pz ligand often shows incorporation of O etc. (such as F, Na) so this highlights the reactivity of complexes involving this lower steric bulk ligand and the chemistry is more difficult than expected and O is extracted from solvent or grease. Since complex **2.2** was isolated in low yield (23%), the same reaction has been repeated to obtain higher yield products and to investigate the source of oxide.

Table 2-2. Selected bond lengths (Å) and angles (º) of **2.2**

Bond lengths					
Sc(1)–O(1)	2.025(17)	Sc(2)–O(1)	1.984(17)	Sc(3)–O(1)	1.985(17)
Sc(1)–N(1)	2.180(2)	Sc(2)–N(8)	2.244(2)	Sc(3)–N(12)	2.277(2)
Sc(1)–N(2)	2.172(2)	Sc(2)–N(9)	2.168(2)	Sc(3)–N(14)	2.218(2)
Sc(1)–N(4)	2.353(2)	Sc(2)–N(10)	2.176(2)	Sc(3)–N(15)	2.178(2)
Sc(1)–N(6)	2.348(2)	Sc(2)–N(11)	2.218(2)	Sc(3)–N(16)	2.168(2)
Sc(1)–N(7)	2.254(2)	Sc(2)–N(13)	2.279(2)	Sc(3)–N(17)	2.243(2)
Sc(1)–N(18)	2.252(2)				
Bond angles					
Sc(2)-O(1)-Sc(1)	122.15(8)	Sc(3)-O(1)-Sc(1)	122.72(8)		
Sc(2)-O(1)-Sc(3)	122.72(8)				

A new pyrazolate complex, $[Sc_2(Me_2pz)_4(Me_2pz(SiMe_2O))_2]_2$ (**2.3**) was synthesised (Figure 2-4) with higher yield (55%). This time the complex incorporated $SiMe_2O$ from the depolymerisation of $[SiMe_2O]_n$ grease used in stopcocks. The unintentional exposure of the reaction mixture to silicon grease during synthesising complex **2.3** caused the formation of a silanoxide-Me_2pz ligand. The silicon grease, $(Me_2SiO)_n$, is commonly used to seal the joints of glassware for manipulating air- and moisture-sensitive compounds.[34] The insertion ability of

$[SiMe_2O]_n$ into nitrogen metal bonds is not unknown[35] and in 3,5-dimethylpyrazolate systems have been shown to repeatedly undergo this chemistry. [23, 36] From the reaction between $[Yb(Me_2pz)_2(MeCp)]$ and $[SiMe_2O]_n$ a moderate yield of (26%) $[Yb(Me_2pz)_2(MeCp)(Me_2pzSiMe_2O)(thf)]_2$ was isolated.[23] Compound $[CpLn(Me_2Pz)(OSiMe_2Me_2Pz]_2$ [Ln = Ho, Dy] has been synthesised as the result of the reaction between $CpLn(Me_2Pz)_2$ and dimethyl silicone grease.[36] Also, complex $[Ce_4O(Me_2pz)_9(Me_2pz(SiMe_2O))_2]$ with silanoxide-Me_2pz ligands has been reported by Werner.[21]

Complex **2.3** ($[Sc_2(Me_2pz)_4(Me_2pz(SiMe_2O))_2]_2$) crystallised as colourless crystals from THF and the structure was solved and refined in the triclinic space group $P\bar{1}$ with two whole molecules occupying the asymmetric unit. The complex is a centrosymmetric dimer in which two silanoxide-Me_2pz ligands cap the metals at opposite sides of the dimer. The anionic oxygen of the silanoxide ligand bridges between the two scandium atoms. Each scandium atom contains two terminal η^2-pyrazolates as observed in the complex **2.2** ($[Sc_3O(Me_2pz)_7(Me_2pzH)_2]$). The reaction has been repeated using different solvents in place of THF (acetonitrile and DME) and in each case the same compound was isolated (Figure 2-4).

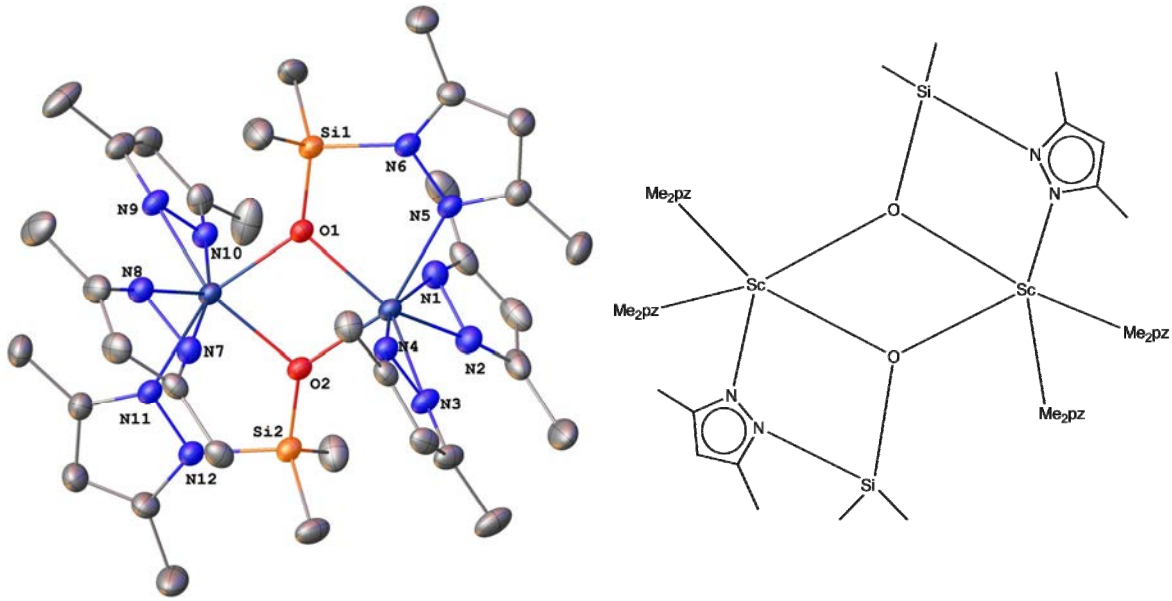

Figure 2-4. *Left:* Molecular structure of $[Sc_2(Me_2pz)_4(Me_2pz(SiMe_2O))_2]_2$ (**2.3**) in THF and DME and acetonitrile. Ellipsoids shown at 50% probability. Hydrogen atoms removed for clarity. *Right*: Simplified diagram of **2.3**.

The seven-coordinate scandium atom has a tetrahedron coordination environment. The

four nitrogen atoms of the pyrazolate ligands are nearly coplanar with the scandium atom and the oxygen atom is located below the plane (O(1)-Sc(1)- Cen(1) = 98.52(3)° and O(1)-Sc(1)-Cen(2)= 132.32(2)°). The N-Sc(1)-N bite angles for the η^2 binding of the pyrazolates are similar (37.24(15)º) and are close to that in compound **2.2** (37.045(13)º).

As shown in Table 2-3, the crystallography data are similar for products obtained from THF and DME but the product from acetonitrile crystallised with differing unit cell dimensions.

Table 2-3. Crystallography data for compound **2.3** ($[Sc_2(Me_2pz)_4(Me_2pz(SiMe_2O))_2]_2$) using different solvents (DME, THF and acetonitrile).

Compound	**2.3 (DME)**	**2.3 (THF)**	**2.3 (Acetonitrile)**
Formula	$(C_{34}H_{54}N_{12}O_2Sc_2Si_2)_2$	$(C_{34}H_{54}N_{12}O_2Sc_2Si_2)_2$	$(C_{17}H_{27}N_6OScSi)_4$
Formula Weight	1617.98	1617.98	808.99
T/K	173(2)	293(2)	293(2)
Crystal System	triclinic	triclinic	triclinic
Space Group	P-1	P-1	P-1
a/Å	11.635(2)	11.625(2)	11.653(2)
b/Å	19.248(4)	19.250(4)	11.729(2)
c/Å	21.092(4)	21.054(4)	16.365(3)
α/°	109.11(3)	108.99(3)	84.76(3)
β/°	103.66(3)	103.69(3)	83.75(3)
γ/°	94.43(3)	94.27(3)	73.96(3)
V/Å^3	4275.0(17)	4269.3(17)	2132.5(8)
Z	2	2	2
Z'	1	1	1
R_{int}	0.0324	0.0398	0.0418
GooF	1.062	1.017	1.069
wR_2 (all data)	0.1200	0.2638	0.4154
wR_2	0.1164	0.2437	0.4246
R_1 (all data)	0.0507	0.1234	0.1705
R_1	0.0451	0.0974	0.1563

The Sc-O (*avg.* 2.115 Å) and Sc-N (*avg.*2.191 Å) bond lengths of **2.3** given in Table 2-4 are shorter than the values reported for the Yb-O (2.250(5) Å) and Yb-N (*avg.* 2332 Å) in the six-coordinate Yb in $[Yb(Me_2pz)_2(MeCp)(Me_2pzSiMe_2O)(thf)]_2$ due to the larger ionic radius

of Yb^{3+} (0.868 Å) compared with Sc^{3+}(0.745 Å).[23] Also, comparing the average Sc-N bond lengths in compounds **2.2** ($[Sc_3O(Me_2pz)_7(Me_2pzH)_2]$.THF) and **2.3**, it is apparent that those in **2.3** are shorter than in **2.2**, even though both Sc^{3+} centres are seven-coordinate. Comparing compound **2.3** with $[CpHo(Me_2Pz)(OSiMe_2Me_2Pz)]_2$ [36] shows that in this centrosymmetric dimer compound**,** each metal centre atom (holmium) is coordinated to two bridging oxygen atoms. The average bond length of Ho-O (2.28 Å) is larger than the Sc-O, which is expected to be due to the larger ionic radii of Ho. However, in both compounds the coordination environment around the silicon atom has the normal tetrahedral arrangement.

Table 2-4. Selected bond lengths (Å) and angles (º) of **2.3**.

Bond lengths			
	DME	THF	Acetonitrile
Sc(1)–O(1)	2.132(14)	2.131(5)	2.133(7)
Sc(1)–O(2)	2.100(16)	2.099(6)	2.086(6)
Sc(1)–N(1)	2.224(19)	2.223(5)	2.182(7)
Sc(1)–N(2)	2.134(18)	2.150(5)	2.146(6)
Sc(1)–N(3)	2.155(19)	2.148(8)	2.158(4)
Sc(1)–N(4)	2.171(19)	2.171(6)	2.167(7)
Sc(1)–N(5)	2.299(2)	2.297(10)	2.278(6)
Sc(2)–O(1)	2.095(16)	2.099(6)	2.086(6)
Sc(2)–O(2)	2.134(14)	2.131(5)	2.133(7)
Sc(2)–N(7)	2.168(18)	2.170(6)	2.168(7)
Sc(2)–N(8)	2.156(18)	2.155(8)	2.158(4)
Sc(2)–N(9)	2.153(19)	2.146(5)	2.146(6)
Sc(2)–N(10)	2.181(19)	2.158(5)	2.182(7)
Sc(2)–N(11)	2.274(2)	2.279(9)	2.278(6)
Si(1) –N(6)	1.796(4)	1.798(4)	1.801(5)
Si(2) –N(12)	1.795(4)	1.777(4)	1.801(5)
Bond angles	DME	THF	Acetonitrile
Cen(1)-Sc(1)-O(2)	96.15(3)	97.28(3)	97.90(3)
Cen(2)-Sc(1)-O(2)	99.46(3)	98.91(3)	98.57(3)
Cen(1)-Sc(1)-Cen(2)	128.719(14)	126.835(14)	132.31

The Si-N distances of 1.79(2) Å in compound **2.3** ([$Sc_2(Me_2pz)_4(Me_2pz(SiMe_2O))_2]_2$)), which is close to the Si-N distance in holmium compound of $[CpHo(Me_2Pz)(OSiMe_2Me_2Pz)]_2$ (1.806(5) Å) [36], shows a normal bond length of Si-N in compound **2.3**.

Compound **2.4** ($[Y_3O(Me_2pz)_9Na_2(Et_2O)_2]$) was synthesised as the result of the reaction using yttrium and Me_2pzH in diethyl ether as solvent (Figure 2-5). The presence of Na in the structure is because of the solvent contamination with Na_2O, as it was stored over sodium pieces. So, due to the high reactivity of Me_2pz, which was observed before, the Na_2O was incorporated into material that crystallised from solution. Compound **2.4** crystallised in the orthorhombic space group *Pna*2_1 with the whole molecule occupying the asymmetric unit.

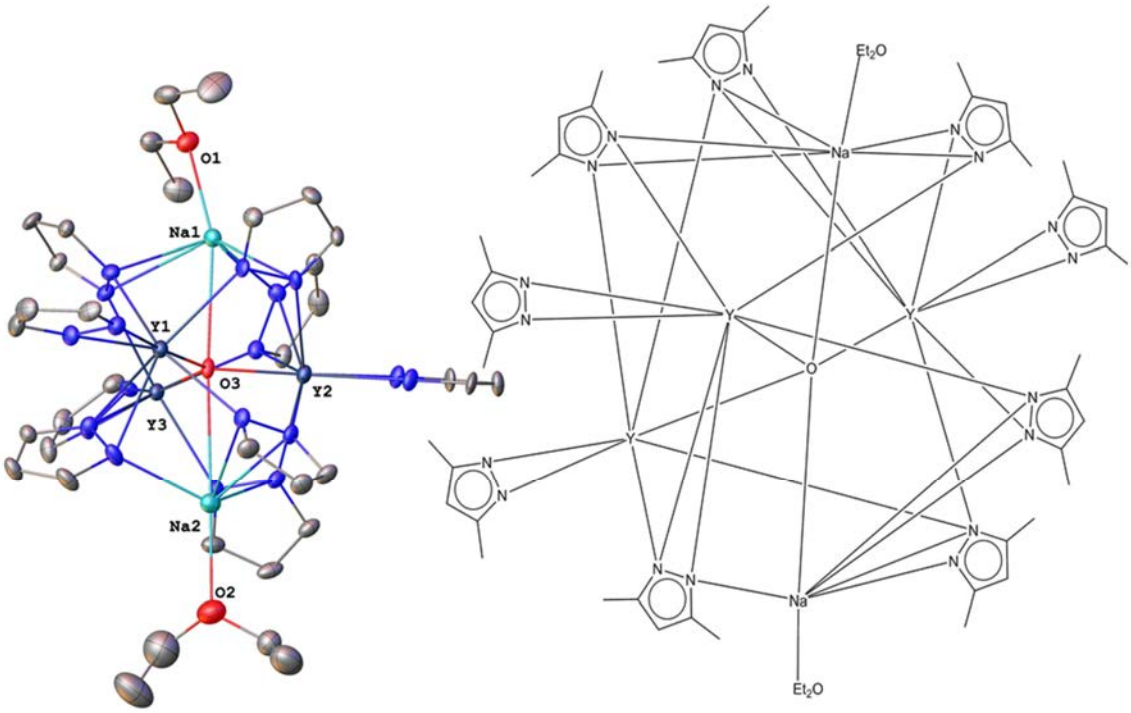

Figure 2-5. *Left*: Molecular structure of $[Y_3O(Me_2pz)_9Na_2(Et_2O)_2]$ (**2.4**). Ellipsoids shown at 50% probability. Hydrogen atoms and methyl groups removed for clarity. *Right*: simplified diagram of **2.4**.

Compound **2.4** has a trinuclear yttrium cage surrounding a trapped Na_2O molecule, with each sodium ligated by a diethyl ether molecule. Y1 and Y2 have two η^2-Me_2pz terminal ligands and three μ_3-η^1:η^1-3,5-dimethylpyrazolate ligands and one η^1 oxygen giving them eight coordination. Y3 is seven coordinate with one η^2-Me_2pz terminal ligand, four μ-η^1:η^1-3,5-

dimethylpyrazolate ligands and one η^1 oxygen. The X-ray crystal structure revealed trigonal bipyramid geometry around oxygen (Figure 2-5).

In compound **2.4**, each sodium is coordinated by two μ-η^2-3,5-dimethylpyrazolate ligands and one μ-η^1-3,5-dimethylpyrazolate ligand. Therefore, to have a clear picture of the molecular geometry of the Na, it is easier to consider the mid points of the N-N bonds of μ-η^2-3,5-dimethylpyrazolate ligand, one nitrogen atom of μ-η^1-3,5-dimethylpyrazolate and two oxygen atoms of the Et_2O and central oxygen as points of attachment to the sodium.

There are two different pyrazolate binding modes in compound **2.4**: η^2 and μ_3- η^1:η^1:η^2. The nitrogen atoms of the terminal η^2-3,5-dimethylpyrazolate ligands (2.371-2.316 Å) are closer to the metal atom (Y) than those of the bridging ligands (2.482-2.618 Å). The Na-O distances (2.774(4)-2.977(5) Å) are significantly different to the Y-O distances (2.116 (4)-2.127(3) Å) (Table 2-5).

Table 2-5. Selected bond lengths (Å) and angles (º) of **2.4**.

Bond Lengths

Y(1) environment		Y(2) environment		Y(3) environment		Na(1) environment		Na(2) environment	
O(3)	2.116(4)	O(3)	2.123(4)	O(3)	2.127(4)	O(1)	2.402(5)	O(2)	2.287(6)
N(12)	2.518(5)	N(52)	2.506(5)	N(11)	2.433(5)	O(3)	2.774(5)	O(3)	2.972(5)
N(82)	2.481(5)	N(62)	2.501(5)	N(21)	2.326(5)	N(11)	2.686(6)	N(32)	2.382(6)
N(41)	2.316(5)	N(71)	2.346(5)	N(22)	2.372(5)	N(12)	2.453(6)	N(51)	2.488(6)
N(42)	2.371(6)	N(72)	2.327(5)	N(31)	2.458(6)	N(81)	2.678(5)	N(52)	2.632(6)
N(31)	2.822(5)	N(81)	2.471(5)	N(51)	2.436(5)	N(82)	2.624(5)	N(61)	2.658(6)
N(32)	2.502(5)	N(91)	2.543(5)	N(92)	2.504(6)	N(91)		N(62)	2.500(6)
N(61)	2.481(5)	N(92)	2.618(5)						

Bond angles

N41-Y1-N42 34.17(18)	N71-Y2-N72 34.23(17)	N21-Y3-N22 34.33(17)
N31-Y1-N32 29.45(14)	N91-Y2-N92 31.29(15)	

Complex **2.4** bears a resemblance to the oxide cages of formulae $[Ln_3O(Me_2pz)_9Na_2(thf)_2]$ (Ln = Y, Ho,Yb, Lu), reported by Schumann and co-workers.[37] Comparing the lengths of the metal to nitrogen bonds of the terminal η^2-3,5-dimethylpyrazolate ligand of compound **2.4** (2.32-2.37 Å) to the previously reported $[Ln_3O(Me_2pz)_9Na_2(thf)_2]$ (Ln = Yb) (2.27-2.34 Å)[37] shows that the difference between Ln-N bond lengths agrees with the difference of ionic radii of seven coordinated Yb (0.925 Å) and Y (0.96 Å). The Na-O distances are almost similar in both compounds (~2.77 Å) (Table 2-5).

By repeating the reaction using yttrium and Me_2pzH in diethyl ether as solvent,

compound **2.5** ($[Y_3O(Me_2pz)_9Na_2(Me_2PzH)_2]$) (Figure 2-6) was synthesised with moderate yield (45%). Compound **2.5** has a trinuclear yttrium cage surrounding a trapped Na_2O molecule, with each sodium ligated by a 3,5-dimethypyrazole. Y1 and Y3 have one η^2-Me_2pz terminal ligands, two μ_3-η^1:η^1-3,5-dimethylpyrazolate ligands and one η^1 oxygen giving them seven coordination. Y2 is eight coordinate with one η^2-Me_2pz terminal ligand, one μ_3-η^1:η^2-3,5-dimethylpyrazolate ligand, one μ_3-η^1:η^1-3,5-dimethylpyrazolate and one η^1 oxygen. The X-ray crystal structure revealed trigonal bipyramid geometry around oxygen.

In compound **2.5**, Na1 is coordinated by three μ-η^2-3,5-dimethylpyrazolate ligands, one η^1-3,5-dimethylpyrazolate ligand and one η^1 oxygen while Na2 is coordinated by two μ-η^2-3,5-dimethylpyrazolate ligands, two η^1-3,5-dimethylpyrazolate ligand and one η^1 oxygen.

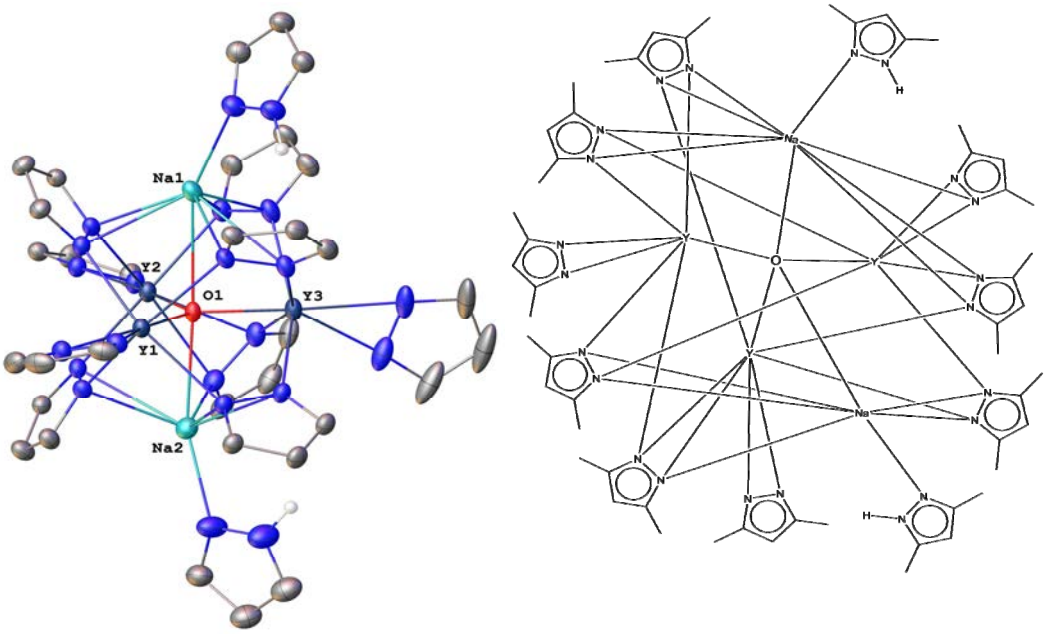

Figure 2-6. *Left*: Molecular structure of $[Y_3O(Me_2pz)_9Na_2(Me_2PzH)_2]$ (**2.5**). Ellipsoids shown at 50% probability. Hydrogen atoms and methyl groups removed for clarity. *Right*: simplified diagram of **2.5**.

There are two different pyrazolate binding modes in compound **2.5**: η^2 and μ_3- η^1:η^1:η^2. The nitrogen atoms of the terminal η^2-3,5-dimethylpyrazolate ligands (2.279-2.357 Å) are closer to the metal atom (Y) than those of the bridging ligands (2.425-2.561 Å). The Na-O distances (2.748(2)-2.893(2) Å) are significantly different to the Y-O distances (2.127 (18)-2.162(19) Å) (Table 2-6).

Table 2-6. Selected bond lengths (Å) and angles (°) of **2.5**.

Bond Lengths

Y(1) environment		Y(2) environment		Y(3) environment		Na(1) environment		Na(2) environment	
O(1)	2.129(18)	O(1)	2.162(19)	O(1)	2.127(18)	O(1)	2.893(2)	O(1)	2.748(2)
N(11)	2.357(2)	N(22)	2.505(2)	N(52)	2.470(2)	N(21)	2.667(2)	N(31)	2.471(3)
N(12)	2.350(2)	N(32)	2.431(2)	N(62)	2.477(3)	N(22)	2.502(3)	N(32)	2.764(3)
N(21)	2.425(2)	N(41)	2.355(2)	N(71)	2.279(3)	N(61)	2.802(3)	N(51)	2.360(3)
N(31)	2.481(2)	N(42)	2.324(2)	N(72)	2.389(3)	N(62)	2.450(3)	N(91)	2.819(3)
N(82)	2.531(2)	N(51)	2.569(2)	N(81)	2.441(2)	N(81)	2.921(3)	N(92)	2.578(3)
N(92)	2.483(2)	N(52)	2.551(2)	N(91)	2.464(2)	N(82)	2.493(3)	N(101)	2.348(3)
		N(61)	2.449(2)			N(111)	2.393(3)		

Bond angles

N11-Y1-N12 34.149(9) N51-Y2-N52 31.378(14) N71-Y3-N72 33.965(10) N41-Y2-N42 34.591(10)

2.2.1.1.3 Rare-earth complexes formed by C-F activation

Due to the high fluorophilicity of rare earth ions, C-F activation was observed in 3,5-dimethypyrazole systems similar to that previously observed in lanthanoid aryloxide complexes [25] and lanthanoid(III) formamidinates.[24] As mentioned previously in this chapter, C-F activation of the $[LnL_2(C_6F_5)]$ intermediate can occur to give a compound containing a fluoride ligand ($[LnL_2F]$) and tetrafluorobenzyne (Equation 2-3, Equation 2-4 and Equation 2-5).

Previously, $[La(Me_2pz)_3(thf)]$ [19, 21] was obtained from an RTP reaction and the tetranuclear compound $[La_4O(Me_2pz)_{10}(Me_2pzH)]$, was obtained by direct treatment of $[La(Me_2pz)_3(thf)]_2$ with $[SiMe_2O]_n$ and crystallisation from PhMe. In this study, a new pyrazolate complex, $[La_4(Me_2pz)_9(\mu_2\text{-}F)_2(\mu_4\text{-}F)(thf)_4].3THF$(**2.6**), was synthesised using an RTP reaction and the final product was the result of C-F activation (Figure 2-7).

Complex **2.6** ($[La_4(Me_2pz)_9(\mu_2\text{-}F)_2(\mu_4\text{-}F)(thf)_4].3THF$) was crystallised as colourless crystals and solved in the monoclinic space group $P2_1/c$ with a whole molecule within the asymmetric unit. Compound **2.6** has two different La centres, in which two La^{3+} ions are eight coordinate and the other two La^{3+} ions are nine coordinate. The eight coordinate La atoms are ligated by one terminal η^2-Me_2pz anion, one thf molecule, three μ-Me_2pz ligands and two μ-F ligands. The nine coordinate La atoms are ligated by two terminal η^2-Me_2pz anions, one μ-

Me_2pz ligand, one thf molecule and two μ-F ligands. The eight coordinate lanthanum accepts trigonal prismatic geometry if the binding site for the terminal η^2-Me_2pz is considered midway between the N–N bond of the pyrazolate. Also, the nine coordinate lanthanum centres are likewise trigonal prismatic if the η^2-Me_2pz ligands are considered similarly bound.

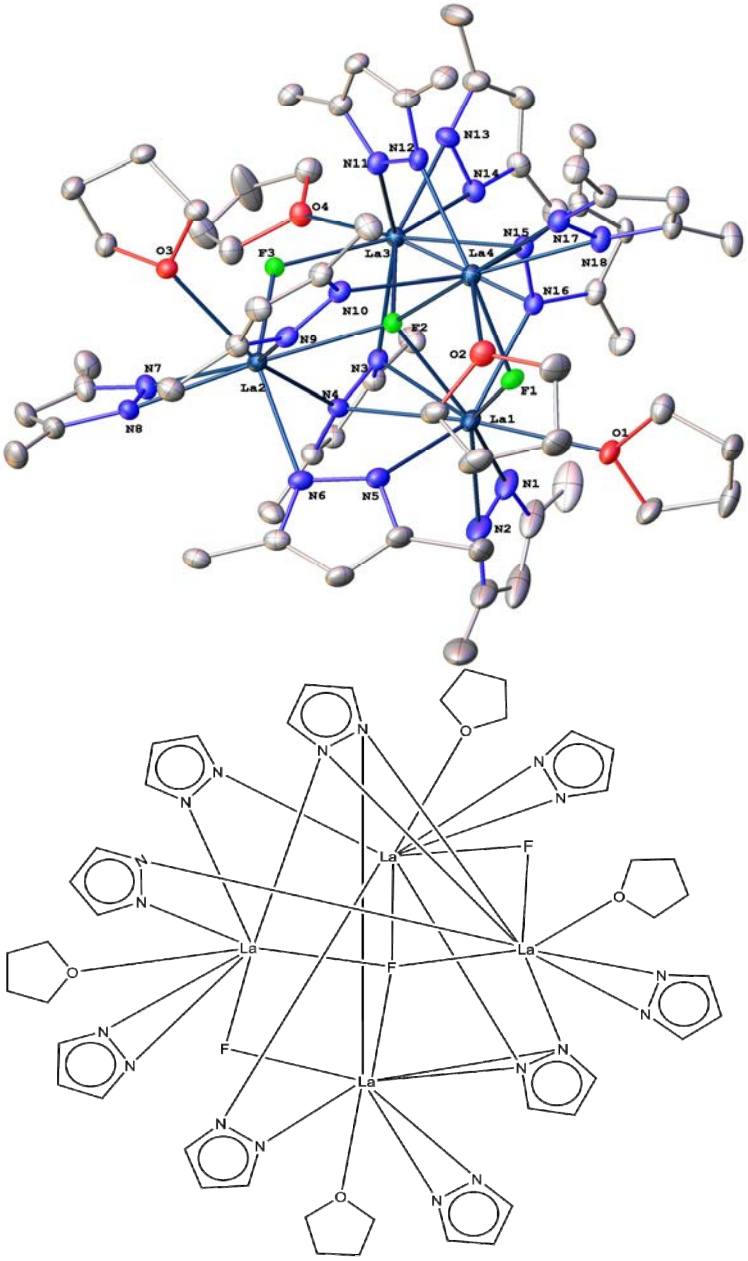

Figure 2-7. *Top*: molecular structure of $[La_4(Me_2pz)_9(\mu_2\text{-}F)_2(\mu_4\text{-}F)(thf)_4].3THF$ (**2.6**). Ellipsoids shown at 50% probability. Hydrogen atoms removed for clarity. *Bottom*: simplified diagram of **2.6**. Methyl groups removed for clarity.

Another significant aspect of the compound **2.6** is the presence of three different pyrazolate bonding modes: η^2, μ- η^1: η^1 and μ- η^2: η^1 along with a shared fluorine between the four lanthanum atoms. The fluorine atom in the centre of the cage adopts tetrahedral geometry, which was observed previously for the central oxygen in $[La_4O(Me_2pz)_{11}K(thf)_2]$ by Werner.[21] There are two different bonding modes for fluorine inside the structure: two μ_2-F which has been observed previously in $[Yb(EtForm)_2(\mu_2\text{-}F)]_2$[38], and one μ_4-F, which is observed for the first time in pyrazolate compounds.

The La-F bond length for the bridging fluoride in complex **2.6** (2.337 Å) is longer than the one in the $[\{Yb(EtForm)_2(\mu_2\text{-}F)\}_2]$ (2.171 Å) [38], which agrees with the difference of ionic radii (Yb^{3+} : 0.868 Å, La^{3+}: 1.16 Å and 1.216 Å for eight and nine coordinate La^{3+} respectively). Despite variation in the coordination numbers of lanthanum centres, the La-N bond lengths in compound **2.6** fall within a narrow range (2.348(4)-2.317(4)(Å)) (Table 2-7). For the η^2-Me_2pz-La ligation, the observed La-N bond lengths (2.458-2.850 Å) (Table 2-7) correspond well with Ln-N distances in the ten-coordinate $[La(Me_2pz)_3(thf)]_2$ complex (La-N : 2.489-2.78 Å).[21]

Table 2-7. Selected bond lengths (Å) and angles (°) of **2.6**.

Bond lengths							
La(1)–F(1)	2.348(4)	La(2)–F(2)	2.547(4)	La (3)–F(2)	2.568(4)	La(4)–F(2)	2.555(4)
La (1)–F(2)	2.569(4)	La (2)–F(3)	2.339(4)	La (3)–F(3)	2.347(4)	La (4)–F(1)	2.317(4)
La (1)–O(1)	2.606(6)	La (2)–O(2)	2.630(6)	La (3)–O(3)	2.603(5)	La (4)–O(4)	2.626(5)
La (1)–N(1)	2.484(6)	La (2)–N(4)	2.722(7)	La (3)–N(3)	2.654(7)	La (4)–N(10)	2.584(6)
La (1)–N(2)	2.460(7)	La (2)–N(6)	2.578(7)	La (3)–N(11)	2.602(8)	La (4)–N(12)	2.571(7)
La (1)-N(3)	2.853(6)	La (2)-N(7)	2.484(7)	La (3)-N(15)	2.446(8)	La (4)-N(13)	2.488(6)
La (1)-N(4)	2.650(6)	La (2)-N(8)	2.508(7)	La (3)-N(16)	2.499(8)	La (4)-N(14)	2.500(7)
La (1)-N(5)	2.563(6)	La (2)-N(9)	2.606(6)	La (1)-N(17)	2.662(6)	La (4)-N(17)	2.714(6)
La(1)- N(18)	2.657(6)			La(1)- N(18)	2.826(7)		
Bond angles							
La(1)-F(2)-La(4)	103.80(14)			La(2)-F(2)-La(4)	129.39(15)		
La(3)-F(2)-La(4)	106.22(15)			La(2)-F(2)-La(3)	104.19(14)		
La(1)-F(2)-La(2)	106.82(15)			La(1)-F(2)-La(3)	104.03(13)		

Repeating the previous reaction with La resulted in the isolation of the compound **2.7** ($[La(Me_2pz)_5Hg_2(C_6F_5)_2(thf)]$) (Figure 2-8). Compound **2.7** was crystallised in the monoclinic space group $P2_1/c$ and the lanthanum centre is nine-coordinate having octahedral geometry if

the binding site is considered midway between the N-N bond of the pyrazolate. The lanthanum ion is ligated by one terminal η^2-pyrazolate ligand and μ-Me_2pz ligands and two bridging μ-η^2:η^2 pyrazolate ligands. The lanthanum atom is coplanar with two nitrogen atoms of the pyrazolate ligands. One pyrazolate and thf are arranged in a *cisoid* fashion.

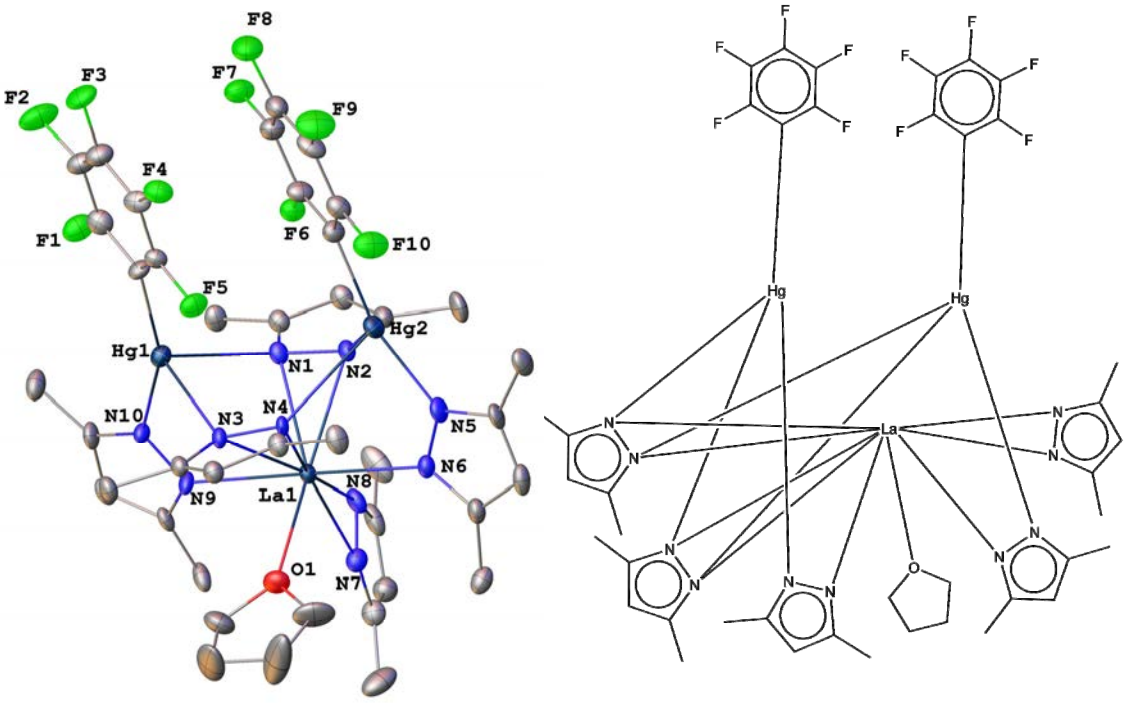

Figure 2-8. *Left:* molecular structure of $[La(Me_2pz)_5Hg_2(C_6F_5)_2(thf)]$ (**2.7**). Ellipsoids shown at 50% probability. Hydrogen atoms removed for clarity. *Right*: simplified diagram of **2.7**.

In the structure of $[Hg_2(Me_2pz)_5(C_6F_5)_2La]$ an open triangle of two mercury atoms and La (Hg…La…Hg : 52.76-74.26º) can be observed that is similar to the triangle of (Hg…Hg…Hg) in the reported $[Hg_3(iPr_2pz)_4(C_6F_5)]$.[39] However, the Hg…Hg is longer because the bond lengths in the triangle in the present case are affected by the inclusion of the larger La^{3+}. Each mercury is linked by three μ-η^1:η^1-3,5-dimethylpyrazolate ligands and terminal C_6F_5 groups. Even the larger Hg-N bonds are well within the sum of the van der Waals radii of mercury (1.9-2 Å,[40, 41] or 2.1-2.2 Å[42]) and nitrogen (1.60 Å[43]). The Hg-C distances [2.072(12) Å, 2.09(14) Å] (Table 2-8) are near the Hg-C bond lengths observed in the homoleptic organomercurial $Hg(C_6F_5)_2$ [Hg-C 2.047(6)-2.052(6) Å] and in the trinuclear $[(Hg(C_6F_4))_3.(C_6H_6)]$ (Hg-C 2.058(8) Å) compound.[44] Both the short and longer Hg-N

distances are close to the values for pseudo-polymeric mercurial pyrazolate (2.5 Å).[45]

Table 2-8. Selected bond lengths (Å) and angles (º) of **2.7**.

Bond lengths					
La(1)–O(1)	2.554(10)	La(1)-N(7)	2.446(12)	Hg(2)–C(2)	2.090(14)
La(1)–N(1)	2.623(11)	La(1)-N(8)	2.470(11)	Hg(2)–N(2)	2.510(10)
La(1)–N(2)	2.599(11)	La(1)-N(9)	2.689(10)	Hg(2)–N(4)	2.708(9)
La(1)–N(3)	2.641(10)	Hg(1)–N(1)	2.662(10)	Hg(2))–N(5)	2.096(12)
La(1)–N(4)	2.653(10)	Hg(1)–N(3)	2.465(10)	Hg(1)–C(1)	2.072(12)
La(1)-N(6)	2.662(11)	Hg(1)–N(10)	2.092(10)		
Bond angles					
N(10)-Hg(1)-N(3)	89.4(4)	N(5)-Hg(2)-N(4)	80.5(4)		
N(10)-Hg(1)-N(1)	81.7(4)	N(5)-Hg(2)-N(2)	89.3(4)		
N(3)-Hg(1)-N(1)	83.8(3)	N(2)-Hg(2)-N(4)	83.2(3)		
C(1)-Hg(1)-N(10)	155.9(5)	C(2)-Hg(2)-N(4)	111.4(5)		
C(1)-Hg(1)-N(3)	109.0(4)	C(2)-Hg(2)-N(5)	160.6(5)		
C(1)-Hg(1)-N(1)	114.9(5)	C(2)-Hg(2)-N(2)	106.9(5)		

Continuing the attempts to synthesise the smaller rare earth 3,5-dimethylpyrazolate complexes, compound $[Er_3F(Me_2pz)_8(thf)_2]$ (**2.8**) was isolated from an RTP reaction involving Er metal, $Hg(C_6F_5)_2$ and 3,5-dimethylpyrazolate, and again is the results of C-F activation (Figure 2-9). Complex **2.8** crystallised in the monoclinic space group $P2_1/c$. The structure of **2.8** is a trimer with the F atom sitting at the centre of the cage with trigonal planar geometry. The Er-F-Er angles are not equal which can be because of coordinated thf to the metal centres. Two erbium atoms (Er2 and Er3) contain one terminal η^2-pyrazolate ligand, and three μ-1κ(*N*):2κ(*N*′)-Me_2pz ligands. Also, the coordination environment of these two metal ions involves one oxygen atom from a tetrahydrofuran molecule. The Er1 ion reveals a coordination environment involving five nitrogen atoms with two η^2-pyrazolate ligands and three μ-1κ(*N*):2κ(*N*′)-Me_2pz ligands. The trimer structure with erbium has been seen previously in the aryloxide complex as $[Er_3(OAr^{OMe})_4(\mu_2\text{-}F)_3(\mu_3\text{-}F)_2(thf)_4].thf.0.5C_6H_{14}$ but the latter structure has five fluorines and the metal centres are one six coordinate Er and two seven coordinate Er.[25] The range of Er-F distances (2.276(4)-2.302(4) Å) (Table 2-9) is similar to

the previously reported Er-F in $[Er_3(OAr^{OMe})_4(\mu_2\text{-}F)_3(\mu_3\text{-}F)_2(thf)_4].thf.0.5C_6H_{14}$.

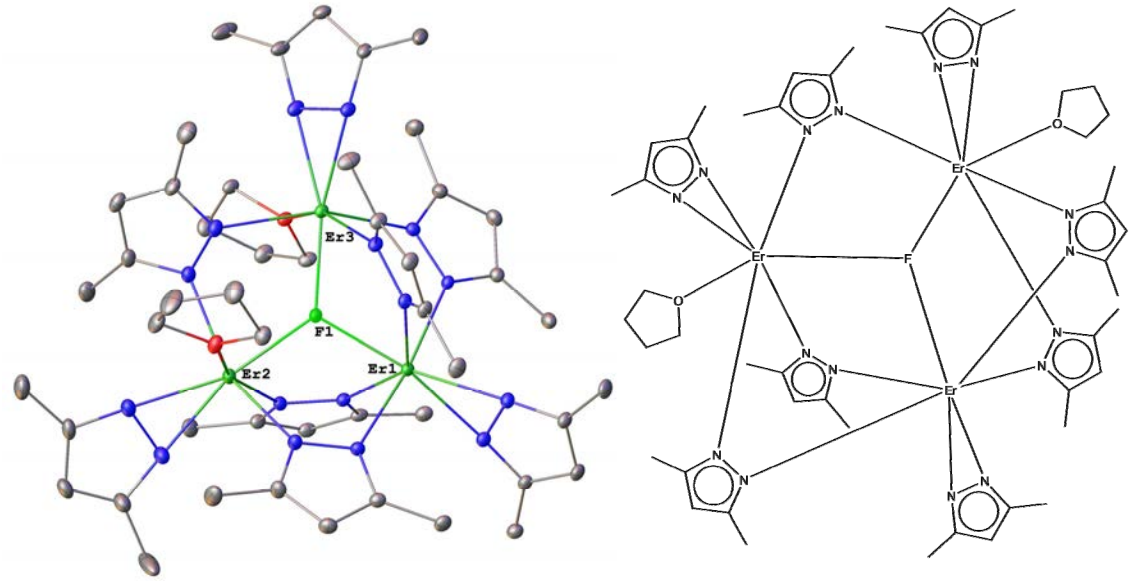

Figure 2-9. *Left:* molecular structure of $[Er_3F(Me_2pz)_8(thf)_2]$ (**2.8**). Ellipsoids shown at 50% probability, Hydrogen atoms removed for clarity. *Right*: simplified diagram of **2.8**.

Table 2-9. Selected bond length (Å) and bond angles (º) for complex **2.8**.

Bond lengths					
Er(1)–F(1)	2.302(4)	Er(2)–F(1)	2.287(4)	Er(3)–F(1)	2.276(4)
Er(1)–N(1)	2.307(6)	Er(2)–O(1)	2.382(6)	Er(3)–O(2)	2.368(5)
Er(1)–N(2)	2.311(7)	Er(2)–N(4)	2.385(7)	Er(3)–N(10)	2.420(7)
Er(1)–N(3)	2.419(6)	Er(2)–N(6)	2.360(7)	Er(3)–N(11)	2.307(7)
Er(1)–N(5)	2.385(6)	Er(2)–N(7)	2.281(8)	Er(3)–N(12)	2.315(6)
Er(1)-N(14)	2.397(6)	Er(2)-N(8)	2.307(7)	Er(3)-N(13)	2.372(6)
Er(1)-N(16)	2.440(6)	Er(2)-N(9)	2.412(7)	Er(3)-N(15)	2.394(6)
Bond angles					
Er(1)–F(1)-Er(2)	115.25(17)	N(1)-Er(1)-N(2)	35.110(2)		
Er(1)–F(1)-Er(3)	116.66(17)	N(11)-Er(3)-N(12)	35.1(2)		
Er(2)–F(1)-Er(3)	128.09(18)	N(7)-Er(2)-N(8)	34.08(3)		

The formation of [Y(η^2-Me$_2$pz)$_2$(μ-Me$_2$pz)$_2$(μ-thf)]$_2$ has been reported previously in which yttrium atoms contain two bridging thf donors (a very uncommon thf binding mode in non-alkaline metal chemistry).[20, 46] Compound **2.9** ([Na(dme)$_3$Y$_3$F(Me$_2$pz)$_9$].3/2DME) was synthesised as the result of using DME as a solvent in the reaction between Me$_2$pzH and yttrium using Hg(C$_6$F$_5$)$_2$ as the oxidant (Figure 2-10).

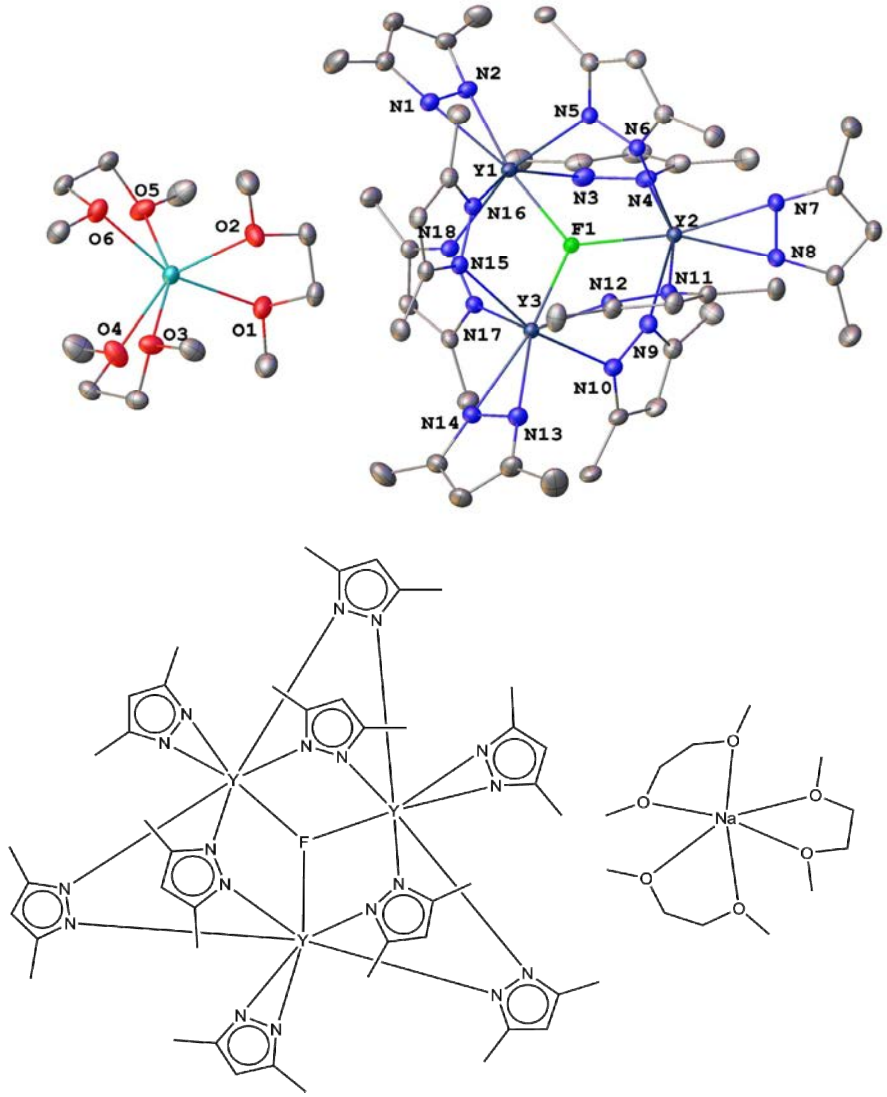

Figure 2-10. *Top:* molecular structure of [Na(dme)$_3$Y$_3$F(Me$_2$pz)$_9$].3/2DME (**2.9**). Ellipsoids shown at 50% probability. Hydrogen atoms removed for clarity. *Bottom*: simplified diagram of **2.9**.

Compound **2.9** crystallised in the triclinic space group $P\bar{1}$ and exhibits a solvent separated ion-pair in the unit cell with 1.5 DME molecules in the lattice. In the reaction in this

study no elemental sodium was used, so the only source of sodium can be the solvent that was kept over the sodium (to keep the solvent dry). Compound **2.9** can be considered a by-product due to the very low yield. Compound **2.9** is a trinuclear anion and the Y_3F forms trigonal planar geometry about the central fluorine atom. The Y-F-Y angles are approximately 120°, and each yttrium ion is coordinated by two nitrogen atoms of chelating 3,5-dimethylpyrazolate ligands and four nitrogens of the bridging 3,5-dimethylpyrazolate ligands. The average Y-N (chelating) distance is 2.333 Å, shorter than the average Y-N (bridging) distance of 2.464 Å. The coordination number of each yttrium in the compound **2.9** is seven. The bite angle is similar for all Y (34.5 Å) (Table 2-10).

Table 2-10. Selected bond lengths (Å) and angles (º) of **2.9**.

Bond lengths					
Y(1)–F(1)	2.24(19)	Y(2)–F(1)	2.249(16)	Y(3)–F(1)	2.239(18)
Y(1)–N(1)	2.332(3)	Y(2)–N(6)	2.468(2)	Y(3)–N(10)	2.424(2)
Y(1)–N(2)	2.309(3)	Y(2)–N(7)	2.339(2)	Y(3)–N(13)	2.324(3)
Y(1)–N(3)	2.464(2)	Y(2)–N(8)	2.310(2)	Y(3)–N(14)	2.327(2)
Y(1)–N(5)	2.393(2)	Y(2)–N(9)	2.453(3)	Y(3)–N(15)	2.418(2)
Y(1)-N(16)	2.477(2)	Y(2)-N(11)	2.406(2)	Y(3)-N(17)	2.465(2)
Y(1)-N(18)	2.409(2)	Y(2)-N(4)	2.401(2)	Y(3)-N(12)	2.440(2)

Bond angles			
Y(1)–F(1)-Y(2)	119.83(7)	N14-Y3-N13	34.57(3)
Y(1)–F(1)-Y(3)	119.82(7)	N1-Y1-N2	34.81(2)
Y(2)–F(1)-Y(3)	120.34(7)	N7-Y2-N8	34.53(3)

2.2.2 Synthesis and structural characterisation of 3,5-di-tert-butylpyrazolate complexes

2.2.2.1 Synthesis and characterisation

Previously, despite the ease of preparation, di-*tert* -butylpyrazole (*t*Bu_2pzH), was not a popular ligand for performing reactions, with only limited reports in the literature. However, the reaction between Na(*t*Bu_2pz) and a nickel(I) salt, which was the first usage of *t*Bu_2pz as a ligand, resulted in the formation of $[Ni(NO)(tBu_2pz)]_2$.[47] A variety of bimetallic rare earth/group one pyrazolate complexes have been reported with the bulky

3,5-di-*tert*-butylpyrazolate (*t*Bu$_2$pz) ligand.[48] Moreover, using a bulky ligand like *t*Bu$_2$pzH has enabled the formation of homoleptic divalent and trivalent mononuclear and dinuclear rare earth metal-organic compounds.[6, 49-52].

A range of complexes using the bulky 3,5-di-*tert*-butylpyrazole (*t*Bu$_2$pzH) ligand and rare earth elements (La, Ce, Sm, Er and Lu) were prepared by redox transmetallation/protolysis (Equation 2-6).

$$2Ln + 3Hg(C_6F_5)_2 + 6\ t\text{Bu}_2\text{pzH} + L \longrightarrow 2Ln(t\text{Bu}_2\text{pz})_3L_2 + 3Hg\downarrow + 6C_6F_5H$$

L = THF, DME

Equation 2-6

The synthesis involves oxidation of the lanthanoid metal by bispentafluorophenyl mercury and protic ligand exchange between the resulting pentafluorophenyl lanthanoid species and 3,5-di-*tert*-butylpyrazole. Although the structures resulting from the middle steps were observed using Me$_2$pzH in the previous section in this study, no intermediate complexes were observed using *t*Bu$_2$pzH and the reactions essentially went as planned. The reaction in Equation 2-6 is presumed to involve redox transmetallation and then ligand exchange, and while the mechanism could follow Equation 2-7 or Equation 2-8 calculations towards the complicated mechanism for this process have been reported.[53]

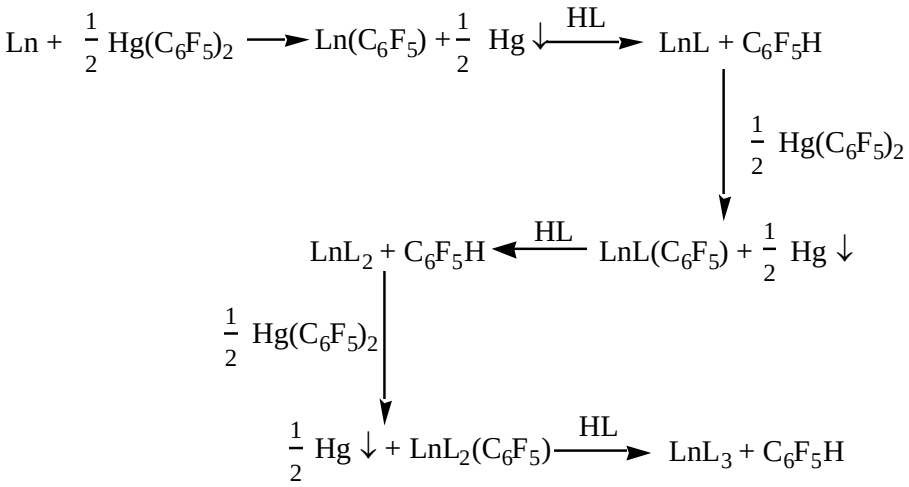

Equation 2-7

Equation 2-8. $2\ Ln + 3\ Hg(C_6F_5)_2 \rightarrow 2\ "Ln(C_6F_5)_3" + 3\ Hg\downarrow \xrightarrow{6HL} 2\ LnL_3 + 6\ C_6F_5H$

The presence of a protic ligand is important for trapping the intermediate species. Ligand exchange (Equation 2-9) will generally occur if the ligand HL is more acidic than C_6F_5H (pK_a = 25.6 in THF)[28] and the reported pK_a for *t*Bu_2pzH is 15.3[54], which is in the correct range for exchange.

Equation 2-9. $\text{"Ln}(C_6F_5)_3\text{"} + 3\ HL \rightarrow LnL_3 + 3\ C_6F_5H$

Since previously monomeric [Nd(*t*Bu_2pz)$_3$(thf)][52] and [Eu(*t*Bu_2pz)$_2$(dme)$_2$][51] had been reported, Sc was chosen for this study since not many RTP reactions have been performed using this metal. Also, Y as Y^{3+} ion, which is diamagnetic, was used in order to facilitate NMR characterisation. Since isolating products out of the selected metals was not successful, attempts were continued to isolate products using other rare earth elements. The structures were established by X-ray crystal structure, ^{1}H NMR spectroscopy, IR spectroscopy and microanalysis. The ^{1}H NMR spectra for three similar compounds [Ln(*t*Bu_2pz)$_3$(thf)$_2$] (Ln = La (**2.10a**), Ce (**2.10b**), Lu (**2.10c**)), confirms the result of X-ray crystal structures. The *t*Bu group resonance occurred at 1.27 ppm and the H4 resonance occurred at 6.34 ppm. The absence of the coordinated thf can be due to its loss during isolation in *vacuo*. The elemental analysis result of **2.10a**, **2.10b** and **2.10c** showed the loss of two thf molecules, which confirmed the loss in *vacuo.* No satisfactory NMR could be obtained for complex **2.11** ([Sm_2(*t*Bu_2pz)$_6$dme$_2$]$_n$) and **2.12** ([Er(*t*Bu_2pz)$_3$dme]) due to paramagnetism. Also a low percentage of carbon was observed along with a low percentage of H for the microanalysis result for complex **2.12,** which can be the result of formation of metal carbides due to the incomplete combustion.

Infrared spectroscopy is a useful initial form of analysis for *t*Bu_2pz complexes due to a very strong ν (NH) absorption at 3229 cm^{-1}, which shows the presence of *t*Bu_2pzH. Therefore, it can be considered a good method for detecting any decomposition or impurities in the products but also to confirm complete deprotonation of the pyrazole.[55] Also, the coordinated solvents can give characteristic spectra. Medium ν (COC) absorptions in the range of 872-876 and 1015-1030 cm^{-1} show the coordinated thf in Ln(*t*Bu_2pz)$_3$(thf)$_2$] complexes, which are lowered from the free ligand values of 912 cm^{-1} for the symmetric and 1070 cm^{-1} for the asymmetric stretch[56, 57] as expected on coordination.[56] A ν(CO) of coordinated dme is seen as a medium absorption between 1018 and 1064 cm^{-1} in the infrared spectrum of [Er(*t*Bu_2pz)$_3$(dme)], and it is lower than the free ligand value of 1105 cm^{-1}.[55]

2.2.2.2 X-ray structure determinations

By performing the RTP reaction in THF, a series of new monomeric lanthanoid complexes ([Ln(*t*Bu$_2$pz)$_3$(thf)$_2$] (Ln = La (**2.10a**), Ce (**2.10b**), Lu (**2.10c**))) with the bulky *t*Bu$_2$pzH ligand has been isolated (Figure 2-11).

Complex **2.10a** is the first structurally characterised complex of monomeric lanthanum resulting from an RTP reaction using the bulky *t*Bu$_2$pzH ligand. Although isolation of [La(*t*Bu$_2$pz)$_3$(thf)] has been confirmed previously using mass spectrometry and IR [52], the crystal structure has not been reported.

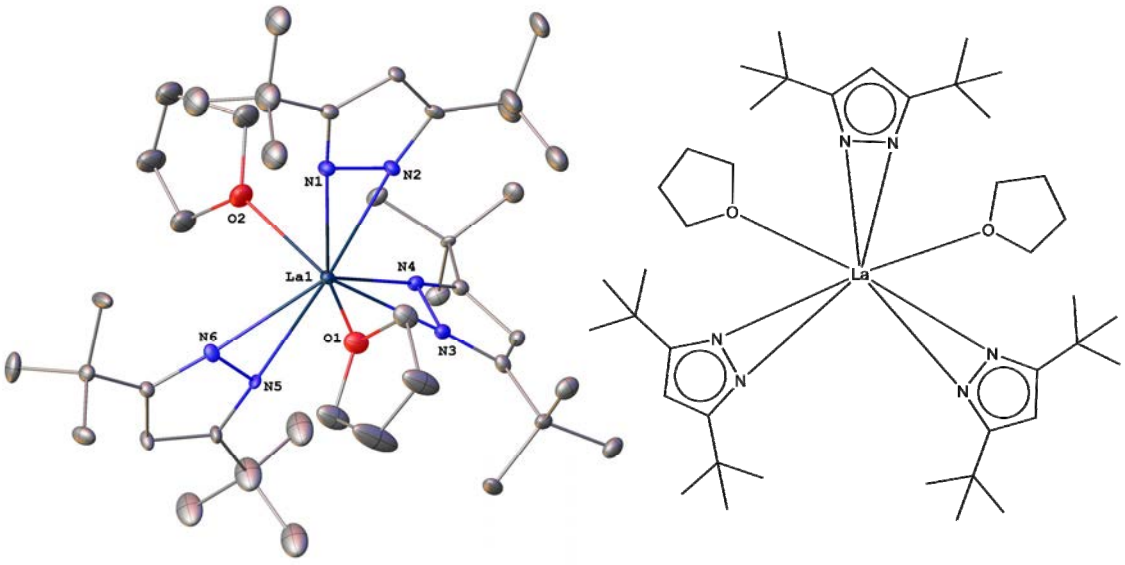

Figure 2-11. *Left:* Molecular structure of [La(*t*Bu$_2$pz)$_3$(thf)$_2$] (**2.10a**). Ellipsoids shown at 50% probability. Hydrogen atoms removed for clarity. Cen 1, Cen 2, and Cen 3 represent the centres of the bonds N1-N2, N3-N4 and N5-N6, respectively). *Right:* simplified diagram of **2.10a**.

While the La^{3+} ion is larger than Nd^{3+}, compound **2.10a** is isostructural with the previously isolated [Nd(*t*Bu$_2$pz)$_3$(thf)] complex, with the central lanthanum atom coordinated by three η^2-(*t*Bu$_2$pz) ligands and two thf ligands that gives eight coordination. To have a clear picture of the molecular geometry of the central La, as was done for the Nd compound,[52] it is easier to consider the mid points of the N-N bonds and oxygen atoms of the thf as the sites of connectivity. Since Cen 1, Cen 2, Cen 3, and La are coplanar, the molecular geometry is an intermediate between a trigonal bipyramid with O1 and O2 apical, and Cen 1, Cen 2, and Cen 3 in the equatorial positions and square pyramidal with Cen 3 apical, and transoid Cen 1, Cen 2, and O1, O2 relationships in the square plane. The La-O1 and La-O2 bond lengths are

2.542(4) Å and 2.545(7) Å respectively and the La-N bond lengths are in the range of 2.468-2.519 Å (Table 2-12). Complex **2.10a** crystallised in the monoclinic space group $P2_1$ and exhibited one molecule in the unit cell. Using the smaller cerium metal resulted in the monomeric [Ce(*t*Bu$_2$pz)$_3$(thf)$_2$] (**2.10b**) compound with the same space group and coordination number as in **2.10a** (Table 2-11). A similar structure to **2.10b** has been reported previously using DFForm (N,N´–bis(2,6-difluorophenyl)formamidine) as a ligand ([Ce(DFForm)$_3$(thf)).[58] The Ce atom in both compounds has a coordination number of eight and the thf ligands have a *transoid* disposition (Figure 2-12).

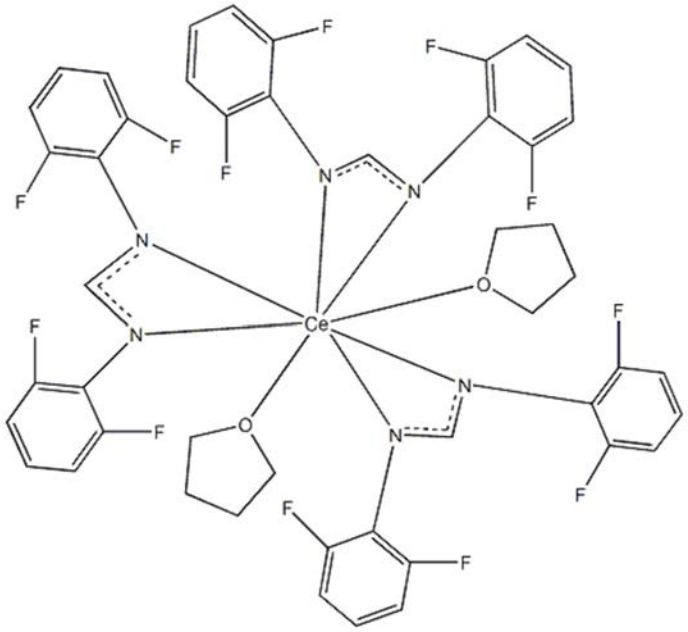

Figure 2-12. Molecular structure of [Ce(DFForm)$_3$(thf)].[58]

The Ce-O1 and Ce-O2 bond lengths are 2.518(6) Å and 2.535(9) Å respectively in complex **2.10b**, which are similar to the Ce-O in the [Ce(DFForm)$_3$(thf)] (2.51-2.50 Å). The Ce-N bond lengths are in the range of 2.508-2.602 Å in the [Ce(DFForm)$_3$(thf)] while the Ce-N in complex **2.10b** is in the range of 2.423-2.537 Å, which is smaller than the reported structure. This difference is due to the bulkier DFForm ligand compared with the *t*Bu$_2$pzH ligand. Also, Lu, which has the smallest ionic radius among the lanthanoids, shows a similar structure ([Lu(*t*Bu$_2$pz)$_3$(thf)] **2.10c**) but crystallised in a different unit cell (Table 2-11) and exhibits four molecules in the asymmetric unit.

Table 2-12 summarises the bond lengths of the obtained complexes, where it can be shown that the difference in Ln-N bond lengths between the metals is within the expected values for the difference of ionic radii/coordination number (La^{3+} = 1.16 Å, Ce^{3+} = 1.143 Å,

Lu^{3+} = 0.977 Å).[32] Subtraction of an ionic radius[32] of an eight-coordinate La^{3+} ion from the La-O distance gives 1.37Å. This difference corresponds closely to the difference (1.34 Å) derived from Ln-O(thf) distances of organolanthanoid-THF complexes with coordination numbers 7-10.[59] However, it contrasts to the differences for THF complexes of bulky lanthanoid aryloxides (1.49-1.59 Å).[60]

Table 2-11. Crystallographic data for compounds **2.10a**, **2.10b**, **2.10c** and [Nd(*t*Bu$_2$pz)$_3$(thf)].

Compound	**2.10a**	**2.10b**	**2.10c**	**[Nd(tBu$_2$pz)$_3$(thf)]**
Formula	$C_{41}H_{73}LaN_6O_2$	$C_{41}H_{73}CeN_6O_2$	$C_{41}H_{73}LuN_6O_2$	$C_{41}H_{73}NdN_6O_2$
Formula Weight	818.94	812.53	858.05	826.3
T/K	100(2)	100(2)	100(2)	165
Crystal System	monoclinic	monoclinic	monoclinic	monoclinic
Space Group	*P2$_1$*	*P2$_1$*	*P2$_1$*	*P2$_1$*
a/Å	9.778(2)	9.950(2)	11.614(2)	9.760(1)
b/Å	19.417(4)	19.874(4)	19.609(4)	19.727(3)
c/Å	11.881(2)	11.999(2)	38.915(8)	11.796(2)
α/°	90	90	90	90
β/°	96.98(3)	97.32(3)	97.48(3)	98.76(1)
γ/°	90	90	90	90
V/Å^3	2239.0(8)	2353.6(8)	8787(3)	2244.7(5)
Z	2	2	8	2
Z'	1	1	4	1
R_{int}	0.0432	0.0583	0.0470	N/A
GooF	1.085	1.011	1.0061	N/A
wR_2 (all data)	0.1274	0.1237	0.1614	N/A
wR_2	0.1271	0.1114	0.1391	N/A
R_1 (all data)	0.0490	0.0639	0.0793	N/A
R_1	0.0487	0.0457	0.0511	0.0398

Table 2-12. Selected bond lengths (Å) for complexes [Ln(*t*Bu$_2$pz)$_3$(thf)] (Ln = La(**2.10a**), Ce(**2.10b**), Lu(**2.10c**).

Bond	2.10a	2.10b	2.10c
Ln1-N1	2.542(7)	2.423(12)	2.281(7)
Ln1-N2	2.468(6)	2.437(13)	2.306(8)
Ln1-N3	2.481(7)	2.425(8)	2.316(6)
Ln1-N4	2.477(6)	2.458(8)	2.313(10)
Ln1-N5	2.480(7)	2.464(10)	2.304(7)
Ln1-N6	2.519(8)	2.454(9)	2.294(8)
Ln1-O1	2.542(6)	2.535(6)	2.302(7)
Ln1-O2	2.545(6)	2.518(9)	2.373(6)
Ionic radii Å (CN)	1.160 (8)	1.143 (8)	0.977 (8)

The use of samarium in place of lanthanum in THF and crystallisation of the product from DME (no suitable crystal formed in THF) led to the isolation of [Sm$_2$(*t*Bu$_2$pz)$_6$(dme)$_2$]$_n$ (**2.11**) (Figure 2-13) that indicates formation of the polymeric complex. Compound **2.11** is similar to two polymeric structures of neodymium complexes that were reported as [Nd(*t*Bu$_2$pz)$_3$(μ-dme)]$_n$[61] and [Nd$_2$(OCH-*i*Pr)$_6$(μ-dme)]$_n$[30] (Figure 2-14). Complex **2.11** crystallised in the triclinic space group $P\bar{1}$ as a 1-D polymer with the whole molecule within the asymmetric unit. The structure indicates a framework, where each *t*Bu$_2$pz ligand coordinates to the central Sm ion in a η^2-coordination mode and successive Sm(*t*Bu$_2$pz) units are bridged by dme in an *anti*-configuration so each samarium atom is eight-coordinate. Although the arrangement of oxygen atoms and centroids (Cn) of pyrazolate N-N bonds around each samarium atom is closest to a square based pyramid[62], the molecular geometry is best described as an intermediate between a trigonal bipyramid and square-based pyramid, considering the centre of pyrazolate N-N bond as the point of attachment to the metal. Complex **2.11** was prepared by a RTP reaction in THF but was crystallised from DME therefore the dme molecule is coordinated with the samarium. The Cn-Ln-Cn angles show a similar variation to those in [Ln(*t*Bu$_2$pz)$_3$(Solv.)$_2$] (Ln=Nd, Er or La and Solv. = THF or DME)[52, 63] (Table 2-13). Comparing the Cn-Ln-Cn angles shows that the Ln(*t*Bu$_2$pz)$_3$ obviously remained the same in

all reported compounds and the coordinated solvents (THF or DME) did not affect the Cn-Ln-Cn angles.

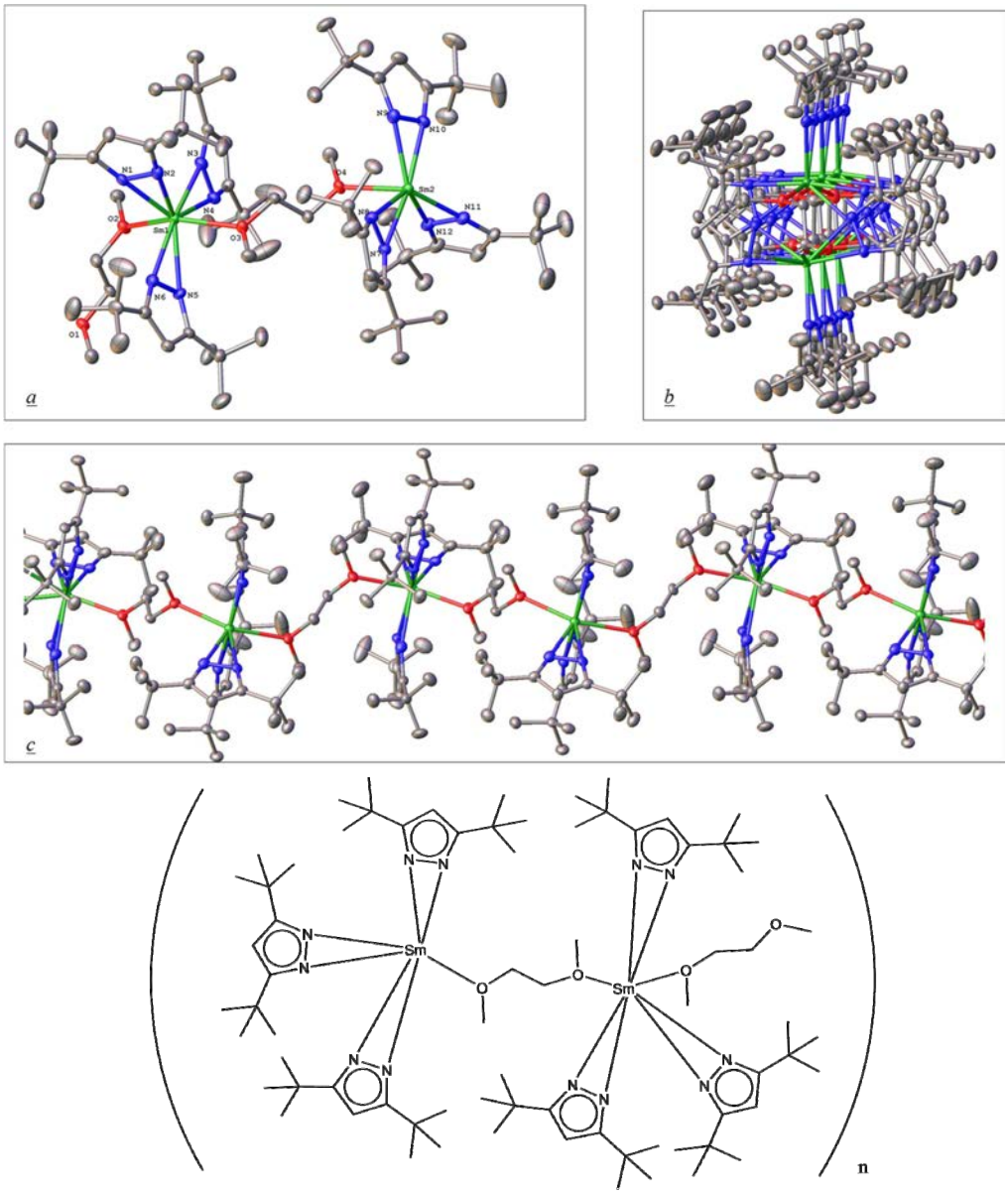

Figure 2-13. *Top:* Molecular structure of $[Sm_2(tBu_2pz)_6(dme)_2]_n$ (**2.11**) showing (a): the asymmetric unit, (b) down the axis of the polymer, (c) along the side of the polymer. Ellipsoids down at 50% probability. Hydrogen atoms were removed for clarity. *Bottom:* simplified diagram of **2.11**.

The O-Sm-O angle is 153.55(9)º compared with 148.27º and 145.2º for $[Ln(tBu_2pz)_3(thf)_2]$ (Ln = La and Nd[52] respectively). In the present structure, similar to that

previously reported $[Nd(tBu_2Pz)_3(\mu\text{-dme})]_n$, monomeric $Sm(tBu_2pz)_3$ units are bridged by dme whereas in the reported $[Nd_2(OCH\text{-}iPr)_6(\mu\text{-dme})]_n$[30] with bridging dme, dimeric $Nd_2(OCH\text{-}iPr)_6$ units are bridged by dme in an infinite linear polymer (Figure 2-14).

Table 2-13. Comparison of the arrangement of the $Ln(tBu_2pz)_3$ unit in different complexes

	$Nd(tBu_2pz)_3(thf)_2$	**$Er(tBu_2pz)_3(thf)_2$**	**$Nd(tBu_2pz)_3(dme)_2$**	**$La(tBu_2pz)_3(thf)_2$**	**$Sm(tBu_2pz)_3(dme)_2$**
Cn-Ln-Cn[°]	140.1	140.3	139.3	144.7	137.6
	110.3	110.6	110.9	108.1	112
	109.6	109.2	109.9	107.2	110.3

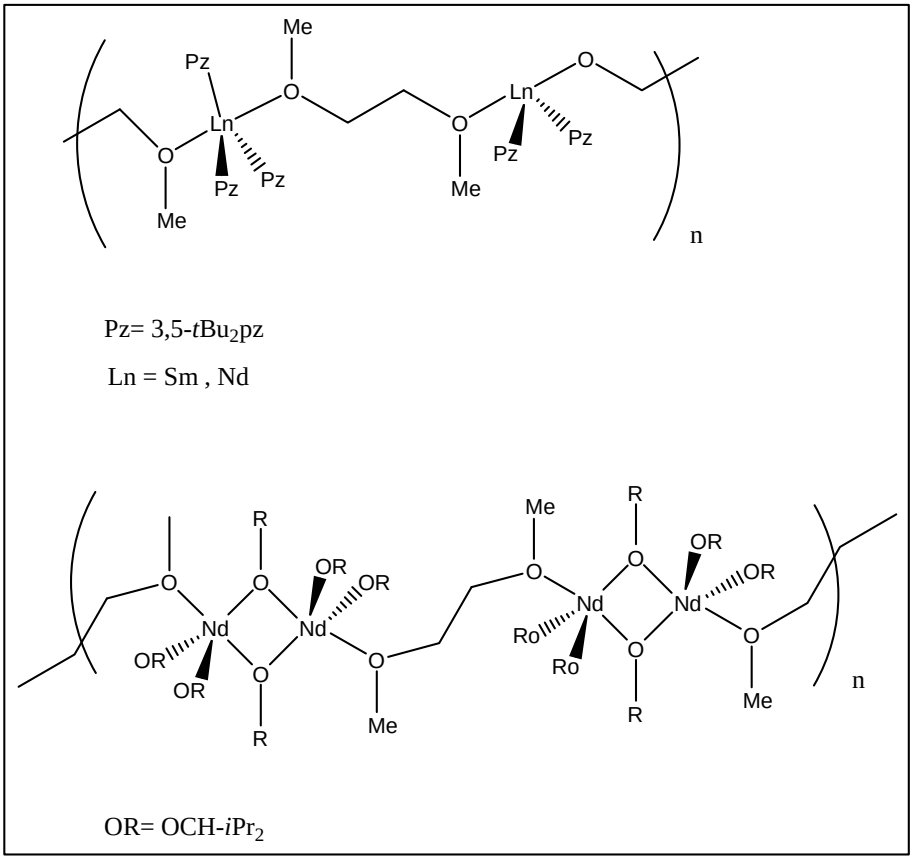

Figure 2-14. Polymeric structures of $[Ln(tBu_2Pz)_3(\mu\text{-dme})]_n$ (Sm , Nd[61])(*top*) and $[Nd_2(OCH\text{-}iPr)_6(\mu\text{-dme})]_n$ [64](*bottom*).

Subtraction of ionic radius[32] of eight-coordinate Sm^{3+} from the average Sm-N distance (Table 2-14) gives a value of 1.33 Å which is similar to $[Nd(tBu_2Pz)_3(\mu\text{-dme})]_n$ (1.32 Å)[61] and equal to those found for eight-coordinate $[Ln(tBu_2pz)_3(thf)_2]$ (1.33 for Ln = Nd or Er)[52, 63] and close to that (1.32 Å) for eight-coordinate $[Sm(Ph_2pz)_2(dme)_2]$[51] and nine-coordinate $[Sm(Ph_2pz)_3(thf)_3]$.3THF (1.30 Å).[65] Subtraction of the ionic radius[32] of eight-coordinate Sm^{3+} from the average Sm-O distance gives 1.43 Å. This value is equal to the one in the previously reported $[Nd(tBu_2Pz)_3(\mu\text{-dme})]_n$ and greater than those found for $[Ln(tBu_2pz)_3(thf)_2]$ (1.35 Å for Ln = Nd or Er)[52, 63] and $[Cp_2Yb(dme)]$ and $[Sm(Ph_2pz)_2(dme)_2]$ (1.33 Å and 1.24 Å respectively where dme is chelating)[51, 66]. This result shows the difference between a chelating ligand and a bridging ligand.

Table 2-14. Selected bond lengths (Å) and angles (º) of **2.11**.

Bond lengths			
Sm(1)–N(1)	2.398(4)	Sm(1)–N(5)	2.451(4)
Sm(1)–N(2)	2.396(5)	Sm(1)–N(6)	2.383(5)
Sm(1)–N(3)	2.397(4)	Sm(1)–O(2)	2.516(4)
Eu(1)–N(4)	2.453(4)	Sm(1)–O(3)	2.512(4)
Sm…..Sm	7.892		
Bond angles			
O(2)-Sm-O(3)	153.577	Cn(2)-Sm-O(2)	82.131
Cn(1)-Sm-Cn(2)	110.391	Cn(3)-Sm-O(2)	89.579
Cn(1)-Sm-Cn(3)	34.112	Cn(1)-Sm-O(3)	104.466
Cn(2)-Sm-Cn(3)	137.529	Cn(2)-Sm-O(3)	85.132
Cn(1)-Sm-O(2)	101.677	Cn(3)-Sm-O(3)	84.311

Following the reactions using tBu_2pzH, an attempt was made to investigate the product of the RTP reaction using erbium in DME solvent. Previously $[Er(tBu_2pz)_3(thf)_2]$ has been reported using THF as solvent.[63] By changing the solvent to DME, $[Er(tBu_2pz)_3(dme)]$ (**2.12**) was synthesised (Figure 2-15). The compound **2.12** is an eight-coordinate monomer with one dme and three η^2-(tBu_2pz) ligands that was crystallised in the triclinic space group $P\bar{1}$ with the whole molecule occupying the asymmetric unit. The arrangement of the centres (Cen) of the pyrazolate N-N bonds and the dme oxygen atoms about Er is intermediate between a square pyramid and a trigonal bipyramid.

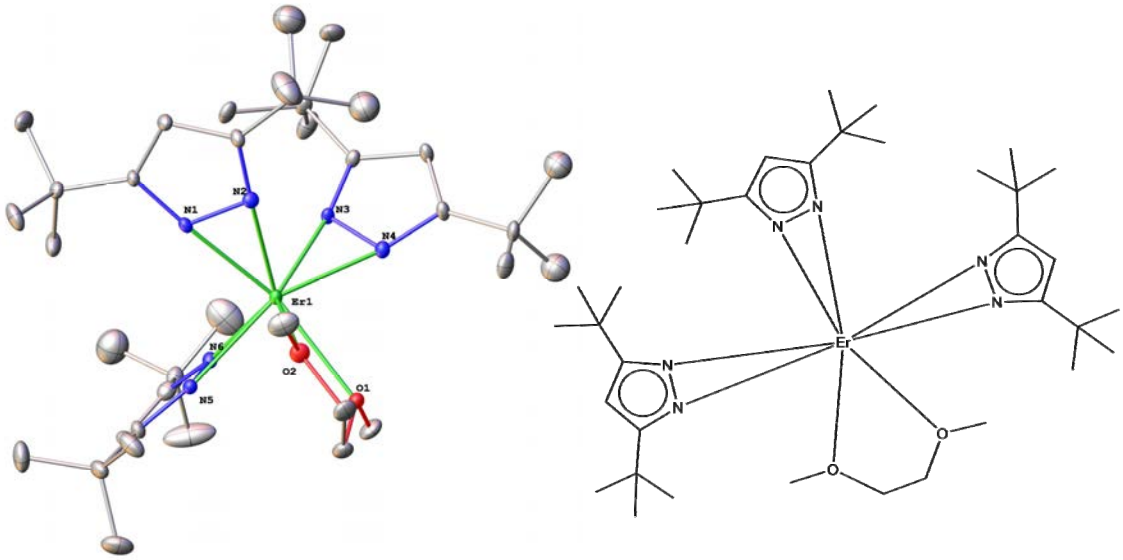

Figure 2-15. *Left:* Molecular structure of [Er(*t*Bu$_2$pz)$_3$(dme)] (**2.12**). Ellipsoids shown at 50% probability. Hydrogen atoms were removed for clarity. *Right:* simplified diagram of **2.12**.

Although Cen(1), Cen(2), Cen(3) and Er are near coplanar and $\sum Cen - Er - Cn$ angles = 360º as expected for a trigonal bipyramid, notable differences in the Cen-Er-Cen can be seen (Table 2-15) and the apical O-Er-O angle is 64.2º. If the structure is viewed as a square pyramid with Cen (3) apical and Cen(1), Cen(2), O (1) and O(2) in the square plane, both *trans* angles, O(1)-Er-O(2) and Cen(1)-Er-Cen(2), are well below 180º.

The listed distances and bond angles (Table 2-15) are similar to [Eu(tBu$_2$pz)$_3$(dme)$_2$], [Er(tBu$_2$pz)$_3$(thf)$_2$] and [Nd(tBu$_2$pz)$_3$(thf)$_2$]. There are differences between corresponding Er-X and Nd-X distances as the result of different ionic radii of eight-coordinate Er^{3+} (1.004Å)[32] and Nd^{3+} (1.109 Å).[32] Also, the differences between eight-coordinate Eu^{3+} (1.066 Å)[32] and Er^{3+} cause differences between Er-X and Eu-X distances.

Table 2-15. Selected bond lengths (Å) and angles (°) of **2.12**.

Bond lengths			
Er(1)–N(1)	2.23(3)	Er(1)–N(5)	2.291(10)
Er(1)–N(2)	2.355(10)	Er(1)–N(6)	2.328(10)
Er(1)–N(3)	2.316(9)	Er(1)–O(1)	2.460(10)
Er(1)–N(4)	2.297(11)	Er(1)–O(2)	2.424(9)
Bond angles			
O(1)-Er-O(2)	64.2(4)	Cn(1)-Er-O(2)	89.89(5)
Cn(1)-Er-Cn(2)	107.878(6)	Cn(2)-Er-O(1)	92.218(6)
Cn(1)-Er-Cn(3)	111.89(5)	Cn(2)-Er-O(2)	124.03(5)
Cn(2)-Er-Cn(3)	135.42(4)	Cn(3)-Er-O(1)	81.33(6)
Cn(1)-Er-O(1)	153.07(19)	Cn(3)-Er-O(2)	101.423(6)

2.2.3 Isolation of 3,5-diphenylpyrazolate complexes

Previous syntheses and structural investigations of some lanthanoid complexes with the bulky 3,5-diphenylpyrazole (Ph_2pzH) ligand have been reported (Equation 2-10).[61, 67]

$$2Ln + 3Hg(C_6F_5)_2 + 6Ph_2pzH \xrightarrow{Solv.} 2[Ln(Ph_2pz)_3(Solv.)n] + 3Hg + 6C_6F_5H$$

Equation 2-10

Since bonding between lanthanoid ions and ligands is highly affected by the large size of these ions, structurally irregular complexes can be isolated due to the steric saturation.[68] Attempts at isolating crystalline products using lanthanum, praseodymium, gadolinium, holmium and lutetium failed due to the formation of a microcrystalline powder upon attempted crystallisation. With the challenge to structurally characterise the mentioned rare-earth 3,5-diphenylpyrazolate complexes, the targeted complexes could not be formed due to the formation of lanthanoid dibenzoylmethanoate complexes. Previously the lanthanoid dibenzylmethanoates ($HNEt_3[Ln(dbm)_4]$) (Ln= La, Nd, Sm, Eu, Tb, Dy, Ho, Er, Tm and Yb) were prepared by stirring the respective oxides in hydrochloric acid followed by refluxing that resulted in the isolation of eight coordinate anions.[69]

3,5-diphenylpyrazole (Ph_2pzH) was prepared by stirring dibenzoylmethane ($(C_6H_5CO)_2CH_2$) and hydrazine hydrate ($NH_2NH_2.H_2O$), with the ratio of 1:1, in ethanol following by refluxing over 3 hours.[70] Due to the presence of dbmH (dibenzoylmethane) as contamination in the starting materials when Ph_2pzH does not form completely during treating dbmH with hydrazine, the eight-coordinate $[Lu(dbm)_3(dme)]$ (**2.13**) (Figure 2-16) was crystallised as the result of usage of the prepared ligand according to the Equation 2-10. Complex **2.13** crystallised in the monoclinic space group $P2_1/c$ with almost similar crystal system to the previously isolated ($HNEt_3[Ln(dbm)_4]$) but with different unit cell data. Selected bond distances and angles are given in Table 2-16. All three dbm^- ligands bind in a bidentate mode. The coordination geometry around the central ion is best described as a distorted square antiprism. The Lu-O bond lengths range from 2.226 Å to 2.510 Å, which can be considered normal for these types of bonds.[71] The decrease in the average bond lengths upon going from the reported lanthanum, neodymium and samarium and isolated lutetium are a result of lanthanoid contraction.

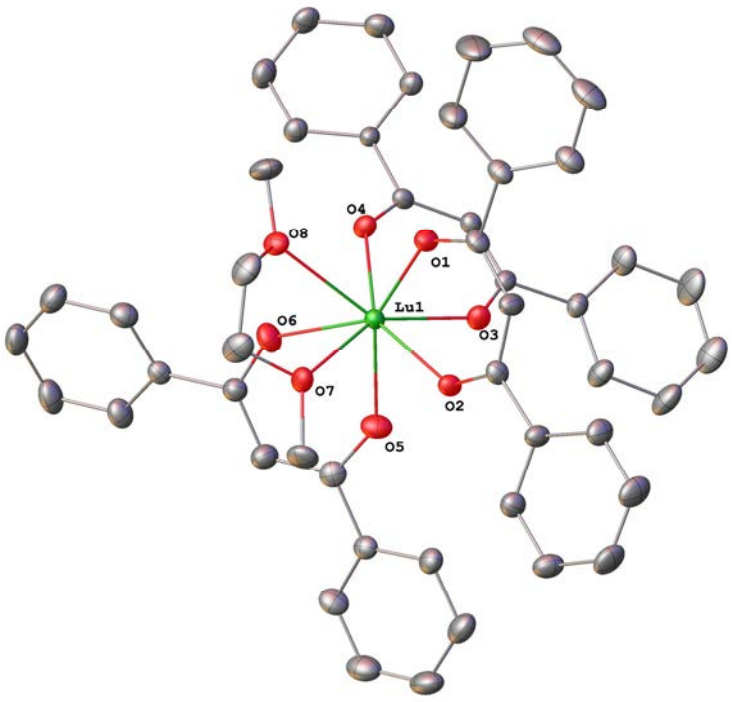

Figure 2-16. Thermal ellipsoid plot of $[Lu(dbm)_3(dme)]$ (**2.13**). Ellipsoids shown at 50% probability, Hydrogen atoms omitted for clarity.

Table 2-16. Selected bond lengths (Å) and angles (°) of **2.13**.

Bond lengths			
Lu(1)–O(1)	2.226(5)	Lu(1)–O(5)	2.241(6)
Lu(1)–O(2)	2.274(4)	Lu(1)–O(6)	2.293(5)
Lu(1)–O(3)	2.260(6)	Lu(1)–O(7)	2.450(5)
Lu(1)–O(4)	2.249(5)	Lu(1)–O(8)	2.510(6)
Bond angles			
O(1)-Lu-O(2)	75.02(18)	O(5)-Lu-O(6)	69.8(2)
O(3)-Lu-O(4)	74.07(19)	O(7)-Lu-O(8)	65.21(18)

Table 2-17. Crystallographic data for compounds $HNEt_3[Ln(dbm)_4]$ (Ln= La,Nd and Sm) and $[Lu(dbm)_3(dme)]$(**2.13**).

Compound	$HNEt_3[La(dbm)_4]$	$HNEt_3[Nd(dbm)_4]$	$HNEt_3[Sm(dbm)_4]$	$[Lu(dbm)_3(dme)]$(**2.13**)
Formula	$C_{66}H_{60}LaNO_8$	$C_{66}H_{60}NNdO_8$	$C_{66}H_{60}NO_8Sm$	$C_{49}H_{43}LuO_8$
Crystal System	monoclinic	monoclinic	monoclinic	monoclinic
Space Group	$P2_1/c$	$P2_1/c$	$P2_1/c$	$P2_1/c$
a/Å	19.044(3)	19.164(15)	23.3(2)	12.4917(14)
b/Å	22.287(2)	22.301(16)	9.023(7)	23.733(3)
c/Å	28.086(4)	27.855(2)	27.473(2)	14.6353(17)
β/°	109.6946(15)	110.0750(9)	112.563(11)	105.431(6)
V/Å^3	11,225.2(3)	11,171.15(14)	5792.00(8)	4182.5(8)
Z	8	8	4	4
R_1	0.0358	0.0301	0.0343	0.0590

Using the same prepared Ph_2pzH and scandium in a RTP reaction (Equation 2-10) resulted in the isolation of six-coordinate $[Sc(dbm)_3]$ (**2.14)** (Figure 2-17). As mentioned, due to the presence of dbmH as contamination in the starting materials, dbm coordinated to the metal centre.

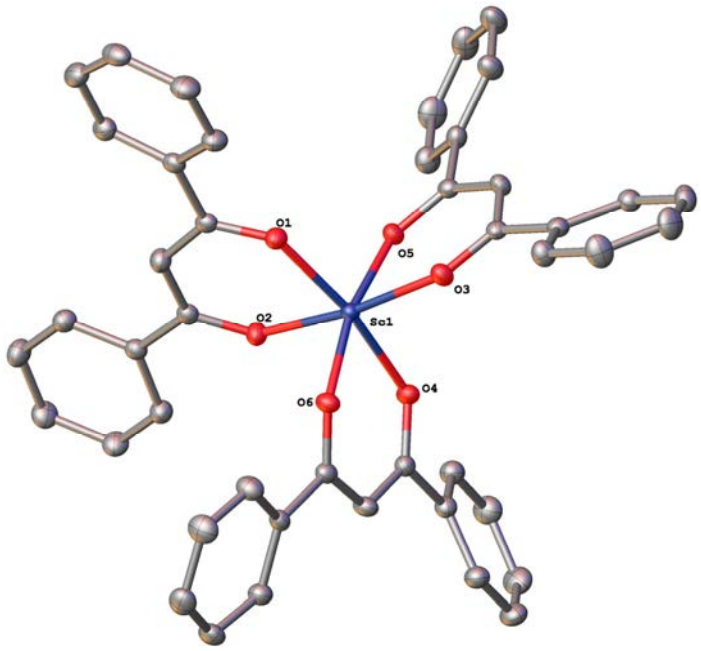

Figure 2-17. Thermal ellipsoid plot of [Sc(dbm)$_3$] (**2.14**). Ellipsoids shown at 50% probability, Hydrogen atoms omitted for clarity.

Compound **2.14** (Figure 2-17) crystallised in the triclinic space group and resembles the previously reported tris(dibenzoylmethanato-O,O')-scandium by E.G. Zaitseva *et.al.*[72]

The Sc-O bond lengths in compound **2.14** range from 2.065 Å to 2.097 Å (Table 2-18). It can be considered normal for this type of bond but are smaller than Lu-O in [Lu(dbm)$_3$] which is reasonable according to the difference between the ionic radii of Sc^{3+} and Lu^{3+} [32] (0.23 Å).

Table 2-18. Selected bond lengths (Å) and angles (º) of **2.14**

Bond lengths			
Sc(1)–O(1)	2.065(12)	Sc(1)–O(4)	2.0915(12)
Sc(1)–O(2)	2.046(12)	Sc(1)–O(5)	2.0974(13)
Sc(1)–O(3)	2.082(12)	Sc(1)–O(6)	2.0870(13)
Bond angles			
O(1)-Sc-O(2)	81.83(5)	O(4)-Sc-O(6)	81.71(5)
O(3)-Sc-O(5)	81.57(5)		

The attempted reaction of Ho metal with 3,5-diphenylpyrazole in THF at room temperature for one week failed to produce single crystals suitable for X-ray determinations. Therefore, the pale pink solution was dried under vacuum and ^{1}H NMR spectrum and IR was carried out on the resulting pale pink powder. The ^{1}H NMR spectrum showed major broadening of the baseline and the signals suggesting the presence of a paramagnetic species. Ph_2pzH does not have a distinct ν (NH) absorption, unlike other pyrazoles.[73] Therefore, IR spectra cannot be useful in establishing deprotonation and coordination of the Ph_2pz^- ion. Moreover, comparing the IR of the isolated product shows that it is not similar to the previously isolated compounds so perhaps a different structural arrangement was present in the complex involving Ho. This will have to be investigated in future work.[67, 74, 75]

2.2.4 Concluding remarks

Performing the RTP reaction using 3,5-dimethylpyrazole and terbium resulted in the easy crystallisation from THF and isolation of $[Tb(Me_2pz)_3(thf)]_2$ (**2.1**), which is isomorphous to the previously reported $[Dy(Me_2pz)_3(thf)]_2$ and analogous to $[Lu(Me_2pz)_3(thf)]_2$.[3] In attempts to synthesise the scandium (III) pyrazolate complexes, the isolation of a trimetallic oxide cage occurred as complex **2.2** ($[Sc_3O(Me_2pz)_7(Me_2pzH)_2]$.THF). The source of oxygen in the structure is probably silicon grease or solvent. Also, similar to previously reported compounds,[21] complex $[Sc_2(Me_2pz)_4(Me_2pz(SiMe_2O))_2]_2$ (**2.3**) has been isolated due to the insertion of the $[SiMe_2O]_n$. Silicon joint grease was determined as one possible source of oxide previously. However, under strict $[SiMe_2O]_n$ free conditions, oxide formation was still observed, showing that another process is likely occurring. Using Et_2O as a solvent in the RTP reaction which is kept over sodium (to make sure the solvent is dry), resulted in the formation of compound **2.4** ($[Y_3O(Me_2pz)_9Na_2(Et_2O)_2]$) because of the presence of Na_2O in the solution. The isolation of rare earth bimetallic oxide cage was observed by Werner as a result of the treatment of $[Ce(Me_2pz)_3(thf)]$ with K(btsa)[21] and by Schumann as a result of reaction between lanthanoid trichlorides with Na(pz) and $Na(pzMe_2)$.[37] The significant aspect of the compound **2.4** is the presence of yttrium with coordination number of seven and eight in the compound. Also, there are two different η^2 and μ_3- η^1: η^1 bonding modes in the compound. By repeating the same RTP reaction using Y and Me_2pzH in the diethyl ether as solvent, compound **2.5** ($[Y_3O(Me_2pz)_9Na_2(Me_2PzH)_2]$) has been isolated. Compound **2.5** has a trinuclear yttrium cage surrounding a trapped Na_2O molecule (solvent was keep over Na to make sure it is dry), with each sodium ligated by a 3,5-dimethypyrazole. Although isolating the common formula of the trivalent rare earth 3,5-dimethylpyrazolate complexes was expected, beside oxide complexes, new complexes as the result of C-F activation occurred as well. Attempting the reaction with large lanthanoid elements resulted in the formation of the complex **2.6** ($[La_4(Me_2pz)_9(\mu_2\text{-}F)_2(\mu_4\text{-}F)(thf)_4]$.3THF). The significant aspect of the compound **2.6**, which is the result of C-F activation, is the presence of three different pyrazolate bonding modes: η^2, μ- η^1: η^1 and μ- η^2: η^1. Also having a fluoride ion (which adopted tetrahedral geometry) shared between the four lanthanum atoms is another significant feature of compound **2.6** that was previously observed for oxygen. Repeating the reaction using lanthanum resulted in the isolation of $[La(Me_2pz)_5Hg_2(C_6F_5)_2(thf)]$ (**2.7**), which can be due to the co-crystallisation of LaL_3 and $LHg(C_6F_5)$ that justify the middle steps during redox transmettalation/protolysis. Using Er, which is a smaller lanthanoid than lanthanum, resulted in the trinuclear structure of

$[Er_3F(Me_2pz)_8(thf)_2]$ (**2.8**). Compound **2.8** has fluorine in the centre, which has been observed previously in the aryloxide complex as $[Er_3(OAr^{OMe})_4(\mu_2\text{-}F)_3(\mu_3\text{-}F)_2(thf)_4].thf.0.5C_6H_{14}$.[25]

The trimer yttrium compound ($[Na(dme)_3Y_3F(Me_2pz)_9].3/2DME$ (**2.9**)) provided a new example of C-F activation. Also, the presence of sodium coordinated with donor solvent by RTP reaction is observed for the first time that has been observed previously by salt elimination.[76]

Continuing the study using bulkier 3,5-di-*tert*-butylpyrazolate (tBu_2pzH) ligand resulted in the formation of the monomeric $[Ln(tBu_2pz)_3(thf)_2]$ (Ln = La, Ce, Lu) complexes, which was expected due to the previously reported $[Ln(tBu_2pz)_3(thf)_2]$ (Ln = Nd and Eu).[52] However, using Sm resulted in the formation of a new polymeric structure ($[Sm_2(tBu_2pz)_6(dme)_2]_n$ (**2.11**)) that is similar to the previously reported $[Nd(tBu_2Pz)_3(\mu\text{-}dme)]_n$.[61] Although previously $[Er(tBu_2pz)_3(thf)_2]$ complex has been reported[63], changing solvent during crystallisation and using DME resulted in the formation of $[Er(tBu_2pz)_3(dme)]$ (**2.12**).

Attempts to isolate product using the bulky 3,5-diphenylpyrazole (Ph_2pzH) ligand with lanthanum, praseodymium, gadolinium, holmium and lutetium failed due to the presence of dbmH as contamination in the starting materials when Ph_2pzH does not form completely during treating dbmH with hydrazine. Therefore, compounds $[Lu(dbm)_3(dme)]$ (**2.13**) and $[Sc(dbm)_3]$ (**2.14**) were isolated as by-products and due to the reaction of dbmH, contamination in the starting materials, with the metal. Compound **2.13** and **2.14** had been reported previously using other reactions rather than RTP (by stirring the respective oxides in hydrochloric acid and following refluxing).

Overall, this chemistry highlights the difficulty in performing Me_2pz chemistry of the lanthanoids compared with other 3,5-disubstituted pyrazolato chemistry. The lack of steric bulk about the Me_2pz ligand presumably allows opening of the coordination sphere of the metal leading to higher reactivity with for example solvent molecules, grease and fluorinated organics.

2.3 Experimental

2.3.1 General considerations

All the lanthanoid metals and their products are air-sensitive and moisture-sensitive, and required manipulation in an inert atmosphere using a glove box, Schlenk flask and vacuum line techniques. All solvents were pre-dried and deoxygenated by refluxing and distillation over sodium or sodium/benzophenone. The lanthanoid metal reagents were purchased as fine powders or metal ingots from Rhone Poulenc or Santoku. Metal ingots were freshly filed under an inert atmosphere into metal filings. 3,5-dimethylpyrazole (Me_2pzH) was purchased from Sigma-Aldrich and 3,5-diphenylpyrazole (Ph_2pzH) and 3,5-di-*tert*-butylpyrazole (tBu_2pzH) were prepared by literature methods.[70, 77] IR data were obtained from Nujol mulls for the region 4000-400 cm^{-1} with a Nicolet-Nexus FT-IR spectrometer. ^1H NMR spectra were recorded with a Bruker Ascend^{TM} 400 (400 MHz) using dry degassed *deutero*-benzene (C_6D_6) as solvent, and resonances were referenced to the residual ^1H resonances of the deuterated solvent. Elemental analyses (C, H, N) were performed by the Micro Analytical Laboratory, Science Centre, London Metropolitan University, England.

$[Tb(Me_2pz)_3(thf)]_2$ (2.1) :

Terbium filings (0.44 g, 1.36 mmol), $Hg(C_6F_5)_2$ (1.07 g, 2 mmol) and Me_2PzH (0.4 g, 4.05 mmol)) were added to a Schlenk flask and dissolved in THF (20 mL) and stirred at room temperature for one week. The solution was separated from the metal residue by filtration and then evaporated to 5mL (*in vacuo*), and cooled for several days without forming suitable crystal. Therefore, the mixture was heated at 60ºC using an oil bath over two nights and cooled slowly. After several weeks, colourless crystals of $[Tb(Me_2pz)_3(thf)]_2$ (**2.1**) were formed, determined by X-ray crystallography. Yield = 0.25 g (73%); IR (crystal oil): ν = 2723 (w), 1709 (vs), 1640(m), 1592 (w), 1573 (w), 1456 (vw), 1376 (vw), 1274 (w), 1260 (w), 1149(m), 915(m), 871(m), 736(w), 727 (w), 672 (vs), 661(s), 654(s), 611(vs), 588 cm^{-1} (s). ^1H NMR could not be obtained owing to paramagnetism. Elemental analysis calcd. (%) for $C_{19}H_{29}TbN_6O$ (M = 516.40 $g.mol^{-1}$): C 44.10, H 5.66, N 16.27. Found: C 44.09, H 5.52, N 16.71.

[$Sc_3O(Me_2pz)_7(Me_2pzH)_2$] (**2.2**):

Scandium filings (0.32 g, 2.3 mmol), $Hg(C_6F_5)_2$ (1.1 g, 2.0 mmol) and Me_2PzH (0.39 g, 4.0 mmol)) were added to a Schlenk flask and dissolved in THF (15 mL) with stirring at room temperature for one week. The resulting pale grey solution was filtered through a pad of Celite from the metal residue and evaporated under vacuum to 5 mL and cooled to -25 °C for several days. Small colourless crystals of **2.2** were produced. Yield = 0.2 g (23%); IR (Nujol, cm^{-1}): ν = 3194 (w), 2726 (m), 1639 (w), 1590 (w), 1509 (s), 1440 (vs), 1304 (m), 1260 (m), 1153 (w), 1076 (m), 1029 (m), 965 (m), 890 (w), 804 (m), 722 (vs), 660 cm^{-1} (wv); ^1H NMR (C_6D_6, 303.2 K): δ = 2.00 (br s, 54 H, Me), 5.68 ppm (br s, 9 H, H4 – Me_2pz), 10.86 ppm (br s, 2 H, Me_2pzH). Elemental analysis calcd. (%) for $C_{45}H_{65}Sc_3N_{18}O$ (M = 1964.6 $g.mol^{-1}$): Sc: 13.36; Found from titration: Sc: 12.89.

[$Sc_2(Me_2pz)_4(Me_2pz(SiMe_2O))_2]_2$ (**2.3**):

Scandium filings (0.32 g, 2.3 mmol), $Hg(C_6F_5)_2$ (1.1 g, 2.0 mmol) and Me_2PzH (0.39 g, 4.0 mmol)) were added to a Schlenk flask and dissolved in THF (15 mL) with stirring at room temperature for one week. The resulting pale grey solution was filtered through a pad of Celite from the metal residue and evaporated under vacuum to 5 mL and cooled in the fridge for several days. Since no product could be isolated, the mixture was heated and cooled down very slowly at room temperature followed by cooling in the fridge and freezer. After 3 weeks compound **2.3** formed as colourless small crystals. Yield = 0.97 g (55%); IR (Nujol, cm^{-1}): ν = 2726 (w), 1591 (w),1519 (m), 1504 (m), 1305 (m), 1154 (m), 1071 (w), 1028 (m), 1009 (w), 956 (w), 845 (vw), 777(m), 722 (w), 660 cm^{-1} (vw). ^1H NMR (C_6D_6, 303.2 K): δ = 0.44 (s, 12 H, Me- $SiMe_2$), 1.78 (br s, 36 H, Me) , 5.4 ppm (s, 6 H, H4 – Me_2pz). Elemental analysis calcd. (%) for $C_{68}H_{108}N_{24}O_4Sc_4Si_4$ (M = 1617.98 $g.mol^{-1}$): Sc 11.11; Found from titration: Sc 10.38.

[$Y_3O(Me_2pz)_9Na_2(Et_2O)_2$] (**2.4**):

Yttrium filings (0.2 g, 2.3 mmol), $Hg(C_6F_5)_2$ (1.1 g, 2.0 mmol) and Me_2PzH (0.4 g, 4.1 mmol)) were added to a Schlenk flask and dissolved in Et_2O (20 mL) with stirring at room temperature for one week. The resulting pale grey solution was filtered through a pad of Celite from the metal residue and evaporated under vacuum to 5 mL and cooled in the fridge for one

month. Colourless block crystals of [$Y_3(Me_2pz)_9Na_2(Et_2O)_2$] formed. Yield =0.18g (61.48%). IR (Nujol, cm^{-1}): ν= 2724 (m), 1671 (w), 1577 (vw), 1518 (s), 1377 (vs), 1316 (m), 1259 (w), 1178 (vw), 1152 (vw), 1090 (w), 1072 (m), 1017 (m), 962 (m), 891 (vw), 795 (m), 727 (m) and 668 cm^{-1} (vw). ^1H NMR (C_6D_6, 303.2 K): δ = 0.81 (t, 12 H, CH_3 Et_2O), 1.91 (s, 36 H, CH_3 (μ_3 -Me_2pz)), 2.03 (s, 18 H, (η^2-Me_2pz)), 2.97 (q, 8 H, CH_2 Et_2O), 5.50 (s, 6 H, H4 (μ_3 -$pzMe_2$)), 6.1 ppm (s, 3H, H4 (η^2-$pzMe_2$)). Elemental analysis calcd. (%) for $C_{53}H_{83}N_{18}Na_2O_3Y_3$, ($M$ = 1317.36 $g.mol^{-1}$): C 47.75, H 6.23, N 18.93. Found: C 45.44, H 6.23, N 17.74. Y: 20.65. Found from titration: Y: 19.98.

[$Y_3(Me_2pz)_9(Me_2pzH)_2Na_2O$] (**2.5**):

Yttrium filings (0.2 g, 2.3 mmol), $Hg(C_6F_5)_2$ (1.1 g, 2.0 mmol) and Me_2PzH (0.4 g, 4.1 mmol)) were added to a Schlenk flask and dissolved in Et_2O (20 mL) with stirring at room temperature for one week. The resulting pale grey solution was filtered through a pad of Celite from the metal residue and evaporated under vacuum to 5 mL and cooled in the fridge for one month. Colourless block crystals of [$Y_3(Me_2pz)_9(Me_2pzH)_2Na_2O$] formed. Yield =0.13g (51.92%). IR (Nujol, cm^{-1}): ν= 3290 (s), 3100 (vs), 2722 (s), 1638 (m), 1575 (m), 1259 (s), 1179 (s), 1152 (s), 1017 (vs), 967 (vs), 916 (m), 833 (m), 772 (vs), 729 (vs), 656 (w), 663 (w), and 679 cm^{-1} (w). ^1H NMR (C_6D_6, 303.2 K): δ = 1.72 (br s, 12 H, Me-pzH), 1.88 (s, 36 H, CH_3 (μ_3 -Me_2pz)), 2.04 (s, 18 H, (η^2-Me_2pz)), 5.51 (s, 8 H, H4 (μ_3 -Me_2pz) + (Me_2pzH)), 6.09 ppm (s, 3H, H4 (η^2-Me_2pz)). Elemental analysis calcd. (%) for $C_{55}H_{79}N_{22}Na_2O_3Y_3$, ($M$ = 1377.11 $g.mol^{-1}$): Y 19.54. Found from titration: Y 19.01.

[$La_4(Me_2pz)_9(\mu_2$-F)$_2(\mu_4$-F)(thf)$_4$].3THF (**2.6**):

Lanthanum filings (0.4 g, 2.8 mmol), $Hg(C_6F_5)_2$ (2.2 g, 4.1 mmol) and Me_2PzH (0.8 g, 8.1 mmol)) were added to a Schlenk flask and dissolved in THF (20 mL) with stirring at room temperature for one week. The pale yellow solution was separated from the metal residue by filtration and evaporated (*in vacuo*), to 5mL and cooled for several days without forming suitable crystal. Therefore, the mixture was heated at 60ºC using an oil bath overnight and cooled down slowly. After two weeks, clear crystals of [$La_4(Me_2pz)_9(\mu_2$-F)$_2(\mu_4$-F)(thf)$_4$].3THF (**2.6**) formed. Yield = 0.57 g (32%); IR (crystal oil): ν = 3313 (w), 3096 (w), 2722 (w), 1570

(m), 1515 (vs), 1308 (s), 1259 (s), 1012 (s), 961 (s), 876 (m), 777 (m), 730 (m), 660 cm^{-1} (w); ^1H NMR (C_6D_6, 303.2 K): δ = 1.39 (m,16 H, β-CH_2(thf)), 2.09 (s, 54 H, Me), 3.52 (m, 16 H, α-CH_2(thf)), 5.86 (br s, 9 H, H4 Me_2pz) ppm. Elemental analysis calcd. (%) for $C_{61}H_{95}F_3La_4N_{18}O_4.3(C_4H_8O)$ (M = 1966.44 $g.mol^{-1}$): C 44.58, H 5.74, N 12.82; calcd for $C_{61}H_{95}F_3La_4N_{18}O_4$ (loss of three THF molecules due to evaporation) (1748.6 $g.mol^{-1}$) : C 41.86, H 5.30, N 14.41. Found: C 41.59, H 5.59, N 14.47.

$[La(Me_2pz)_5Hg_2(C_6F_5)_2(thf)]$ (**2.7**):

Lanthanum filings (0.4 g, 2.8 mmol), $Hg(C_6F_5)_2$ (2.2 g, 4.1 mmol) and Me_2PzH (0.8 g, 8.1 mmol)) were added to a Schlenk flask and dissolved in THF (20 mL) with stirring at room temperature for 8 days. The bright red solution was separated from the metal residue by filtration and then evaporated (*in vacuo*), to 5mL and cooled for several days without forming suitable crystal. Therefore, the mixture was heated at 60ºC using an oil bath over two nights and cooled down slowly. After three weeks, clear crystals of $[La(Me_2pz)_5Hg_2(C_6F_5)_2(thf)]$ (**2.7**) formed. Yield = 1g (44%); IR (crystal oil): ν = 2724 (vw), 1637 (w), 1572 (vw), 1151 (w), 1073 (vw), 1009 (vw), 883 (w), 775 (vw), 730 (vw), 655cm^{-1} (m); ^1H NMR (C_6D_6, 303.2 K): δ = 1.18 (m, 4 H, β-CH_2(thf)), 1.78 (br s, 30 H, Me), 3.32 (m, 4 H, α-CH_2(thf)), 5.52 ppm (br s, 5 H, H4 – Me_2pz). ^{19}F NMR (C_6D_6, 303.2 K, δ_{ppm}) : -117.22, -152.16, -159.79. Elemental analysis calcd. (%) for $C_{41}H_{43}F_{10}Hg_2LaN_{10}O$ (M = 1421.94 $g.mol^{-1}$): C 34.63, H 3.048, N 9.85, La 9.76. Found: C 36.59, H 4.65, N 14.24; Found from titration: La 8.74.

$[Er_3F(Me_2pz)_8(thf)_2]$ (**2.8**)

Erbium metal (0.45 g, 1.36 mmol), $Hg(C_6F_5)_2$ (1.07 g, 2 mmol), and Me_2PzH (0.4 g, 4.05 mmol) were stirred in THF (15 mL) for two days. The pale pink solution was filtered from the metal residues. The solution was evaporated to 5mL (*in vacuo*), then the mixture was heated at 60ºC using an oil bath overnight and cooled down slowly. After one week, pale pink crystals of $[Er_3F(Me_2pz)_8(thf)_2]$ (**2.8**) formed and composition was determined by X-ray crystallography. Crystal yield = 0.54 g (76%); IR (crystal oil): ν = 2725 (w), 1567 (w), 1521 (vs), 1317(s), 1260 (m), 1171 (w), 1071 (m),1028 (s), 969 (m), 913 (w), 873 (w), 770(m), 738(m), 727(w), 673(vs), 659 (w), 587 cm^{-1} (w). ^1H NMR could not be obtained owing to paramagnetism. Elemental analysis cacld. (%) for: $C_{40}H_{56}Er_3FN_{16}.2(C_4H_8O_2)$ (1425.98 $g.mol^{-}$

[1]): Er 34.89; Found using titration: Er 33.75.

$[Na(dme)_3Y_3F(Me_2pz)_9]_2$ .3/2 DME(2.9):

Yttrium filings (0.2 g, 2.3 mmol), $Hg(C_6F_5)_2$ (1.1 g, 2.0 mmol) and Me_2PzH (0.4 g, 4.1 mmol)) were added to a Schlenk flask and dissolved in DME (20 mL) with stirring at room temperature for one week. The resulting very pale brown solution was filtered through a pad of Celite from the metal residue and evaporated under vacuum to 5 mL and cooled in the fridge for several days. Two sets of product was formed: colourless hexagonal crystals of $[Na(dme)_3Y_3F(Me_2pz)_9]$ and a white powder. White powder product was not suitable for X-ray crystallography determination. The reaction has been repeated and the same crystal structure formed. Microanalysis/ titration could not be done due to the very low yield of the reaction. IR (Nujol, cm^{-1}): ν= 2726 (m), 1592 (w), 1305 (s), 1155 (m), 1029 (m), 1009 (w), 969 (w), 890 (w), 774(w), 722(vs), 661 cm^{-1} (vw). ^1H NMR (C_6D_6, 303.2 K): δ = 1.82 (br s, 54 H, Me), 2.88 (s, 18 H, CH_3 dme), 3.09 (br s, 12 H, CH_2 dme), 5.48 ppm (s, 9 H, H4 – Me_2pz).

$[La(tBu_2pz)_3(thf)_2]$ (**2.10a**)

Lanthanum filings (0.08 g, 0.6 mmol), $Hg(C_6F_5)_2$ (0.535 g, 1.0 mmol) and tBu_2pzH (0.4 g, 2.0 mmol)) were added to a Schlenk flask and dissolved in THF (15 mL) by stirring at room temperature. The bright grey solution was separated from the metal residue by filtration. The solution was evaporated to 5mL (*in vacuo*) and cooled down slowly in the fridge and freezer. After several weeks clear $[La(tBu_2pz)_3(thf)_2]$ (**2.10a**) crystals formed. Yield = 0.36 g (66%); IR (crystal oil): ν = 3105 (m), 2704 (w), 1575 (w), 1560 (s),1412 (s), 1310 (s),1421 (vs), 1223(s), 1104 (m), 1015 (m), 992 (m), 916 (m), 875 (m), 787 (s), 725 (s), 669 (w), 626 cm^{-1} (m); ^1H NMR (C_6D_6, 303.2 K): δ = 1.10 (br s, 54 H, *t*Bu), 6.06 ppm (br s, 3 H, H4 – pz). The coordinated thf in the structure might evaporate under vacuum during drying the product and leaving only the residue thf in the structure. Elemental analysis calcd. (%) for $C_{33}H_{57}LaN_6.2(C_4H_8O)$ (M = 818.94 $g.mol^{-1}$)): C 60.13, H 8.738, N 10.262; calcd for $C_{33}H_{57}LaN_6$ (loss of two THF molecules due to evaporation) (674.72 $g.mol^{-1}$): C 57.73, H 8.15, N 12.44. Found: C 57.63, H 8.68, N 9.75.

[Ce(*t*Bu$_2$pz)$_3$(thf)$_2$] (**2.10b**)

Cerium filings (0.084 g, 0.6 mmol), Hg(C_6F_5)$_2$ (0.535 g, 1.0 mmol) and *t*Bu$_2$pzH (0.4 g, 2.0 mmol)) were added to a Schlenk flask and dissolved in THF (15 mL) with stirring at room temperature. The pale green solution was separated from the metal residue by filtration and evaporated to 5mL (*in vacuo*). The solution was cooled down slowly in the fridge and freezer. After several weeks colourless [Ce(*t*Bu$_2$pz)$_3$(thf)$_2$] (**2.10b**) crystals formed. Yield = 0.3 g (55%); IR (crystal oil): ν = 2724(w), 1558(m), 1519 (s), 1501 (m), 1413(m), 1291 (m), 1250 (m), 1203 (m), 1141 (m), 1107 (w), 1015 (m), 1002 (m), 990 (m), 934 (vw), 872 (vw), 797 (s), 720 (vw), 667 (m), 625 cm^{-1} (vw); ^{1}H NMR (C_6D_6, 303.2 K): δ = 1.15 (br s, 54 H, *t*Bu), 6.14 ppm (br s, 3 H, H4 – pz). The coordinated thf in the structure might evaporate under vacuum during drying the product, leaving only residue thf in the structure. Elemental analysis calcd. (%) for $C_{33}H_{57}CeN_6$. 2(C_4H_8O) (M = 812.53 g.mol^{-1})): C 60.04, H 8.66, N 10.25; calcd for $C_{33}H_{57}CeN_6$ (loss of two THF molecules due to evaporation) (675.11 g.mol^{-1}): C 58.65, H 9.14, N 12.44. Found: C 59.02, H 9.75, N 10.36.

[Lu(*t*Bu$_2$pz)$_3$(thf)$_2$] (**2.10c**)

Lutetium filings (0.1 g, 0.6 mmol), Hg(C_6F_5)$_2$ (0.535 g, 1.0 mmol) and *t*Bu$_2$pzH (0.4 g, 2.0 mmol)) were added to a Schlenk flask and dissolved in THF (15 mL) by stirring at room temperature for two weeks. The pale grey solution was separated from the metal residue by filtration and evaporated to 5mL (*in vacuo*). The solution was cooled down slowly in the fridge and freezer. After one week, colourless [Lu(*t*Bu$_2$pz)$_3$(thf)$_2$] (**2.10c**) crystals formed. Yield = 0.41 g (72%); IR (crystal oil): ν = 2727(w), 1569(m), 1314 (w), 1285(m), 1250 (w), 1225 (w), 1204 (w), 1128 (vw), 1107 (vw), 1019 (m), 994 (m), 920 (m), 873 (m), 790 (m), 723 (s), 668 (w), 627 cm^{-1} (vw); ^{1}H NMR (C_6D_6, 303.2 K): δ = 1.15 (br s, 54 H, *t*Bu), 6.14 ppm (br s, 3 H, H4 – pz). The coordinated thf in the structure might evaporate under vacuum during drying the product and only residue thf left in the structure could be seen at δ = 3.05 ppm. Elemental analysis calcd. (%) for $C_{33}H_{55}LuN_6$. 2(C_4H_8O) (M = 858.18 g.mol^{-1})): Lu 20.63; Found from titration: 19.48.

[Sm$_2$(*t*Bu$_2$pz)$_6$(dme)$_2$]$_n$ (**2.11**)

Samarium filings (0.09 g, 0.6 mmol), Hg(C_6F_5)$_2$ (0.535 g, 1.0 mmol) and *t*Bu$_2$pzH (0.4

g, 2.0 mmol)) were added to a Schlenk flask and dissolved in THF (15 mL) by stirring at room temperature for two weeks. The dark red solution was separated from the metal residue by filtration and evaporated to 5mL (*in vacuo*). The solution was cooled down slowly in the fridge and freezer but no suitable crystal formed. Therefore, the reaction solution evaporated (*in vacuo*) leaving a red powder. The powder was dissolved in hot DME (5 mL), and slowly cooled, forming small red crystal of $[Sm_2(tBu_2pz)_6(dme)_2]_n$ (**2.11**). Yield = 0.64 g (62%); IR (Nujol oil): ν = 3110 (m), 2725(m), 1575(m), 1519 (m), 1502(s), 1307(m), 1288 (m), 1250 (m), 1224 (m), 1206 (m), 1108 (w), 1050 (m), 1017 (m), 992 (m), 900 (m), 790 (s), 723 (s), 627 cm^{-1} (m); No satisfactory ^1H NMR spectrum could be obtained owing to paramagnetism. Elemental analysis calcd. (%) for $C_{74}H_{134}Sm_2N_{12}O_4$ (M = 1556.62 $g.mol^{-1}$): C 57.09, H 8.67, N 10.79; Found: C 56.67, H 8.51, N 10.54.

[Er(*t*Bu$_2$pz)$_3$(dme)] (**2.12**)

Erbium filings (0.1 g, 0.6 mmol), $Hg(C_6F_5)_2$ (0.535 g, 1.0 mmol) and *t*Bu$_2$pzH (0.4 g, 2.0 mmol)) were added to a Schlenk flask and dissolved in THF (15 mL) by stirring at room temperature for two weeks. The pale pink solution was separated from the metal residue by filtration and evaporated to 5mL (*in vacuo*). The solution was cooled down slowly in the fridge and freezer but no suitable crystal formed. Therefore, the reaction solution evaporated (*in vacuo*), leaving a pink powder. The powder was dissolved in hot DME (5 mL), and slowly cooled producing small pink needle shaped crystals of $[Er(tBu_2pz)_3(dme)]$ (**2.12**). Yield = 0.36 g (68%); IR (Nujol oil): ν = 2728(vw), 1569(m), 1518 (s), 1414(m), 1315(m), 1278 (w), 1250 (m), 1225 (w), 1204 (wv), 1107 (m), 1064 (m), 1018 (m), 995 (m), 925 (vw), 870 (s), 831 (m), 785 (vs), 723 (vs), 694 (vw), 629 cm^{-1} (m). No satisfactory ^1H NMR spectrum could be obtained owing to paramagnetism. Elemental analysis calcd. (%) for $C_{33}H_{57}ErN_6$ ($C_4H_8O_2$) (M = 797.25 $g.mol^{-1}$): Er 21.16; Found from titration: Er 20.66.

[Lu(dbm)$_3$(dme)] (**2.13**)

Lutetium filings (0.1 g, 0.6 mmol), $Hg(C_6F_5)_2$ (0.3 g, 1.36 mmol) and Ph_2pzH (0.4 g, 1.81 mmol)) were added to a Schlenk flask and dissolved in DME (15 mL) by stirring at room temperature for one week. The pale yellow solution was separated from the metal residue by filtration and evaporated to 5mL (*in vacuo*). The solution was cooled slowly and, since no

suitable crystal formed, the solution was layered by hexane, resulting in the formation of two crystal sets: red crystals of [Lu(dbm)$_3$(dme)] (**2.13**) and hexagonal colourless crystals. X-ray crystallographic analysis of the hexagonal colourless crystals indicated large amount of disorder, which could not be resolved.

[Sc(dbm)$_3$] (**2.14**)

Scandium filings (0.3 g, 1.00 mmol), Hg(C_6F_5)$_2$ (0.26 g, 0.5 mmol) and Ph_2pzH (0.3 g, 1.36 mmol)) were added to a Schlenk flask and dissolved in DME (15 mL) by stirring at room temperature for two weeks. The pale grey solution was separated from the metal residue by filtration and evaporated to 5mL (*in vacuo*). The solution was cooled slowly and, since no suitable crystal formed, the solution was layered by hexane, resulting in the formation of two product sets (similar to lutetium reaction): colourless hexagonal shaped crystals of [Sc(dbm)$_3$] (**2.14**) and white powder. The white powder product was not suitable for X-ray crystallography determination.

2.4 Crystallographic data

Complexes were immersed in viscous hydrocarbon oil (Paraton-N) and measured on either a Bruker APEX II CCD diffractometer/on a 'Bruker P4' diffractometer with integration and absorption corrections completed using Apex II program suite, or at the Australian Synchrotron on the MX1 at 173 K using a single wavelength (λ = 0.712 Å). The data and integration were completed by Blue ice [78] and XDS [79] software programs. Structural solutions were obtained by either direct methods [80] or the Patterson method [80] and solutions were refined using full matrix least squares methods against F^2 using SHELX2014, via OLEX 2 [81] interface.

[Tb(Me$_2$pz)$_3$(thf)]$_2$ (2.1) : $C_{19}H_{29}N_6OTb$, (M = 516.40) , triclinic, P-1 (no. 2), a = 10.684(2) Å, b = 10.699(2) Å, c = 11.124(2) Å, α = 77.42(3)°, β = 68.78(3)°, γ = 60.37(3)°, V = 1029.2(5) Å^3, T = 173(2) K, Z = 2, Z' = 1, μ(MoK$_\alpha$) = 3.456 mm^{-1}, 9522 reflections measured, 4838 unique (R_{int} = 0.0417), which were used in all calculations. The final wR_2 was 0.0908 (all data) and R_1 was 0.0299 (I > 2σ (I)).

[Sc$_3$O(Me$_2$pz)$_7$(Me$_2$pzH)$_2$] (2.2): $C_{45}H_{65}N_{18}OSc_3$ (M = 1009.03): monoclinic, $P2_1/n$ (No. 14), a = 17.671(4) Å, b = 15.822(3) Å, c = 19.912(4) Å, β = 90.10(3)°, α = γ = 90°, V =

5567.2(19) Å^3, T = 100(2) K, Z = 4, Z' = 1, μ (MoKa) = 0.404 mm^{-1}, 46994 reflections measured, 12640 unique (R_{int} = 0.0674), which were used in all calculations. The final wR_2 was 0.1488 (all data) and R_1 was 0.0588 (I > 2σ (I)).

[Sc$_2$(Me$_2$pz)$_4$(Me$_2$pz(SiMe$_2$O))$_2$]$_2$ (2.3): $C_{68}H_{108}N_{24}O_4Sc_4Si_4$, ($M$ = 1617.98), triclinic, P-1 (no. 2), a = 11.625(2) Å, b = 19.250(4) Å, c = 21.054(4) Å, α = 108.99(3)°, β = 103.69(3)°, γ = 94.27(3)°, V = 4275.0(17) Å^3, T = 173(2) K, Z = 2, Z' = 1, μ(MoK$_\alpha$) = 0.418 mm^{-1}, 34831 reflections measured, 17710 unique (R_{int} = 0.0398), which were used in all calculations. The final wR_2 was 0.2638 (all data) and R_1 was 0.0974 (I > 2σ (I)).

[Y$_3$(Me$_2$pz)$_9$Na$_2$(Et$_2$O)$_2$] (**2.4**): $C_{53}H_{83}N_{18}Na_2O_3Y_3$, ($M$ = 1317.36), orthorhombic, $Pna2_1$ (no. 33), a = 18.935(4) Å, b = 19.797(4) Å, c = 16..671(3) Å, α = 90(3)°, β = 90(3)°, γ = 90(3)°, V = 6249(2) Å^3, T = 293(2) K, Z = 4, Z' = 1, μ(MoK$_\alpha$) = 2.831 mm^{-1}, 69051 reflections measured, 16977 unique (R_{int} = 0.0853), which were used in all calculations. The final wR_2 was 0.1509 (all data) and R_1 was 0.0524 (I > 2σ (I)).

[Y$_3$(Me$_2$pz)$_9$(Me$_2$pzH)$_2$Na$_2$O] (**2.5**): $C_{55}H_{79}N_{22}Na_2OY_3$, ($M$ = 1377.11), monoclinic, $P2_1/n$ (no. 14), a = 16.686(3) Å, b = 18.416(4) Å, c = 20.664(4) Å, α = γ = 90°, β = 97.16(3)°, V = 6300(2) Å^3, T = 173(2) ºK, Z = 4, Z' = 1, μ(MoK$_\alpha$) = 2.811 mm^{-1}, 92573 reflections measured, 17383 unique (R_{int} = 0.0668), which were used in all calculations. The final wR_2 was 0.1434 (all data) and R_1 was 0.0527 (I > 2σ (I)).

[La$_4$(Me$_2$pz)$_9$(μ$_2$-F)$_2$(μ$_4$-F)(thf)$_4$].3THF (2.6): $C_{73}H_{112}F_3La_4N_{18}O_7$, ($M$= 1966.44), monoclinic, $P2_1/c$ (no. 14), a = 14.348(3) Å, b = 18.730(4) Å, c = 31.528(6) Å, β = 97.06(3)°, α = γ = 90°, V = 8409(3) Å^3, T = 100(2) K, Z = 4, Z' = 1, μ(MoK$_\alpha$) = 2.057 mm^{-1}, 100563 reflections measured, 15499 unique (R_{int} = 0.1473), which were used in all calculations. The final wR_2 was 0.2123 (all data) and R_1 was 0.0753 (I > 2σ (I)).

[La(Me$_2$pz)$_5$Hg$_2$(C$_6$F$_5$)$_2$(thf)] (2.7): $C_{41}H_{43}F_{10}Hg_2LaN_{10}O$, ($M$ = 1421.94), monoclinic, $P2_1/c$ (no. 14), a = 17.770(4) Å, b = 12.197(2) Å, c = 22.826(5) Å, β = 110.83(3)°, α= β= 90°, V = 4623.8(18) Å^3, T = 100(2) K, Z = 4, Z' = 1, μ(MoK$_\alpha$) = 7.616 mm^{-1}, 89789 reflections measured, 13241 unique (R_{int} = 0.0795), which were used in all calculations. The final wR_2 was 0.1901 (all data) and R_1 was 0.0949 (I > 2σ (I)).

[$Er_3F(Me_2pz)_8thf_2$] (2.8): $C_{48}H_{72}Er_3FN_{16}O_2$, ($M$ = 1425.99), monoclinic, $P2_1/c$ (no. 14), a = 22.394(5) Å, b = 16.777(3) Å, c = 16.987(3) Å, β = 97.43(3)°, $\alpha = \gamma$ = 90°, V = 6329(2) Å^3, T = 293(2) K, Z = 4, Z' = 1, μ (MoK$_\alpha$) = 3.990 mm^{-1}, 59901 reflections measured, 15673 unique (R_{int} = 0.0537), which were used in all calculations. The final wR_2 was 0.1750 (all data) and R_1 was 0.0501 (I > 2σ (I)).

[$Na(dme)_3Y_3F(Me_2pz)_9]_2$.3/2 DME (2.9): $C_{120}H_{188}FN_{36}Na_2O_{15}Y_6$, ($M$ = 2992.49), triclinic, P-1 (no. 2), a = 15.287(3) Å, b = 23.167(5) Å, c = 24.499(5) Å, α = 102.45(3)°, β = 106.30(3)°, γ = 107.03(3)°, V = 7532(3) Å^3, T = 173(2) K, Z = 2, Z' = 1, μ (MoK$_\alpha$) = 2.359 mm^{-1}, 70825 reflections measured, 35890 unique (R_{int} = 0.0761), which were used in all calculations. The final wR_2 was 0.1919 (all data) and R_1 was 0.0654 (I > 2σ (I)).

[La($t$$Bu_2pz)_3(thf)_2$] (2.10a): $C_{41}H_{73}LaN_6O_2$, (M = 818.94), monoclinic, $P2_1$ (No. 4), a = 9.778(2) Å, b = 19.417(4) Å, c = 11.881(2) Å, β = 96.98(3)°, $\alpha = \beta$ = 90°, V = 2239.0(8) Å^3, T = 100(2) K, Z = 2, Z' = 1, μ(MoK$_\alpha$) = 0.987 mm^{-1}, 27605 reflections measured, 7803 unique (R_{int} = 0.0432), which were used in all calculations. The final wR_2 was 0.1274 (all data) and R_1 was 0.0487 (I > 2σ (I)).

[Ce($t$$Bu_2pz)_3(thf)_2$] (2.10b): $C_{41}H_{73}CeN_6O_2$, (M = 812.53), monoclinic, $P2_1$ (no. 4), a = 9.950(2) Å, b = 19.874(4) Å, c = 11.999(2) Å, β = 97.32(3)°, $\alpha = \gamma$ = 90°, V = 2353.6(8) Å^3, T = 296(2) K, Z = 2, Z' = 1, μ(MoK$_\alpha$) = 1.002 mm^{-1}, 20200 reflections measured, 7841 unique (R_{int} = 0.0583), which were used in all calculations. The final wR_2 was 0.1237 (all data) and R_1 was 0.0457 (I > 2σ (I)).

[Lu($t$$Bu_2pz)_3(thf)_2$] (2.10c): $C_{41}H_{73}LuN_6O_2$, (M = 858.05), monoclinic, $P2_1$ (no. 4), a = 11.614(2) Å, b = 19.609(4) Å, c = 38.915(8) Å, β = 97.48(3)°, $\alpha = \gamma$ = 90°, V = 8787(3) Å^3, T = 296(2) K, Z = 8, Z' = 4, μ(Mo K$_\alpha$) = 2.285 mm^{-1}, 103749 reflections measured, 48196 unique (R_{int} = 0.0470), which were used in all calculations. The final wR_2 was 0.1614 (all data) and R_1 was 0.0511 (I≥2σ (I)).

[$Sm_2(tBu_2pz)_6(dme)_2]_n$ (2.11): $C_{74}H_{134}N_{12}O_4Sm_2$, ($M$ = 1556.62), triclinic, P-1 (no. 2), a = 14.251(3) Å, b = 14.566(3) Å, c = 20.686(4) Å, α = 94.03(3)°, β = 99.66(3)°, γ = 99.91(3)°, V = 4148.1(15) Å^3, T = 173(2) K, Z = 2, Z' = 1, μ(MoK$_\alpha$) = 1.451 mm^{-1}, 38960 reflections

measured, 19726 unique (R_{int} = 0.0366), which were used in all calculations. The final wR_2 was 0.1537 (all data) and R_1 was 0.0579 (I > 2σ (I)).

[Er(tBu$_2$pz)$_3$(dme)] (2.12): $C_{37}H_{67}ErN_6O_2$, (M = 795.22), triclinic, P-1 (No. 2), a = 10.4393(8) Å, b = 11.4782(9) Å, c = 19.4437(15) Å, α = 85.327(4)°, β = 76.343(4)°, γ = 72.891(3)°, V = 2163.6(3) Å^3, T = 296(2) K, Z = 2, Z' = 1, μ(MoK$_\alpha$) = 1.974 mm^{-1}, 22476 reflections measured, 7581 unique (R_{int} = 0.0868), which were used in all calculations. The final wR_2 was 0.2906 (all data) and R_1 was 0.1073 (I > 2σ (I)).

[Lu(dbm)$_3$(dme)] (2.13): $C_{49}H_{43}LuO_8$, (M = 934.80), monoclinic, $P2_1/c$ (no. 14), a = 12.4917(14) Å, b = 23.733(3) Å, c = 14.6353(17) Å, β = 105.431(6)°, α = γ = 90°, V = 4182.5(8) Å^3, T = 298(2) K, Z = 4, Z' = 1, μ(MoK$_\alpha$) = 2.415 mm^{-1}, 55326 reflections measured, 12210 unique (R_{int} = 0.1481), which were used in all calculations. The final wR_2 was 0.2064 (all data) and R_1 was 0.0590 (I > 2σ (I)).

[Sc(dbm)$_3$] (2.14): $C_{45}H_{33}O_6Sc$, (M = 714.67), triclinic, P-1 (No. 2), a = 10.388(2) Å, b = 11.511(2) Å, c = 16.039(3) Å, α = 107.92(3)°, β = 96.57(3)°, γ = 101.97(3)°, V = 1752.1(7) Å^3, T = 173(2) K, Z = 2, Z' = 1, μ(MoK$_\alpha$) = 0.262 mm^{-1}, 14284 reflections measured, 7306 unique (R_{int} = 0.0226), which were used in all calculations. The final wR_2 was 0.0974 (all data) and R_1 was 0.0379 (I > 2σ (I)).

2.5 References

1. S. Trofimenko, *Chem. Rev.*, 1972, **72**, 497-509.
2. S. Trofimenko, *Prog. Inorg. Chem.*, 1986, **34**, 115-210.
3. G. B. Deacon, R. Harika, P. C. Junk, B. W. Skelton, D. Werner and A. H. White, *Eur. J. Inorg. Chem.*, 2014, 2412-2419.
4. G. B. Deacon, E. E. Delbridge, C. M. Forsyth, B. W. Skelton and A. H. White, *J. Chem. Soc., Dalton Trans.*, 2000, 745-751.
5. C. Yélamos, M. J. Heeg and C. H. Winter, *Inorg. Chem.*, 1998, **37**, 3892-3894.
6. G. B. Deacon, E. E. Delbridge, B. W. Skelton and A. H. White, *Angew. Chem. Int. Ed. Engl.*, 1998, **37**, 2251-2252.
7. G. B. Deacon, E. E. Delbridge and C. M. Forsyth, *Angew. Chem. Int. Ed.*, 1999, **38**, 1766-1767.
8. L. R. Falvello, J. Fornies, A. Martin, R. Navarro, V. Sicilia and P. Villarroya, *Chem. Commun.*, 1998, 2429-2430.
9. J. R. Perera, M. J. Heeg, H. B. Schlegel and C. H. Winter, *J. Am. Chem. Soc*, 1999, **121**, 4536-4537.
10. A. A. Mohamed, *Coord. Chem. Rev.*, 2010, **254**, 1918-1947.
11. A. P. Sadimenko and S. S. Basson, *Coord. Chem. Rev.*, 1996, **147**, 247-297.
12. M. A. Halcrow, *Dalton Trans.*, 2009, 2059-2073.
13. L. Zhang, X. Zhou, R. Cai and L. Weng, *J. Organomet. Chem.*, 2000, **612**, 176-181.
14. H. Schumann, J. Loebel, J. Pickardt, C. Qian and Z. Xie, *Organometallics*, 1991, **10**, 215-219.
15. D. Pfeiffer, B. J. Ximba, L. M. Liable-Sands, A. L. Rheingold, M. J. Heeg, D. M. Coleman, H. B. Schlegel, T. F. Kuech and C. H. Winter, *Inorg. Chem.*, 1999, **38**, 4539-4548.
16. G. B. Deacon, C. M. Forsyth, A. Gitlits, R. Harika, P. C. Junk, B. W. Skelton and A. H. White, *Angew. Chem. Int. Ed. Engl.*, 2002, **41**, 3249-3251.
17. G. Deacon, B. Gatehouse, S. Nickel and S. Platts, *Aust. J. Chem.*, 1991, **44**, 613-621.
18. X. Zhou, L. Zhang, R. Ruan, L. Zhang, R. Cai and L. Weng, *Chin. Sci. Bull.*, 2001, **46**, 723-726.
19. J. E. Cosgriff, G. B. Deacon, B. M. Gatehouse, P. R. Lee and H. Schumann, *Z. Anorg. Allg. Chem.*, 1996, **622**, 1399-1403.
20. R. Harika, Ph.D Thesis, Monash University, 2003.
21. D. Werner, Ph.D Thesis, Monash University, 2015.
22. S. Cotton, in *Comprehensive Coordination Chemistry II*, ed. J. A. M. J. Meyer, Pergamon,

Oxford, 2003, pp. 93-188.

23. X. Zhou, H. Ma, X. Huang and X. You, *J. Chem. Soc., Chem. Commun*, 1995, 2483-2484.
24. M. L. Cole, G. B. Deacon, C. M. Forsyth, P. C. Junk, K. Konstas and J. Wang, *Chem. Eur. J*, 2007, **13**, 8092-8110.
25. G. B. Deacon, G. D. Fallon, C. M. Forsyth, S. C. Harris, P. C. Junk, B. W. Skelton and A. H. White, *Dalton Trans*, 2006, 802-812.
26. G. B. Deacon, C. M. Forsyth and S. Nickel, *J. Organomet. Chem*, 2002, **647**, 50-60.
27. J. Townley, Ph.D Thesis, Monash University, 2010.
28. G. Deacon, C. Forsyth and B. Gatehouse, *Aust. J. Chem.*, 1990, **43**, 795-806.
29. M. L. Cole, G. B. Deacon, P. C. Junk, K. Konstas and P. W. Roesky, *Eur. J. Inorg. Chem.*, 2005, 1090-1098.
30. D. M. Barnhart, D. L. Clark, J. C. Huffman, R. L. Vincent and J. G. Watkin, *Inorg. Chem.*, 1993, **32**, 4077-4083.
31. W. J. Evans, *Angew. Chem. Int. Ed.*, 1997, **36**, 2693-2693.
32. R. Shannon, *Acta Cryst., Sect. A*, 1976, **32**, 751-767.
33. X. Zhou, Z. Huang, R. Cai, L. Zhang, Y. Liu and C. Duan, *Synth. React. Inorg. Met.-Org. Chem.*, 2000, **30**, 649-662.
34. L.-C. Pop and M. Saito, *Coord. Chem. Rev.*, 2016, **314**, 64-70.
35. C. Jones, P. C. Junk, S. G. Leary and N. A. Smithies, *J. Chem. Soc., Dalton Trans.*, 2000, 3186-3190.
36. X.-g. Zhou, Z.-e. Huang, R.-f. Cai, L.-b. Zhang, L.-x. Zhang and X.-y. Huang, *Organometallics*, 1999, **18**, 4128-4133.
37. H. Schumann, P. R. Lee and J. Loebel, *Angew. Chem. Int. Ed.*, 1989, **28**, 1033-1035.
38. M. L. Cole, G. B. Deacon, C. M. Forsyth, P. C. Junk, K. Konstas, J. Wang, H. Bittig and D. Werner, *Chem. Eur. J*, 2013, **19**, 1410-1420.
39. J. Hitzbleck, G. B. Deacon and K. Ruhlandt-Senge, *Eur. J. Inorg. Chem.*, 2007, 592-601.
40. R. D. Chambers, G. E. Coates, J. G. Livingstone and W. K. R. Musgrave, *J. Chem. Soc*, 1962, 4367-4371.
41. K. R. Flower, V. J. Howard, S. Naguthney, R. G. Pritchard, J. E. Warren and A. T. McGown, *Inorg. Chem.*, 2002, **41**, 1907-1912.
42. S. S. Batsanov, *J. Chem. Soc., Dalton Trans.*, 1998, 1541-1546.
43. S. C. Nyburg and C. H. Faerman, *Acta Crystallographica Section B*, 1985, **41**, 274-279.
44. M. Tsunoda and F. P. Gabbaï, *J. Am. Chem. Soc.*, 2000, **122**, 8335-8336.
45. N. Masciocchi, G. A. Ardizzoia, A. Maspero, G. LaMonica and A. Sironi, *Inorg. Chem.*, 1999,

38, 3657-3664.

46. S.-Á. Cortés-Llamas, R. Hernández-Lamoneda, M.-Á. Velázquez-Carmona, M.-A. Muñoz-Hernández and R. A. Toscano, *Inorg. Chem.*, 2006, **45**, 286-294.
47. K. S. Chong, S. J. Rettig, A. Storr and J. Trotter, *Can. J. Chem.*, 1979, **57**, 3090-3098.
48. G. B. Deacon, E. E. Delbridge, D. J. Evans, R. Harika, P. C. Junk, B. W. Skelton and A. H. White, *Chem. Eur. J.*, 2004, **10**, 1193-1204.
49. F. T. Edelmann, in *Comprehensive Organometallic Chemistry II*, eds. F. G. A. Stone and G. Wilkinson, Elsevier, Oxford, 1995, pp. 11-212.
50. R. Anwander, in *Lanthanides: Chemistry and Use in Organic Synthesis*, Springer, 1999, pp. 1-61.
51. G. B. Deacon, E. E. Delbridge, B. W. Skelton and A. H. White, *Eur. J. Inorg. Chem.*, 1999, 751-761.
52. J. E. Cosgriff, G. B. Deacon, B. M. Gatehouse, H. Hemling and H. Schumann, *Angew. Chem. Int. Ed. Engl.*, 1993, **32**, 874-875.
53. J. Lefevre, G. B. Deacon, P. C. Junk and L. Maron, *Chem. Commun.*, 2015, **51**, 15173-15175.
54. A. L. Llamas-Saiz, C. Foces-Foces, F. H. Cano, P. Jimenez, J. Laynez, W. Meutermans, J. Elguero, H.-H. Limbach and F. Aguilar-Parrilla, *Acta Cryst.*, 1994, **B50**, 746-762.
55. E. C. Joanna, Ph. D Thesis, Monash University, 1996.
56. R. J. H. Clark, J. Lewis, D. J. Machin and R. S. Nyholm, *J. Chem. Soc.*, 1963, 379-387.
57. J. Lewis, J. R. Miller, R. L. Richards and A. Thompson, *J. Chem. Soc.*, 1965, 5850-5860.
58. D. Werner, G. B. Deacon, P. C. Junk and R. Anwander, *Chem. Eur. J.*, 2014, **20**, 4426-4438.
59. G. B. Deacon, P. I. Mackinnon, T. W. Hambley and J. C. Taylor, *J. Organomet. Chem.*, 1983, **259**, 91-97.
60. G. Deacon, T. Feng, S. Nickel, M. Ogden and A. White, *Aust. J. Chem.*, 1992, **45**, 671-683.
61. J. E. Cosgriff, G. B. Deacon, G. D. Fallon, B. M. Gatehouse, H. Schumann and R. Weimann, *Chem. Ber.*, 1996, **129**, 953-958.
62. M. Johnson, J. C. Taylor and G. W. Cox, *J. Appl. Crystallogr.*, 1980, **13**, 188-189.
63. J. Cosgriff, G. Deacon, B. Gatehouse, H. Hemling and H. Schumann, *Aust. J. Chem.*, 1994, **47**, 1223-1235.
64. P. B. Hitchcock, A. V. Khvostov, M. F. Lappert and A. V. Protchenko, *Dalton Trans.*, 2009, 2383-2391.
65. S. Beaini, G. B. Deacon, M. Hilder, P. C. Junk and D. R. Turner, *Eur. J. Inorg. Chem.*, 2006, 3434-3441.
66. J. Jin, S. Jin and W. Chen, *J. Organomet. Chem.*, 1991, **412**, 71-75.

67. S. Beaini, G. B. Deacon, E. E. Delbridge, P. C. Junk, B. W. Skelton and A. H. White, *Eur. J. Inorg. Chem.*, 2008, 4586-4596.
68. N. Marques, A. Sella and J. Takats, *Chem. Rev.*, 2002, **102**, 2137-2160.
69. S. Akerboom, M. S. Meijer, M. A. Siegler, W. T. Fu and E. Bouwman, *J. Lumin.*, 2014, **145**, 278-282.
70. J. Elguero, E. Gonzalez and R. Jacquier, *Bull. Soc. Chim. Fr.*, 1968, 707-713.
71. A. G. Orpen, L. Brammer, F. H. Allen, O. Kennard, D. G. Watson and R. Taylor, *J. Chem. Soc., Dalton Trans.*, 1989, S1-S83.
72. E. G. Zaitseva, l. A. Baidina, P. A. Stabnikov, S. V. Borisov and I. K. Igumenov, *J. Struct. Chem.*, 1990, **31**, 184-182.
73. D. H. Williams and I. Fleming, *Spectroscopic Methods in Organic Chemistry*, McGraw-Hill, 1995.
74. J. E. Cosgriff, G. B. Deacon and B. M. Gatehouse, *Aust. J. Chem.*, 1993, **46**, 1881-1896.
75. M. Wiecko, G. B. Deacon and P. C. Junk, *Chem. Commun.*, 2010, **46**, 5076-5078.
76. M. L. Cole and P. C. Junk, *Chem. Commun.*, 2005, 2695-2697.
77. C. Fernández-Castaño, C. Foces-Foces, N. Jagerovic and J. Elguero, *J. Mol. Struct.*, 1995, **355**, 265-271.
78. T. M. McPhillips, S. E. McPhillips, H.-J. Chiu, A. E. Cohen, A. M. Deacon, P. J. Ellis, E. Garman, A. Gonzalez, N. K. Sauter, R. P. Phizackerley, S. M. Soltis and P. Kuhn, *J. Synchrotron Rad.*, 2002, **9**, 401-406.
79. W. Kabsch, *J. Appl. Cryst.*, 1993, **26**, 795-800.
80. G. Sheldrick, *Acta Crystallogra., Sect. A*, 2008, **64**, 112-122.
81. O. V. Dolomanov, L. J. Bourhis, R. J. Gildea, J. A. K. Howard and H. Puschmann, *J. Appl. Cryst.*, 2009, **42**, 339-341.

Chapter 3

Synthesis of Rare Earth Pyrazolate Complexes Using High Temperature Solvent-free Reactions

---

3. Chapter 3

3.1 Introduction

The synthesis of complexes with solely nitrogen coordination as well as the formation of homoleptic complexes of rare earth elements is complicated due to the oxophilic character of these elements.[1] The presence of coordinating solvent molecules are quite often essential in the synthesis routes for solubility reasons. Solvent free elevated temperature reactions can be a useful route towards homoleptic complexes, and interesting structural features can be expected due to the lanthanoid represent a satisfied coordination sphere.

Homoleptic trivalent and divalent lanthanoid complexes $Ln(L)_n$ (n = 2 or 3) have been isolated by the direct thermal reactions. The reactions were performed using lanthanoid metals and the conjugate acids (HL) of the target ligand. This potentially simple route involves reactions at elevated temperatures (200-300 ºC) under solventless conditions. Using this method, a range of rare earth phenolate and pyrazolate complexes have been obtained (Equation 3.1) (OAr = 2,6-di-tert-butyl-4-X-phenolate; pz = pyrazolate).[2-10] Alternatively, by using metathesis reactions under the same conditions (Equation 3.2) some heterobimetallic rare earth phenolate and pyrazolate complexes have been obtained as well.[11, 12]

$$Ln + n\,LH \longrightarrow [Ln(L)n] + n/_2\,H_2$$

L = OAr, Ph_2pz, $t Bu_2pz$

n = 2, 3

Equation 3.1

$$LnCl_3 + 4\,[M(tBu_2pz)] \longrightarrow [M\{Ln(tBu_2pz)_4] + 3\,MCl$$

(M = K or Na)

Ln = Tb, Ho, Er

Equation 3.2

For transition metal complexes, the structures of $[Ti(Me_2pz)_4]$[13, 14] and $[Ta(Me_2pz)_4]$[15] were the first structurally characterised homoleptic pyrazolate complexes.

Using solvent-free elevated-temperature reaction commonly provides the formation of homoleptic complexes whilst the majority of lanthanoid-pyrazolate complexes are of a heteroleptic nature $[Ln(R_2pz)_n(S)_m]$[11, 12, 16-26] [R = *t*Bu, Me, Ph; *n* = 2, 3; S = co-ligand/solvent (e.g. dme, thf)].

The bimetallic $[K\{Er(tBu_2pz)_4]$[12] was the first homoleptic Ln-pyrazolate complex that was prepared by an elevated temperature metathesis reaction between $ErCl_3$ and $[K(tBu_2pz)]$ in the presence of the non-coordinating tetramethylbenzene as a flux (Equation 3.3).

$$ErCl_3 + 4\,[K(tBu_2pz)] \longrightarrow [K\{Er(tBu_2pz)_4\}] + 3\,KCl$$

Equation 3.3

$[K(18\text{-crown-6})(dme)(PhMe)\{Er(tBu_2pz)_4\}]$[12] (Figure 3-1) which is the first example of a discrete mononuclear η^2-pyrazolatolanthanoid (III) complex was synthesised by extraction of $[K\{Er(tBu_2pz)_4\}]$ with 18-crown-6, toluene and dme.

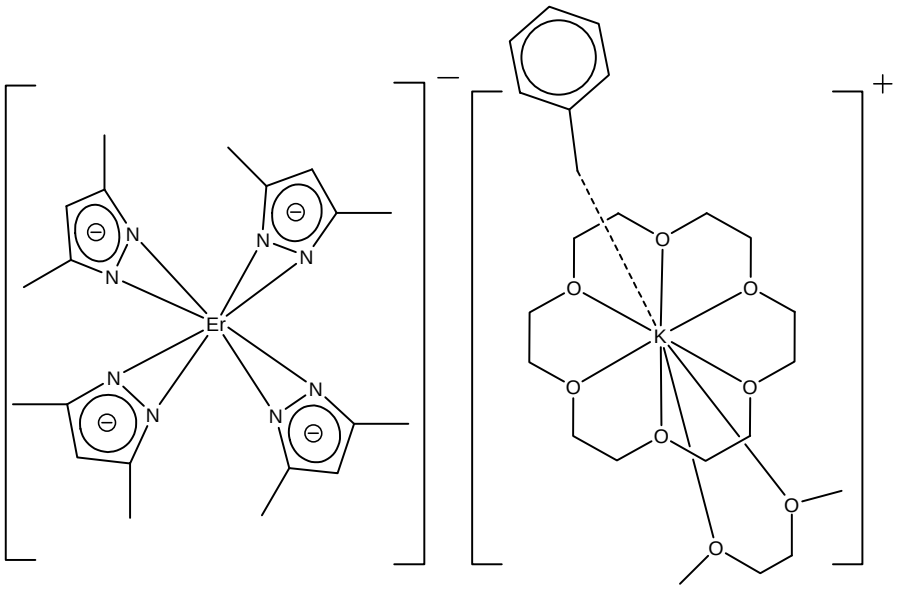

Figure 3-1. The structure of $[K(18\text{-crown-6})(dme)(PhMe)\{Er(tBu_2pz)_4\}]$[12]; methyl groups of *t*Bu removed for clarity.

By using high temperature direct redox [8, 9, 16, 27] (Equation 3.4) or metathesis reactions [11, 12] (Equation 3.3), a number of homoleptic Ln-pyrazolate complexes (pyrazolate = Ph_2pz, tBu_2pz) have been synthesised.

$$Ln + n\ R_2pzH \longrightarrow [Ln(R_2pz)_n] + n/2\ H_2$$

Ln = Sc, La, Nd, Eu, Lu (R = *t*Bu; *n* = 3)

Ln = Yb (R = *t*Bu; *n* = 2.5)

Ln = Sc, La, Nd, Er, Lu (R = Ph; n = 3)

Equation 3.4

The versatility of pyrazolate ligand is highlighted by the isolation of monomeric $[Sc(tBu_2pz)_3]$[9] (Figure 3-2), the tetranuclear divalent $[Eu_4(tBu_2pz)_8]$[9] (Figure 3-3) and the mixed-valent $[Yb_2(tBu_2pz)_5]$ species (Figure 3-4).[8] Also, the isolation of the mentioned complexes clearly shows the variance in structural behaviour of the Ln-pyrazolate systems.

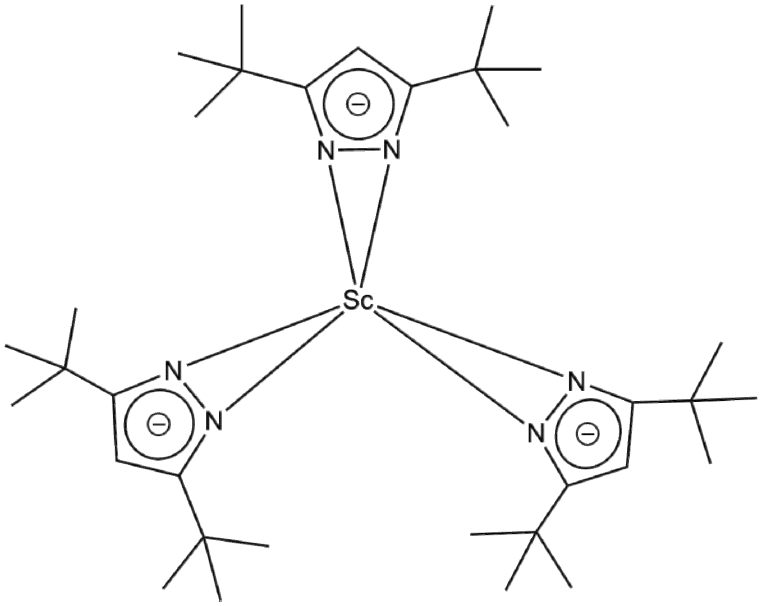

Figure 3-2. The structure of the monomeric $[Sc(tBu_2pz)_3]$[9] complex.

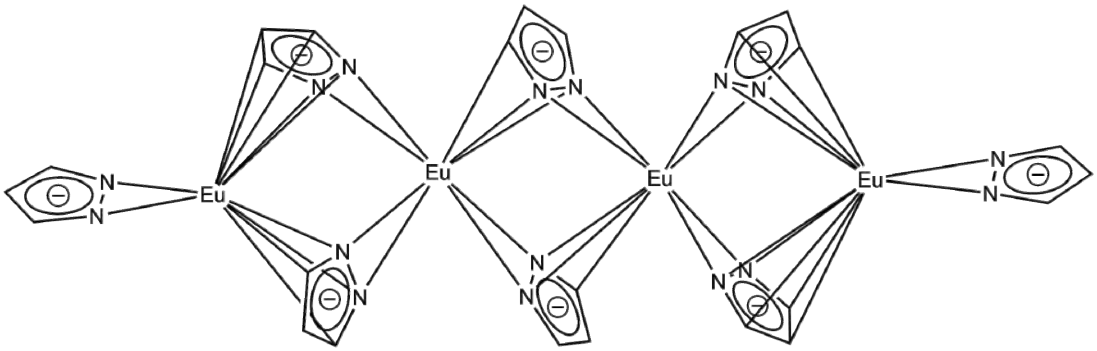

Figure 3-3. The structure of $[Eu_4(tBu_2pz)_8]$;[9] *t*Bu groups removed for clarity.

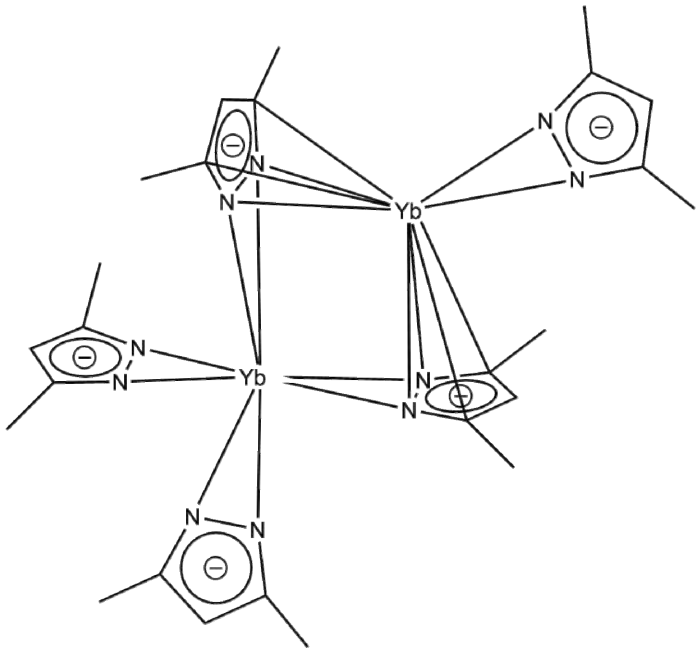

Figure 3-4. The structure of $[Yb_2(tBu_2pz)_5]$;[8] *t*Bu groups removed for clarity.

By the reaction of europium metal with a melt of pyrazole, bright yellow crystals of $[Eu(pz)_2(pzH_2)]_\infty$ were obtained as the first unsubstituted pyrazolate and the first unsubstituted Cp analogue complex of rare earth elements.[28] Showing the versatility of this synthetic method, homoleptic rare earth dipyridylamides $[Ln_2(N(NC_5H_4)_2)_6]$ (Ln = Ce, Nd, Sm, Ho, Er, Tm, Yb and Sc) were obtained using elevated temperature reactions.[29]

Moreover, several homoleptic bimetallic alkali metal-Ln-pyrazolate complexes have been successfully prepared in which some new pyrazolate coordination modes to both the

alkali and lanthanoid metals were established.[11, 30] Three new charge-separated bimetallic complexes [Na(18-crown-6)(dme){Sm(*t*Bu$_2$pz)$_4$}].PhMe, [Na(B18-crown-6)(dme){Nd(*t*Bu$_2$pz)$_4$}].PhMe (B18-crown-6 = benzo-18-crown-6) and [Na(B18-crown-6)(dme){Yb(*t*Bu$_2$pz)$_4$}]$_2$ were isolated by extraction of the [LnNa$_3$(*t*Bu$_2$pz)$_6$]$_n$ (Ln = Nd, Sm, Yb) with the appropriate crown ether and DME/toluene.[31] In all the reported charge-separated bimetallic complexes, [Ln(*t*Bu$_2$pz)$_4$] was surrounded solely by four η^2-*t*Bu$_2$pz nitrogen-bonded ligands (Figure 3-5).

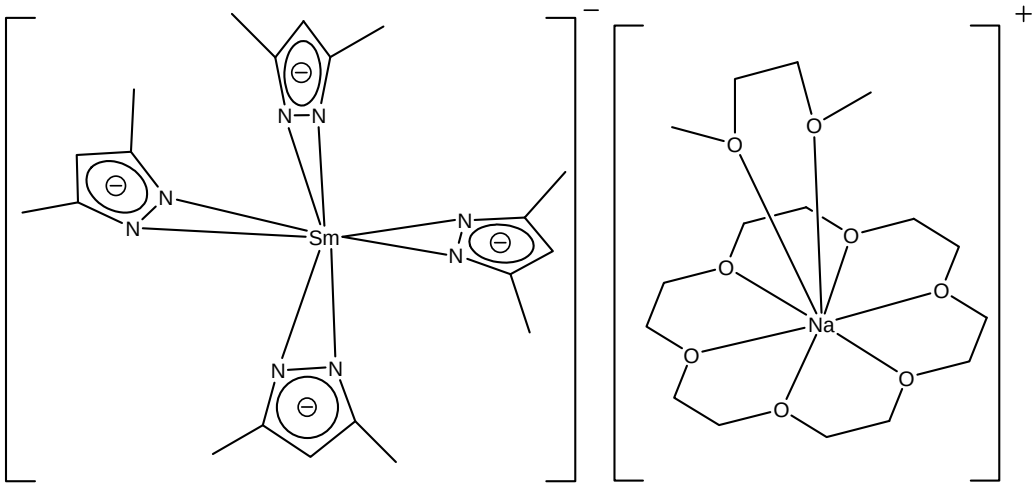

Figure 3-5. The structure of [Na(18-crown-6)(dme){Sm(*t*Bu$_2$pz)$_4$}].PhMe; methyl groups of *t*Bu groups and H atoms removed for clarity.

3.1.1 Current study

This chapter discusses the synthesis and structural characterisation of a variety of rare earth pyrazolate complexes using three different pyrazoles: 3,5-dimethylpyrazole (Me_2pzH), 3,5-di-*tert*-butylpyrazole (*t*-Bu_2pzH) and 3,5-diphenylpyrazole (Ph_2pzH). There are some notable developments in this study such as isolation of the homoleptic $[La(Me_2pz)_3]_n$ which has bridging η^2:η^5-Me_2pz bonding modes with a twelve-coordinate lanthanum. Isolation of another heteroleptic complex ($[Pr(Ph_2pz)_2(Ph_2pz(SiMe_2O))]_2$) bearing a fragment derived from silicon grease in the structure which is a notable feature in this study since previously, reactions with silico-grease has been reported as a result of RTP reaction with scandium and cerium.[32] Also, using the bulkiest *t*Bu_2pzH among the three ligands resulted in the isolation of the isomorphous $[Ln(tBu_2pz)_3]_2$ (Ln= Er and Ce) compounds despite their different ionic radii as was expected from previously reported structures.[9]

3.2 Results and discussion

Glossary of compounds and codes

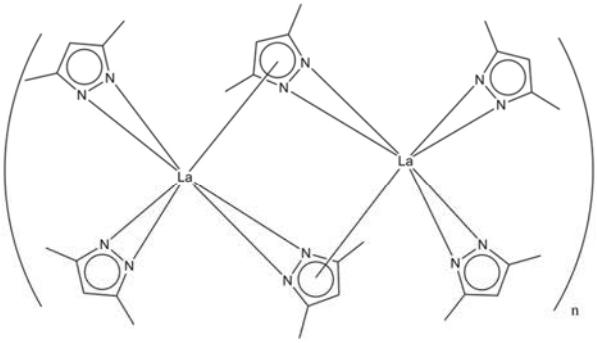

$[La(Me_2pz)_3]_\infty$ (**3.1**)

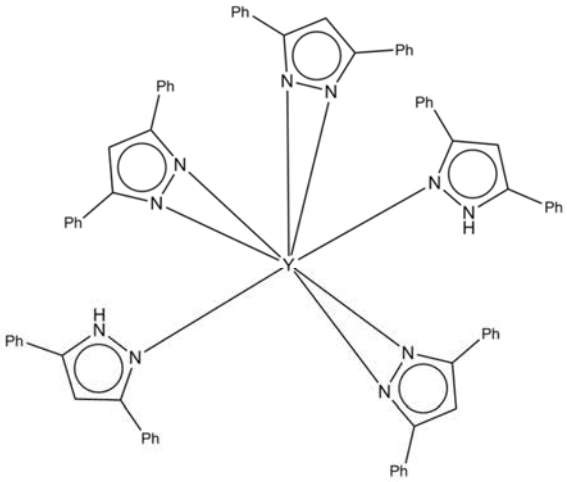

$[Y(Ph_2pz)_3(Ph_2pzH)_2]$ (**3.2**)

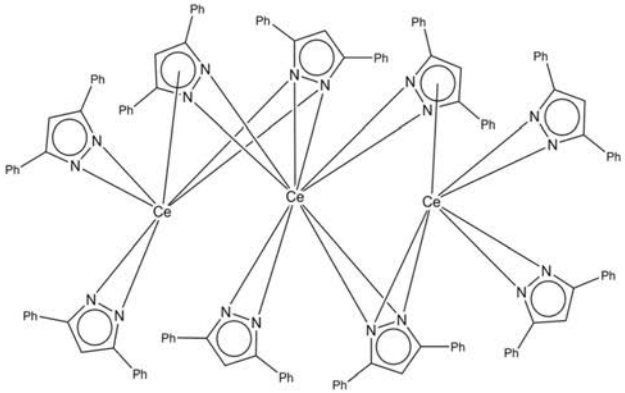

$[Ce_3(Ph_2pz)_9]$ (**3.3**)

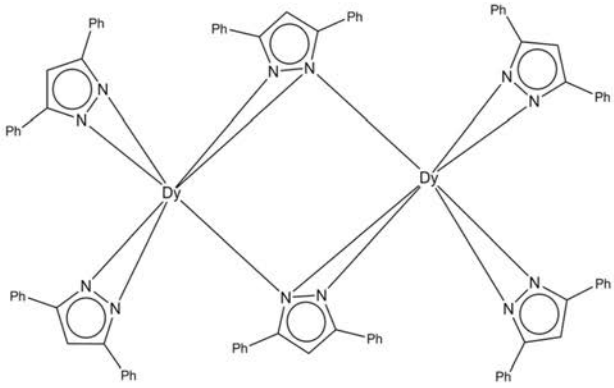

$[Dy_2(Ph_2pz)_6]$ (**3.4**)

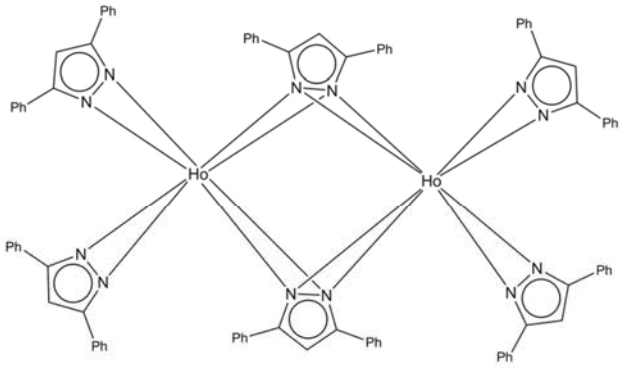

$[Ho_2(Ph_2pz)_6]$ (**3.5**)

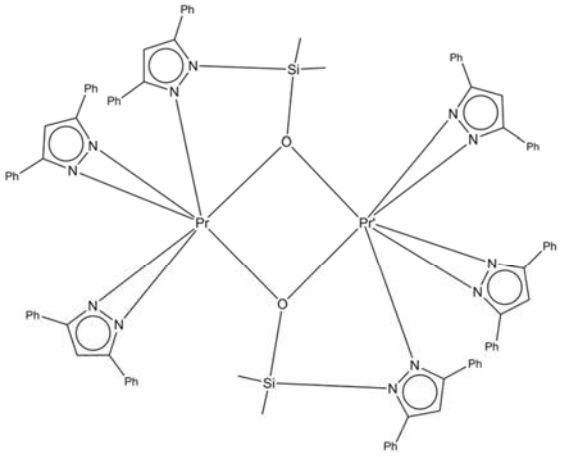

$[Pr(Ph_2pz)_2(Ph_2pz(SiMe_2O))]_2$ (**3.6**)

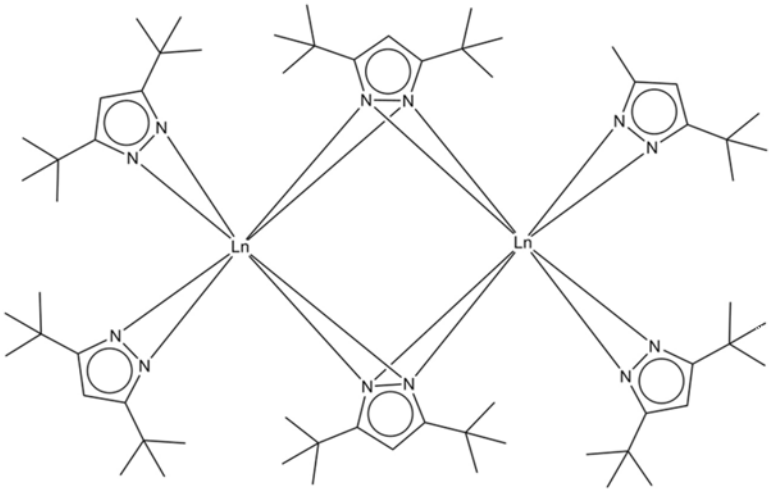

Ln = Ce, Er

$[Ce(t\text{Bu}_2pz)_3]_2$(**3.7**)

$[Er(t\text{Bu}_2pz)_3]_2$(**3.8**)

3.2.1 Synthesis and characterisation

Direct thermal reactions were performed using rare earth metals (RE = Sc, Y and La-Lu) , Me_2pzH, tBu_2pzH and Ph_2pzH and several drops of Hg. The reagents were sealed under reduced pressure in a Carius tube at $\approx 10^{-2}$ Torr and heated at 200-300ºC over 336 hours, resulting in various homoleptic and heteroleptic complexes (Equation 3.5).

$$Ln + nLH \xrightarrow[200\text{-}300^{\circ}C]{Hg} Ln(L)n + n/_2\ H_2$$

LH = Me_2pzH, tBu_2pzH and Ph_2pzH

Ln = Sc, Y and La-Lu

Equation 3.5

Addition of mercury metal has been shown previously to be an important reagent in these direct syntheses as it is necessary to activate the lanthanoid metals by forming an amalgam on the metal surface.[6, 17] Although it was difficult to obtain pure crystalline material due to contamination of the crystals with excess metal filings or powder, using non-polar solvents was not suitable either due to the insolubility of most of the reagents in these solvents. Extraction with toluene, which is the common solution for extracting product of the elevated temperature reactions, is not always possible because of the limited solubility of some complexes.[11] Using a polar solvent (DME or THF) can sometime alter the crystal composition.[11, 33, 34] Therefore, to isolate the product, the reaction mixture was cooled down to the melting point of the ligand. The excess of unreacted reagents were sublimed to the other side of the tube in a temperature gradient starting from the melting point of ligand to room temperature in 3 h to give the crystals of the final products. Also, the usage of a flux in the reaction process was sometimes necessary because an inert flux can provide the suitable reaction environment. Three different fluxes, 1,2,4,5-tetramethylbenzene, 1,3,5-triphenylbenzen and 1,2,3,4-tetrahydroquinoline, were investigated in this study. Among the three mentioned fluxes, 1,2,4,5-tetramethylbenzene worked best during the reactions. Since all the reported products in this study were handpicked crystals, microanalysis data could not be obtained due to the contamination of the crystals with excess Ln metal or flux. Moreover, solubility limitations preclude the determination of NMR spectra in C_6D_6.

IR was performed as Nujol mulls. It should be considered that unlike other pyrazoles,

Ph_2pzH does not have a distinct ν(NH) adsorption and this is probably a consequence of its existence in a hydrogen-bonded tetrameric form,[35] as ν(NH) adsorption of hydrogen-bonded N-H bonds are often broadened.[36] Infrared spectra are therefore not very useful for establishing complete deprotonation and coordination of the Ph_2pz^- ion. However, IR spectra comparison with the previously reported structures provides evidence for complex formation. The presence of the absorption at ea. 3342 cm^{-1} for complex **3.2 (**[$Y(Ph_2pz)_3(Ph_2pzH)_2$]) justifies the presence of Ph_2pzH in the structure. Also, the presence of absorption at 3346 cm^{-1} and 3236 cm^{-1} for complexes **3.7** ([$Ce(t Bu_2pz)_3]_2$) and **3.8** ([$Er(t Bu_2pz)_3]_2$) respectively is due to an impurity of $t Bu_2pzH$ in the isolated complexes.

3.2.2 X-ray crystal structure determinations

Single crystals of all the following reported structures except complex [$La(Me_2pz)_3$](**3.1**) were obtained directly from the Carius tubes and mounted on glass fibres. A series of homoleptic and heteroleptic complexes are reported and discussed using Ph_2pzH as ligand. Moreover, for the first time a structure containing silicon from a high temperature reaction is reported in this study ([$Pr(Ph_2pz)_2(Ph_2pz(SiMe_2O))]_2$ (**3.6**)). Complexes [$Ce(t Bu_2pz)_3]_2$ (**3.7**) and [$Er_2(Ph_2pz)_6$] (**3.8**) are isotypic and are discussed together.

3.2.2.1 3,5-dimethylpyrazolate complexes (Me_2pz)

Previous attempts to isolate homoleptic complexes [$Ln(Me_2pz)_3$] using the elevated temperature reactions were problematic since crystals could not be directly obtained from the high temperature reactions. The product of the reactions to isolate [$Ln(Me_2pz)_3$] was not toluene soluble and THF, which is a more polar solvent, was used to extract the final product.[33] [$La(Me_2pz)_3$(thf)] was isolated after extraction which was similar to the previously reported [$La(Me_2pz)_3$(thf)][37] compound obtained from RTP reaction. However, in this study, the isolation of the homoleptic $[La(Me_2pz)_3]_n$ shows another surprising ligation for lanthanoid pyrazolates. Previously, no complex using 3,5-dimethylpyrazolate in elevated temperature reactions were reported. Figure 3-6 and Figure 3-7 shows the fascinating X-ray crystal structure of [$La(Me_2pz)_3$] (**3.1**).

The lanthanum metal centre is surrounded by three near-planar $\eta^2(N,N')$ Me_2pz

ligands, (Figure 3-7), and the polymer is grown by two Me_2pz ligands (N1/N2 & N3/N4) which engage in additional μ-η^5(N_2C_3) coordination with two different adjacent symmetry equivalent lanthanum atoms (Figure 3-6, La1′ and La1″).

The η^5 coordination of the Me_2pz ligands in the axial positions, gives the lanthanum centre a coordination number of 12, and a simplified geometry best described as distorted trigonal bi-pyramidal (Figure 3-7) (if the centroids of the axial η^5-pz rings and the N-N centroids of the equatorial pz ligands are considered).

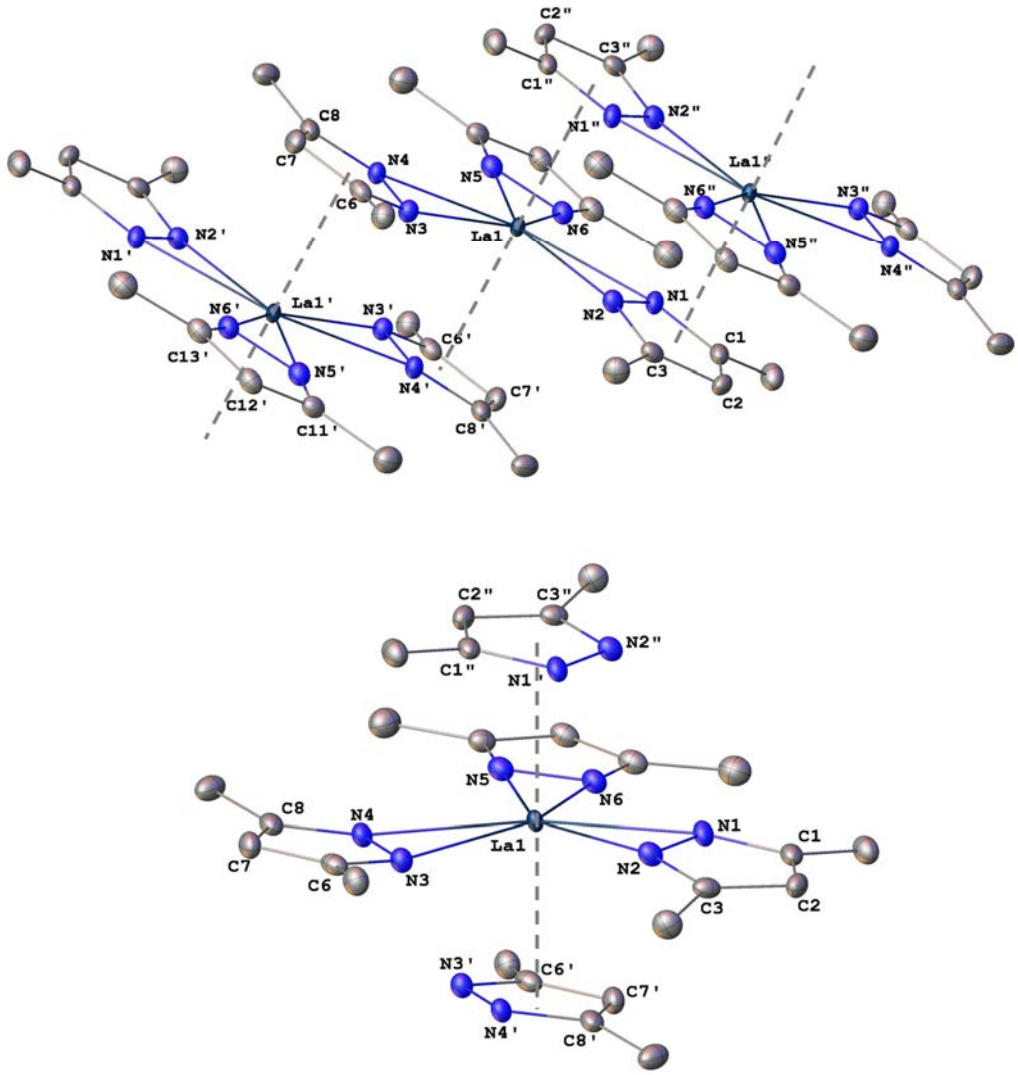

Figure 3-6. X-ray crystal structure of $[La(Me_2pz)_3]_\infty$ (**3.1**). Top: view from alongside the polymer down the *a* axis, bottom: bonding around the La centre. Ellipsoids shown at 50% probability, hydrogen atoms removed for clarity.

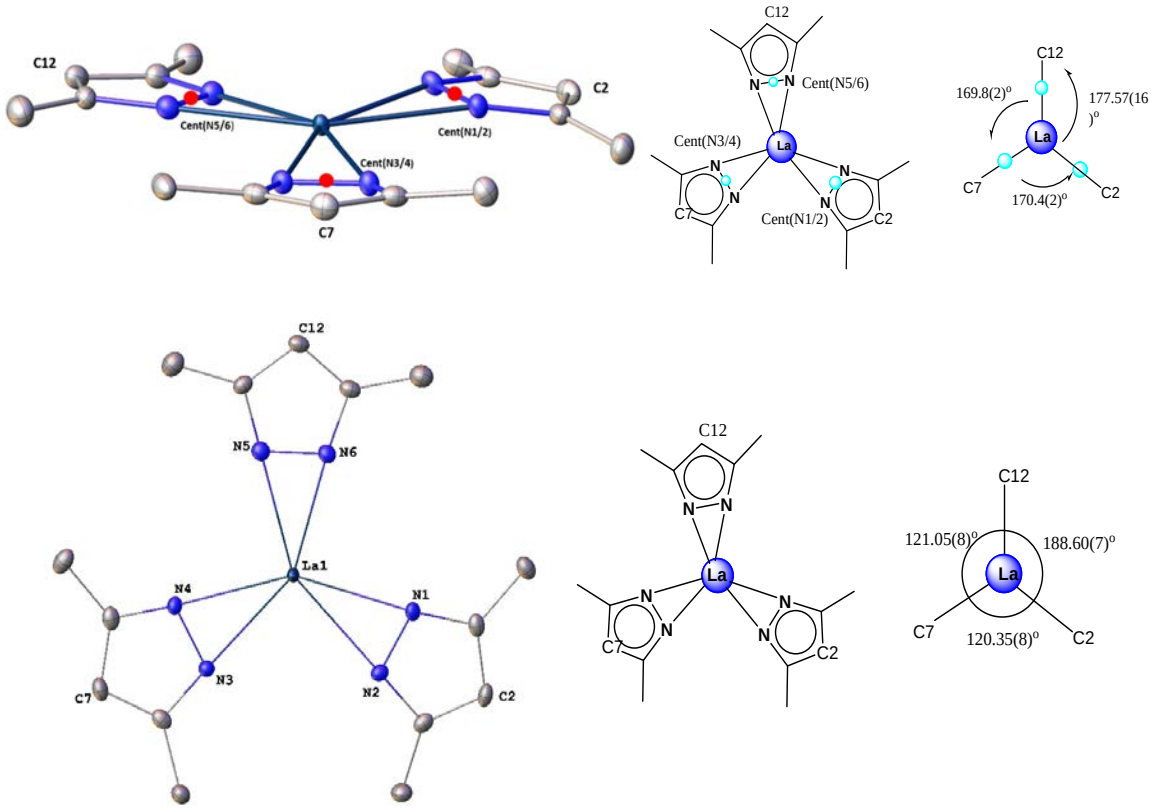

Figure 3-7. Asymmetric unit of **3.1** showing the Me_2pz ligands are not coplanar (top), but are arranged in a near trigonal planar manner around the La centre (bottom).

The η^5 bonding is supported by comparison with similar La–C bond lengths ([La(Odbp)$_3$], [$Me_2Si(C_{13}H_8)(C_5H_4BNEt_2)$]LaI(THF) and [$La_2(Odbp)_6$]),[17, 38, 39] and gives the Me_2pz ligands a "cyclopentadienyl (Cp)" type coordination, that has only a few examples in rare earth pz chemistry.[28, 40-42]

Examining the previously reported [$Ln(Me_2pz)_3(thf)]_2$ (Ln = La, Ce, Pr)[40] complexes shows that they exhibit two μ-$\eta^2(N,N')$:$\eta^5(N_2C_3)$ Me_2pz ligands, along with four terminal $\eta^2(N,N')$ Me_2pz, capped by two terminal thf ligands.

Figure **3-8** shows these dimeric thf derivatives.

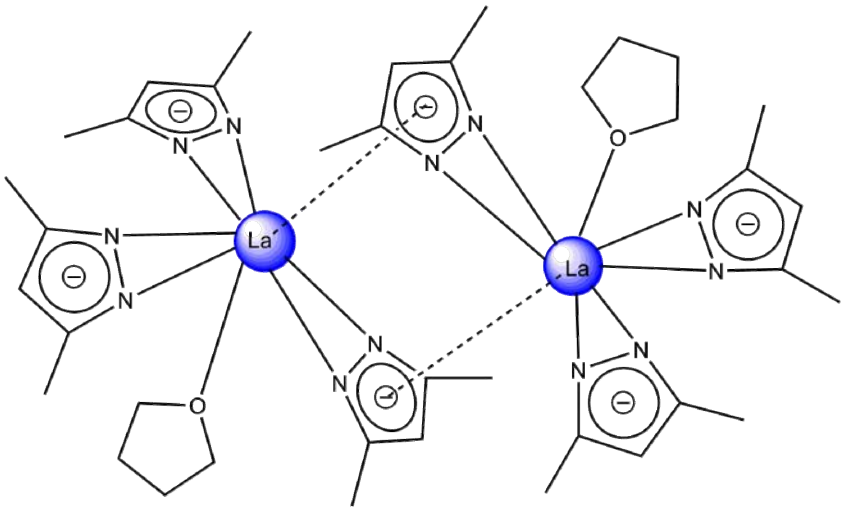

Figure 3-8. [La(Me$_2$pz)$_3$(thf)]$_2$ having coordination mode of μ-η^2(*N*,*N*′):η^5(*N*$_2$*C*$_3$) Me$_2$pz ligands, along with four terminal η^2(*N*,*N*′) Me$_2$pz.[40]

Comparing the complex **3.1 (**[La(Me$_2$pz)$_3$]) with the previously reported divalent [Eu(pz)$_2$(pz-H)$_2$]$_\infty$[28] shows the presence of η^5-Cp binding mode in both of them. The Eu-N distances in [Eu(pz)$_2$(pz-H)$_2$]$_\infty$ range from 2.65 Å for Pz amides to 2.73-3.10 Å for pyrazolate-N donor bond and N atoms participating in the η^5-coordination. However, the La-N distances in **3.1** range from 2.516 to 3.245 Å (Table 3-1) and are comparable to the Eu-N distances in complex [Eu(pz)$_2$(pz-H)$_2$]$_\infty$. This may be due to the different coordination numbers and different oxidation states of the metal centres.

Table 3-1. Selected bond lengths (Å) and angles (º) of **3.1**.

Bond lengths			
La(1)–N(1)	2.587(4)	La(1)–C(6′)	3.137(5)
La(1)–N(2)	2.599(4)	La(1)–C(7′)	3.245(6)
La(1)–N(3)	2.617(3)	La(1)– C(8′)	3.114(5)
La(1)–N(4)	2.566(3)	La(1)-Cent(N1′-C5′)	2.821(2)
La(1)–N(5)	2.516(3)	La(1)-Cent(N3′-C8′)	2.872(2)
La(1)–N(6)	2.475(3)		
Bond angles			
Cent(N3′-C8′)-La1-Cent(N1′-C5′)	177.04(4)		
Cent(N1-C5)-La1-Cent(N1′-C5′)	92.98(5)		
Cent(N1-C5)-La1-Cent(N6′-C8′)	88.65(5)		

Considering the interest to examine if the coordination geometry in complex **3.1** extends to the other rare earth metals, attempts were performed using the high temperature synthesis with cerium metal. At the end of the reaction, a yellow product was observed in the tube. No suitable crystals were formed directly after cooling the sealed tube slowly. Hot toluene was used to extract the product. The final light yellow amorphous material was insoluble in C_6D_6, toluene-d_8 and THF-d_8 and no ^1H NMR could be obtained. Perhaps the insolubility of the product is due to the formation of a polymeric structure. Comparisons between the IR of the isolated yellow product and the complex **3.1** indicates a different composition. Attempts were done to run the X-ray as well. Although the sample gave reflections (a = 18.06 Å, b = 18.06 Å, c = 4.25 Å, α = 90º, β = 90º, γ = 120º), the structural solution appeared unsolvable. Also, the sample seemed reasonably resilient to oxidation, as in the crystallography oil it did not change colour, which is unlike $[Ce(Me_2pz)_3]$[40, 43] species. Therefore, it seems that it is some polymeric species, but it does not appear to have pz in it anymore. In the olex2 solution, a (Me)C(=N)-CH-C(Me)(=N) type ligand could be observed which means the pz ligand was perhaps broken up. Unfortunately, the solution of the crystal structure was not of good quality.

3.2.2.2 3,5- diphenylpyrazolate complexes (Ph_2pz)

A change in the steric demands of the ligands in homoleptic complexes can lead to different binding modes. A series of homoleptic and heteroleptic rare earth complexes with 3,5-diphenylpyrazole (Ph_2pzH) has been reported previously.[10, 16] To investigate the effect of changing the bulkiness of 3,5-substituents on the pyrazolate ligand on the final product, attempts have been made to isolate some unreported rare earth complexes involving 3,5-diphenylpyrazole as the ligand.

Figure 3-9 depicts the crystal structure of heteroleptic $[Y(Ph_2pz)_3(Ph_2pzH)_2]$ complex (**3.2**) which is isostructural to the previously reported $[Ln(Ph_2pz)_3(Ph_2pzH)_2]$ (Ln = La, Nd, Gd, Yb).[16] The complex is an eight-coordinate monomer with three chelating η^2-Ph_2pz and two unidentate η^1-Ph_2pzH ligands. Bond distances for complex **3.2** are listed in Table 3-2. The complex crystallises in the monoclinic space group *C2/c* with the metal atom disposed on a crystallographic *2*-axis, that also passes through the midpoint of N(21)-N(21´) bond and C(24) of the pyrazolate ring ligand (2) (Figure 3-9 bottom). The Y atom is co-planar with the ring plane of ligand 2 (Figure 3-9 top) and symmetrically η^2-coordinated by its two nitrogen

atoms. Moreover, although ligand 1 and 1´ are tilted slightly away from co-planarity with the axis, the *2*-axis relates the pair.

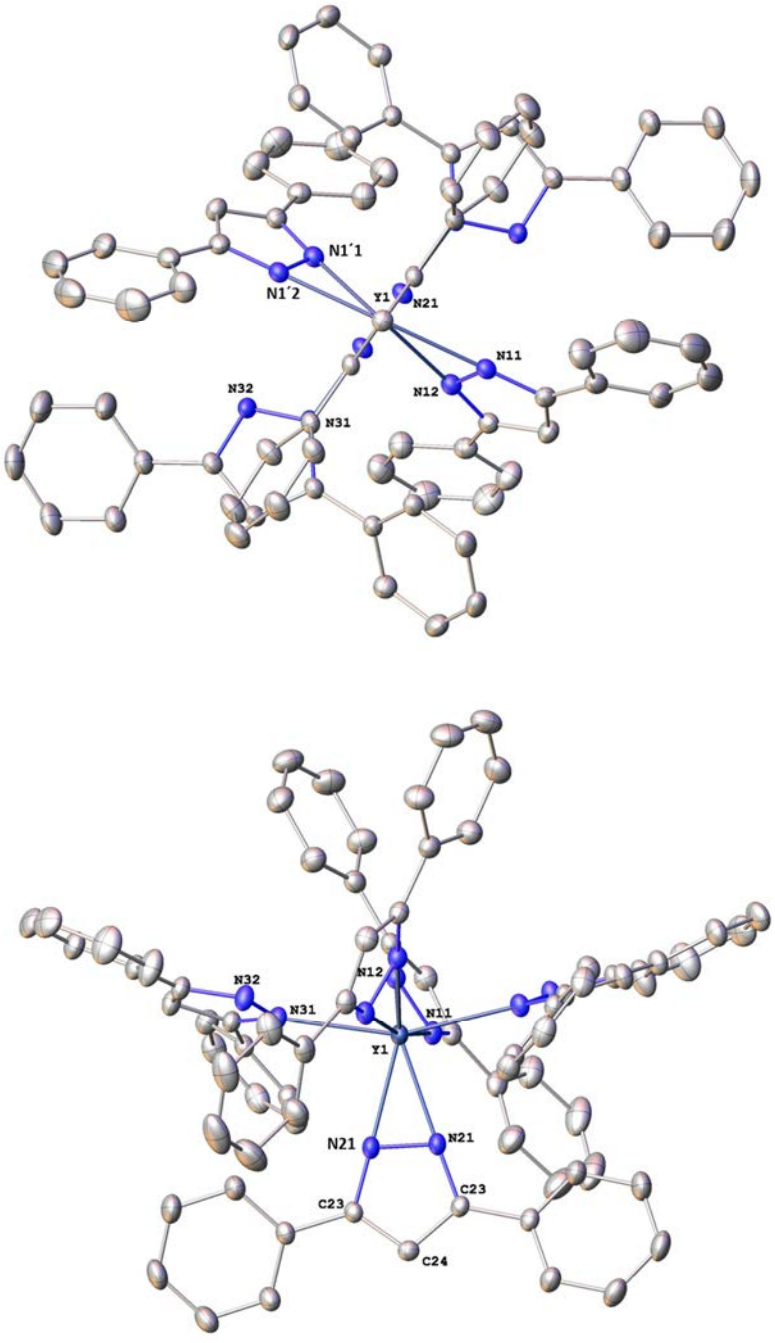

Figure 3-9. Top: Projection of [Y(Ph$_2$pz)$_3$(Ph$_2$pzH)$_2$] (**3.2**) down the *2*-axis. Bottom: Projection of [Y(Ph$_2$pz)$_3$(Ph$_2$pzH)$_2$] normal to the *2*-axis. Ellipsoids shown at 50% probability and H atoms are removed for clarity.

The Y-N(Ph_2pz) distance (2.336 Å) is shorter than Ln-$N_{terminal}$ for the [Ln(Ph_2pz)$_3$(Ph_2pzH)$_2$] (Ln = La, Nd and Gd). On the other hand, the Y-$N_{terminal}$ is somewhat longer than the average Yb-N distance (2.32 Å)[16] in the ytterbium complex due to the smaller ionic radius of eight-coordinate Yb^{3+} compared with Y^{3+}.[44]

Complex **3.2** can be viewed as having a distorted trigonal bipyramidal geometry, if the centres (Cent) of the N-N bonds of the η^2-pyrazolate ligands are treated as unidentate donors. These occupy equatorial sites, and the η^1-Ph_2pzH ligands apical positions with an average bond angles of 158.75º for N(31)-Y-N(31´), which is comparable with N(Ph_2pz)-Ln-N(Ph_2pz) (159.7º) in [Ln(Ph_2pz)$_3$(Ph_2pzH)$_2$] (Ln = La, Gd and Nd). Moreover, complex **3.2** is similar to the previously reported [Y(Ph_2pz)$_3$$thf_2$][22], an eight-coordinate monomer, where the thf ligands replace the unidentate Ph_2pzH ligands.

Table 3-2. Selected bond lengths and angles for complex **3.2**.

Bond length Å			
Y(1)-N(11)	2.367(6)	Y(1)-N(21)	2.346(6)
Y(1)-N(12)	2.355(4)	Y(1)-N(31)	2.561(6)
Bond angles^o			
N(31)-Y-N(31´)	158.75	N(12)-Y-N(11)	33.88

Continuing with the rare earth series using cerium metal and Ph_2pzH resulted in the isolation of [Ce_3(Ph_2pz)$_9$] (**3.3**) (Figure 3-10) in a non-linear (bowed) trinuclear arrangement, which has been observed previously with La and Nd.[16] Ce(1) and Ce(3) atoms are linked to a central Ce(2) atom by two terminal η^2-3,5-diphenylpyrazolate ligands each through a pair of bridging pyrazolate ligands (μ-η^2:η^2). The central cerium (Ce (2)) has one η^2-pyrazolate ligand. A quasi-2-axis bisects Ce (2) and the associated terminal ligand which is bonded via a η^2 bonding mode (N9/N10). Attachment of this donor group is accompanied with the non-linear Ce_3 array (Ce…Ce…Ce 136.744(4) º). With ten nitrogen donor atoms, trivalent Ce(2) is similar to the previously reported trivalent ten-coordinate cerium-pyrazolate complex ([Ce(Me_2pz)$_4$]$_2$).[43] Ce (2) atom in complex **3.3** is ten-coordinated with coordination to one terminal η^2-pyrazolate and four μ-η^2:η^2 –bridging Ph_2pz ligands. Ce (1) and Ce (3) have only eight nitrogen donors. The closely similar Ce-N distances for the terminal η^2-Ph_2pz groups of Ce (1-3) (Table 3-3) suggest that the differences of coordination number between Ce(1,3)

and Ce(2) is not that significant. Figure 3-10 (bottom) shows that ligands 4 and 7 are tilted from the usual position for η^2:η^2-bonding towards Ce (1) and Ce (3), respectively. Bridging ligands 4 and 7 are nearly parallel with the terminal ligands 1 and 8, respectively and their planes intersect the Ce (1, 3)…Ce (2) line at *ca*. 45º. Ligands 4 and 7 are nearly coplanar with Ce (2) indicative of σ- η^2 bonding. Four of the terminal ligands are symmetrically η^2 attached (Table 3-3) with the difference between bond lengths of Ce (*n*1)-N (*n*1) and Ce-N (*n*2) (n = 1, 2, 5 and 9) less than 0.02 Å. Ligand 8 is slightly unsymmetrically chelated with bond length differences of 0.1 Å. Ligand 9 on the eight-coordinate Ce (3) is the most symmetrically bound (Table 3-3).

The μ-η^2:η^2 and μ-η^5:η^2 ligands in $[Ce_3(Ph_2pz)_9]$ chelate (η^2) Ce(2) in an unsymmetrical fashion (Table 3-3). The differences between Ce (2)-N (*n*1) and Ce (2)-N (*n*2) (*n* = 3, 4, 6, 7) range from 0.16 Å to 0.33 Å, though the upper limit is well below the highest reported value for unsymmetrical η^2-bonding (0.45-0.60 Å).[11, 45, 46] Ligands 3 and 6 (μ-η^5:η^2 bonded) are more symmetrically chelated to Ce (1) and Ce (3) and the Ce (1, 3)-N distances for the η^5-bonded ligands 4, 7 are close to each other (Table 3-3). Bridging of the μ-η^2:η^2 ligands is unsymmetrical, with N (31) and N (61) closer to Ce (1, 3) than to the more crowded Ce (2). On the other hand, N (32) and N (62) are somewhat closer to Ce (2). A lack of excessive crowding at ten-coordinate Ce (2) is suggested by the Ce (2)-N (51, 52) distances of the terminal ligand 5 (Table 3-3) which is away from the adjacent ligands (Figure 3-10 bottom).

Table 3-4 shows the distances of the Ce(1,3)…C(ligand 4,7), which are close to the previously reported values for $[Ln_3(Ph_2pz)_9]$ (Ln = La, Nd)[16] and supports the presence of μ-η^5:η^2-coordination. Thus, the Ce(1,3)-C distances are comparable with those in the previously reported complex **3.1** ($[La(Me_2pz)_3]_\infty$) in this study , (2.87(4)-3.13(4) Å) for the η^5-pyrazolate-La, and also with the μ-η^5:η^2 Cp ligands in $[LaCp_3]_n$.[47] Moreover, subtraction of ionic radii[44] of eight-coordinate Ce^{3+} from the Ce-C(pz) distances (Table 3-4) gives 1.78-1.97 Å (av. 1.87 Å) which matches well with those of reported $[Ln_3(Ph_2pz)_9]$ (Ln = La, Nd)(1.81-2 Å).[16]

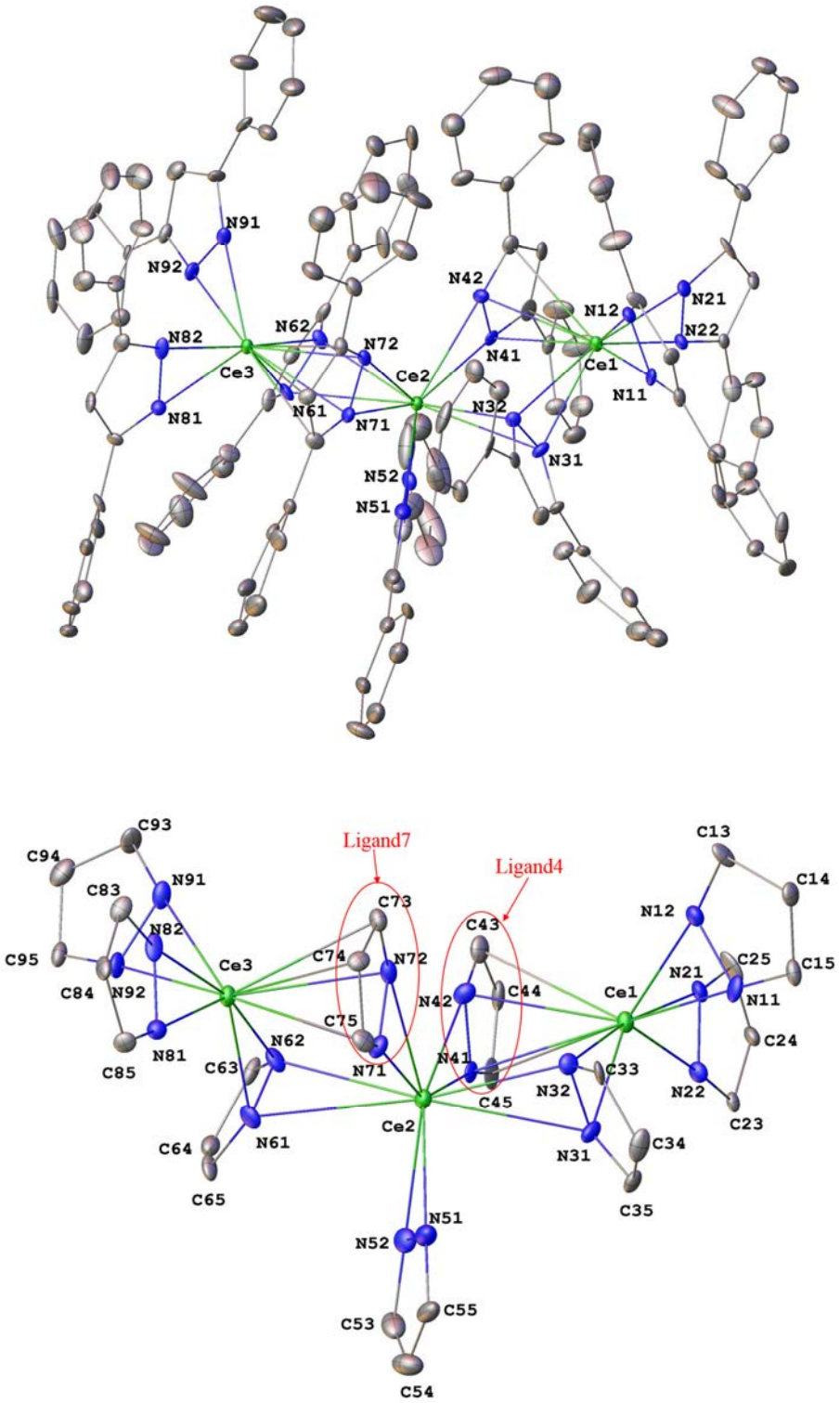

Figure 3-10. *Top*: The X-ray crystal structure of $[Ce_3(Ph_2pz)_9]$ (**3.3**) Down: projection of 3.3 normal to its quasi-2-axis showing μ-η^5:η^2 binding of pyrazolate ligands 4 and 7;

ellipsoids shown at 50% probability and H atoms are removed for clarity.

Table 3-3. Selected bond distances in $[Ce_3(Ph_2pz)_9]$ (**3.3**) (Å).

Ce (1) environment		Ce (2) environment		Ce (3) environment	
Atom	Bond length	Atom	bond length	Atom	bond length
N11	2.44(2)	N31	2.83(2)	N61	2.55(2)
N12	2.41(2)	N32	2.55(2)	N62	2.72(2)
N21	2.39(2)	N41	2.524(19)	N71	2.67(2)
N22	2.447(19)	N42	2.68(2)	N72	2.692(19)
N31	2.56(2)	N51	2.40(2)	N81	2.52(2)
N32	2.704(19)	N52	2.41(2)	N82	2.424(18)
N41	2.742(17)	N61	2.88(2)	N91	2.43(2)
N42	2.71(2)	N62	2.60(2)	N92	2.433(19)
		N71	2.502(19)		
		N72	2.81(2)		

Table 3-4. Ce(1,3)…C(pz) (ligand 4,7) distances (Å) for $[Ce_3(Ph_2pz)_9]$ and the corresponding residual values Δr (Å) obtained by the subtraction of the ionic radii[44] for eight-coordinate Ce^{3+} from Ce(1,3)…C(pz) distances.

Bond	length	Δr	bond	Length	Δr
Ce(1)…C(43)	2.93(3)	1.78	Ce(3)…C(73)	2.97(2)	1.82
Ce(1)…C(44)	3.12(19)	1.97	Ce(3)…C(74)	3.11(2)	1.96
Ce(1)…C(45)	3.02(2)	1.87	Ce(3)…C(75)	2.98(3)	1.83

Comparing complex **3.3** with the reported complex $[Ce(Me_2pz)_4]_2$ by Werner[43] shows that in $[Ce(Me_2pz)_4]_2$ the cerium atoms are coordinated by three terminal (Ce-$N_{av.,term}$: 2.36 Å) and two μ-η^2:η^2 –bridging Me_2pz ligands (Ce-$N_{av.,bridg}$: 2.60 Å), making each cerium atom ten-coordinate. However, Ce (2) atom in complex **3.3** is ten-coordinated with coordination to one terminal η^2-pyrazolate and four μ-η^2:η^2–bridging Ph_2pz ligand. Interestingly, trivalent $[Ce(Me_2pz)_3(thf)]_2$, where Ce^{3+} is smaller than Ce^{4+} by 0.18 Å, is also ten-coordinate,[40] but the bridging Me_2pz ligands are μ-η^2 (*N,N´*):η^5 (N_2C_3) bonded,

contrasting the μ-η^2 (*N,N´*):η^2 (*N,N´*) bonding in **3.3** ([$Ce_3(Ph_2pz)_9$]). Although previously trinuclear homoleptic [$Ln_3(Ph_2pz)_9$] complexes (Ln = La, Nd) have been reported,[16] this is the first time that a trinuclear homoleptic cerium pyrazolate compound is reported. Similar to compound **3.3**, the central atom in the [$Ln_3(Ph_2pz)_9$] (Ln = La, Nd) is ten coordinate.

The dysprosium complex of [$Dy_2(Ph_2pz)_6$] (**3.4**) is displayed in Figure 3-11. The isolated structure of holmium [$Ho_2(Ph_2pz)_6$] (**3.5**) is very similar to **3.4**. Both complexes are dimeric with two terminal η^2-Ph_2pz ligands. Although both of them have two bridging Ph_2pz groups, complex **3.4** ([$Dy_2(Ph_2pz)_6$]) has μ-η^2:η^1 –Ph_2pz bond while complex **3.5** (**[**$Ho_2(Ph_2pz)_6$]) contains μ-η^2:η^2 –Ph_2pz as a bridging ligand which is in good agreement with the difference between the ionic radii of Dy^{3+} and Ho^{3+} (0.97 Å and 1.015 Å respectively).[44] Therefore, Dy metal in complex **3.4** is seven-coordinate while Ho metal centres are eight-coordinate in complex **3.5** (Figure 3-11 and Figure 3-12). Furthermore, complex [$Dy_2(Ph_2pz)_6$] crystallises in the triclinic space group *P-1* with one and half dimer within the asymmetric unit while complex [$Ho_2(Ph_2pz)_6$] crystallises in the monoclinic space group *P21/c* with one molecule within the asymmetric unit. There is a little variation in Ln-$N_{terminal}$ bond lengths within each of the two structures (Table 3-5). All the four terminal ligands chelate in a symmetrical fashion (Table 3-5) in complex **3.4** and **3.5** with the variation in the corresponding Ln-N(*n*1)/Ln-N(*n*2) distances ranging from zero (Ln = Ho(1), *n* = 2) to 0.033 Å (Ln = Ho(1), *n* = 1). The average Ln-$N_{terminal}$ is 2.29 Å and 2.28 Å for Dy and Ho respectively, which is larger than the one for the Lu (2.25 Å).[16] The Dy…Dy separation and Ho…Ho separation is larger than that in [$Ln(Me_2pz)_3(thf)]_2$ (Ln = Dy and Ho),[40] consistent with enlarged steric crowding due to the larger Ph_2pz ligands. Similarly, the average Ln-N_{bridge} in **3.4** and **3.5** is larger than Ln-N_{bridge} in [$Ln(Me_2pz)_3(thf)]_2$. The bridging ligands in **3.5** chelate the metal centres more symmetrically than the μ-η^2:η^2 ligands in complex **3.3** ([$Ce_3(Ph_2pz)_9$]) and also it is more symmetrically for Ho(1) than Ho(2) (Table 3-5).

The pyrazolate planes of the bridging ligands in complex **3.4** are inclined to the Dy…Dy axis (tilt angles are 78.12(3)º and 77.41(3)º). In contrast, the pyrazolate planes of the bridging ligands in **3.5** lie quasi-normal (90.6(2)-91.9(2)º) to the Ho(1)…Ho(2) line in complex **3.5**. Thus, according to Figure 3-12 bottom, the terminal Ph_2pz ligands are disposed unsymmetrically in a helical fashion relative to the Ho-Ho line. By contrast with complex **3.3** ([$Ce_3(Ph_2pz)_9$]), there are no close Ln…C contacts in complex **3.5**. The greater inclination in complex **3.4** rather than **3.5** affect the disposition of the terminal ligands (Figure 3-11 bottom).

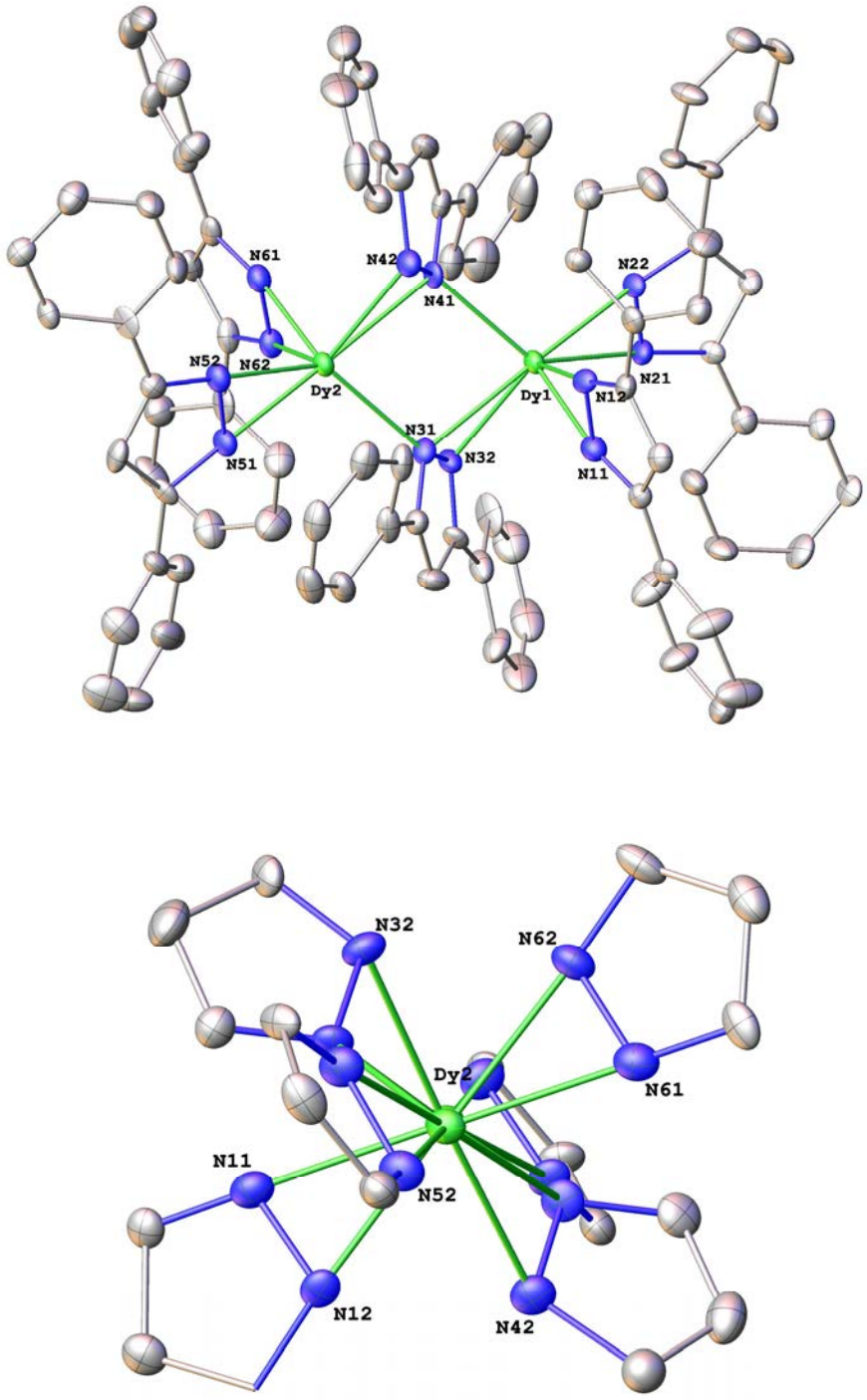

Figure 3-11. Top: crystal structure of $[Dy_2(Ph_2pz)_6]$ (**3.4**) normal to the Dy…Dy line. Ellipsoids shown at 50% probability, hydrogen atoms removed for clarity. Bottom: projection of $[Dy_2(Ph_2pz)_6]$ down the Ho…Ho line. Phenyl groups omitted in the bottom projection.

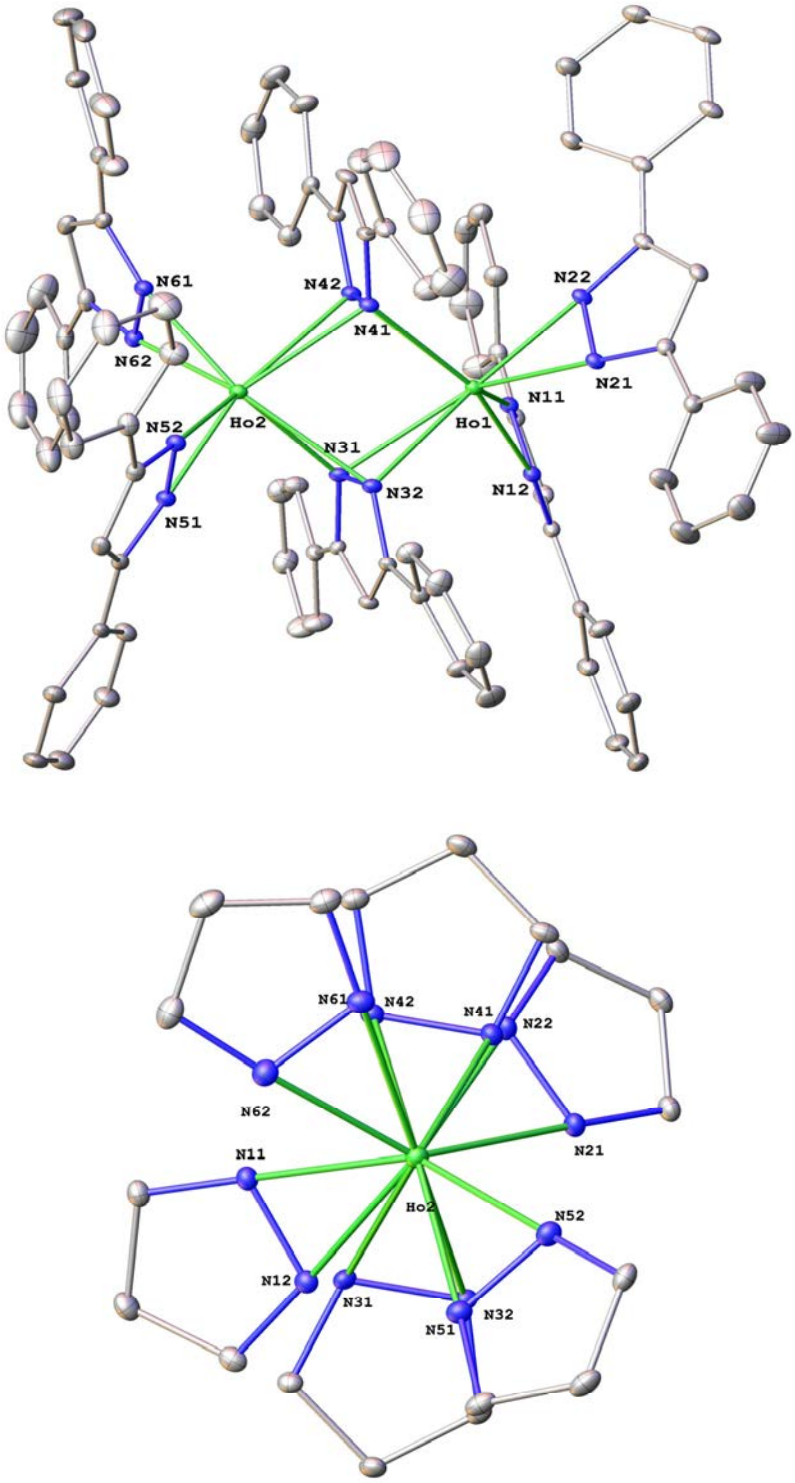

Figure 3-12. Top: crystal structure of [$Ho_2(Ph_2pz)_6$] (**3.5**) normal to the Ho…Ho line. Ellipsoids shown at 50% probability, hydrogen atoms removed for clarity. Bottom: projection of [$Ho_2(Ph_2pz)_6$] down the Ho…Ho line. Phenyl groups omitted in the bottom projection.

Table 3-5. Selected bond distances in complex **3.4** and 3.5 (Å).

Ln (1) environment			*Ln (2) environment*		
Atoms	*Bond lengths*		***Atoms***	*bond lengths*	
	Dy	***Ho***		***Dy***	***Ho***
Ln(1)-N11	2.305(14)	2.254(3)	Ln(2)-N51	2.266(13)	2.265(6)
Ln(1)-N12	2.301(11)	2.287(4)	Ln(2)-N52	2.297(13)	2.297(6)
Ln(1)-N21	2.311(12)	2.288(3)	Ln(2)-N61	2.295(14)	2.297(7)
Ln(1)-N22	2.284(13)	2.288(3)	Ln(2)-N62	2.298(12)	2.294(5)
Ln(1)-N31	2.505(13)	2.498(3)	Ln(2)-N41	2.525(12)	2.449(3)
Ln(1)-N32	2.399(13)	2.501(3)	Ln(2)-N42	2.409(14)	2.600(3)
Ln(1)-N41	2.445(12)	2.473(4)	Ln(2)-N31	2.470(12)	2.404(4)
Ln(1)-N42	-	2.422(4)	Ln(2)-N32	-	2.545(4)

As mentioned before, a series of compounds using lanthanoid metals (La, Nd, Gd, Tb, Er and Yb) with Ph_2pzH have been reported.[16] Praseodymium was expected to have a similar crystal structure to La and Nd as it falls between those two elements in the Ln series. Surprisingly treating praseodymium with Ph_2pzH in a solid state reaction resulted in another heteroleptic complex **3.6** ($[Pr(Ph_2pz)_2(Ph_2pz(SiMe_2O))]_2$) (Figure 3-13) having silicon in the structure. It is the first time that a complex having a silanoxide-pyrazolate ligand from sealed tube reaction has been prepared. It is expected that dimethylsilicon grease, used as a sealant while sealing the high temperature test tubes, upon work up was depolymerized by the reactive praseodymium pyrazolate species. Complex **3.6** crystallises in the monoclinic system with half a dimer within the asymmetric unit. Each praseodymium is ligated by a pair of terminal η^2 pyrazolate ligands, and the complex is centrosymmetric in which two silanoxide-Ph_2pz ligands cap at two opposite ends of the dimer. The anionic oxygen of the silanoxide ligand is bridging between the two praseodymium atoms (Figure 3-13). The seven-coordinate praseodymium atom has a trigonal bipyramid coordination environment considering the centre of the N-N vector of the pz ligands as binding sites. The four nitrogen atoms are nearly in the same plane with the praseodymium atom and the oxygen atom is located below the plane (Cent (N11/12)-Pr1-Cent (N21/22) = 135.29º,

Cent (N11/12)-Pr1-O1 = 99.86º and Cent (N21/22)-Pr1-O1 = 98.12º) (Table 3-6).

The difference between the coordination number of seven in complex **3.6** and ten in the reported $[Pr(Me_2pz)_3(thf)]_2$[40] can be due to the different steric bulk of Ph_2pz and Me_2pz ions. Furthermore, the environment around the Pr metals is similar to previously reported complex ($[Sc(Me_2pz)_2(Me_2pz(SiMe_2O))]_2$.solv) in chapter 2 despite the smaller size of Sc and less steric bulkiness of Me_2pz compared with Ph_2pz.

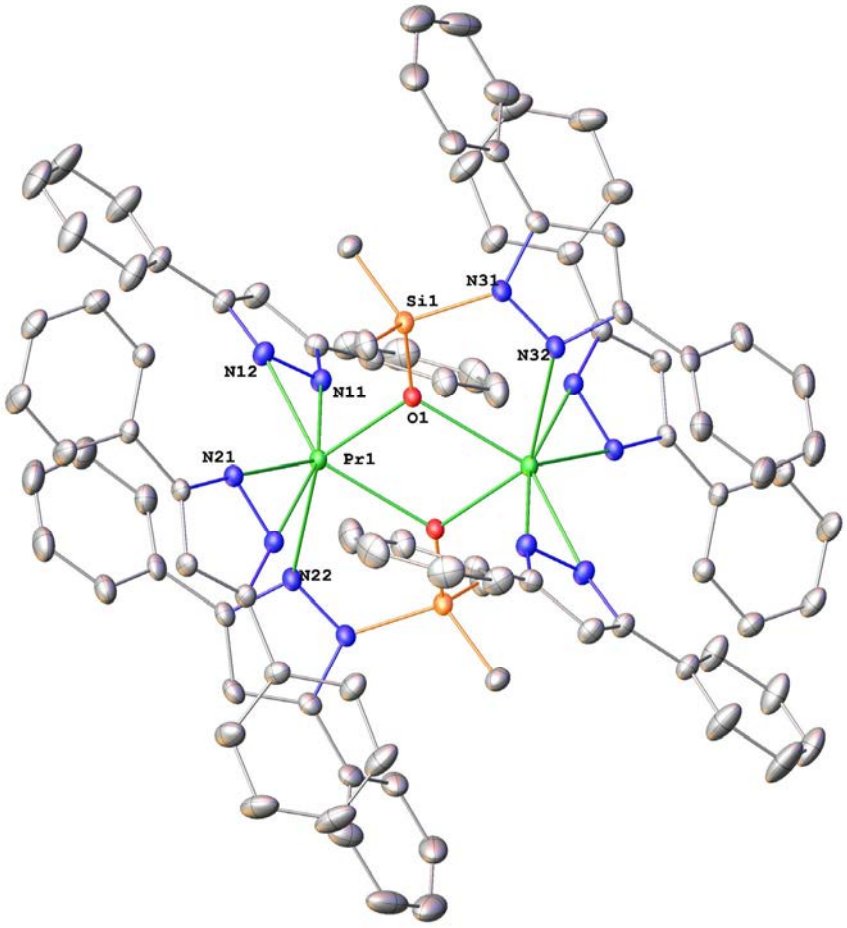

Figure 3-13. Crystal structure of $[Pr(Ph_2pz)_2(Ph_2pz(SiMe_2O))]_2$ (**3.6**). Ellipsoids shown at 50% probability, hydrogen atoms removed for clarity.

The Pr-O and Pr-N bonds lengths of **3.6** given in Table 3-6 are larger than the values reported for the related ($[Sc(Me_2pz)_2(Me_2pz(SiMe_2O))]_2$.solv) (chapter 2). Also comparing the average bond lengths of Pr-N of the terminal ligand in complex $[Pr(Me_2pz)_3(thf)]_2$ (2.444 Å) with those in the complex **3.6** (2.453 Å) shows that although the coordination around Pr in the two complexes is different, it did not affect the bond lengths of terminal ligands. The bite angles N (11)-Pr-N(12) (32.75(10)º) and N(21)-Pr-N(22) (32.69(3)º) are similar to the

previously reported compounds (**3.2** ([$Y(Ph_2pz)_3(Ph_2pzH)_2$]) and **3.3** ([$Ce_3(Ph_2pz)_9$])) but they are smaller than the bite angle of N-Sc(1)-N in complex [$Sc(Me_2pz)_2(Me_2pz(SiMe_2O))]_2$.solv) (37.045(13)º) which can be due the bulkier Ph_2pzH compared with Me_2pzH.

Table 3-6. Selected bond lengths (Å) and angles (º) of **3.6**.

Bond lengths Å			
Pr(1)-N(11)	2.461(6)	Pr(1)-N(21)	2.490(9)
Pr(1)-N(12)	2.438(6)	Pr(1)-N(31)	2.423(7)
Pr(1)-O(1)	2.358(5)		
Bond anglesº			
Cent(N11/12)-Pr1- Cent(N21/22)	135.28(9)	Cent(N21/22)-Pr1-O1	95.12(2)
Cent(N11/12)-Pr1-O1	99.86(3)	N(12)-Pr-N(11)	32.75(10)
N(21)-Pr-N(22)	32.69(3)		

3.2.2.3 3,5-di- tert-butylpyrazolate rare earth complexes (tBu2pz)

Previous results that were reported in this study using Me_2pzH and Ph_2pzH, showed different complexes with new bonding modes and new features. The homoleptic rare earth pyrazolate complexes involving the *t*Bu_2pz ligands, [$Sc(tBu_2pz)_3$], [$Ln_2(tBu_2pz)_6$] (Ln = La, Nd, Sm, Lu), [$Eu_4(tBu_2pz)_8$] and [$Yb_2(tBu_2pz)_5$], have been reported.[9] Therefore, the bulkier *t*Bu_2pzH was used in this study as well to isolate new compounds and investigate the effect of steric bulkiness of the ligand while completing the rare earth series for the homoleptic compounds.

While using cerium as the metal in the solid state reaction, a compound was isolated similar to its neighbours in the lanthanoid series.[43, 48] Figure 3-14 shows the isolated crystal structure of [$Ln(tBu_2pz)_3]_2$ (Ln = Ce) (**3.7**) which is similar to the previously reported complexes of [$Ln_2(tBu_2pz)_6$] (Ln = La, Nd, Lu, Yb).[9] Each cerium ion is eight coordinate with two terminal η^2-pyrazolate ligands and two bridging μ-η^2:η^2 ligands. Considering the structure **3.7** (Figure 3-14, bottom) when it is viewed down the Ce…Ce* axis (* denotes the inversion relation), it can be seen that there is incomplete overlap between 3* and 2 and between 2* and 3 and the bridging ligands (1, 1*) are twisted to either side. This can result from accommodation of the bulkiness of the *tert*-butyl groups that is consistent with

dodecahedral stereochemistry about the metals.

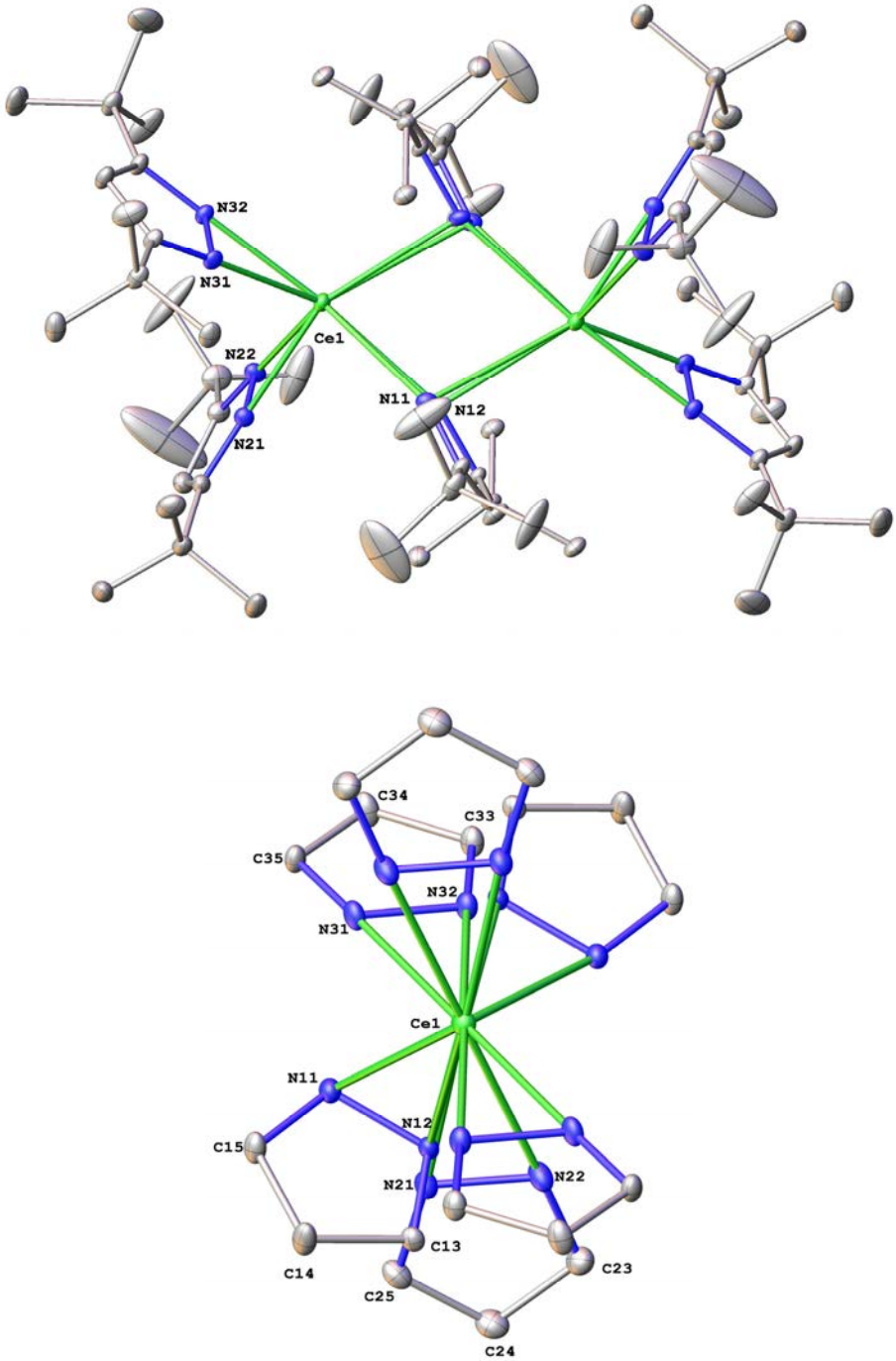

Figure 3-14. Top: crystal structure of [Ce(*t*Bu$_2$pz)$_3$]$_2$ (**3.7**) normal to the Ce…Ce vector. Ellipsoids shown at 50% probability, hydrogen atoms removed for clarity. Bottom: projection of [Ce(*t*Bu$_2$pz)$_3$]$_2$ down the Ce…Ce vector; *tert*-butyl groups are removed for clarity.

The bridging ligands lie with the pyrazolate plane quasi-normal to the Ce…Ce* axis. This is clearly evident from the angle between the Ce…Ce* vector and the C3N2 plane of the bridging ligand (ligand 1; 86.28(3)º) .The terminal ligands are symmetrically η^2 coordinated with the maximum variation in Ce-N (21) and Ce-N (22) bond lengths of 0.07Å (Table 3-7). The terminal Ce-N (average = 2.434 Å) bond lengths are close to the previously reported $[La(t\text{Bu}_2\text{pz})_3]_2$ (average = 2.453 Å) which is consistent with the small difference in radii between eight coordinate La^{3+} and Ce^{3+} but is higher than the $[Ln(t\text{Bu}_2\text{pz})_3]_2$ (Ln = Nd, Yb and Lu) which is in agreement with the reduction in the radius for eight coordinate Ln^{3+} from Ce^{3+} to Lu^{3+}.[44] Thus, chelation is unsymmetrical with the difference between Ce-N (11) and Ce-N (12) and between Ce*-N (11) and Ce*-N (12) of 0.114, 0.139 Å respectively (Table 3-7). Also, comparing the mentioned bond difference with the previously reported bond difference in $[Ln(t\text{Bu}_2\text{pz})_3]_2$ (Ln = Nd, Yb and Lu)[9] shows that the asymmetry in chelation increased with reduction in Ln^{3+} size which is consistent with increased steric strain. Comparing the values for the N(N1)-Ce-N(n2) bite angles (Table 3-7) with the previously reported structures[9] show the expected increase with the decrease in lanthanoid ion size for both bridging and terminal pyrazolate ligands.

The μ-η^2:η^2 binding has been observed previously in this study in complex **3.5** ($[Ho_2(Ph_2pz)_6]$). Also, recently this binding has been observed in $[Ce(Me_2pz)_4]_2$ which was obtained via a protolysis reaction employing the silamide precursor ($Ce[N(SiHMe_2)_2]_4$).[43] The terminal (term) bond lengths and bridging bond lengths in **3.7** ($Ce\text{-}N_{av.,\ bridge:}$ 2.677 Å and $Ce\text{-}N_{av.,\ term}$: 2.434 Å) are larger than bonds in $[Ce(Me_2pz)_4]_2$ which can be due to the higher coordination number in $[Ce(Me_2pz)_4]_2$ and different oxidation state of cerium in two compounds. Moreover, in the same research, by protolysis of $Ce[N(SiMe_3)_2]_3$ with three equivalents of $t\text{Bu}_2\text{pzH}$, the trivalent complex $[Ce(t\text{Bu}_2\text{pz})_3]_2$ was reported. Comparing the terminal ligand bonds and bridging ligand bonds in both structures shows similar values.

Table 3-7. Selected bond distances (Å) and bond angles (º) in complex **3.7**.

Bond length Å			
Ce-N(11)	2.656(3)	Ce-N(21)	2.395(4)
Ce-N(12)	2.542(3)	Ce-N(22)	2.466(4)
Ce-N(11*)	2.824(3)	Ce-N(31)	2.458(4)
Ce-N(12*)	2.686(3)	Ce-N(32)	2.419(3)
Ce-Ce*	4.089(9)		
Bond angles^{o}			
N(11)-Ce-N(12)	31.05(12)	N(31)-Ce-N(32)	33.47(12)
N(21)-Ce-N(22)	33.17(14)	N(11*)-Ce-N(12*)	29.2(14)

[Er(*t*Bu$_2$pz)$_3$]$_2$ (**3.8**) is structurally similar to its Ln neighbours. Similar to previously isolated structures, **3.8** crystallises in the triclinic space group *P-1* with half a dimer within asymmetric unit. The erbium atoms are each ligated by a pair of terminal η^2-*t*Bu$_2$pz anions and two μ-η^2:η^2 ligands, so that the Er^{3+} can be considered as eight-coordinate. Since angle between Er-Er* line and the C_3N_2 plane of the bridging ligands is 90.51(3)º, the bridging ligand is less tilted compared with the one in the complex **3.7** ([Ce(*t*Bu$_2$pz)$_3$]$_2$) (86.28(3)º) and previously reported complexes.[9] Comparing the structure of **3.8** (Figure 3-15) with the structure of **3.7**, when they are viewed down the Ln…Ln* axis, shows that although there is incomplete overlap between 3* and 2 and between 2* and 3 in complex **3.7**, there is almost complete overlap between the terminal ligands in complex **3.8**.

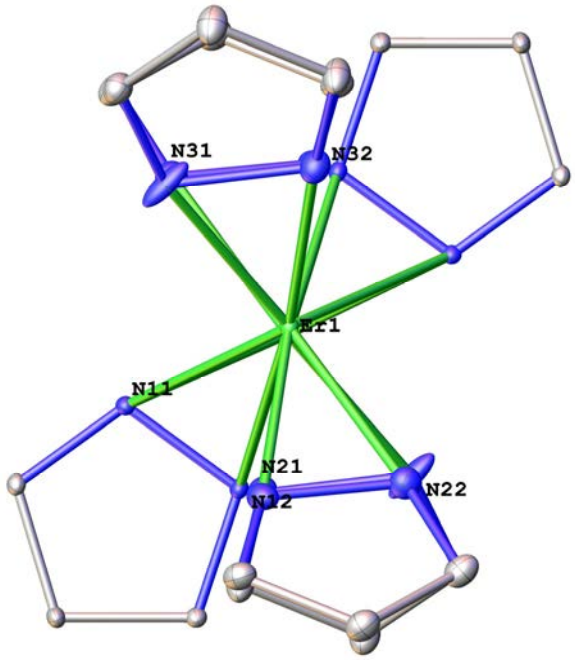

Figure 3-15. Projection of [Er(*t*Bu$_2$pz)$_3$]$_2$ (**3.8**) down the Er…Er vector; *tert*-butyl groups removed for clarity.

Bond lengths differences of terminal Er-N (Table 3-8) with the previously reported isomorphous structures are consistent with the difference between ionic radii for eight-coordinated Ln^{3+} from La^{3+} to Er^{3+}.[9, 44] Values for the bite angles (Table 3-8) show the expected increase with decrease in lanthanoid ion size for both bridging and terminal pyrazolate comparing complex **3.8** and **3.7**.

Table 3-8. Selected bond distances (Å) and bond angles (º) in complex **3.8**.

Bond length Å			
Er-N(11)	2.535(6)	Er-N(21)	2.254(10)
Er-N(12)	2.458(6)	Er-N(22)	2.287(8)
Er-N(11*)	2.571(6)	Er-N(31)	2.359(10)
Er-N(12*)	2.465(6)	Er-N(32)	2.299(10)
Er-Er*	3.650 (6)		
Bond anglesº			
N(11)-Er-N(12)	32.458 (14)	N(31)-Er-N(32)	36.2(3)
N(21)-Er-N(22)	38.08(4)	N(11*)-Er-N(12*)	32.155(4)

Both η^2 and μ-η^2:η^2 bonds are present in the compound [Er(*t*Bu$_2$pz)$_3$]$_2$ (**3.8**). Similar bonding modes have been observed in the [Na(*t*Bu$_2$pzH){Er(*t*Bu$_2$pz)$_4$}].PhMe.[11] The bite angles are larger than those of [Na(*t*Bu$_2$pzH){Er(*t*Bu$_2$pz)$_4$}].PhMe complex. Also comparing the Er-N bond lengths in both complexes shows almost similar bond lengths since Er in both complexes is eight-coordinate (Er-N $_{avg.\ term}$: 2.31 Å & Er-N $_{avg.bridg}$: 2.417Å vs Er-N $_{avg.\ term}$: 2.29 & Er-N $_{avg.bridg}$: 2.50Å bond lengths in [Na(*t*Bu$_2$pzH){Er(*t*Bu$_2$pz)$_4$}].PhMe and **3.8** respectively). Moreover, previously eight-coordinate erbium structures have been reported having η^2-pyrazolate bond. Comparing complex **3.8** with the previously reported structure [Er(tBu$_2$pz)$_3$(dme)] (chapter 2) shows the larger bite angle in complex **3.8** which can be due to the absence of coordinate solvent ligand but the Er-N$_{avg.}$ of η^2 bonds are similar in both structures.

Attempts have been made to isolate suitable crystals for X-ray using gadolinium, dysprosium and holmium which failed due to the inability to get X-ray quality crystals. However, it can be assumed that [Ln$_2$(*t*Bu$_2$pz)$_6$] can be isolated with the mentioned metals considering the trend of [Ln$_2$(*t*Bu$_2$pz)$_6$] structures from La-Lu.

3.2.3 Concluding remarks

The direct reaction between lanthanoid metals and three kinds of pyrazole (3,5-dimethyl pyrazole, 3,5-diphenylpyrazole and 3,5-di-*tert*-butylpyrazole) is a simple route to isolate homoleptic and heteroleptic rare-earth pyrazolates. Due to the less steric bulkiness of 3,5-dimethylpyrazole, a homoleptic twelve-coordinate structure has been synthesized which is an η^2:η^5-Me_2pz-bridged coordination polymer with 12-coordinate La atoms in an η^5:η^5 Me_2pz sandwich. A decrease in steric demand in homoleptic complexes can lead to unusual bonding modes as some coordination sites are no longer blocked. The lower coordination numbers of nine and eight occurred using bulkier 3,5-diphenylpyrazole. Moreover, both homoleptic and heteroleptic complexes have been isolated using 3,5-diphenylpyrazole. Among the varied structures observed, the most notable feature are the bowed trinuclear arrangement in $[Ce_3(Ph_2pz)_9]$ (**3.3**) ,which has both μ-η^2:η^2 and μ-η^2:η^5 bonding modes with Ph_2pz ligands, and a higher coordination number for the central than the terminal Ce atoms. Also, the isolation of heteroleptic $[Pr(Ph_2pz)_2(Ph_2pz(SiMe_2O))]_2$ (**3.6**) was similar to a previously isolated Sc compound despite the smaller size of Sc and less steric bulkiness of Me_2pz compared with Ph_2pz. The higher coordination number of compounds using 3,5-dimethylpyrazole and 3,5-diphenylpyrazol than 3,5-di-*tert*-butylpyrazolate complexes are clearly indicative of reduction in bulkiness from *t*Bu_2pz to Me_2pz.

With considering reported structure in this chapter, it can be assumed that the series of possible complexes from elevated temperature reaction using rare-earth elements and 3,5-diphenylpyrazole and 3,5-di-*tert*-butylpyrazole is almost complete. However, due to the isolation of $[La(Me_2pz)_3]_n$, this work is incomplete using the less bulky 3,5- dimethyl pyrazole which may result in some new pyrazolate binding modes.

3.3 Experimental

3.3.1 General considerations

All the lanthanoid metals and their products are air-sensitive and moisture-sensitive, and therefore required manipulation in an inert atmosphere using a glove box, Schlenk flask and vacuum line techniques. All solvents were pre-dried and deoxygenated by refluxing and distillation over sodium or sodium/benzophenone. The lanthanoid metal reagents were purchased as fine powders or metal ingots from Rhone Poulenc or Santoku. Metal ingots were freshly filed under an inert atmosphere into metal filings. 3,5-dimethylpyrazole (Me_2pzH) was purchased from Sigma-Aldrich and 3,5-diphenylpyrazole (Ph_2pzH) and 3,5-di-*tert*-butylpyrazole (*t*-Bu_2pzH) were prepared by literature methods.[49, 50] IR data were obtained from Nujol mulls for the region 4000-400 cm^{-1} with a Nicolet-Nexus FT-IR spectrometer. The intensity of transmittance in IR data is reported as vw(very weak), w(weak), m(medium), s(strong) and vs(very strong).

Rare earth metal and pyrazolate ligand and flux were sealed in a Carius tube at $\approx 10^{-2}$ Torr. The Carius tube was heated between 220-270ºC up to 336 hours. A thermocouple was used to control the temperature of the furnace precisely. For isolating the product, the reaction mixture was cooled down to the melting point of ligand. In this way the excess of unreacted reagents were sublimed to the other side of the tube in a temperature gradient from melting point of ligand to room temperature in 3 h to give the crystals of final products. In the case that crystals could not be hand-picked directly after reaction, the complex was extracted with hot toluene. No NMR details could be obtained due to insolubility of some of the complexes or the possibility of reaction between complex and NMR solvent. Also, microanalysis could not be obtained for complexes due to metal filings (or powder) contaminating the crystal surface.

3.3.2 Synthesis of 3,5-dimethylpyrazolate complexes

$[Ln(Me_2pz)_3]_\infty$ (3.1):

La (0.14 g, 1.0 mmol), Me_2pzH (0.15 g, 1.5 mmol) and 1,2,4,5-tetramethylbenzene (0.20 g, 1.5mmol, used as flux) were sealed in a Carius glass tube under vacuum. The tube was heated at 220 °C for 78 h. The reaction mixture was extracted with hot toluene (10mL) to give a colourless solution, which was reduced in volume (*in vacuo*). After a few hours,

colourless single crystals of $[La(Me_2pz)_3]_\infty$ (**3.1**) formed and were suitable for structural determination by X-ray crystallography. IR (Nujol): ν = 3105 (w), 1554 (w), 1515 (s), 1300(m), 1282 (m), 1068(w), 1036 (m), 1004(m), 957(m), 866(w), 792(m), 776(m), 729(m), 681 cm^{-1}(m). No NMR details could be obtained due to insolubility of the compound.

3.3.3 Synthesis of 3,5-diphenylpyrazlate complexes

$[Y(Ph_2pz)_3(Ph_2pzH)_2]$ (**3.2**):

Y (0.04 g, 0.226 mmol), Ph_2pzH (0.15 g, 1.5 mmol) and 1,2,4,5-tetramethylbenzene (0.20 g, 1.5mmol, used as flux) and mercury metal (two drops) were sealed in a Carius glass tube under vacuum. The tube was heated at 250-270 °C for 336 h. colourless crystals were hand-picked for structural determination by X-ray crystallography. IR (Nujol): ν = 3340 (w), 2726(m), 1605 (m), 1532 (w), 1304(w), 1154 (m), 1071(m), 1019 (w), 1002(vw), 968(m), 912(w), 833(vw), 812(vw), 799(vw), 755(m), 722(m), 703(vw), 684 cm^{-1}(w).

$[Ce_3(Ph_2pz)_9]$ (**3.3**):

Ce (0.063 g, 0.226 mmol), Ph_2pzH (0.15 g, 1.5 mmol) and 1,2,4,5-tetramethylbenzene (0.20 g, 1.5mmol, used as flux) and mercury metal (two drops) were sealed in a Carius glass tube under vacuum. The tube was heated at 250-270 °C for 336 h. yellow crystals were hand-picked for structural determination by X-ray crystallography. IR (Nujol): ν = 2726 (m), 1602 (vw), 1304(m), 1155 (m), 1072(w), 1021 (vw), 967(m), 916(vw), 836(w), 722 cm^{-1}(s).

$[Dy_2(Ph_2pz)_6]$ (**3.4**):

Dy (0.064 g, 0.226 mmol), Ph_2pzH (0.15 g, 1.5 mmol) and 1,2,4,5-tetramethylbenzene (0.20 g, 1.5mmol, used as flux) and mercury metal (two drops) were sealed in a Carius glass tube under vacuum. The tube was heated at 250-270 °C for 336 h. Crystals were hand-picked for structural determination by X-ray crystallography. IR (Nujol): ν = 2727 (w), 1603 (m), 1562 (w), 1535(vw), 1294 (m), 1221(w), 1155 (m), 1072(m),

1054(w), 1024(m), 999(w), 968(s), 914(m), 844(w), 805(w), 753(vs), 722(vs), 686 cm^{-1}(m).

$[Ho_2(Ph_2pz)_6]$ (**3.5**):

Ho (0.064 g, 0.226 mmol), Ph_2pzH (0.15 g, 1.5 mmol) and 1,2,4,5-tetramethylbenzene (0.20 g, 1.5mmol, used as flux) and mercury metal (two drops) were sealed in a Carius glass tube under vacuum. The tube was heated at 250-270 °C for 336 h. Pale pink crystals were hand-picked for structural determination by X-ray crystallography. IR (Nujol): ν = 2726 (w), 1605 (m), 1532(m), 1512 (vw), 1337(vw), 1313 (vw), 1282(vw), 1242(m), 1153(m), 1137(w), 1070(vw), 1088(m), 1002(m), 968(m), 911(m), 866(w), 833(w), 811(w), 755(s),703(vw), 683 cm^{-1}(s).

$[Pr(Ph_2pz)_2(Ph_2pz(SiMe_2O))]_2$ (**3.6**):

Pr (0.064 g, 0.226 mmol), Ph_2pzH (0.15 g, 1.5 mmol) and 1,2,4,5-tetramethylbenzene (0.20 g, 1.5mmol, used as flux) and mercury metal (two drops) were sealed in a Carius glass tube under vacuum. The tube was heated at 250-270 °C for 336 h. Pale green crystals were hand-picked for structural determination by X-ray crystallography. IR (Nujol): ν = 3105 (vw), 2726 (w), 1605 (m), 1303(m), 1155 (m), 1072(w), 1022 (w), 963(m), 910(vw), 866(vw), 843(vw), 804(vw), 758(m), 722(m), 686(w), 668 cm^{-1}(w).

3.3.4 Synthesis of 3,5-di-tert-butylpyrazolate complexes

$[Ce(tBu_2pz)_3]_2$ (**3.7**):

Ce (0.1 g, 0.366 mmol), *t*Bu_2pzH (0.2 g, 1.1 mmol) and 1,2,4,5-tetramethylbenzene (0.20 g, 1.5mmol, used as flux) and mercury metal (two drops) were sealed in a Carius glass tube under vacuum. The tube was heated at 270-300 °C for 240 h. Pale yellow crystals were hand-picked for structural determination by X-ray crystallography. IR (Nujol): ν = 3346 (slight impurity) (vw), 2726 (w), 1559 (vw), 1501(w), 1413 (vw), 1303(m), 1251 (m), 1224(m), 1169(vw), 1016(vw), 979(w), 890(vw), 794(m),723 n(s), 668 cm^{-1}(vw).

[Er(*t*Bu$_2$pz)$_3$]$_2$ (3.8):

Er (0.122 g, 0.366 mmol), *t*Bu$_2$pzH (0.2 g, 1.1 mmol) and 1,2,4,5-tetramethylbenzene (0.20 g, 1.5mmol, used as flux) and mercury metal (two drops) were sealed in a Carius glass tube under vacuum. The tube was heated at 270-300 °C for 240 h. Pale pink crystals were hand-picked for structural determination by X-ray crystallography. IR (Nujol): ν = 3236 (w), 2725 (w), 1559 (m), 1506(m), 1305(m), 1251 (m), 1226(w), 1204 (w), 1168(m), 1021(m), 1003(m), 992(m), 890(vw), 866(m), 793(w),722(s), 667 cm^{-1}(vw).

3.3.5 Crystallographic data

Complexes were immersed in viscous hydrocarbon oil (Paraton-N) and measured on either a Bruker APEX II CCD diffractometer/on a 'Bruker P4' diffractometer with integration and absorption corrections completed using Apex II program suite, or at the Australian Synchrotron on the MX1 using a single wavelength (λ = 0.712 Å). The data and integration were completed by Blue ice [51] and XDS [52] software programs. Structural solution were obtained by either direct methods or Patterson method and solution were refined using full matrix least squares methods against F^2 using SHELX2014, via OLEX 2 [53] interface.

[Ln(Me$_2$pz)$_3$]$_\infty$ (3.1): $C_{15}H_{21}LaN_6$, (M = 424.29), triclinic, P-1 (No. 2), a = 7.996(16) Å, b = 10.246(2) Å, c = 10.755(2) Å, α = 71.42(3)°, β = 79.55(3)°, γ = 81.91(3)°, V = 818.1(3) Å^3, T = 100(2) K, Z = 2, Z' = 1, μ (MoK$_\alpha$) = 2.617, 2858 reflections measured, 2858 unique which were used in all calculations. The final wR_2 was 0.069 (all data) and R_1 was 0.0268 (I > 2σ(I)).

[Y(Ph$_2$pz)$_3$(Ph$_2$pzH)$_2$] (3.2): $C_{75}H_{57}N_{10}Y$ (M = 1187.21): monoclinic, $C2/c$ (No. 15), a = 20.0146(6) Å, b = 14.0349(4) Å, c = 22.0146(6) Å, β = 103.986(10)°, α = γ = 90°, V = 6075.9(3) Å^3, T = 296(2) K, Z = 4, Z' = 0.5, μ (MoKa) = 1.013, 36900 reflections measured, 6955 unique (R_{int} = 0.0772) which were used in all calculations. The final wR_2 was 0.1181 (all data) and R_1 was 0.0444 (I > 2σ(I)).

[Ce$_3$(Ph$_2$pz)$_9$] (3.3): $C_{135}H_{99}Ce_3N_{18}$ (M = 2393.68): monoclinic, $P2_1/n$ (No. 14), a = 19.3383(16) Å, b = 20.3172(15) Å, c = 28.831(3) Å, β = 80.226(6)°, α = γ = 90°, V =

11163.5(16) Å^3, T = 296.15 K, Z = 4, Z' = 1, μ (MoKa) = 0.7107, 71731 reflections measured, 19572 unique (R_{int} = 0.2393) which were used in all calculations. The final wR_2 was 0.4144(all data) and R_1 was 0.1483 (I > 2σ(I)).

[Dy$_2$(Ph$_2$pz)$_6$] (**3.4**): $C_{90}H_{66}Dy_2N_{12}$, (M = 2462.82) , triclinic, P-1 (No. 2), a = 13.618(3) Å, b = 18.695(4) Å, c = 23.173(5) Å, α = 70.65(3)°, β = 75.13(3)°, γ = 79.42(3)°, V = 5348(2) Å^3, T = 100(2) K, Z = 2, Z' = 1.5, μ(MoK$_a$) = 2.138, 57348 reflections measured, 25463 unique (R_{int} = 0.0618) which were used in all calculations. The final wR_2 was 0.3649 (all data) and R_1 was 0.1402 (I > 2σ(I)).

[Ho$_2$(Ph$_2$pz)$_6$] (**3.5**): $C_{90}H_{66}Ho_2N_{12}$ (M = 1645.40): monoclinic, $P2_1/c$ (No. 14), a = 13.1038(4) Å, b = 19.0758(5) Å, c = 30.2903(9) Å, β = 98.7740(10)°, α = γ = 90°, V = 7482.9(4) Å^3, T = 296.15 K, Z = 4, Z' = 1, μ (MoKa) = 2.155, 104731 reflections measured, 21852 unique (R_{int} = 0.0850) which were used in all calculations. The final wR_2 was 0.1257(all data) and R_1 was 0.0464 (I > 2σ(I)).

[Pr(Ph$_2$pz)$_2$(Ph$_2$pz(SiMe$_2$O))]$_2$ (**3.6**): $C_{94}H_{78}N_{12}O_2Pr_2Si_2$ (M = 1745.68): monoclinic, $C2/c$(No. 15), a = 24.3219(8) Å, b = 14.8996(5) Å, c = 23.6906(8) Å, β = 104.573(2)°, α = γ = 90°, V = 8309.0(5) Å^3, T = 296.15(2) K, Z = 4, Z' = 0.5, μ (MoKa) = 1.244, 57708 reflections measured, 12166 unique (R_{int} = 0.0574) which were used in all calculations. The final wR_2 was 0.0926(all data) and R_1 was 0.0348 (I > 2σ(I)).

[Ce(*t*Bu$_2$pz)$_3$]$_2$ (**3.7**): $C_{66}H_{114}Ce_2N_{12}$, (M = 1349.88) , triclinic, P-1 (No. 2), a = 12.297(3) Å, b = 14.166(3) Å, c = 20.728(4) Å, α = 80.34(3)°, β = 89.21(3)°, γ = 80.65(3)°, V = 3511.9(13) Å^3, T = 100(2) K, Z = 4, Z' = 1, μ(MoK$_a$) = 1.325, 36686 reflections measured, 16438 unique (R_{int} = 0.0648) which were used in all calculations. The final wR_2 was 0.1437 (all data) and R_1 was 0.0477 (I > 2σ(I)).

[Er(*t*Bu$_2$pz)$_3$]$_2$ (**3.8**): $C_{66}H_{114}Er_2N_{12}$, (M = 1405.17) , triclinic, P-1 (No. 2), a = 12.155(3) Å, b = 15.950(3) Å, c = 21.085(4) Å, α = 106.00(3)°, β = 90.12(3)°, γ = 112.36(3)°, V = 3607.8(15) Å^3, T = 293(2) K, Z = 2, Z' = 1, μ(MoK$_a$) = 2.351, 48839 reflections measured, 17305 unique (R_{int} = 0.0586) which were used in all calculations. The final wR_2 was 0.2062 (all data) and R_1 was 0.0700 (I > 2σ(I)).

3.4 References

1. P. J. Davidson, M. F. Lappert and R. Pearce, *Acc. Chem. Res.*, 1974, **7**, 209-217.
2. D. Bradley, R. C. Mehrotra, I. Rothwell and A. Singh, *Alkoxo and aryloxo derivatives of metals*, Academic Press, 2001.
3. F. Nief, *Eur. J. Inorg. Chem.*, 2001, 891-904.
4. K. Müller-Buschbaum and C. C. Quitmann, *Z. Anorg. Allg. Chem.*, 2003, **629**, 1610-1616.
5. K. Müller-Buschbaum and C. C. Quitmann, *Z. Anorg. Allg. Chem.*, 2004, **630**, 131-136.
6. G. B. Deacon, C. M. Forsyth, P. C. Junk, B. W. Skelton and A. H. White, *Chem. Eur. J*, 1999, **5**, 1452-1459.
7. G. B. Deacon, P. E. Fanwick, A. Gitlits, I. P. Rothwell, B. W. Skelton and A. H. White, *Eur. J. Inorg. Chem.*, 2001, 1505-1514.
8. G. B. Deacon, A. Gitlits, B. W. Skelton and A. H. White, *Chem. Commun.*, 1999, 1213-1214.
9. G. B. Deacon, A. Gitlits, P. W. Roesky, M. R. Bürgstein, K. C. Lim, B. W. Skelton and A. H. White, *Chem. Eur. J.*, 2001, **7**, 127-138.
10. G. B. Deacon, C. M. Forsyth, A. Gitlits, R. Harika, P. C. Junk, B. W. Skelton and A. H. White, *Angew. Chem. Int. Ed. Engl.*, 2002, **41**, 3249-3251.
11. G. B. Deacon, E. E. Delbridge, D. J. Evans, R. Harika, P. C. Junk, B. W. Skelton and A. H. White, *Chem. Eur. J.*, 2004, **10**, 1193-1204.
12. G. B. Deacon, E. E. Delbridge and C. M. Forsyth, *Angew. Chem. Int. Ed.*, 1999, **38**, 1766-1767.
13. I. A. Guzei and C. H. Winter, *Inorg. Chem.*, 1997, **36**, 4415-4420.
14. I. A. Guzei, A. G. Baboul, G. P. A. Yap, A. L. Rheingold, H. B. Schlegel and C. H. Winter, *J. Am. Chem. Soc.*, 1997, **119**, 3387-3388.
15. I. A. Guzei, G. P. A. Yap and C. H. Winter, *Inorg. Chem.*, 1997, **36**, 1738-1739.
16. G. B. Deacon, C. M. Forsyth, A. Gitlits, B. W. Skelton and A. H. White, *Dalton Trans.* , 2004, 1239-1247.
17. G. B. Deacon, T. Feng, C. M. Forsyth, A. Gitlits, D. C. R. Hockless, Q. Shen, B. W. Skelton and A. H. White, *J. Chem. Soc., Dalton Trans.*, 2000, 961-966.
18. J. E. Cosgriff and G. B. Deacon, *Angew. Chem. Int. Ed.*, 1998, **37**, 286-287.
19. J. E. Cosgriff, G. B. Deacon and B. M. Gatehouse, *Aust. J. Chem.*, 1993, **46**, 1881-1896.
20. J. E. Cosgriff, G. B. Deacon, B. M. Gatehouse, H. Hemling and H. Schumann, *Angew. Chem. Int. Ed. Engl.*, 1993, **32**, 874-875.
21. J. Cosgriff, G. Deacon, B. Gatehouse, H. Hemling and H. Schumann, *Aust. J. Chem.*, 1994,

47, 1223-1235.

22. J. E. Cosgriff, G. B. Deacon, B. M. Gatehouse, P. R. Lee and H. Schumann, *Z. Anorg. Allg. Chem.*, 1996, **622**, 1399-1403.
23. G. B. Deacon, E. E. Delbridge, G. D. Fallon, C. Jones, D. E. Hibbs, M. B. Hursthouse, B. W. Skelton and A. H. White, *Organometallics*, 2000, **19**, 1713-1721.
24. G. B. Deacon, E. E. Delbridge, B. W. Skelton and A. H. White, *Eur. J. Inorg. Chem.*, 1998, 543-545.
25. G. B. Deacon, E. E. Delbridge, B. W. Skelton and A. H. White, *Eur. J. Inorg. Chem.*, 1999, 751-761.
26. S. Beaini, G. B. Deacon, M. Hilder, P. C. Junk and D. R. Turner, *Eur. J. Inorg. Chem.*, 2006, 3434-3441.
27. G. B. Deacon, C. M. Forsyth, A. Gitlits, R. Harika, P. C. Junk, B. W. Skelton and A. H. White, *Angew. Chem. Int. Ed.*, 2002, **41**, 3249-3251.
28. K. Müller-Buschbaum and C. C. Quitmann, *Z. Anorg. Allg. Chem.*, 2004, **59b**, 562-566.
29. K. Müller-Buschbaum and C. C. Quitmann, *Inorg. Chem.*, 2006, **45**, 2678-2687.
30. S. Beaini, G. B. Deacon, C. M. Forsyth and P. C. Junk, *Z. Anorg. Allg. Chem.*, 2008, **634**, 2903-2906.
31. S. Beaini, Ph.D Thesis, Monash University, 2007.
32. D. Werner, Ph.D Thesis, Monash University, 2015.
33. R. Harika, Ph.D Thesis, Monash University, 2003.
34. J. Townley, Ph.D Thesis, Monash University, 2010.
35. F. Aguilar-Parrilla, G. Scherer, H. H. Limbach, M. d. l. C. Foces-Foces, F. Hernandez Cano, J. A. S. Smith, C. Toiron and J. Elguero, *J. Am. Chem. Soc.*, 1992, **114**, 9657-9659.
36. A. L. Llamas-Saiz, C. Foces-Foces, F. H. Cano, P. Jimenez, J. Laynez, W. Meutermans, J. Elguero, H.-H. Limbach and F. Aguilar-Parrilla, *Acta Cryst.*, 1994, **B50**, 746-762.
37. R. Kempe, H. Noss and T. Irrgang, *J. Organomet. Chem.*, 2002, **647**, 12-20.
38. C. Wang, L. Xiang, X. Leng and Y. Chen, *Organometallics*, 2016, **35**, 1995-2002.
39. M. L. Cole, G. B. Deacon, P. C. Junk, K. M. Proctor, J. L. Scott and C. R. Strauss, *Eur. J. Inorg. Chem.*, 2005, 4138-4144.
40. G. B. Deacon, R. Harika, P. C. Junk, B. W. Skelton, D. Werner and A. H. White, *Eur. J. Inorg. Chem.*, 2014, 2412-2419.
41. C. C. Quitmann, V. Bezugly, F. R. Wagner and K. Müller-Buschbaum, *Z. Anorg. Allg. Chem.*, 2006, **632**, 1173-1186.
42. J. Hitzbleck, G. B. Deacon and K. Ruhlandt-Senge, *Eur. J. Inorg. Chem.*, 2007, 592-601.

43. R. Anwander, D. Werner, G. B. Deacon and P. C. Junk, *Dalton Trans.*, 2017.
44. R. Shannon, *Acta Cryst., Sect. A*, 1976, **32**, 751-767.
45. W. Zheng, N. C. Mösch-Zanetti, T. Blunck, H. W. Roesky, M. Noltemeyer and H.-G. Schmidt, *Organometallics*, 2001, **20**, 3299-3303.
46. W. Zheng, M. J. Heeg and C. H. Winter, *Angew. Chem. Int. Ed.*, 2003, **42**, 2761-2764.
47. S. H. Eggers, J. Kopf and R. D. Fischer, *Organometallics*, 1986, **5**, 383-385.
48. D. Werner, G. B. Deacon, P. C. Junk and R. Anwander, *Chem. Eur. J.*, 2014, **20**, 4426-4438.
49. C. Fernández-Castaño, C. Foces-Foces, N. Jagerovic and J. Elguero, *J. Mol. Struct.*, 1995, **355**, 265-271.
50. J. Elguero, E. Gonzalez and R. Jacquier, *Bull. Soc. Chim. Fr.*, 1968, 707-713.
51. T. M. McPhillips, S. E. McPhillips, H.-J. Chiu, A. E. Cohen, A. M. Deacon, P. J. Ellis, E. Garman, A. Gonzalez, N. K. Sauter, R. P. Phizackerley, S. M. Soltis and P. Kuhn, *J. Synchrotron Rad.*, 2002, **9**, 401-406.
52. W. Kabsch, *J. Appl. Cryst.*, 1993, **26**, 795-800.
53. O. V. Dolomanov, L. J. Bourhis, R. J. Gildea, J. A. K. Howard and H. Puschmann, *J. Appl. Cryst.*, 2009, **42**, 339-341.

Chapter 4

Synthesis and characterisation of some main group metal pyrazolate complexes

4. Chapter 4

4.1 Introduction

As it has been observed previously in this study, pyrazolate ligands have high coordination flexibility. Therefore, a considerable amount of structurally varied derivatives have been synthesised.[1] The formation of di- and polynuclear complexes is facile due to the two adjacent Lewis basic N-donor atoms which provides a bridging platform for metal centres.[2-6] Advances such as the first example of η^2-pyrazolate ligand coordination to a group 13 element,[7, 8] new coordination modes for acetylide groups[9] and stabilization of the bridging alkyl and hydride groups in pyrazolate-bridged dimers[10-12] have resulted from employing pyrazolate ligands in main-group metal chemistry as bridging scaffolds. The polynuclear potassium pyrazolate species obtained by Winter,[13] $[K(Ph_2pz)(thf)]_6$, was the first structurally documented group 1 complex, with an η^2-pyrazolate coordination unit, which was incorporated into the new μ_3-η^1:η^2:η^1 arrangement. This arrangement was suggested as a common one among group 1 complexes which was supported later by the isolation of monomeric [K(η^2-3,5-Ph_2pz)(η^6-18-crown-6)].[14] Also, various properties of alkali metals, particularly their high reactivity, made a range of syntheses possible that resulted in the advances in this area. Organoalkali reagents have been involved in addition and substitution reactions for the preparation of the organic and other organometallic complexes,[15]as well as acting as Brønsted bases when treated with protic reagents.[16] The reactivity of organoalkali complexes increases as the alkali metal gets heavier and the bonding within them are ionic (with iconicity increasing down the group) or electrostatic in nature.[16] Organolithium derivatives are the most extensively studied complexes of this group. Since the reactivity of these compounds are comparable to Grignard reagents, the interest in using them in synthesis has progressively increased.[17] Later, with understanding of the usage of heavier organoalkali compounds, several researches were performed to isolate the heavy organoalkali products.[18] Organoalkali reagents and/or complexes are generally synthesised by the following methods: direct synthesis[19] (Equation 4-1) which is predominantly used for the synthesis of organolithium complexes but it is not useful for heavier organoalkali derivatives. This method usually requires high speed stirring for metal dispersions in order to obtain good yields with heavier organoalkali derivatives which is a limitation of using this method.[20]

Equation 4-1. $2\ M + RX \longrightarrow RM + MX$

$X = Cl, Br$

Metallation[21, 22] involves replacement of hydrogen by the alkali metal and can occur via three ways depending on the type of organic group substituent.

- Direct reaction with the alkali metal (Equation 4-2)

Equation 4-2. $2\ M + 2\ RH \longrightarrow 2\ MR + H_2$

- Treatment of the organic molecule with an organoalkali compound (Equation 4-3)

Equation 4-3. $MR + R'H \longrightarrow MR' + RH$

- Reaction of organoamido or organoalkali reagents with an acidic organic complex (Equation 4-4).

Equation 4-4. $MNR_2 + R'H \longrightarrow MR' + HNR_2$

Transmetallaton[23] requires transferring the organic group (R) from less electropositive metal than the alkali metal which occurs in the reaction of an organometallic compound with an alkali metal (Equation 4-5) or organoalkali metal compound (Equation 4-6). Organomercury compounds have also been found useful in the preparation of heavy alkali metal complexes (Equation 4-7).

Equation 4-5. $M + RM' \longrightarrow RM + M'$

Equation 4-6. $RM + R'M' \longrightarrow R'M + RM'$

Equation 4-7. $2\ M + HgR_2 \longrightarrow 2\ MR + Hg$

Metal-halogen exchange [24, 25] which is mainly used for lithium derivatives, but can sometimes be used for the preparation of some sodium and potassium compounds (Equation 4-8). Polar solvents such as THF and Et_2O are preferred for these reactions because the reaction is solvent dependent.

Equation 4-8. $MR + R'X \longrightarrow MR' + RX$

By utilizing $Hg(C_6F_5)_2$ through transmetallation/ligand exchange, several group II pyrazolate compounds, $[M(Ph_2pz)_2(thf)_4]$ (M = Ca, Sr, Ba), have been prepared.[6] Alternatively, direct reaction of the alkaline earth metals with 3,5-diphenylpyrazole at

elevated temperatures under solventless conditions yielded similar compounds upon extraction with THF or DME. In the same study, compounds $[M(Me_2pz)_2(Me_2pzH)_4]$ (M = Ca, Sr, Ba) were prepared by protolysis of $[M\{N(SiMe_3)_2\}(thf)_2]$ (M = Ca, Sr, Ba) with Me_2pzH in THF and by direct metalation with Me_2pzH in liquid NH_3/THF.[6] Later, three more group I structures ($[Li(Ph_2pz)(OEt_2)_2$, $[Na(Ph_2pz)(thf)]_4$ and $[Na(t Bu_2pz]_n]$) were reported which portrayed an important advance in group I pyrazolate chemistry.[26]

Since Zn^{2+} has a closed shell d^{10} electron configuration it can be considered as a main group element and is therefore included in this chapter. The interest in chemistry of organozinc pyrazolate complexes increased due to the formation of dimeric compounds with four-coordinate Zn centres which has been promoted by compartmental multidentate pyrazolate ligands.[27-29] The formation of three structurally diverse alkylzinc pyrazolates via the reaction of R_2Zn (R = Et, *t*Bu) with 3,5-diphenylpyrazole has been reported.[30] The character of both the Zn-bonded alkyl substituents and solvents used resulted in the determination of the new reported structures which provided a new look at the aggregation and stabilization of alkylzinc species ($[t BuZn(Ph_2pz)]_3$, $[Et_2Zn_3(Ph_2pz)_4]$ and $[Et_2Zn_2(Ph_2pz)_2(\mu\text{-thf})]$.[30]

Following the development of researchers interest to extend their studies from lanthanoid pyrazolate to the structural chemistry of main group pyrazolates, several structures have been reported using aluminium reagents. From the metathesis reaction between $AlCl_3$ and the appropriate potassium 3,5-disubstituted pyrazolate $[K(t Bu_2pz)]$, the complex $[Al(t Bu_2pz)_3]$ was obtained which was the first monomeric homoleptic tris(pyrazolato) complex of any element.[8] Later, by a redox transmetallation/ligand exchange reaction between Al metal, $Hg(C_6F_5)_2$ and 3,5-di-*tert*-butyl-pyrazole in THF, $[Al(t Bu_2pz)_3(thf)]$ was isolated.[31]

4.1.1 Current study

As was highlighted in the first chapter of this thesis, this PhD study is focused on the preparation of pyrazolate complexes. While the rare earth pyrazolate complexes were prepared by redox transmetallation reactions in chapter 2, the compounds prepared in this chapter were prepared by metalation reactions using a range of pyrazolates (3,5-dimethylpyrazole (Me_2pzH), $C_5N_3H_7O_2$ (Me_2pzHNO_2), 3,5-di-*tert*-butypyrazole (tBu_2pzH) and 3,5-diphenylpyrazole (Ph_2pzH)). By using *n*BuLi reagent, complexes $[Li_4(Me_2pz)_4(OEt_2)_4]$ (**4.1**) and $[Li_6(Me_2pz)_6(tmeda)_2]$ (**4.2**) were isolated. The lithium complexes were prepared and isolated as they would be very useful reagents in metathesis chemistry. The hexameric pyrazolate complex using *n*BuLi is being reported for the first time in this study. Also, the presence of three different coordination modes in compound **4.2**, μ-η^2:η^2, μ-η^1:η^1 and μ-η^2:η^1, is a notable feature in complex **4.2**. By using the 4-nitropyrazolate (Me_2pzNO_2), a new polymeric complex $[Li_2(C_5N_3H_6O_2)_2(thf)_2]_n$ (**4.3**) is now reported. Continuing the study using $ZnEt_2$ as the metallating reagent resulted in the isolation of $[Zn(tBu_2pz)_2(tBu_2pzH)_2].1/2THF$ (**4.4**). In attempts to explore the reactions between $AlMe_3$ and pyrazole proligands with different ratios, $[AlMe_2(Ph_2pz)]_2.1/2THF$ (**4.5**) with bridging $AlMe_2$ group was obtained.

4.2 Results and discussion

Glossary of compounds and codes

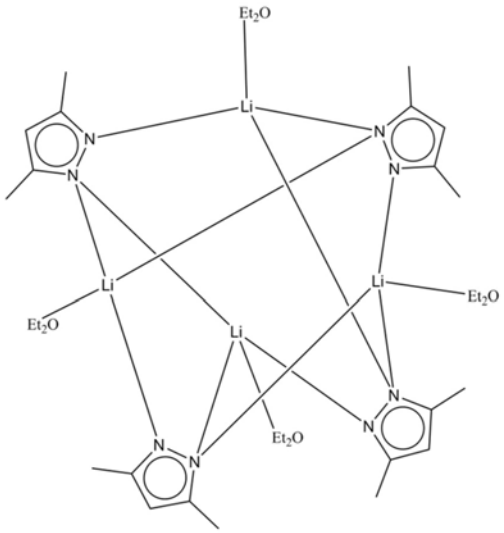

4.1 ($[Li_4(Me_2pz)_4(OEt_2)_4]$)

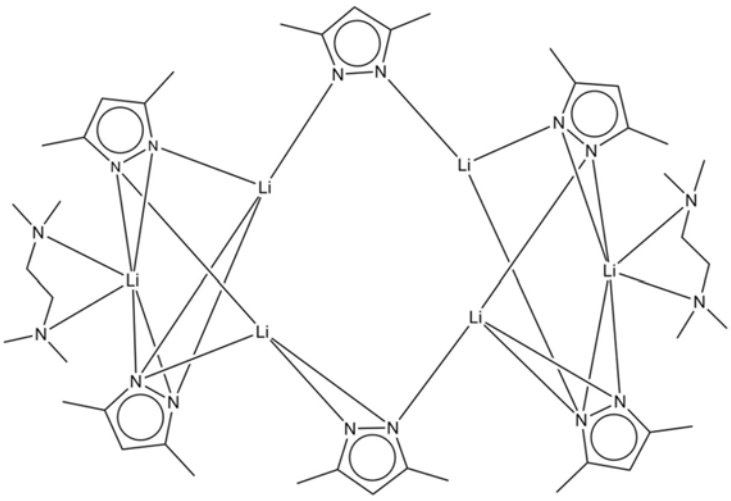

4.2 ($[Li_6(Me_2pz)_6(tmeda)_2]$)

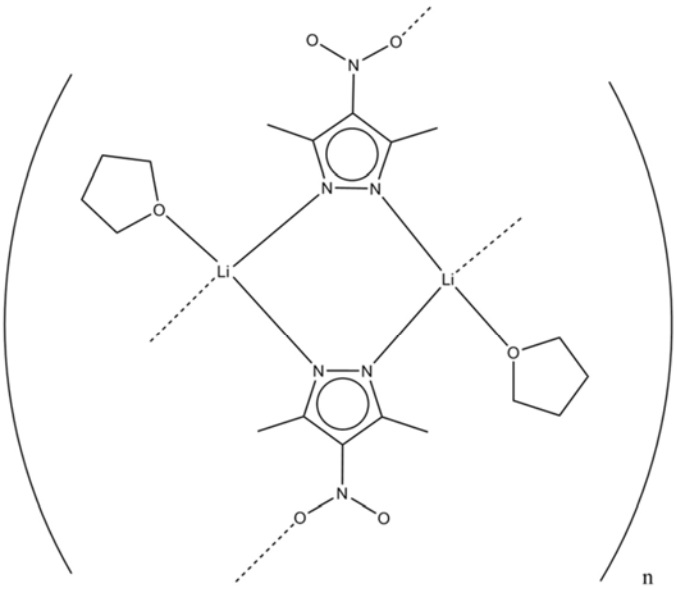

4.3 ($[Li_2(C_5N_3H_6O_2)_2(thf)_2]_n$)

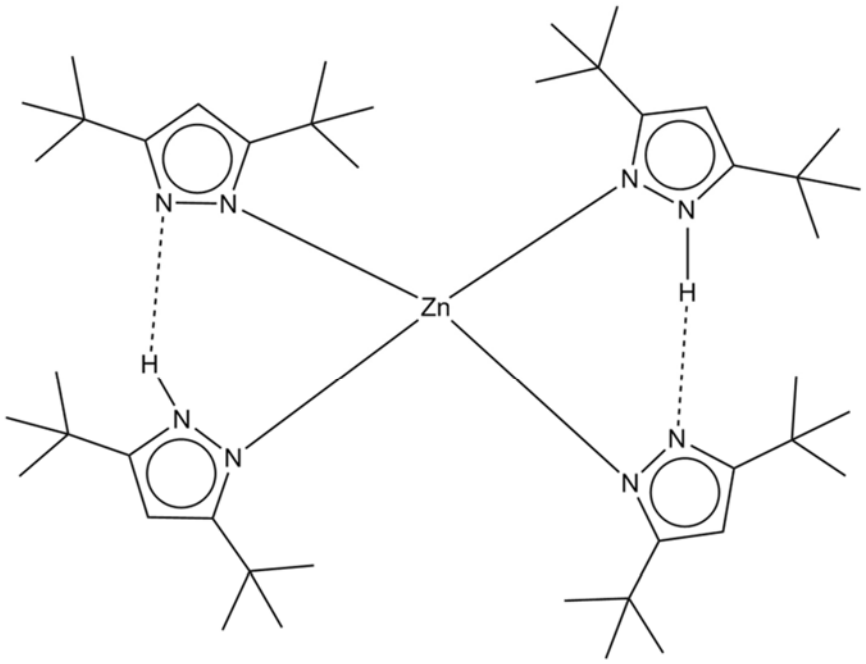

4.4 ({[Zn(*t*Bu$_2$pz)$_2$(*t*Bu$_2$pzH)$_2$].1/2THF})

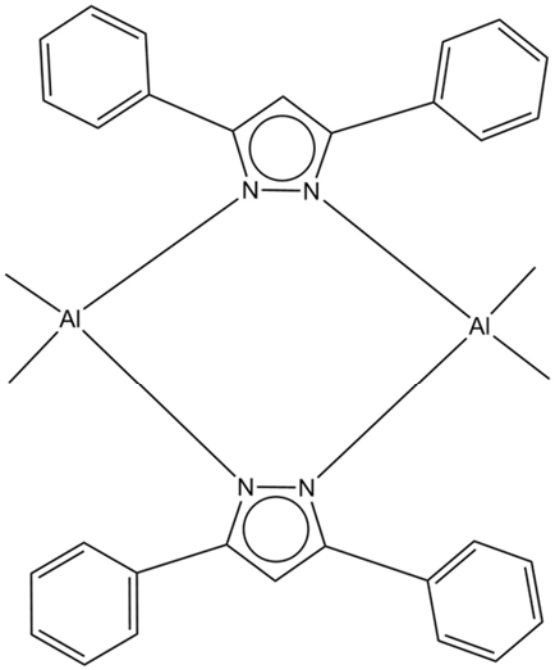

4.5 ({[AlMe$_2$(Ph$_2$pz)]$_2$.1/2THF})

4.2.1 Synthesis and characterization of pyrazolate complexes of lithium

Treatment of different pyrazoles (Me_2pzH and Me_2pzHNO_2) with *n*BuLi at room temperature in different solvents such as tetrahydrofuran (THF), diethyl ether (Et_2O) and hexane/TMEDA afforded three different compounds $[Li_4(Me_2pz)_4(OEt_2)_4]$ (**4.1**), $[Li_6(Me_2pz)_6(tmeda)_2]$ (**4.2**) and $[Li_2(C_5N_3H_6O_2)_2(thf)_2]_n$ (**4.3**) after filtration and concentration of the solution (Equation 4-9).

Equation 4-9. $$x\mathrm{R_2pzH} + xn\mathrm{BuLi} \xrightarrow{\textit{Solvent}} [\mathrm{Li(R_2pz)(solvent)}]_x + xn\mathrm{BuH}$$

Solvent = THF, Et_2O and hexane/TMEDA

R = Me, NO_2

The ^{1}H NMR spectrum of compound **4.1** ($[Li_4(Me_2pz)_4(OEt_2)_4]$) shows no NH resonances at ~10 ppm which indicates the complete deprotonation of the pyrazole. Also, the presence of a triplet signal at ~ 1.01 ppm and quartet at signal at 3.15 ppm are the result of coordinated Et_2O in the structure. Similarly, the IR spectrum is devoid of any NH absorption at 3100-3400 cm^{-1}.

Complete deprotonation of the pyrazole in the compound **4.2** ($[Li_6(Me_2pz)_6(tmeda)_2]$) can be confirmed by the absence of the NH resonance at ~10 ppm in the ^{1}H NMR spectrum. Also, the IR spectrum is devoid of any NH absorption at 3100-3400 cm^{-1}.

The ^{1}H NMR spectrum of compound **4.3** ($[Li_2(C_5N_3H_6O_2)_2(thf)_2]_n$) shows the presence of two resonances at 1.70 and 3.42 ppm that is the result of coordinated thf in the structure. The peak at 2.28 ppm is assigned to hydrogen atoms of CH_3 groups present in the ligand.

The integration in the NMR spectra of **4.1**, **4.2** and **4.3** show the compositions in solution are consistent with their X-ray crystal structures (see below).

4.2.1.1 X-ray structure of pyrazolato compounds invlving lithium

The X-ray crystal structure in Figure 4-1 shows the formation of an Et_2O-solvated tetrameric lithium pyrazolate complex of $[Li_4(Me_2pz)_4(OEt_2)_4]$ (**4.1**), with the whole molecule occupying the asymmetric unit. The structure consists of four lithium ions bridged by three pyrazolate ligands. The coordination sphere of the lithium ion is completed by one Et_2O molecule in η^1 bonding mode (Figure 4-1) that forms four-coordinate lithium centres.

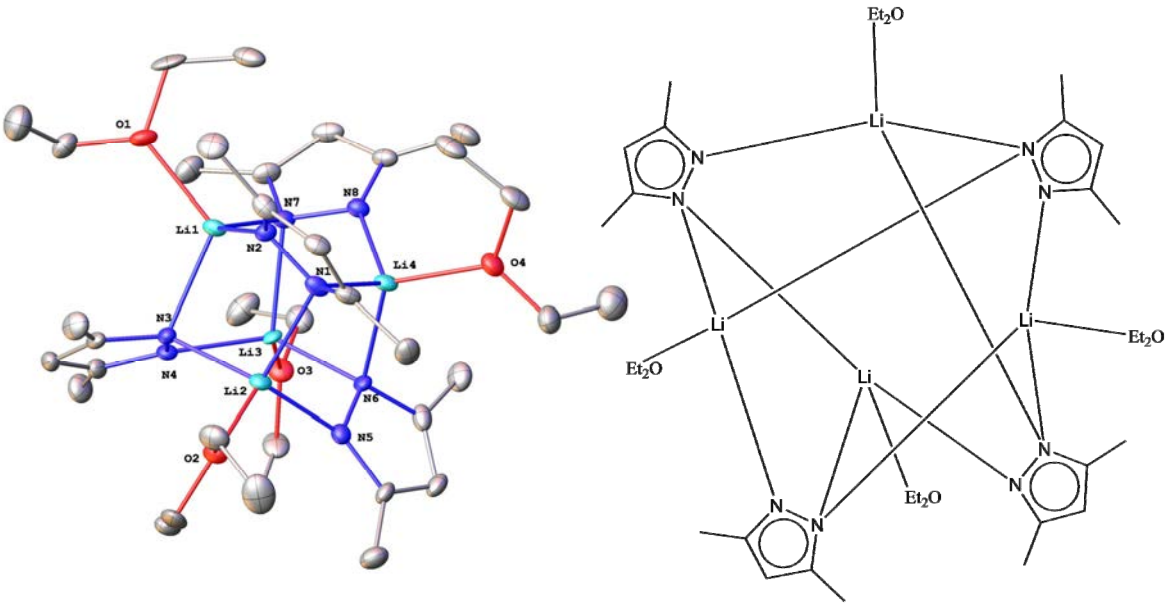

Figure 4-1. *Left:* X-ray crystal structure of the $[Li_4(Me_2pz)_4(OEt_2)_4]$ (**4.1**); hydrogen atoms removed for clarity; Ellipsoids are shown at 50% probability. *Right:* simplified diagram of **4.1**.

Each lithium atom is arranged in a distorted tetrahedral fashion (Figure 4-2). One nitrogen from each pyrazolate ring coordinate one lithium atom with a shorter Li-N distance (2.0-2.052 Å) and the other coordinates two lithium atoms with longer Li-N distances (2.11-2.18 Å) (Table 4-1). These Li-N bond lengths are comparable to those observed in other pyrazolato lithium complexes such as $[Li(tBu_2pz)]_4$ (1.94-2.11 Å)[32] and $[HC(Me_2pz)_3]Li(\eta^3\text{-}BH_4)$ (2.038-2.09 Å).[33] Tetrahedral and octahedral arrangements about Li are common in aggregated lithium structures such as $[MeLi]_4$, $[EtLi]_4$, $[(SiMe_3)Li]_4$, $[CyLi]_6$, $[^iPrLi]_6$, etc.[34-37] The Li-Li distances in **4.1** [3.06 (2)- 3.069(19) Å] are somewhat longer than those found in lithium-based tetramers (e.g., $[Li(tBu_2pz)]_4$ (2.812(4)-3.095(4)

Å).[32] The expansion of the lithium core in **4.1** can be ascribed to the interaction of each triangular face of the tetrahedron with two nitrogen atoms of the pyrazolate ligand instead of only one atom (carbon or silicon) in $[MeLi]_4$, $[EtLi]_4$, $[(SiMe_3)Li]_4$, etc.[38]

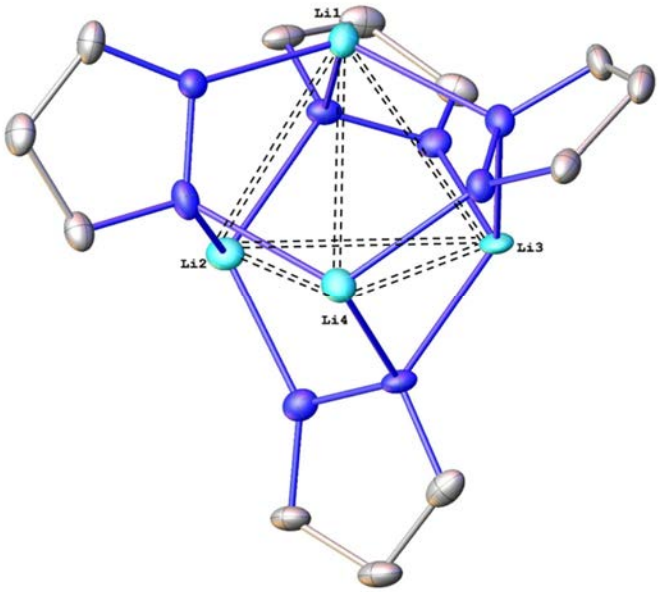

Figure 4-2. Perspective view of complex $[Li_4(Me_2pz)_4(OEt_2)_4]$ (**4.1**) showing the thermal ellipsoids at the 50% probability level (hydrogen atoms and methyl groups removed for clarity).

Thus, **4.1** has the pyrazolate coordination of μ_3- η^1:η^1:η^1 which previously was observed in $[Tl_3(Ph_2pz)_3]$[39] and $[Na_7(t Bu_2pz)_6(OH)]$[32]. Comparing the previously Et_2O-solvated pyrazolate complex of $[Li(Ph_2pz)(OEt_2)]_2$ [26] with compound **4.1** shows the transition from μ-η^2:η^1 in $[Li(Ph_2pz)(OEt_2)]_2$ [26] (Figure 4-3) to the μ_3-η^1:η^1:η^1 in **4.1**. This transition can be attributed to the lower steric demand of the Me_2pz ligand around Li^+ in compound **4.1** than the one in $[Li(Ph_2pz)(OEt_2)]_2$.[26] However, the similar coordination (μ_3-η^1:η^1:η^1) of the pyrazolate ligand was seen in $[Li(tBu_2pz)]_4$ [32] although **4.1** is an Et_2O-solvated pyrazolate complex and $t Bu_2pz$ and Me_2pz have different steric bulk.

Table 4-1. Selected bond lengths (Å) and angles (º) of **4.1**.

Li (1) environment		**Li(2) environment**		**Li(3) environment**		**Li (4) environment**	
Atom	Bond length	Atom	Bond length	Atom	Bond length	Atom	Bond length
N2	2.014(18)	N1	2.150(16)	N4	2.112(16)	N1	2.16(2)
N3	2.130(17)	N3	2.159(18)	N6	2.112(16)	N8	2.053(19)
N7	2.185(19)	N5	2.00(2)	N7	2.161(16)	N6	2.122(19)
O1	2.06(2)	O2	2.074(17)	O3	2.062(16)	O4	2.029(17)
Li1-Li2	3.06(2)	Li1-Li3	3.07(2)	Li2-Li3	3.17(2)	Li1-Li4	3.24(3)
Li2-Li4	3.037(19)	Li3-Li4	3.070(19)				

Bond Angles (º)					
Li(1)-Li(2)-Li(4)	64.3(6)	Li(2)-Li(1)-Li(3)	62.3(6)	Li(1)-Li(3)-Li(4)	63.7(6)
Li(2)-Li(4)-Li(3)	62.6(5)	Li(2)-Li(3)-Li(4)	58.2(4)	Li(3)-Li(2)-Li(4)	59.2(5)
Li(2)-Li(1)-Li(4)	57.6(5)	Li(4)-Li(1)-Li(3)	58.1(5)		

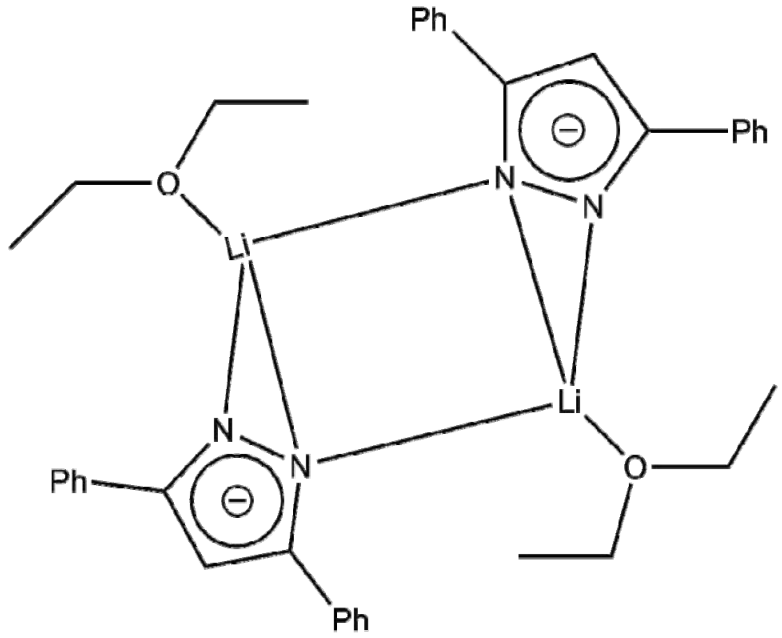

Figure 4-3. Structure of the dimeric $[Li(Ph_2pz)(Et_2O)]_2$,[26] phenyl rings and hydrogen atoms removed for clarity.

Previously, the formation of complex $[(Me_2pz)(thf)Li]$ has been reported as a result of treatment of *n*BuLi with Me_2pzH based on ^1H NMR and IR data without crystal structure. By changing the solvent system of the reaction to the combination of hexane/TMEDA (TMEDA:Me_2pzH:1:1) a new structure of $[Li_6(Me_2pz)_6(tmeda)_2]$ (**4.2**) with new features was

isolated (Figure 4-4).

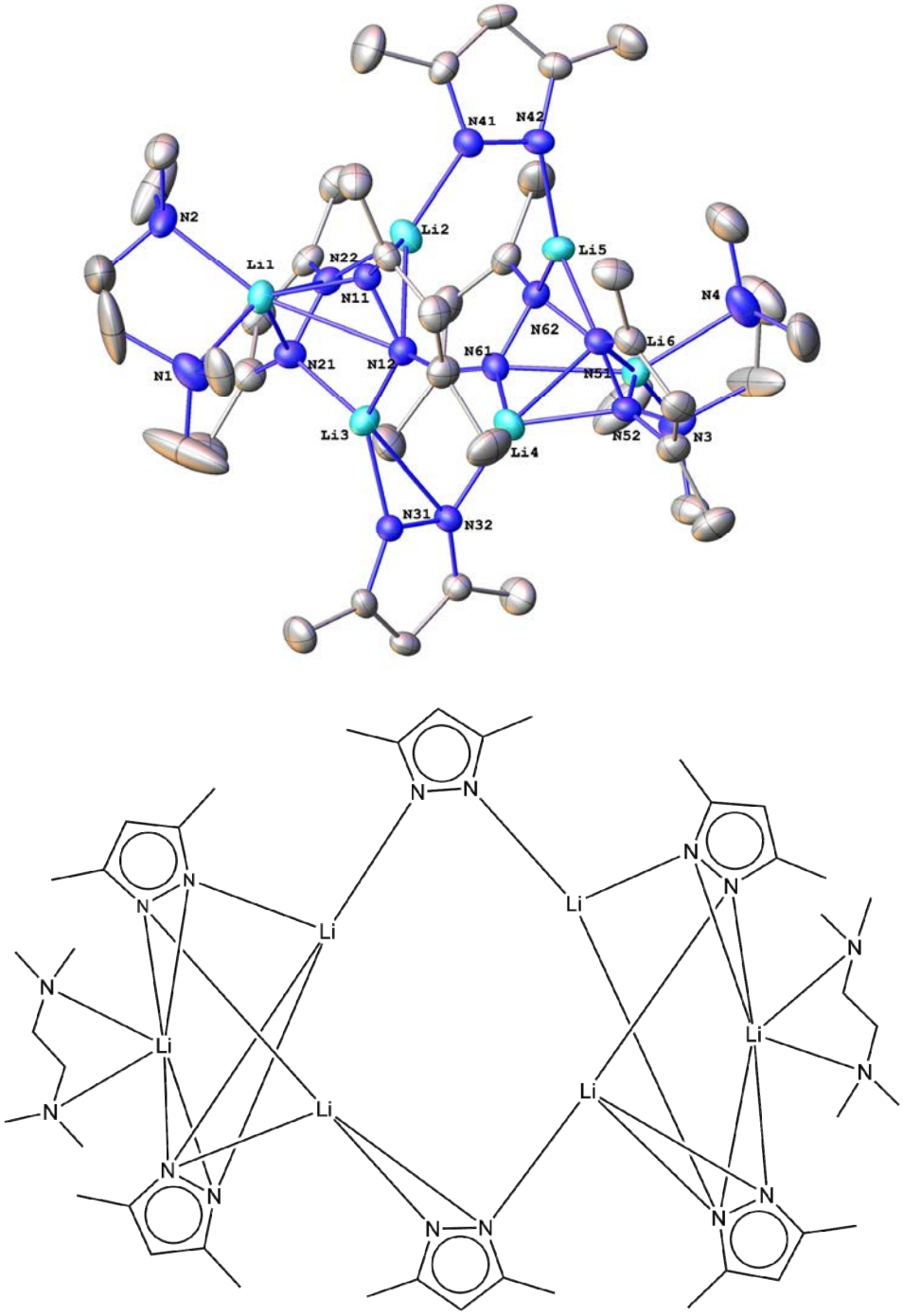

Figure 4-4. *Top:* X-ray crystal structure of the complex $[Li_6(Me_2pz)_6(tmeda)_2]$ (**4.2**) showing the thermal ellipsoids at the 50% probability level (hydrogen atoms and methyl groups have been removed for clarity); Bottom: simplified diagram of **4.2**.

Previously, it has been reported *n*BuLi forms hexameric aggregates in non-coordinating solvents[40] and dimers in the presence of TMEDA and exists in a tetramer-dimer equilibrium in THF.[41, 42] In this study, the formation of the hexameric structure using hexane/TMEDA as solvent and pyrazolate ligand is being reported for the first time. X-ray crystallography of $[Li_6(Me_2pz)_6(tmeda)_2]$ (**4.2**) shows the formation of a tmeda-solvated hexameric lithium pyrazolate complex. Compound **4.2** has the unusual pyrazolate coordination of μ-η^1:η^2, which has been observed previously in the dimeric $[Li(Ph_2pz)(OEt_2)]_2$[26] and is reminiscent of carboxylate[43] and formamidinate[44-47] chemistry. Compound **4.2** contains six lithium ions having two η^2:η^2:η^1:η^1, one η^1:η^1:η^1 and three η^1:η^2:η^1 pyrazolate ligands forming six (Li1 and Li6), three (Li5) and four (Li2, Li3 and Li4) coordinate lithium atoms. Also, there are three kinds of bridging bonds in the compound **4.2** (μ-η^2:η^2, μ-η^1:η^1 and μ-η^2:η^1) (Figure 4-5). The six-coordinate terminal lithium atoms have a distorted tetrahedral coordination environment considering the centre (Cent) of the N-N vector as the binding site of pyrazolate around (Figure 4-5).

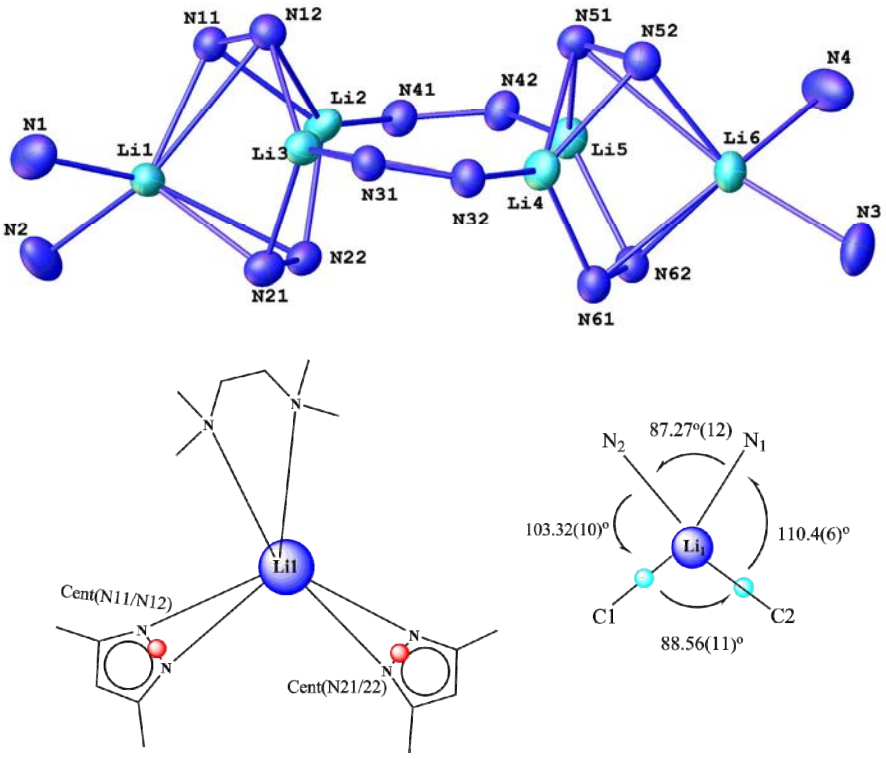

Figure 4-5. *Top:* asymmetric unit of **4.2** along the x axis; *Bottom*: the distorted tetrahedral arrangement of ligands around terminal lithium atom (C1 = Cent (N11/N12) and C2 = Cent (N21/N22)).

Comparing the Li-N (nitrogen of the pz ligand) bond length (Table 4-2) in the μ-η^2:η^1

(ave. 1.96 Å) with the previously reported distances in $[Li(Ph_2pz)(OEt_2)]_2$[26] (2.04 Å) and $[Li(tBu_2pz)(tBu_2pzH)]_2$ [32] (2.06Å) (Figure 4-6) shows a smaller distance in the η^1-interaction which can be due to the lower bulkiness of the Me_2pz^- ion. The η^2-bridging bond lengths in compound **4.2** (1.94(7) Å, 2.65(7) Å) are greater than the similar bonding in the $[Li(Ph_2pz)(OEt_2)]_2$[26] (1.954, 2.236 Å) and $[Li(tBu_2pz)(tBu_2pzH)]_2$ [32] (2.009, 2022 Å).

Table 4-2. Selected bond lengths (Å) and angles (º) of **4.2**.

Li1		**Li2**		**Li3**		**Li4**		**Li5**		**Li6**	
Atom	Bond length	Atom	Bond length	Atom	Bond length	Atom	Bond length	Atom	Bond length	Atom	Bond length
N1	2.111(7)	N41	1.979(7)	N21	2.004(7)	N32	1.965(7)	N42	1.971(7)	N3	2.114(7)
N2	2.111(7)	N11	2.051(7)	N12	2.995(7)	N51	2.318(7)	N51	2.013(7)	N4	2.120(7)
N11	2.060(7)	N12	2.486(7)	N31	2.983(7)	N52	2.031(7)	N62	2.031(7)	N51	2.719(7)
N12	2.646(7)	N22	1.982(7)	N32	2.650(7)	N61	1.989(7)			N52	2.047(7)
N21	2.122(7)									N61	2.374(7)
N22	2.398(7)									N62	2.146(7)

Bond Angles

N(1)-Li(1)-N(2)	87.3(3)	N(21)-Li(1)-N(22)	35.51(15)	N(11)-Li(1)-N(12)	31.56(14)
N(11)-Li(2)-N(12)	34.23(4)	N(51)-Li(6)-N(52)	30.31(8)	N(61)-Li(6)-N(62)	35.59(8)
N(51)-Li(4)-N(52)	36.95(4)	N(32)-Li(4)-N(61)	126.05(6)	N(42)-Li(5)-N(62)	130.72(3)
N(42)-Li(5)-N(51)	124.74(12)	N(51)-Li(5)-N(62)	104.32(12)		

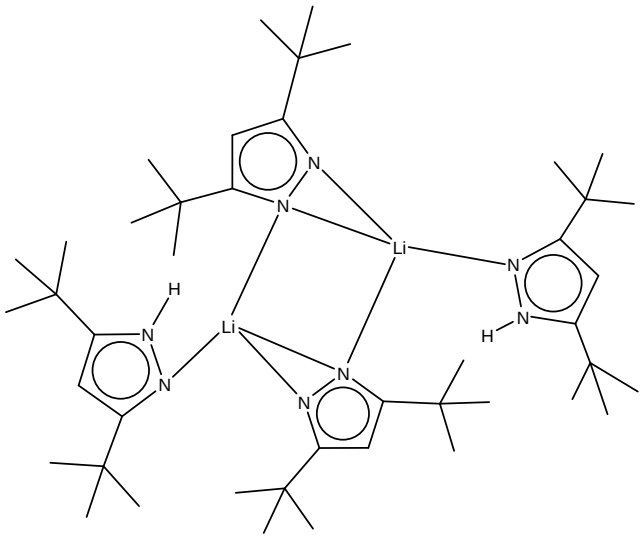

Figure 4-6. Structure of $[Li(tBu_2pz)(tBu_2pzH)]_2$ [32]; hydrogen atoms removed for clarity.

Performing a reaction using *n*BuLi and a nitro derivative of 3,5-dimethylpyrazole (3,5-di-*tert*-butyl-4-nitropyrazole) is being reported for the first time in this study. According to the previous study of the nitro group on the solid-state structure of 4-nitropyrazoles, it has been reported that the 4-nitro substituent can result in decreasing pK_a (pK_a 3,5-dimethylpyrazole = 15 and pK_a 3,5-dimethyl-4-nitropyrazole = 10.65).[48] Using 3,5-dimethyl-4-nitropyrazole resulted in a structure which consists of a dinuclear asymmetric unit which is part of a large polymeric network ($[Li_2(C_5N_3H_6O_2)_2(thf)_2]_n$ **4.3** (Figure 4-7)). So far, many coordination polymers of *d*-block transition metal elements have been reported ($\{[Cu(bpe)_2]^+\}_\infty$, $\{[Cu(diaz)_2]PF_6\}_\infty$ etc.).[49] Also, a series of compounds using lanthanoids and a ligand having nitro group (potassium *o*-nitrophenolate) which formed polymeric structures was reported later ($[(THF)_4\{K(o\text{-}O_2N\text{-}C_6H_4\text{-}O)_4Ln\}_4]_n$ (Ln = Y, Er, Lu); $[[K_2(o\text{-}O_2N\text{-}C_6H_4\text{-}O)_5Tb]_n]$ etc.).[50] Complex **4.3** crystallised in the monoclinic space group $P2_1/n$ with half the dimer within the asymmetric unit. The $[Li_2(C_5N_3H_6O_2)_2(thf)_2]$ units are bridged by a O_2N group in an *anti*-configuration. The lithium atom is coordinated by two pyrazolate ligands in $\mu\text{-}\eta^1\text{:}\eta^1$ fashion (the most common pyrazolate ligation for non-rare earth complexes).[51] Lithium ions complete their respective coordination spheres with a thf and coordination number of four in a tetrahedral coordination geometry around them. The two thf molecules are arranged in a *cisoid* fashion. Bond lengths and angles are available in Table 4-3. Comparing the N-O bond length in compound **4.3** with the previously reported N-O bond lengths shows that the formation of the O…Li bond does not affect the length of nitro groups bonds in the ligand. [48] The Li…O that formed with nitro group is longer than the formed Li…O with thf (2.002 Å and 1.995(9) Å respectively). The Li-Li distances in compound **4.3** ($[Li_2(C_5N_3H_6O_2)_2(thf)_2]_n$) (3.525 (13) Å) are longer than in compound **4.1** ($[Li_4(Me_2pz)_4(Et_2O)_4]$) [3.06 (2)- 3.069(19) Å]. Similar to the complex $[Li(t\text{Bu}_2pz)(thf)]_2$,[52] a six-membered ring of Li_2N_4 and two thf molecules are arranged in a *cisoid* fashion which minimize the steric bulk in the complex. The Li–N bond length values in **4.3** (2.042(10)-2.018(10) Å) are similar to the sum of covalent radii of Li and N (1.99 Å)[53] but longer than those found in $[Li(t\text{Bu}_2pz)(thf)]_2$ (1.942(5) Å and 1.952(5) Å).[52]

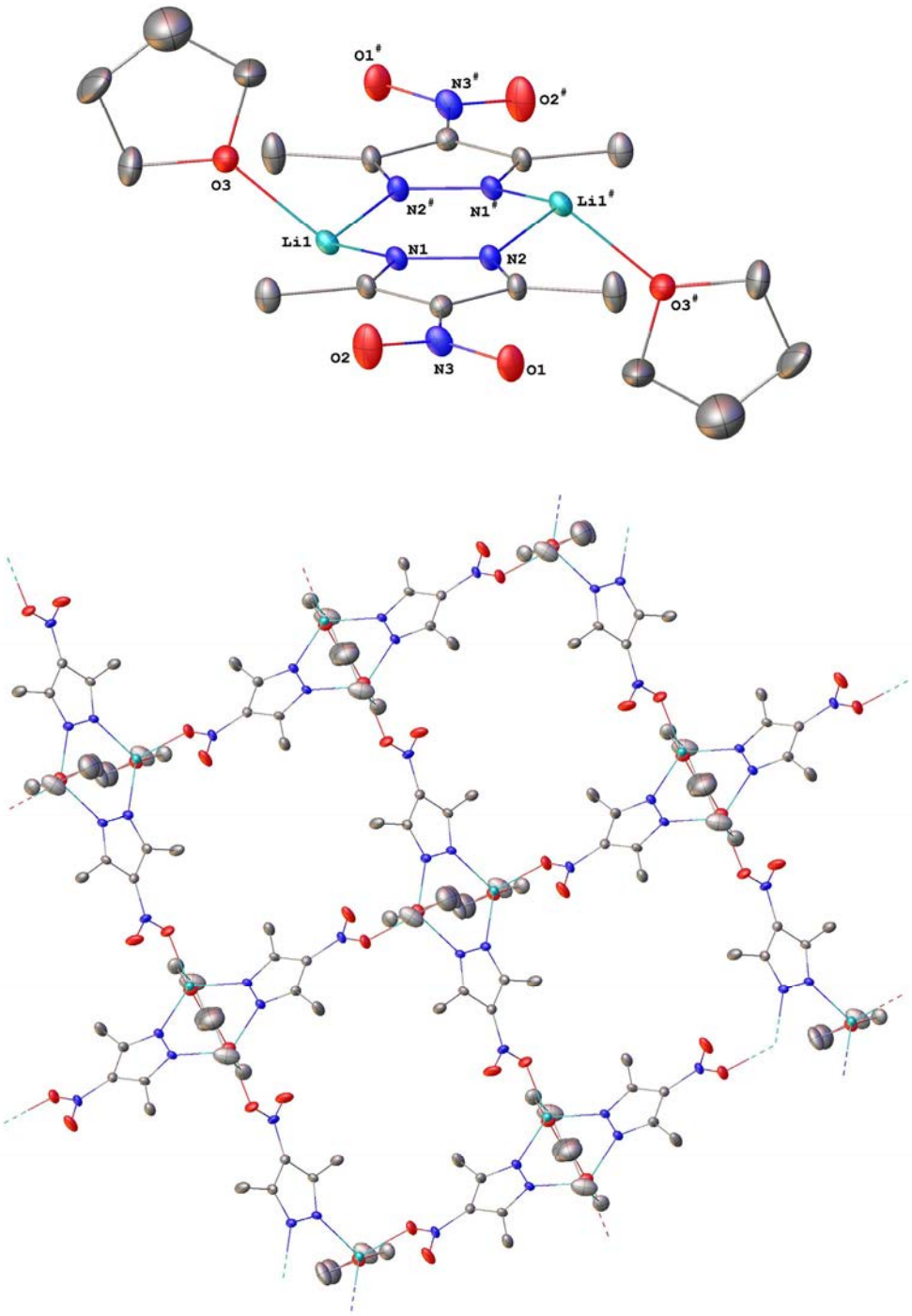

Figure 4-7. *Top:* the X-Ray crystal structure of $[Li_2(C_5N_3H_6O_2)_2(thf)_2]_n$ (**4.3**) showing the asymmetric unite; ellipsoids shown at 50% probability; H atoms removed for clarity. *Bottom*: The polymeric $[Li_2(C_5N_3H_6O_2)_2(thf)_2]_n$; ellipsoids shown at 50% probability; H atoms removed for clarity. Symmetry equivalents used: #1 = ½-X, 1/2+Y, 3/2-Z; #2 = 1-X, 1-Y, 2-Z; #3 = -1/2-X, -1/2+Y, 3/2-Z.

Table 4-3. Selected bond lengths (Å) and angles (º) for **4.3**; symmetry equivalents used: #1 = ½-X, 1/2+Y, 3/2-Z; #2 = 1-X, 1-Y, 2-Z; #3 = -1/2-X, -1/2+Y, 3/2-Z

Bond lengths			
Li(1)–O(3)	1.995(9)	Li(1)$^{\#}$–O(3)$^{\#}$	1.995(9)
Li(1)–N(1)	2.042(10)	Li(1)$^{\#}$–N(1)$^{\#}$	2.042(10)
Li(1)–N(2)$^{\#}$	2.018(10)	Li(1)$^{\#}$–N(2)	2.018(10)
Li(1) –Li(1)$^{\#}$	3.525(13)		
Bond angles			
Li(1)–N(1)–N(2)	120.8(6)	O(3)–Li(1)–N(1)	106.883(2)
O(2)–N(3)–O(1)	121(1)	Li(1)–N(2)$^{\#}$–N(1)$^{\#}$	120.972(6)
Li(2)$^{\#}$–N(1)$^{\#}$–Li(1)$^{\#}$	120.807(6)	N(1)$^{\#}$–Li(1)$^{\#}$–N(2)	115.514(1)
Li(1)$^{\#}$–N(2)–N(1)	120.972(3)	N(1)–Li(1)–N(2)$^{\#}$	115.5(1)

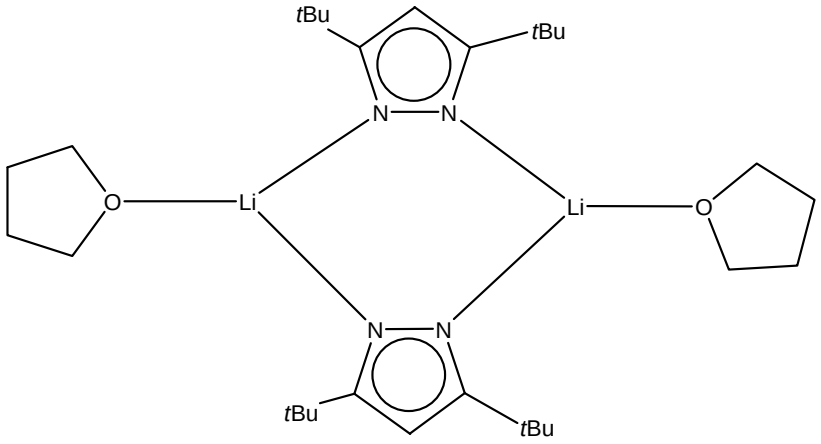

Figure 4-8. Structure of [Li(*t*Bu$_2$pz)(thf)]$_2$.[52]; hydrogen atoms removed for clarity.

4.2.2 Synthesis and characterisation of a zinc pyrazolato compound

4.2.2.1 Spectral analysis

The infrared spectrum of the crystalline material for $[Zn(tBu_2pz)_2(tBu_2pzH)_2].1/2THF$ (**4.4**) reflects the presence of NH absorption at 3137 cm^{-1} which shows the presence of the coordinated *t*Bu2pzH in the structure. In spite of the fact that there are two *t*Bu2pzH rings in $[Zn(tBu_2pz)_2(tBu_2pzH)_2].1/2THF$, only one bond assignable to this ring stretching vibration is observed at 1574 cm^{-1}. It can be likely a consequence of the hydrogen bonding associated with these ligands. The absence of the stretching vibration for all pyrazolate rings was observed previously in $[Zn_2(Me_2pz)_4(Me_2pzH)]$[54] due to the presence of the very strong hydrogen bonding. Considering the presence of both *t*Bu2pz and *t*Bu2pzH in the structure, two individual set of peaks were observed in the ^1H NMR spectra. The signal at 1.10 and 5.96 ppm are assigned to the *t*Bu and H4 of *t*Bu2pzH respectively. The signals at 1.52 ppm and 6.09 ppm represents the *t*Bu and H4 of *t*Bu2pz. The broad signal at 10.33 ppm is assigned to the two hydrogen atoms of *t*Bu2pzH.

4.2.2.2 X-ray crystal structure of pyrazolate compounds with zinc

As mentioned before, using pyrazolate ligands with main group metals resulted in many advances such as the first example of η^2- pyrazolate ligand coordination to the metal[7] or stabilization of the bridging alkyl and hydride group in pyrazolate bridging dimers.[10] Poly(1-pyrazolate)borate zinc complexes were first reported by Trofimenko *et al.*[55] Later, zinc and boron centres were featured in a number of polynuclear pyrazolyl bridged species.[56] Most of the mentioned complexes were not characterised in the solid state using X-ray crystallography. Later, a number of structural reports appeared. Ehlert *et al* reported $[Zn_2(Me_2pz)_4(Me_2pzH)]$ (Figure 4-9).[54]

Recently, by treating 3,5-diphenylpyrazole with $ZnEt_2$ the compounds $[(Et_2Zn_3(Ph_2pz))_4]$ (Figure 4-10) and $[(EtZn(Ph_2pz))_2(\mu\text{-THF})]$ [30] (Figure 4-11) have been reported.

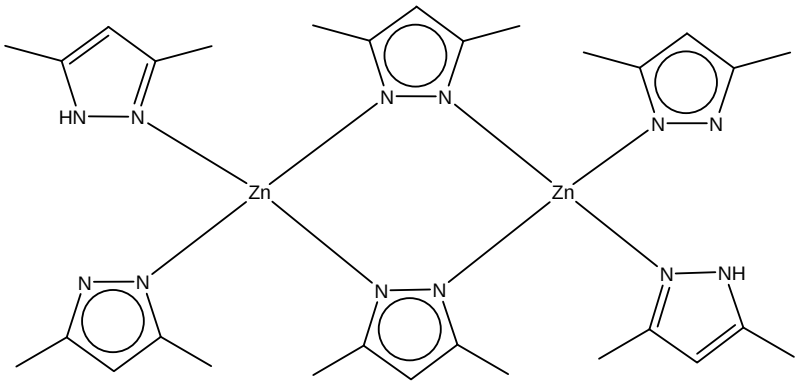

Figure 4-9. Structure of $[Zn_2(Me_2pz)_4(Me_2pzH)_2]$[54]; hydrogen atoms removed for clarity.

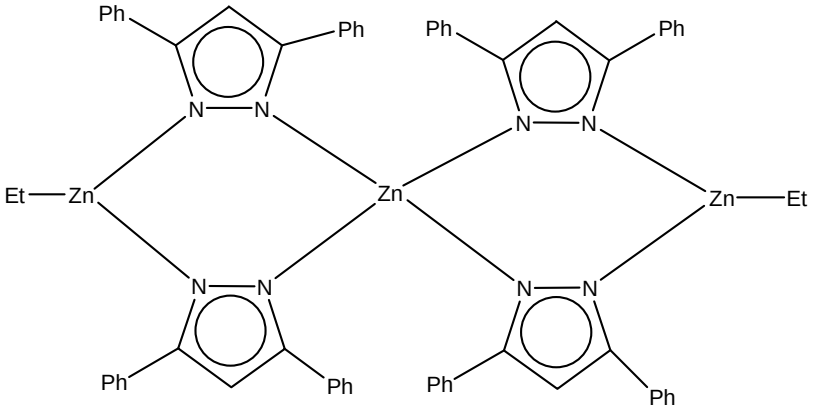

Figure 4-10. Structure of $[(Et_2Zn_3(Ph_2pz))_4]$[54]; Hydrogen atoms removed for clarity.

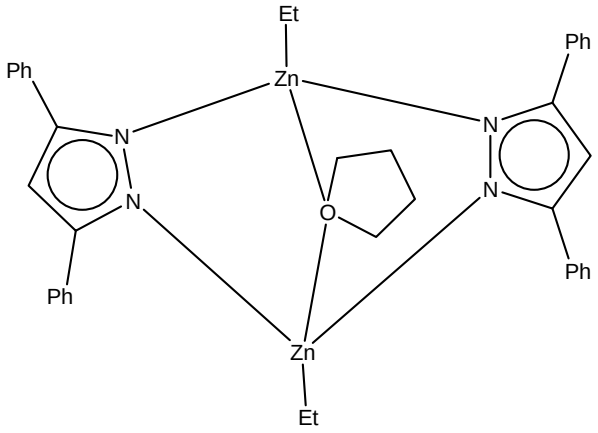

Figure 4-11. Structure of $[(EtZn(Ph_2pz))_2(\mu\text{-THF})]$ [30] ; Hydrogen atoms removed for clarity.

Since no compounds were previously reported using 3,5-di-*tert*-butylpyrazole, the compound {[Zn(tBu$_2$pz)$_2$(tBu$_2$pzH)$_2$].1/2THF} (**4.4**) (Figure 4-12) is being reported for the first time. The molecular structure (Figure 4-12) is monomeric and consists of two pyrazolate ions and two neutral *t*Bu$_2$pzH molecules. The monomeric compound **4.4** crystallised in the monoclinic *P2$_1$/n* space group having half of a THF lattice solvate. The zinc atom is coordinated in a tetrahedral fashion (N–Zn–N = 106.2(12)–110.5(12)º). The two Zn–N(3) and Zn–N(6) bonds are similar (within 3 e.s.d.s) to the other two Zn–N bonds even though two coordinated pyrazolate ions are charged while the other two ligands are neutral (Table 4-4).

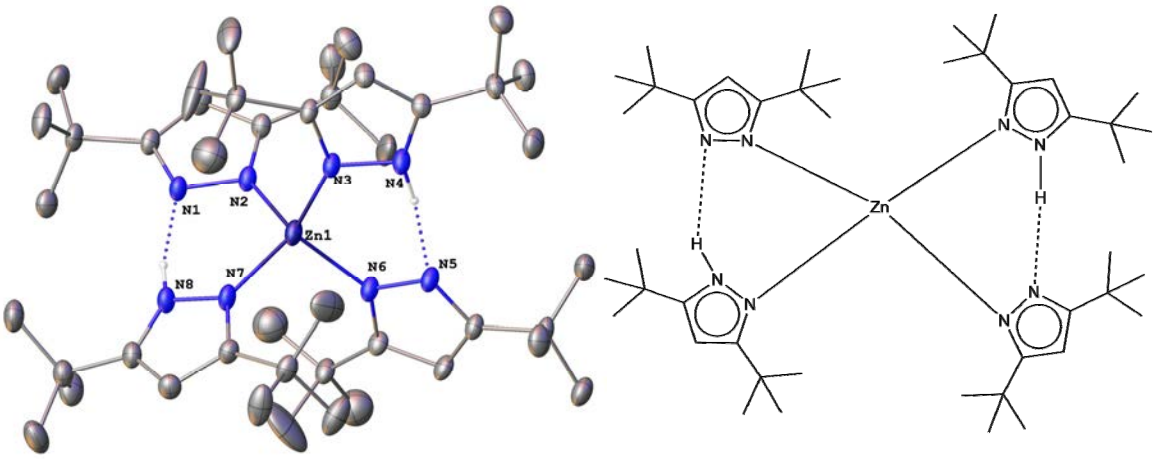

Figure 4-12. *Left:* the X-ray crystal structure of {[Zn(*t*Bu$_2$pz)$_2$(*t*Bu$_2$pzH)$_2$].1/2THF} (**4.4**); ellipsoids shown at 50% probability; H atoms are removed for clarity. *Right*: simplified diagram of **4.4**.

Table 4-4. Selected bond lengths (Å) and angles (º) for compound **4.4**.

Bond lengths			
Zn(1)–N(2)	2.036(4)	Zn(1)–N(3)	2.024(4)
Zn(1)–N(6)	2.021(4)	Zn(1)–N(7)	2.036(5)
Bond angles			
N(2)–Zn(1)–N(7)	110.59(17)	N(6)–Zn(1)–N(3)	109.41(17)
N(7)–Zn(1)–N(6)	106.34(19)	N(3)–Zn(1)–N(2)	106.25(19)
N(3)–Zn(1)–N(7)	113.06(19)	N(6)–Zn(1)–N(2)	111.28(17)
H(1)–N(1)–N(2)	112.48(9)	H(8)–N(8)–N(7)	121.84(8)

The Zn metal centre is coordinated by two pyrazolate ligands and two pyrazole molecules via four η^1 bonding modes. The Zn-N distances are between 2.021(4) Å and 2.036(4) Å which is in the expected range. [30] Similar to the previously reported zinc compounds, [30, 32] the coordination number of zinc in compound **4.4** is four with close to tetrahedral geometry about Zn^{2+}. Hydrogen bonding occurs between two pyrazole molecules [N(8)–H(8)… N(1), H…N = 1.87 (4) Å, N–H…N = 165.73º and N(4)–H(4)… N(5), H…N = 1.71 Å (4) Å, N–H…N = 158.04º]. The presence of the hydrogen bond was observed in the previously reported $[Zn_2(Me_2pz)_4(Me_2pzH)]$[54] compound. The Zn-N distance in compound **4.4** is very close to the similar Zn-N bond in the reported $[Zn_2(Me_2pz)_4(Me_2pzH)_2]$ (2.025 Å).[54]

4.2.3 Synthesis and characterisation of an aluminium pyrazolato compounds

4.2.3.1 Spectral analysis

The N-H stretching absorptions of the pyrazoles at 3300-3100 cm^{-1} are not observed in the IR spectra of pyrazolate aluminium complex, indicating complete deprotonation. The very strong band around 679 cm^{-1} in compound **4.5** ($[AlMe_2(Ph_2pz)]_2$.1/2THF) is attributed to an Al-C(Me) stretching absorption.[57] The ^1H NMR spectrum of the compound **4.5** shows resonances at δ = 1.40 and 3.55 ppm which are attributed to the THF molecule in the lattice. The resonance at δ = -0.66 is attributed to the 12 hydrogens of four methyl groups of $AlMe_2$. The resonance at δ = 6.26 ppm is attributed to the two backbone hydrogens of the pyrazolato ligand and the resonance at δ = 7.03 ppm is attributed to the 12 hydrogens in total in *meta* and *para* positions of the phenyl groups. The resonance at the δ = 7.42 ppm is attributed to the eight hydrogens in *ortho* position. The elemental analysis confirmed the composition of the bulk material was identical to the found in the X-ray crystal structure.

4.2.3.2 X-ray structure of {[$AlMe_2(Ph_2pz)]_2$.1/2THF}

As observed around 50 years ago, pyrazolate ligands have been widely employed in complexes of transition metals and exhibit either η^1-bonding to a single metal atom or ion, or form an η^1, η^1-bridge between two metal centres.[58, 59] Several years later, it was observed that the pyrazolate ligand can coordinate in an η^2, η^5 and μ bonding modes to metal centres.[60,

[61] Also, since alkyl-bridged ligands in group 13 complexes gained a significant interest in olefin polymerization [62-66], researches was performed using aluminium because of the possibility of bridging the saturated hydrocarbon groups between two aluminium centres.[67-75] Therefore, a number of researches were performed to isolate products using pyrazolate ligands and aluminium. A number of pyrazolatoaluminium complexes have been structurally characterised, showing the methyl group bridging between two aluminium(III) centres through three-centre-two-electron bonding such as [$Me_2Al(\mu\text{-}Ph_2pz)(\mu\text{-}Me)AlMe_2$], [$Et_2Al(\mu\text{-}Ph_2pz)(\mu\text{-}Et)AlEt_2$] and [$(n\text{Pr})_2Al(\mu\text{-}t\text{Bu}_2pz)(\mu\text{-}n\text{Pr})Al(n\text{Pr})_2$].[10, 11, 76] They were prepared by metallation of the pyrazole by the corresponding alkyl aluminium. Also, some 3,5-di-tert-butylpyrazolato[8, 77] and 3,5-dimethylpyrazolato[78] aluminium derivatives have been investigated and characterized.

Treatment of 3,5-diphenylpyrazole with an excess of trimethylaluminium ($AlMe_3$, 3 equiv.) in THF at ambient temperature led to the formation of complex **4.5** ({[$AlMe_2(Ph_2pz)]_2$.1/2THF}) (Figure 4-13).

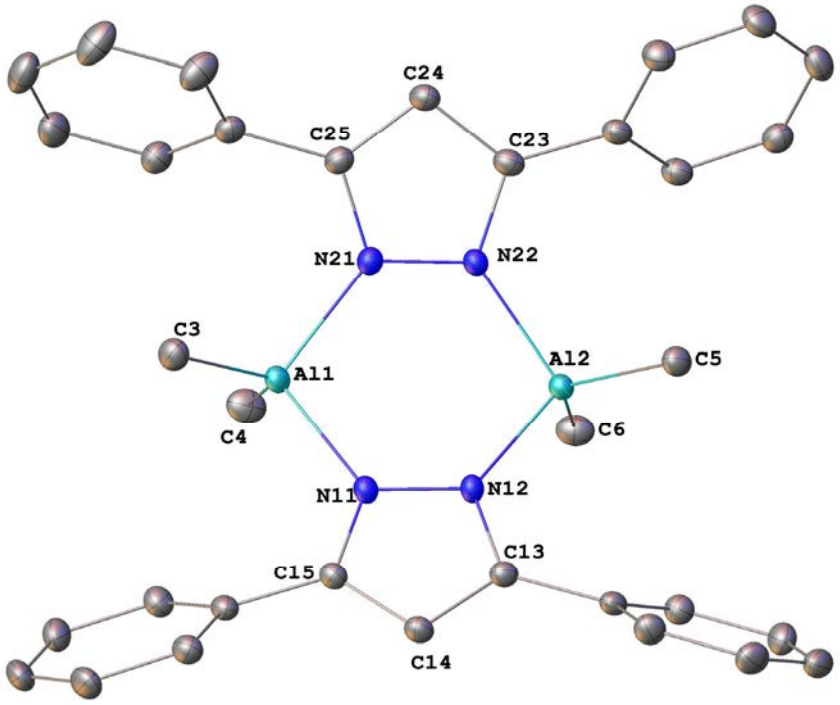

Figure 4-13. The X-Ray crystal structure of {[$AlMe_2(Ph_2pz)]_2$.1/2THF} (**4.5**); ellipsoids shown at 50% probability; hydrogen atoms removed for clarity.

Compound **4.5** crystallised in the triclinic crystal system, space group *P*-1. Compound **4.5** is a dimeric molecule with a six-membered Al_2N_4 ring and four terminal methyl groups (Figure 4-13) comparable to those observed in the pyrazolato derivatives [(η^1, η^1-pz)(μ-Al)Me_2],[79] [(η^1, η^1-3,5-*t*Bu_2pz)(μ-Al)Me_2]$_2$ [77] and [Me_2Al(μ-Al)]$_2$ [80]. Two phenylpyrazolato groups serve as bridges between the two aluminium atoms, and the six-membered Al_2N_4 ring consists of four nitrogen atoms from two phenylpyrazolato groups and two aluminium atoms. The Al_2N_4 ring features a twisted conformation due to the bulky phenyl groups. The environment around aluminium can be considered as distorted tetrahedral. Both the Al-N and Al-C bond lengths (e.g. Al1-N11: 1.962(5) Å, and Al1-C4: 1.971(5) Å) are comparable to the bond lengths in [(η^1, η^1-3,5-*t*Bu_2pz)(μ-Al)Me_2]$_2$ (Al(1)-N(1): 1.9638(13) Å; and Al(1)-C(6): 1.962(2) Å) (Figure 4-14).[77] The N-Al-N angle (e.g. N11-Al1-N21: 102.48(2)º) (Table 4-5) is somewhat larger than the corresponding one in [(η^1, η^1-3,5-*t*Bu_2pz)(μ-Al)Me_2]$_2$ (N(1)-Al(1)-N(2): 99.3º).[77] Also, the C(4)-Al(1)-C(3) angle is 125.05(16)º somewhat larger than the corresponding one in [(η^1, η^1-3,5-*t*Bu_2pz)(μ-Al)Me_2]$_2$ (C(5)-Al(1)-C(10): 121.80(9)º).[77]

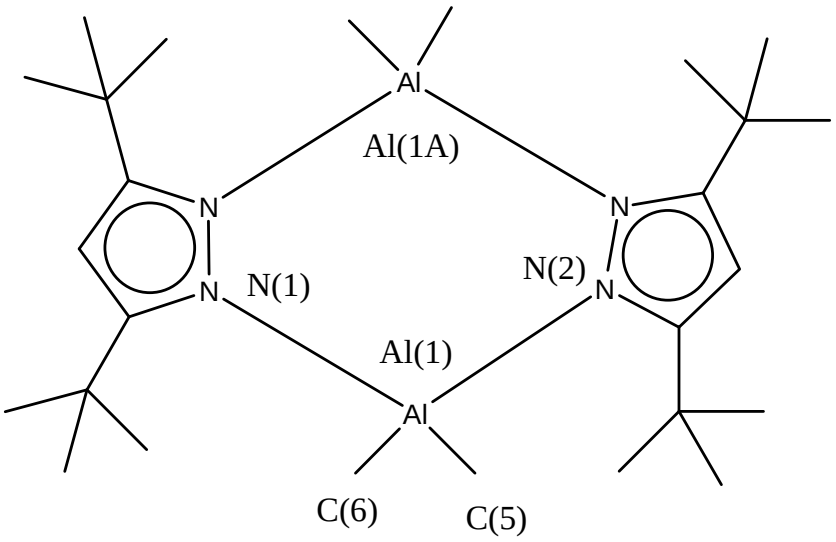

Figure 4-14. Structure of the complex [(η^1, η^1-3,5-*t*Bu_2pz)(μ-Al)Me_2]$_2$ [77]; hydrogen atoms removed for clarity.

Table 4-5. Selected bond lengths (Å) and angles (º) for compound **4.5**.

Bond lengths			
Al(1)–N(11)	1.957(5)	Al(12)–N(12)	1.961(7)
Al(1)–N(21)	1.952(7)	Al(12)–N(22)	1.963(6)
Al(1)–C(3)	1.969(5)	Al(12)–C(5)	1.977(4)
Al(1)–N(4)	1.971(5)	Al(1)–N(6)	1.969(4)
Bond angles			
N(11)–Al(1)–N(12)	102.48(2)	N(12)–Al(2)–N(22)	102.53(2)
C(3)-Al(1)-C(4)	125.055(16)	C(5)-Al(2)-C(6)	125.42(2)

4.2.4 Concluding remarks

The successful preparation and characterisation of $[Li_4(Me_2pz)_4(OEt_2)_4]$ **(4.1)**, $[Li_6(Me_2pz)_6(tmeda)_2]$ **(4.2)** and $[Li_2(C_5N_3H_6O_2)_2(thf)_2]_n$ **(4.3)** portray advances in lithium pyrazolate chemistry. Comparing the previously Et_2O-solvated pyrazolate complex of $[Li(Ph_2pz)(OEt_2)]_2$ [26] with compound **4.1** shows the transition from μ-η^2:η^1 in $[Li(Ph_2pz)(OEt_2)]_2$ [26] to the μ_3-η^1:η^1:η^1 due to the less steric demand of Me_2pz ions around Li^+. $[Li_6(Me_2pz)_6(tmeda)_2]$ **(4.2)** reveals an important advance in lithium pyrazolate chemistry, as no hexameric pyrazolate structure of lithium using THF/TMEDA was reported before. Lithium ions have three different coordination numbers in compound **4.2** (six, three and four). Also, three kind of bridging bonds were observed in the compound **4.2** (μ-η^2:η^2, μ-η^1:η^1 and μ-η^2:η). Using 3,5-di-*tert*-butyl-4-nitropyrazole resulted in a new polymeric chain of $[Li_2(C_5N_3H_6O_2)_2(thf)_2]_n$ **(4.3)** in which the $[Li_2(C_5N_3H_6O_2)_2(thf)_2]$ units are bridged by O_2N group in an *anti*-configuration.

A new alkylzinc derivative of 3,5-di-*tert*-butylpyrazole ($[Zn(tBu_2pz)_2(tBu_2pzH)_2]$.1/2THF (**4.4**)) with two pyrazolate ions and two neutral *t*Bu_2pzH molecules was prepared. Hydrogen bonding occurs between two pyrazole molecules.

The compound $[AlMe_2(Ph_2pz)]_2$.1/2THF **(4.5)** prepared by reaction of $AlMe_3$ with Ph_2pzH in a 3:1 ratio. The crystal structure of **4.5** features two phenylpyrazolato groups serve as bridges between the two aluminium atoms.

Overall, this chapter presents a small contribution to the main group chemistry involving pyrazolates, while presenting several compounds that can be used in future metathesis chemistry (lithium complexes) but also compounds that have alkyl groups (Zn and Al complexes) that can be further substituted/elaborated in protolysis reactions.

4.3 Experimental

4.3.1 General considerations

Synthetic operations were carried out under an inert atmosphere of dry nitrogen using standard Schlenk and vacuum line techniques. All solvents were freshly distilled over sodium or sodium/benzophenone prior to use. 3,5-dimethylpyrazole (Me_2pzH) was purchased from Sigma-Aldrich and 3,5-diphenylpyrazole (Ph_2pzH) and 3,5-di-*tert*-butylpyrazole (tBu_2pzH) were prepared by literature methods.[81, 82] The starting materials, Me_2pzHNO_2 was kindly provided by our collaborator, Dr llya Taidakov, from the P.N. Lebedev Institute of Physics of Russian Academy of science, Moscow. Trimethylaluminum ($AlMe_3$), *n*-butyllitium (*n*BuLi) and diethylzinc ($ZnEt_2$) were purchased from Aldrich and used as received. IR spectra were obtained from Nujol mulls for the region 4000-400 cm^{-1} with a Nicolet-Nexus FT-IR spectrometer. The ^1H NMR spectra were recorded with a Bruker Ascend^{TM} 400 (400 MHz) using dry degassed *deutero*-benzene (C_6D_6) as solvent, and resonances were referenced to the residual ^1H resonances of the deuterated solvent. Elemental analyses (C, H, N) were performed by the Micro Analytical Laboratory, Science Centre, London Metropolitan University, England.

$[Li_4(Me_2pz)_4(Et_2O)_4]$ (4.1)

*n*BuLi (1.6 mL of a 2.5 M solution in hexane; 4 mmol) was added by a syringe to a stirring solution of Me_2pzH (0.4g; 4 mmol) in Et_2O (20mL) using Schlenk line. After 1 day stirring, the solution was concentrated to ~10 mL, and cooled overnight causing the formation of colourless crystals. Yield = 0.36g (51.15%); IR (crystal oil): ν = 2722 (m), 1515 (s), 1316 (m), 1260 (w), 1152 (m), 1076 (m), 1017 (s), 966 (m), 727 (vw), 843 (w), 774 (m), 737 (s), 691 (vw), 668 (vw) and 656 cm^{-1} (m); ^1H NMR (C_6D_6, 303.2 K): δ = 0.79 (t, 24 H, CH_3 Et_2O), 1.90 (s, 24 H, CH_3 (Me_2pz)), 2.93 (q, 16 H, CH_2 Et_2O), 5.67 (s, 4 H, H4–Me_2pz)),). Elemental analysis calcd. (%) for $Li_4C_{36}H_{66}N_8O_4$ (M = 703.744 $g.mol^{-1}$): C 61.443, H 9.596, N 15.923; calcd for $Li_4C_{20}H_{28}N_8$ (loss of four Et_2O molecules due to evaporation) (408.26 $g.mol^{-1}$): C 58.84, H 6.85, N 27.44. Found from microanalysis: C 56.65, H 8.00, and N 24.22.

[$Li_6(Me_2pz)_6(tmeda)_2$] (4.2)

*n*BuLi (1.6 mL of a 2.5 M solution in hexane; 4 mmol) was added by a syringe to a stirring solution of Me_2pzH (0.4g; 4 mmol) in hexane and TMEDA (4mmol, 0.6 mL) (TMEDA:Me_2pzH:1:1) (20mL) using Schlenk line. After 1 day stirring, the solution was concentrated to ~10 mL, and cooled overnight causing the formation of colourless crystals. Yield = 0.271g (48.11%); IR (crystal oil): ν = 3098(m), 2716 (m), 1562 (w), 1378 (vs), 1378 (vs), 1316 (vs), 1289 (vs), 1246 (s), 1180 (m), 1157 (s), 1129 (s), 1098 (m), 1067 (s), 1019 (vs), 948 (vs), 881 (w), 828 (s), 766 (vs), 737 (vs), 688 (m) and 663 cm^{-1} (m); ^1H NMR (C_6D_6, 303.2 K): δ = 1.90 (m, 60 H, CH_3 tmeda and Me_2pz), 2.22 (s, 24 H, CH_2 (tmeda)), 5.89 (s, 6 H, (H4–Me_2pz)).

[$Li_2(C_5N_3H_6O_2)_2(thf)_2]_n$ (4.3)

*n*BuLi (0.56 mL of a 2.5 M solution in hexane; 1.4 mmol) was added by a syringe to a stirring solution of 3,5-di-*tert*-butyl-4-nitropyrazole (0.2 g; 1.4 mmol) in THF (20mL) using Schlenk line. After 1 day stirring, the solution was concentrated to ~5 mL, and cooled for 4 days, causing the formation of red crystals. Yield = 0.14g (45.62%); IR (crystal oil): ν = 3381(m), 2782 (m), 1529 (m), 1163 (s), 1046 (m), 977 (m), 891 (m), 823 (vw), 770 (m), and 722 cm^{-1} (s); ^1H NMR (C_6D_6, 303.2 K): δ = 1.70 (m, 8 H, β-CH_2(thf)), 2.28 (s, 12 H, CH_3 (pz)), 3.42 (m, 8 H, α-CH_2(thf)). Elemental analysis calcd. (%) for $(LiC_9H_{14}N_3O_3)_2$ (M = 438.34 $g.mol^{-1}$): C 49.323, H 6.438, N 19.172; Found from microanalysis: C 49.17, H 6.50, and N 19.26.

[Zn(*t*$Bu_2pz)_2$(*t*$Bu_2pzH)_2$].1/2THF (4.4)

$ZnEt_2$ (0.12 mL of a 15 W% solution in toluene; 0.5 mmol) was added by a syringe to a stirring solution of *t*Bu_2pzH (0.2 g; 1 mmol) in THF (20mL) using Schlenk line. After 1 day stirring, the solution was concentrated to ~5 mL, and cooled for one week, causing the formation of colourless crystals. Yield = 0.07 g (34.18%); IR (crystal oil): ν = 3137(w), 2724 (m), 1571 (m), 1290 (s), 1204 (m), 1133 (m), 1117 (w), 1083 (m), 1016 (m), 976 (w), 916 (w), 801 (m), 782 (m), 725 (s), and 629 cm^{-1} (w); ^1H NMR (C_6D_6, 303.2 K): δ = 1.10 (s, 36 H, *t*Bu (*t*Bu_2pzH), 1.52 (s, 36 H, *t*Bu (*t*Bu_2pz), 5.96 (s, 2 H, H4 – *t*Bu_2pzH), 6.09 ppm (s, 2

H, H4 – *t*Bu$_2$pz), 10.33 (br s, 2 H, H4 – *t*Bu$_2$pz). Elemental analysis calcd. (%) for $ZnC_{44}H_{78}N_8$ (Loss of ½ THF molecule due to evaporation) (M = 783.82 g.mol^{-1}): C 67.41, H 9.95, N 14.28; Found from microanalysis: C 68.50, H 8.76, and N 14.27.

[AlMe$_2$(Ph$_2$pz)]$_2$.1/2THF (4.5)

Under Schlenk line, a solution of AlMe$_3$ (0.45 mL of a 2.0 M solution in toluene; 0.3 mmol) was added dropwise to a suspension of Ph$_2$pzH ligand (0.2g, 0.9 mmol) in 20 mL THF under vigorous stirring. Instant gas formation was observed. The clear solution was stirred overnight at ambient temperature, and then evaporated (*in vacuo*), to less than 5mL and cooled slowly. Colourless crystalline product was obtained after four days and all the characterisations were performed on the crystalline compound. Yield = 0.103 g (41.84%); IR (Nujol oil): ν = 2725(m), 1575(w), 1543 (m), 1302(s), 1197(s), 1157 (m), 1109 (m), 1073 (m), 1008 (m), 967 (m), 917 (m), 869 (vw), 845 (vw), 808 (m), 759 (vs), 721 (vs), 697 cm^{-1} (vs); ^{1}H NMR (C_6D_6, 303.2 K): δ = -0.66 (s, 12 H, AlMe$_2$), 1.40 (m, 2 H, β-CH$_2$(thf)), 3.55 (m, 2 H, α-CH$_2$(thf)), 6.26 (s, 2 H, 4-H (Ph$_2$pz)), 7.03 (br, m, 12 H, *m*-, *p*-H (Ph$_2$pz)), 7.42 (br m, 8 H, *o*-H (Ph$_2$pz)). Elemental analysis calcd. (%) for $C_{34}H_{32}Al_2N_4$. (Loss of ½ THF molecule due to evaporation) (M = 550.30 g.mol^{-1})): C 74.20, H 5.81, N 10.17; Found from microanalysis: C 73.51, H 6.06, N 12.85.

4.3.2 Crystallographic data

Complexes were immersed in viscous hydrocarbon oil (Paraton-N) and measured on either a Bruker APEX II CCD diffractometer/on a 'Bruker P4' diffractometer with integration and absorption corrections completed using Apex II program suite, or at the Australian Synchrotron on the MX1 at 173 K using a single wavelength (λ = 0.712 Å). The data and integration were completed by Blue ice [83] and XDS [84] software programs. Structural solutions were obtained by either direct methods [85] or the Patterson method [85] and solutions were refined using full matrix least squares methods against F^2 using SHELX2014, via OLEX 2 [86] interface.

$[Li_4(Me_2pz)_4(Et_2O)_4]$ (4.1) : $C_{36}H_{66}N_8O_4Li_4$, (M = 703.75) , monoclinic, *Cc* (no. 9), a = 40.918(6) Å, b = 15.595(3) Å, c = 15.601(3) Å, α = 90°, β = 112.29(15)°, γ = 90°, V = 3212(3) Å^3, T = 296(2) K, Z = 8, Z' = 2, μ(MoK$_a$) = 0.065 mm^{-1}, 14.894 reflections measured, 6842 unique (R_{int} =0.1456), which were used in all calculations. The final wR_2 was 0.2005 (all data) and R_1 was 0.0685 (I > 2σ (I)).

$[Li_6(Me_2pz)_6(tmeda)_2]$ (4.2) : for $C_{42}H_{74}Li_6N_{16}$ (M =844.81 g/mol): orthorhombic, space group $P2_12_12_1$ (no. 19), a = 13.296(3) Å, b = 13.384(3) Å, c = 29.598(6) Å, $\alpha = \beta = \gamma = 90°$, V = 5267.1(18) Å^3, Z = 4, Z' = 1, T = 173.15 K, μ(MoKα) = 0.065 mm^{-1}, *Dcalc* = 1.065 g/cm^3, 56913 reflections measured (3.34° ≤ 2Θ ≤ 52.744°), 10661 unique (R_{int} = 0.0379) which were used in all calculations. The final wR_2 was 0.1751 (all data) and R_1 was 0.0664 (I > 2σ(I)).

$[Li_2(C_5N_3H_6O_2)_2(thf)_2]_n$ (4.3) : for $C_{18}H_{28}Li_2N_6O_6$ (M =438.34 g/mol): monoclinic, space group $P2_1/n$ (no. 14), a = 8.2926(5) Å, b = 12.8207(8) Å, c = 11.3992(6) Å, β = 98.151(2)°, V = 1199.68(12) Å^3, Z = 2, Z' = 0.5, T = 296.15 K, μ(MoKα) = 0.090 mm^{-1}, *Dcalc* = 1.213 g/cm^3, 3152 reflections measured (4.808° ≤ 2Θ ≤ 59.14°), 892 unique (R_{int} = 0.0263) which were used in all calculations. The final wR_2 was 0.2185 (all data) and R_1 was 0.0672 (I > 2σ(I)).

$[Zn(tBu_2pz)_2(tBu_2pzH)_2]$.1/2THF (4.4) : $C_{44}H_{55}N_8Zn$ (M =819.87 g/mol): monoclinic, space group $P2_1/n$ (no. 14), a = 10.954(2) Å, b = 33.040(6) Å, c = 14.287(2) Å, α = 90°, β = 103.954(9)°, γ = 90°, V = 5017.9(16) Å^3, Z = 4, Z' = 1, T = 296(2) K, μ(MoKα) = 0.523 mm^{-1}, *Dcalc* = 1.008 g/cm^3, 42288 reflections measured (2.466° ≤ 2Θ ≤ 49.996°), 8805 unique (R_{int} = 0.1251) which were used in all calculations. The final wR_2 was 0.3438 (all data) and R_1 was 0.1092 (I > 2σ(I)) and.

$[AlMe_2(Ph_2pz)]_2$.1/2THF (4.5) : $C_{36}H_{38}Al_2N_4O$ (M =592.63 g/mol): triclinic, space group *P-1* (no. 2), a = 10.522(2) Å, b = 11.172(2) Å, c = 14.019(3) Å, α = 85.63(3)°, β = 82.31(3)°, γ = 79.68(3)°, V = 1604.4(6) Å^3, Z = 2, Z' = 1, T = 293(2) K, μ(MoKα) = 0.125 mm^{-1}, *Dcalc* = 1.227 g/cm^3, 17946 reflections measured (2.936° ≤ 2Θ ≤ 63.75°), 7243 unique (R_{int} = 0.0265, R_{sigma} = 0.0285) which were used in all calculations. The final wR_2 was 0.1941 (all data) and R_1 was 0.0635 (I > 2σ(I)).

4.4 References

1. S. Fustero, M. Sánchez-Roselló, P. Barrio and A. Simón-Fuentes, *Chem. Rev.*, 2011, **111**, 6984-7034.
2. G. L. Monica and G. A. Ardizzoia, in *Prog. Inorg. Chem.*, John Wiley & Sons, Inc., 2007, pp. 151-238.
3. M. A. Halcrow, *Dalton Trans.*, 2009, 2059-2073.
4. J. Klingele, S. Dechert and F. Meyer, *Coord. Chem. Rev.*, 2009, **253**, 2698-2741.
5. M. Viciano-Chumillas, S. Tanase, L. J. de Jongh and J. Reedijk, *Eur. J. Inorg. Chem.*, 2010, 3403-3418.
6. J. Hitzbleck, A. Y. O'Brien, C. M. Forsyth, G. B. Deacon and K. Ruhlandt-Senge, *Chem. Eur. J*, 2004, **10**, 3315-3323.
7. W. Zheng, N. C. Mösch-Zanetti, T. Blunck, H. W. Roesky, M. Noltemeyer and H.-G. Schmidt, *Organometallics*, 2001, **20**, 3299-3303.
8. G. B. Deacon, E. E. Delbridge, C. M. Forsyth, P. C. Junk, B. W. Skelton and A. H. White, *Aust. J. Chem.*, 1999, **52**, 733-740.
9. W. Zheng, A. Stasch, J. Prust, H. W. Roesky, F. Cimpoesu, M. Noltemeyer and H.-G. Schmidt, *Angew. Chem. Int. Ed.*, 2001, **40**, 3461-3464.
10. Z. Yu, M. J. Heeg and C. H. Winter, *Chem. Commun.*, 2001, 353-354.
11. Z. Yu, J. M. Wittbrodt, M. J. Heeg, H. B. Schlegel and C. H. Winter, *J. Am. Chem. Soc.*, 2000, **122**, 9338-9339.
12. Z. Yu, J. M. Wittbrodt, A. Xia, M. J. Heeg, H. B. Schlegel and C. H. Winter, *Organometallics*, 2001, **20**, 4301-4303.
13. C. Yélamos, M. J. Heeg and C. H. Winter, *Inorg. Chem.*, 1998, **37**, 3892-3894.
14. W. Zheng, Mary J. Heeg and Charles H. Winter, *Eur. J. Inorg. Chem.*, 2004, 2652-2657.
15. E. W. Abel, F. G. A. Stone and G. Wilkinson, *Comprehensive Organometallic Chemistry II: A Review of the Literature 1982-1994*, Elsevier Science & Technology Books, 1995.
16. R. B. King, *Encyclopedia of Inorganic Chemistry*, Wiley, 2005.
17. A. W. Parkins and R. C. Poller, *An Introduction to Organometallic Chemistry*, Macmillan, 1986.
18. G. Wilkinson, R. D. Gillard and J. A. McCleverty, *Comprehensive coordination chemistry: the synthesis, reactions, properties & applications of coordination compounds. Main group and early transition elements*, Pergamon Press, 1987.

19. E. Müller and D. Ludsteck, *Chem. Ber.*, 1954, **87**, 1887-1895.
20. I. Fatt and M. Tashima, *Alkali Metal Dispersions*, Van Nostrand, 1961.
21. H. Gilman and J. W. Morton, *Org. React.*, 1954, **8**, 258-304.
22. R. G. Jones and R. J. Gildea, *Org. React.*, 1951, **6**, 339-366.
23. D. J. Peterson, *Organomet. Chem. Rev. (A)*, 1972, **7**.
24. W. E. Parham and L. D. Jones, *J. Org. Chem*, 1976, **41**, 1187-1191.
25. W. J. Trepka and R. J. Sonnenfeld, *J. Organomet. Chem.*, 1969, **16**, 317-320.
26. S. Beaini, G. B. Deacon, A. P. Erven, P. C. Junk and D. R. Turner, *Chem.Asian.J*, 2007, **2**, 539-550.
27. T. Kloubert, C. Müller, S. Krieck, T. Schlotthauer, H. Görls and M. Westerhausen, *Eur. J. Inorg. Chem.*, 2012, DOI: 10.1002/ejic.201200876, 5991-6001.
28. B. Schowtka, H. Görls and M. Westerhausen, *Z. Anorg. Allg. Chem.*, 2014, **640**, 907-915.
29. T. Kloubert, H. Görls and M. Westerhausen, *Z. Anorg. Allg. Chem.*, 2010, **636**, 2405-2408.
30. S. Komorski, M. K. Leszczyński, I. Justyniak and J. Lewiński, *Inorg. Chem.*, 2016, **55**, 5104-5106.
31. J. M. Bakker, L. J. Barbour, G. B. Deacon, P. C. Junk, G. O. Lloyd and J. W. Steed, *J. Organomet. Chem.*, 2010, **695**, 2720-2725.
32. S.-Á. Cortés-Llamas, R. Hernández-Lamoneda, M.-Á. Velázquez-Carmona, M.-A. Muñoz-Hernández and R. A. Toscano, *Inorg. Chem.*, 2006, **45**, 286-294.
33. D. L. Reger, J. E. Collins, M. A. Matthews, A. L. Rheingold, L. M. Liable-Sands and I. A. Guzei, *Inorg. Chem.*, 1997, **36**, 6266-6269.
34. Nanjo. M, Sekiguchi. A and Sakurai. H, *Bull. chem. Soc. Jpn*, 1999, **72**, 1387-1393.
35. U. Siemeling, T. Redecker, B. Neumann and H.-G. Stammler, *J. Am. Chem. Soc.*, 1994, **116**, 5507-5508.
36. R. Zerger, W. Rhine and G. Stucky, *J. Am. Chem. Soc.*, 1974, **96**, 6048-6055.
37. E. Weiss and G. Hencken, *J. Organomet. Chem.*, 1970, **21**, 265-268.
38. J. L. Kisko, T. Hascall, C. Kimblin and G. Parkin, *J. Chem. Soc., Dalton Trans.*, 1999, 1929-1936.
39. G. B. Deacon, E. E. Delbridge, C. M. Forsyth, B. W. Skelton and A. H. White, *J. Chem. Soc., Dalton Trans.*, 2000, 745-751.
40. D. Margerison and J. P. Newport, *Trans. Faraday Soc.*, 1963, **59**, 2058-2063.
41. D. Seebach, R. Hässig and J. Gabriel, *Helv. Chim. Acta*, 1983, **66**, 308-337.
42. W. Bauer and P. v. R. Schleyer, *J. Am. Chem. Soc.*, 1989, **111**, 7191-7198.
43. G. Meyer, *J. Alloys Compd.*, 2000, **300**, 113-122.

44. M. L. Cole, P. C. Junk and L. M. Louis, *J. Chem. Soc., Dalton Trans.*, 2002, 3906-3914.
45. M. L. Cole, A. J. Davies, C. Jones and P. C. Junk, *J. Organomet. Chem.*, 2004, **689**, 3093-3107.
46. J. Baldamus, C. Berghof, Marcus L. Cole, E. Hey-Hawkins, Peter C. Junk and Lance M. Louis, *Eur. J. Inorg. Chem.*, 2002, 2878-2884.
47. P. C. Junk and M. L. Cole, *Chem. Commun.*, 2007, 1579-1590.
48. A. L. Llamas-Saiz, C. Foces-Foces, F. H. Cano, P. Jimenez, J. Laynez, W. Meutermans, J. Elguero, H.-H. Limbach and F. Aguilar-Parrilla, *Acta Cryst.*, 1994, **B50**, 746-762.
49. A. J. Blake, N. R. Champness, P. Hubberstey, W.-S. Li, M. A. Withersby and M. Schröder, *Coord. Chem. Rev.*, 1999, **183**, 117-138.
50. M. R. Bürgstein, M. T. Gamer and P. W. Roesky, *J. Am. Chem. Soc.*, 2004, **126**, 5213-5218.
51. G. Deacon, B. Gatehouse, S. Nickel and S. Platts, *Aust. J. Chem.*, 1991, **44**, 613-621.
52. M.-Á. Velázquez-Carmona, A.-J. Metta-Magaña, S.-A. Cortés-Llamas, V. Montiel-Palma and M.-Á. Muñoz-Hernández, *Polyhedron*, 2009, **28**, 205-208.
53. B. Cordero, V. Gomez, A. E. Platero-Prats, M. Reves, J. Echeverria, E. Cremades, F. Barragan and S. Alvarez, *Dallton Trans*, 2008, 2832-2838.
54. M. K. Ehlert, S. J. Rettig, A. Storr, R. C. Thompson and J. Trotter, *Can. J. Chem.*, 1990, **68**, 1494-1498.
55. J. P. Jesson, S. Trofimenko and D. R. Eaton, *J. Am. Chem. Soc.*, 1967, **89**, 3148-3158.
56. J. Bielawski, T. G. Hodgkins, W. J. Layton, K. Niedenzu, P. M. Niedenzu and S. Trofimenko, *Inorg. Chem.*, 1986, **25**, 87-90.
57. J. Yamamoto and C. A. Wilkie, *Inorg. Chem.*, 1971, **10**, 1129-1133.
58. S. Trofimenko, *Chem. Rev.*, 1972, **72**, 497-509.
59. S. Trofimenko, *Prog. Inorg. Chem*, 1986, **34**, 115-210.
60. N. C. Mösch-Zanetti, R. Krätzner, C. Lehmann, T. R. Schneider and I. Usón, *Eur. J. Inorg. Chem.*, 2000, 13-16.
61. J. R. Perera, M. J. Heeg, H. B. Schlegel and C. H. Winter, *J. Am. Chem. Soc*, 1999, **121**, 4536-4537.
62. M. Watanabi, C. N. McMahon, C. J. Harlan and A. R. Barron, *Organometallics*, 2001, **20**, 460-467.
63. M. Bochmann, *J. Chem. Soc., Dalton Trans.*, 1996, 255-270.
64. C. J. Harlan, S. G. Bott and A. R. Barron, *J. Am. Chem. Soc.*, 1995, **117**, 6465-6474.
65. A. R. Barron, *Organometallics*, 1995, **14**, 3581-3583.
66. S. Pasynkiewicz, *Polyhedron*, 1990, **9**, 429-453.

67. F. A. Cotton, G. Wilkinson, C. A. Murillo and M. Bochmann, *Advanced Inorganic Chemistry*, Wiley, New York, sixth edn., 1996.
68. N. N. Greenwood and E. A. Earnshaw, in *Chemistry of the Elements (Second Edition)*, Butterworth-Heinemann, Oxford, 1997, pp. 216-267.
69. T. Mole, *Organoaluminium compounds*, Elsevier Pub. Co., 1972.
70. V. R. Magnuson and G. D. Stucky, *J. Am. Chem. Soc.*, 1969, **91**, 2544-2550.
71. W. J. Evans, R. Anwander and J. W. Ziller, *Organometallics*, 1995, **14**, 1107-1109.
72. J. Klosin, G. R. Roof, E. Y. X. Chen and K. A. Abboud, *Organometallics*, 2000, **19**, 4684-4686.
73. A. Cottone and M. J. Scott, *Organometallics*, 2000, **19**, 5254-5256.
74. A. J. R. Son, M. G. Thorn, P. E. Fanwick and I. P. Rothwell, *Organometallics*, 2003, **22**, 2318-2324.
75. G. S. Hair, A. H. Cowley, J. D. Gorden, J. N. Jones, R. A. Jones and C. L. B. Macdonald, *Chem. Commun.*, 2003, 424-425.
76. C. T. Sirimanne, Z. Yu, M. J. Heeg and C. H. Winter, *J. Organomet. Chem.*, 2006, **691**, 2517-2527.
77. W. Zheng, H. Hohmeister, N. C. Mösch-Zanetti, H. W. Roesky, M. Noltemeyer and H.-G. Schmidt, *Inorg. Chem.*, 2001, **40**, 2363-2367.
78. J. Lewiński, J. Zachara, P. Goś, E. Grabska, T. Kopeć, I. Madura, W. Marciniak and I. Prowotorow, *Chem. Eur. J*, 2000, **6**, 3215-3227.
79. C.-C. Chang, T.-Y. Her, F.-Y. Hsieh, C.-Y. Yang, M. Y. Chiang, G.-H. Lee, Y. Wang and S.-M. Peng, *J. Chin. Chem. Soc.*, 1994, **41**, 783-789.
80. A. Arduini and A. Storr, *J. Chem. Soc., Dalton Trans.*, 1974, 503-506.
81. C. Fernández-Castaño, C. Foces-Foces, N. Jagerovic and J. Elguero, *J. Mol. Struct.*, 1995, **355**, 265-271.
82. J. Elguero, E. Gonzalez and R. Jacquier, *Bull. Soc. Chim. Fr.*, 1968, 707-713.
83. T. M. McPhillips, S. E. McPhillips, H.-J. Chiu, A. E. Cohen, A. M. Deacon, P. J. Ellis, E. Garman, A. Gonzalez, N. K. Sauter, R. P. Phizackerley, S. M. Soltis and P. Kuhn, *J. Synchrotron Rad.*, 2002, **9**, 401-406.
84. W. Kabsch, *J. Appl. Cryst.*, 1993, **26**, 795-800.
85. G. Sheldrick, *Acta Crystallogra., Sect. A*, 2008, **64**, 112-122.
86. O. V. Dolomanov, L. J. Bourhis, R. J. Gildea, J. A. K. Howard and H. Puschmann, *J. Appl. Cryst.*, 2009, **42**, 339-341.

Chapter 5

Concluding Remarks

5. Chapter 5

Investigation of the synthesis of novel pyrazolate rare earth complexes and Li, Zn and Al pyrazolate complexes has yielded 29 new pyrazolate compounds. The initial focus of this thesis was to isolate rare earth pyrazolate complexes using RTP and high-temperature solvent-free reactions. However, attempts to synthesise the scandium (III) pyrazolate complexes using 3,5-dimethylpyrazole as the pro-ligand and $Hg(C_6F_5)_2$ using RTP reaction resulted in the isolation of oxide cage complexes. The pyrazolate oxide cage complexes were isolated previously by other researchers. Werner reported the isolation of a lanthanum oxide cage of formula $[La_4O(Me_2pz)_{10}(Me_2pzH)]$.[1] Although it was assumed that 3,5-dimethylpyrazole reacts easily, performing several RTP reactions showed that it a highly reactive ligand that resulted in complexes contain oxygen and fluorine. This was clearly demonstrated by isolation of a variety of complexes in chapter **2** such as $[Sc_3O(Me_2pz)_7(Me_2pzH)_2]$ (**2.2**), $[La_4(Me_2pz)_9(\mu_2\text{-}F)_2(\mu_4\text{-}F)(thf)_4].3THF$ (**2.6**), $[La(Me_2pz)_5Hg_2(C_6F_5)_2(thf)]$ (**2.7**) and $[Er_3F(Me_2pz)_8thf_2]$ (**2.8**). Also, isolation of $[Sc(Me_2pz)_2(Me_2pz(SiMe_2O))]_2$ (**2.3**) can confirm that the source of oxygen in the structure is silicon grease or solvent. The insertion of the $[SiMe_2O]_n$ was also observed previously by Werner.[1] However, under strict $[SiMe_2O]_n$ free conditions, oxide formation was still observed, showing that another process is likely occurring. Using Et_2O as the solvent in the RTP reaction, which is kept over sodium (to ensure the solvent is dry), resulted in the formation of compound **2.4** ($[Y_3O(Me_2pz)_9Na_2(Et_2O)_2]$) and **2.5** ($[Y_3(Me_2pz)_9(Me_2pzH)_2Na_2O]$). The presence of Sodium in the structure presumably arose from Na_2O in the solvent. Werner observed the isolation of a rare earth bimetallic oxide cage as a result of the treatment of $[Ce(Me_2pz)_3(thf)]$ with K(btsa)[1] and Schumann similarly isolated a bimetallic as a result of the reaction between lanthanoid trichlorides with Na(pz) and $Na(pzMe_2)$.[2] It can be concluded the reactive $Y(Me_2pz)$, trapped the Na_2O present in the solvent. Attempting the reaction with larger lanthanoid element (La) resulted in the formation of the complex **2.6** ($[La_4(Me_2pz)_9(\mu_2\text{-}F)_2(\mu_4\text{-}F)(thf)_4].3THF$). The presence of fluorine in the structure is the result of C-F activation and the high fluorophilicity of lanthanoids. Isolation of $[La(Me_2pz)_5Hg_2(C_6F_5)_2(thf)]$ (**2.7**) can confirm the presence of LaL_3 and $LHg(C_6F_5)$ during RTP reaction and provides evidence towards intermediates in these reactions. Performing an RTP reaction using Er, which is a smaller lanthanoid than lanthanum, resulted in the trinuclear structure $[Er_3F(Me_2pz)_8(thf)_2]$ (**2.8**). Compound **2.8**

again has fluorine in the compound, presumably from C-F activation which has been observed previously in the aryloxide complex $[Er_3(OAr^{OMe})_4(\mu_2\text{-}F)_3(\mu_3F)_2(thf)_4].thf.0.5C_6H_{14}$.[3] Also, the trimeric yttrium compound ($[Na(dme)_3Y_3F(Me_2pz)_9].3/2DME$ (**2.9**)) provided a new example of C-F activation. The presence of sodium coordinated with donor solvent by RTP reaction is observed for the first time, only previously observed in salt elimination reactions.[4]

Performing RTP reactions using the bulkier *t*Bu$_2$pzH as the pro-ligand were less problematic and pz compounds were isolable. Attempts to isolate products resulted in the monomeric [Ln(*t*Bu$_2$pz)$_3$(thf)$_2$] (Ln = La, Ce, Lu) complexes, which was expected due to the previously reported [Ln(*t*Bu$_2$pz)$_3$(thf)$_2$] (Ln = Nd and Eu).[5] However, using Sm resulted in the formation of a new polymeric structure ($[Sm_2(tBu_2pz)_6(dme)_2]_n$ (**2.11**)) that is similar to the previously reported $[Nd(tBu_2Pz)_3(dme)]_n$.[6]

Attempts to isolate targeted products using the bulky 3,5-diphenylpyrazole (Ph$_2$pzH) pro-ligand with lanthanum, praseodymium, gadolinium, holmium and lutetium in the RTP reactions failed due to the presence of dbmH (dibenzoylmethane) as a contamination in the starting materials when Ph$_2$pzH does not form completely during treating dbmH with hydrazine. Therefore, compounds [Lu(dbm)$_3$(dme)] (**2.13**) and [Sc(dbm)$_3$] (**2.14**) were isolated as crystals as by-products. Compound **2.13** and **2.14** had been reported previously using reactions other than RTP (by stirring the respective oxides in hydrochloric acid and following refluxing) by E.G. Zaitseva *et.al*.[7]

This chemistry highlights the difficulty in performing Me$_2$pz chemistry of the lanthanoids compared with other 3,5-disubstituted pyrazolato chemistry. The lack of steric bulk of the Me$_2$pz ligand presumably allows opening of the coordination sphere of the metal leading to higher reactivity with for example solvent molecules, grease and fluorinated organics.

Solvent-free elevated temperature reactions can be a useful route towards homoleptic complexes, and interesting structural features can be expected because the lanthanoid ion has to satisfy its coordination sphere with only pz$^-$ ligands. In this study in chapter **3**, the direct reaction between lanthanoid metals and three kinds of pyrazoles (3,5-dimethyl pyrazole, 3,5-diphenylpyrazole and 3,5-di-*tert*-butylpyrazole) is a simple route that resulted in the isolation of homoleptic and heteroleptic (due to coordinated pzH) rare earth pyrazolates. Due to the lower steric bulk of 3,5-dimethylpyrazole, a homoleptic twelve-coordinate La structure has been synthesized which is a η^2:η^5-Me$_2$pz-bridged coordination polymer with 12-coordinate

La atoms in a η^5:η^5 Me_2pz sandwich. The η^5 bonding gives the Me_2pz ligands a "cyclopentadienyl (Cp)" type coordination, which has only a few examples in rare earth pz chemistry. Thus, both homoleptic and heteroleptic complexes have been isolated using 3,5-diphenylpyrazole ($[Ce_3(Ph_2pz)_9]$, $[Dy_2(Ph_2pz)_6]$, $[Y(Ph_2pz)_3(Ph_2pzH)_2]$ and $[Pr(Ph_2pz)_2(Ph_2pz(SiMe_2O))]_2$). While using cerium as the metal in the solid state reaction, a compound was isolated similarly to its neighbours in the lanthanoid series ($[Ce(t\text{Bu}_2pz)_3]_2$ (**3.7**)).[8, 9] Considering the reported structures in chapter **3** that resulted from high-temperature solvent-free reactions, it can be assumed that the series of possible complexes from elevated temperature reaction using rare earth elements and 3,5-diphenylpyrazole and 3,5-di-*tert*-butylpyrazole is almost complete. However, due to the isolation of $[La(Me_2pz)_3]_n$, this work is incomplete using the less bulky 3,5-dimethyl pyrazole which may result in some new pyrazolate binding modes and this is suggested as future work in this exciting field.

Due to the isolation of a variety of rare earth pyrazolate compounds in this study, further studies were performed using Li (nBuLi was used as the metalation reagent), Al and Zn alkyls in chapter **4** to investigate the characteristics of pyrazolate ligands towards main group elements. The successful preparation and characterisation of $[Li_4(Me_2pz)_4(Et_2O)_4]$ **(4.1)**, $[Li_6(Me_2pz)_6(tmeda)_2]$ **(4.2)** and $[Li_2(C_5N_3H_6O_2)_2thf_2]_n$ **(4.3)** portray advances in lithium pyrazolate chemistry. $[Li_6(Me_2pz)_6(tmeda)_2]$ **(4.2)** reveals an important advance in lithium pyrazolate chemistry, as no hexamer pyrazolate structure of lithium using THF/TMEDA was reported before. Overall, these reported lithium compounds can be used in future metathesis chemistry.

Previously a series of compounds using lanthanoids and a ligand having a nitro group were reported later ($[(THF)_4\{K(o\text{-}O_2N\text{-}C_6H_4\text{-}O)_4Ln\}_4]_n$ (Ln = Y, Er, Lu); $[[K_2(o\text{-}O_2N\text{-}C_6H_4\text{-}O)_5Tb]_n]$ etc.).[10] In this study for the first time, metallating 3,5-di-*tert*-butyl-4-nitropyrazole with *n*BuLi resulted in a structure which consists of a dinuclear structure which is part of a large polymeric network ($[Li_2(C_5N_3H_6O_2)_2(thf)_2]_n$ (**4.3).**

Poly(1-pyrazolate)borate zinc complexes were first reported by Trofimenko *et al.*[11] Later, zinc and boron centres were featured in some polynuclear pyrazolyl bridged species.[12] Most of the mentioned complexes were not characterised by X-ray crystallography. Recently, Ehlert *et al* reported the dimer $[Zn_2(Me_2pz)_4(Me_2pzH)]$.[13] Now in this study by metallating 3,5-di-*tert*-butylpyrazole by $ZnEt_2$, a new alkylzinc derivative of ($[Zn(t\text{Bu}_2pz)_2(t\text{Bu}_2pzH)_2]$.1/2THF (**4.4**)) with two pyrazolate ions and two neutral $t\text{Bu}_2pzH$ molecules was isolated. Hydrogen bonding occurs between two pyrazole molecules.

Previously, some 3,5-di-tert-butylpyrazolato[14, 15] and 3,5-dimethylpyrazolato[16] aluminium derivatives have been investigated and characterized. In this study, the compound $[AlMe_2(Ph_2pz)]_2.1/2THF$ **(4.5)** prepared by reaction of $AlMe_3$ with Ph_2pzH in a 3:1 ratio. The crystal structure of **4.5** features two phenylpyrazolato groups serving as bridges between the two aluminium atoms.

Overall, this chemistry represents the significant aspect of pyrazolato compounds isolated from redox transmetallation/protolysis and high temperature reaction using lanthanoids besides main group element (Li, Zn and Al) pyrazolato compounds.

5.1 References

1. D. Werner, Ph.D Thesis, Monash University, 2015.
2. H. Schumann, P. R. Lee and J. Loebel, *Angew. Chem. Int. Ed.*, 1989, **28**, 1033-1035.
3. G. B. Deacon, G. D. Fallon, C. M. Forsyth, S. C. Harris, P. C. Junk, B. W. Skelton and A. H. White, *Dalton Trans*, 2006, 802-812.
4. M. L. Cole and P. C. Junk, *Chem. Commun.*, 2005, 2695-2697.
5. J. E. Cosgriff, G. B. Deacon, B. M. Gatehouse, H. Hemling and H. Schumann, *Angew. Chem. Int. Ed. Engl.*, 1993, **32**, 874-875.
6. J. E. Cosgriff, G. B. Deacon, G. D. Fallon, B. M. Gatehouse, H. Schumann and R. Weimann, *Chem. Ber.*, 1996, **129**, 953-958.
7. E. G. Zaitseva, l. A. Baidina, P. A. Stabnikov, S. V. Borisov and I. K. Igumenov, *J. Struct. Chem.*, 1990, **31**, 184-182.
8. R. Anwander, D. Werner, G. B. Deacon and P. C. Junk, *Dalton Trans.*, 2017.
9. D. Werner, G. B. Deacon, P. C. Junk and R. Anwander, *Chem. Eur. J.*, 2014, **20**, 4426-4438.
10. M. R. Bürgstein, M. T. Gamer and P. W. Roesky, *J. Am. Chem. Soc.*, 2004, **126**, 5213-5218.
11. J. P. Jesson, S. Trofimenko and D. R. Eaton, *J. Am. Chem. Soc.*, 1967, **89**, 3148-3158.
12. J. Bielawski, T. G. Hodgkins, W. J. Layton, K. Niedenzu, P. M. Niedenzu and S. Trofimenko, *Inorg. Chem.*, 1986, **25**, 87-90.
13. M. K. Ehlert, S. J. Rettig, A. Storr, R. C. Thompson and J. Trotter, *Can. J. Chem.*, 1990, **68**, 1494-1498.
14. W. Zheng, H. Hohmeister, N. C. Mösch-Zanetti, H. W. Roesky, M. Noltemeyer and H.-G. Schmidt, *Inorg. Chem.*, 2001, **40**, 2363-2367.
15. G. B. Deacon, E. E. Delbridge, C. M. Forsyth, P. C. Junk, B. W. Skelton and A. H. White, *Aust. J. Chem.*, 1999, **52**, 733-740.
16. J. Lewiński, J. Zachara, P. Goś, E. Grabska, T. Kopeć, I. Madura, W. Marciniak and I. Prowotorow, *Chem. Eur. J*, 2000, **6**, 3215-3227.

Publication

Dalton Transactions

COMMUNICATION

View Article Online
View Journal

Cite this: DOI: 10.1039/c8dt00338f

Received 25th January 2018,
Accepted 4th April 2018

DOI: 10.1039/c8dt00338f

rsc.li/dalton

Unique and contrasting structures of homoleptic lanthanum(III) and cerium(III) 3,5-dimethylpyrazolates†

Daniel Werner, [a] Uwe Bayer, [a] Nazli E. Rad,[b] Peter C. Junk, *[b] Glen B. Deacon *[c] and Reiner Anwander *[a]

Homoleptic $[La(Me_2pz)_3]_n$ (Me_2pz = 3,5-dimethylpyrazolato) is a μ–η^2:η^5-Me_2pz coordination polymer with 12-coordinate La atoms in an unusual η^5:η^5 Me_2pz sandwich, whilst the cerium congener forms a molecular tetrametallic cage $[Ce_4(Me_2pz)_{12}]$ featuring six different Me_2pz coordination modes.

With some twenty different known binding modes,[1] several of which were developed through rare-earth metal derivatives,[2–6] the capacity for innovation or surprises in pyrazolate (1,2-diazocyclopentadienide) complexes might appear exhausted. However, through exclusive coordination of the relatively sterically undemanding 3,5-dimethylpyrazolato ligand (Me_2pz) to the large lanthanide ions (La^{3+}, Ce^{3+}), we have accessed polymeric $[La(Me_2pz)_3]$ (**1**), solely bridged by η^2:η^5-bonded ligands such that the metal is in an η^5-pz sandwich, and also tetrametallic $[Ce_4(Me_2pz)_{12}]$ (**2**), which has six different pyrazolato binding modes. Hitherto, a homoleptic η^5-pz sandwich complex has been observed only for molecular $[Ru(\eta^5\text{-}Me_2pz)_2]$,[7] whilst the coordination variety in **2** is unprecedented.

Following the reaction of lanthanum metal with 3,5-dimethylpyrazole in the presence of 1,2,4,5-tetramethylbenzene, crystallisation from toluene gave polymeric homoleptic $[La(Me_2pz)_3]$ (**1**) (Scheme 1 (i)). After crystallisation, **1** was insoluble in non-coordinating solvents, making purification and subsequent characterisation difficult. However, an amorphous analytically pure sample of the same compound (with a nearly identical IR spectrum) was obtained by protonolysis of lanthanum tris[bis(trimethylsilyl)amide] with 3,5-dimethylpyrazole (Scheme 1 (ii)). When switching to cerium, a characterisable product could not be obtained from the reaction of

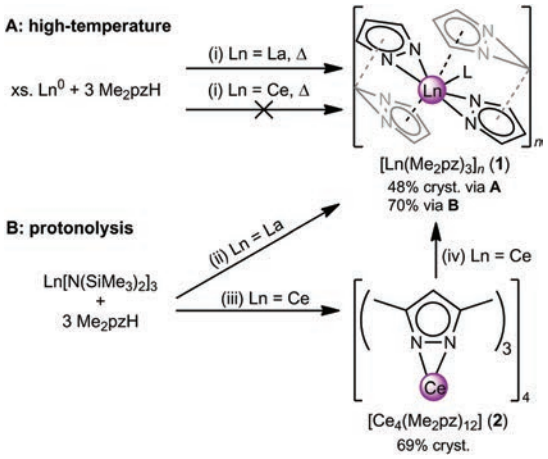

Scheme 1 Synthesis of homoleptic rare-earth metal pyrazolate complexes. High-temperature synthesis **A**: (i) reagents were sealed under vacuum, heated to 220–270 °C, with 1,2,4,5-tetramethylbenzene, loss of dihydrogen. After reaction, crystallisation was performed from hot toluene (L = Me_2pz). Protonolysis **B**: (ii) reagents stirred in toluene, loss of 3 $HN(SiMe_3)_2$; (iii) toluene solution of Me_2pzH added dropwise to a toluene solution of $Ce[N(SiMe_3)_2]_3$; for Ln = Ce crystallisation at −35 °C gave crystals of $[Ce_4(Me_2pz)_{12}]$·PhMe (**2**·PhMe), for Ln = La a white powder of $[La(Me_2pz)_3]_n$ (**1**) formed immediately (Me groups omitted); (iv) heating in toluene converted **2** into an insoluble material, presumably a polymeric variant like **1**. Note: Me_2pz bonding in schematic of **1** and **2** are simplified.

cerium metal with 3,5-dimethylpyrazole (Scheme 1 (i)). The corresponding silylamine elimination however gave the tetrametallic species $[Ce_4(Me_2pz)_{12}]$·toluene (**2**·toluene) when the reagents were combined under mild conditions (namely slow combination of reagents without stirring, Scheme 1 (iii)). Complex **2** is soluble in C_6D_6, toluene, and even *n*-hexane. The ^1H NMR spectrum of **2** in C_6D_6 is consistent with multiple Me_2pz environments, which persist in solution but their complexity defies any detailed interpretation (Fig. S4†). The ambient and lower-temperature proton spectra of a variable-temperature (VT) NMR spectroscopic study of re-crystallised **2** (−80 to +80 °C, Fig. S5–S8†) indicated nearly as many Me and

[a]*Institut für Anorganische Chemie, University of Tübingen (EKUT), Auf der Morgenstelle 18, 72076, Germany. E-mail: reiner.anwander@uni-tuebingen.de*
[b]*College of Science & Engineering, James Cook University, Townsville, Qld, 4811, Australia*
[c]*School of Chemistry, Monash University, Clayton, Victoria 3800, Australia*

†Electronic supplementary information (ESI) available: Experimental details, FTIR data and X-ray crystallographic information. CCDC 1441020 (**2**·PhMe), 1813156–1813158. For ESI and crystallographic data in CIF or other electronic format see DOI: 10.1039/c8dt00338f

H4(pz) signals as required for the different pyrazolato ligands present (in total 12). Unsurprisingly, a pronounced signal shifting was observed upon lowering the temperature, stretching a range from +66 to −61 ppm at −80 °C.

At higher temperatures less but significantly broadened signals appeared (*ca.* 8). Upon re-cooling the sample from +80 to 25 °C the original spectrum was retrieved. Independently performed protonolyses of $Ce[N(SiMe_3)_2]_3$ with one and two equiv. of 3,5-dimethylpyrazole indicated formation of complex **2** from the outset, as revealed by NMR spectroscopy (Fig. S9†), most likley *via* ligand redistribution (not shown in Scheme 1).

By distinct crystallisation procedures, we have obtained the Ce_4 cluster as $[Ce_4(Me_2pz)_{12}]\cdot 0.75n$-hexane (**2**·0.75*n*-hexane) and solvent-free $[Ce_4(Me_2pz)_{12}]$ (**2**) in addition to the toluene solvate (see ESI†), thereby showing the durability of the tetrametallic arrangement. Earlier we found that rapid addition and stirring the reagents in the silylamine elimination reaction gave $Ce(Me_2pz)_3$ as an insoluble powder,[8] the IR spectrum of which has now been found to match that of **1**.

The solid-state structure of polymeric $[La(Me_2pz)_3]_n$ (**1**, Fig. 1) is unexpected and fascinating. The La centre is surrounded by three near-planar $\eta^2(N,N')$ Me_2pz ligands (N1/2, N3/4, N5/6), while the polymer is grown by two Me_2pz ligands (N1/2 & N3/4) which engage in additional μ–$\eta^5(N_2C_3)$ coordination to two adjacent symmetry-equivalent La atoms (Fig. 1, La1′ and La1″). The η^5 coordination of the Me_2pz ligands in the axial positions (Cent–La1–Cent′: 177.04(4)°) gives the lanthanum centre a formal coordination number of 12, and a simplified (centroid) geometry best described as distorted trigonal bi-pyramidal. The validity of the η^5 bonding is supported by comparisons with reported π-C–La bond lengths.[9–13] The Me_2pz ligands thus display a "Cp"-type coordination, which is rarely observed in rare-earth pz chemistry,[6,14–16] and not at all involving an η^5-pz sandwich. Such sandwich-type bonding is restricted to monomeric complexes $[Ru(\eta^5\text{-pz})_2]$,[7] and is further related to the heteroleptic pentamethylcyclopentadienyl diphenylimidazolato complex $[Ru(Ph_2\text{-}\eta^5\text{-}C_3HN_2)(Cp^*)]$.[17] The structure contrasts that of polymeric $[LaCp_3]_n$, in which the metal is bound by two terminal Cp ligands and by two μ–η^5:η^2 ligands, one bound η^5 and one η^2, giving a tetrahedral array of centroids/centres[18] (see also an analogous μ–1η^5:2κ-bridged polymorph).[19]

The formation of a colourless precipitate on treatment of dimeric $[La(Me_2pz)_2(\mu\text{-}\eta^5\text{:}\eta^2\text{-}Me_2pz)(thf)]_2$ with non-polar solvents[16] is likely attributable to the conversion of the dimer into polymeric **1** *via* elimination of thf and a coordination switch of one terminal η^2-pyrazolato into a μ–η^5:η^2-Me_2pz ligand (Scheme S1†).‡ By contrast, $[Ln(Me_2pz)_2(\mu\text{-}1\kappa(N)\text{:}2\kappa(N')\text{-}Me_2pz)(\mu\text{-}1:2\kappa^2(O)thf)]_2$ (Ln = Nd – Lu),§ with different bridging ligand coordination, are stable in toluene and C_6D_6.[16]

X-ray crystallography established that **2** and **2**·solv (solv = toluene or 0.75*n*-hexane) all contain the homoleptic tetrametallic complex $[Ce_4(Me_2pz)_{12}]$ (Fig. 2). In **2**, each cerium environment is unique, with two ten-coordinate cerium atoms (Ce2, Ce4), one 9-coordinate cerium atom (Ce1), and one 8-coordinate cerium atom (Ce3). The most remarkable feature of **2** is the variety of different coordination modes adopted by the Me_2pz ligands. In total, there are six different binding modes, including two common, one unusual, and three unprecedented ones in rare-earth metal pz chemistry (Fig. 2**a**–**f**, for Me_2pz coordination overview). Five Me_2pz ligands (N1/2, N3/4, N13/14, N19/20, N23/24), coordinate to the cerium atoms in typical (for rare-earth metals)[3,6,8,14–16,20–23] η^2 coordination (Fig. 2**a**), whereas the other seven Me_2pz ligands are bridging either between two, three, or four metal centres. Three Me_2pz ligands (N5/N6, N15/16, N21/22), bridge in a μ–1κ(*N*):2κ(*N*′) manner (Fig. 2**b**), a common binding mode observed in transition metal pz complexes,[1,24] with some examples in rare-earth metal chemistry.[6,16,21,25,26] One Me_2pz ligand (N7/8), bridges between two metals in a twisted μ–1$\eta^2(N,N')$:2κ(*N*)

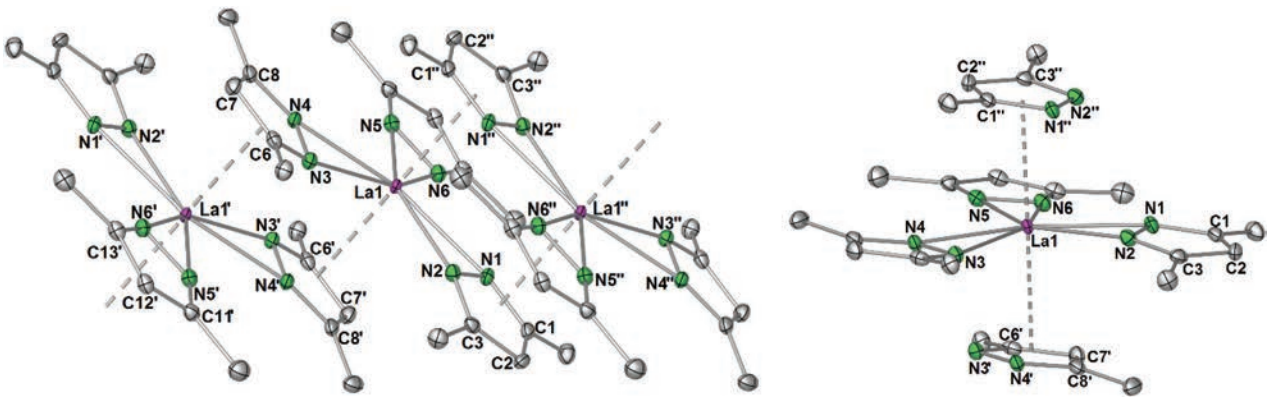

Fig. 1 Solid-state structure of $[La(Me_2pz)_3]_n$ (**1**). Left: View from alongside the polymer along the *a*-axis, right: Encapsulation of the La centre by Me_2pz. Ellipsoids shown at 50% probability, hydrogen atoms omitted for clarity. Selected bond lengths (Å) and angles (°) for **1**: La–N1: 2.587(4), La1–N2: 2.599(4), La1–N3: 2.617(3), La1–N4: 2.566(3), La1–N5: 2.516(3), La1–N6: 2.475(3), La1–N1′: 2.903(4), La1–N2′: 2.879(4), La1–C1′: 3.134(5), La1–C2′: 3.229(5), La1–C3′: 3.114(5), La1–N3′: 2.900(4), La1–N4′: 2.884(4), 2.903(4) La1–C6′: 3.137(5), La1–C7′: 3.245(6), La1–C8′: 3.114(5), La1–Cent (N1′–C5′): 2.821(2), La1–Cent(N3′–C8′): 2.872(2), Cent(N3′–C8′)–La1–Cent(N1′–C5′): 177.04(4), Cent(N1–C5)–La1–Cent(N1′–C5′): 92.98(5), Cent (N1–C5)–La1–Cent(N6′–C8′): 88.65(5) (for further structural diagrams please refer to ESI†).

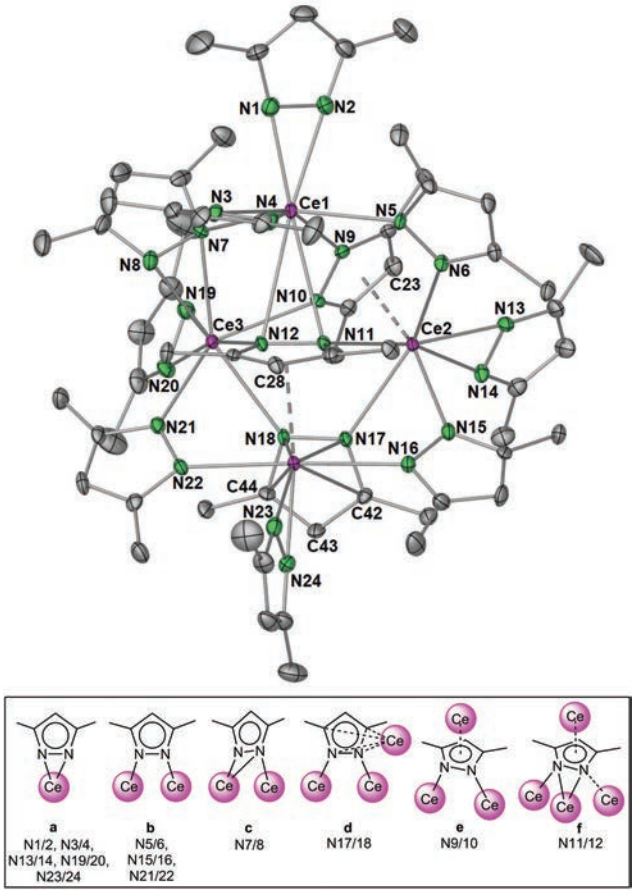

Fig. 2 Top: Molecular structure of $[Ce_4(Me_2pz)_{12}]$ (**2**), ellipsoids shown at 50% probability, hydrogen atoms, solvent of crystallisation omitted for clarity. See Fig. S3† for bond lengths and angles. Bottom: Schematic of Me_2pz coordination modes.

array (Fig. 2**c**), with a few examples in rare-earth metal pz chemistry.[2,8] Two Me_2pz ligands bridge between three cerium atoms. One ligand (N17/N18), bridges in a μ_3–$1\eta^4(C,N,N',C')$:$2\kappa(N)$:$3\kappa(N')$ manner (Fig. 2**d**), a mode unprecedented in rare-earth metal chemistry, but related to the μ_3–$1\eta^2(N,N')$:$2\kappa(N)$:$3\kappa(N')$ binding in rare-earth alkali metal bimetallics $[Na_2Ln_3O(Me_2pz)_9(Do)_2]$ (Ln = Ho, Do = Me_2pzH; Ln = Yb, Do = thf).[20] The η^4 binding of this Me_2pz ligand is exemplified by the large distance between the C4 carbon atom (C43) and cerium at 3.355(5) Å. This distance is far from that observed in the other μ_3-Me_2pz ligand (N9/N10, Fig. 2**e**), which coordinates in a μ_3-$1\eta^5(N_2C_3)$:$2\kappa(N)$:$3\kappa(N')$ manner. There the analogous Ce–C23 distance is at 3.147(5) Å, an acceptable range for η^5-pz-Ce coordination.[16] Bonding mode **e** of the N9/N10 ligand has been observed only in one other rare-earth metal complex,[6] but there are a few derivatives of other metals known.[24] The final, and most remarkable coordination mode, is for the central μ_4-Me_2pz ligand (N12/N11) which bridges μ_4–$1\eta^5(N_2C_3)$:$2\eta^2(N,N')$:$3\kappa(N)$:$4\kappa(N')$, between all four cerium atoms (Fig. 2**f**). Although a novel pz coordination to rare-earth metals (and homometallic complexes in general), this unusual bridging has been observed in one heterometallic pz system, namely $[K_2Mn_4(CO)_{12}(pz)_6(EtO)_2]$.[27] Overall the structure of **2**, with 6 different binding modes, highlights the versatility of these ligands, and further emphasises that pz coordination chemistry still astounds.

For La, regardless of the synthesis protocol applied, only the polymeric form could be obtained. However, for the slightly smaller cerium ion, upon refluxing the tetramer (**2**) in toluene, an insoluble white powder was obtained. The IR spectrum of the latter matched well with **1** and the previously reported amorphous $[Ce(Me_2pz)_3]$, which was obtained by stirring the reagents in toluene,[8] and is therefore assumed to be the polymeric form. Nevertheless, the solid-state structures of complexes **1** and **2** show extraordinary pz-coordination features, such as the "Cp"-analogous sandwich-type Me_2pz coordination in **1**, which generates a polymeric network, or the large array of pz coordination modes displayed in **2**. Such observations emphasise how the pz ligand class can adopt a diverse array of structures, and that the structural outcome is influenced by the synthesis and a subtle difference in ion size (~0.017 Å).[28]

Conflicts of interest

There are no conflicts of interest.

Acknowledgements

We thank the German Science Foundation (grant AN 238/16-1) and the Australian Research Council (DP16010640) for funding.

Notes and references

‡ By extension a similar de-solvation process likely occurs with the two other isostructural dimers $[Ln(Me_2pz)_3(thf)]_2$ (Ln = Ce, Pr).[16]

§ κ (kappa) nomenclature: "The kappa convention is used to specify bonding from isolated donor atoms to one or more central atoms...the term η^1 is not used...".[29]

1 M. A. Halcrow, *Dalton Trans.*, 2009, 2059–2073.
2 G. B. Deacon, A. Gitlits, P. W. Roesky, M. R. Bürgstein, K. C. Lim, B. W. Skelton and A. H. White, *Chem. – Eur. J.*, 2001, **7**, 127–138.
3 G. B. Deacon, C. M. Forsyth, A. Gitlits, R. Harika, P. C. Junk, B. W. Skelton and A. H. White, *Angew. Chem., Int. Ed.*, 2002, **41**, 3249–3251.
4 G. B. Deacon, C. M. Forsyth, A. Gitlits, B. W. Skelton and A. H. White, *Dalton Trans.*, 2004, 1239–1247.
5 G. B. Deacon, E. E. Delbridge, D. J. Evans, R. Harika, P. C. Junk, B. W. Skelton and A. H. White, *Chem. – Eur. J.*, 2004, **10**, 1193–1204.
6 C. C. Quitmann, V. Bezugly, F. R. Wagner and K. Müller-Buschbaum, *Z. Anorg. Allg. Chem.*, 2006, **632**, 1173–1186.

7 J. R. Perera, M. J. Heeg, H. B. Schlegel and C. H. Winter, *J. Am. Chem. Soc.*, 1999, **121**, 4536–4537; See also ref. 17 for an analagous η^5-imidazolate sandwich.
8 D. Werner, G. B. Deacon, P. C. Junk and R. Anwander, *Dalton Trans.*, 2017, **46**, 6265–6277.
9 G. B. Deacon, T. Feng, C. M. Forsyth, A. Gitlits, D. C. R. Hockless, Q. Shen, B. W. Skelton and A. H. White, *J. Chem. Soc., Dalton Trans.*, 2000, 961–966.
10 C. Wang, L. Xiang, X. Leng and Y. Chen, *Organometallics*, 2016, **35**, 1995–2002.
11 M. L. Cole, G. B. Deacon, P. C. Junk, K. M. Proctor, J. L. Scott and C. R. Strauss, *Eur. J. Inorg. Chem.*, 2005, 4138–4144.
12 L. C. H. Gerber, E. Le Roux, K. W. Törnroos and R. Anwander, *Chem. – Eur. J.*, 2008, **14**, 9555–9564.
13 A. S. Filatov, A. Y. Rogachev and M. A. Petrukhina, *J. Mol. Struct.*, 2008, **890**, 116–122.
14 C. C. Quitmann and K. Müller-Buschbaum, *Z. Naturforsch. B*, 2004, **59**, 562–566.
15 J. Hitzbleck, G. B. Deacon and K. Ruhlandt-Senge, *Eur. J. Inorg. Chem.*, 2007, 592–601.
16 G. B. Deacon, R. Harika, P. C. Junk, B. W. Skelton, D. Werner and A. H. White, *Eur. J. Inorg. Chem.*, 2014, 2412–2419.
17 J. R. Perera, M. J. Heeg and C. H. Winter, *Organometallics*, 2000, **19**, 5263–5265.
18 S. H. Eggers, J. Kopf and R. D. Fischer, *Organometallics*, 1986, **5**, 383–385.
19 J. Rebizant, C. Apostolidis, M. R. Spirlet and B. Kanellakopulos, *Acta Crystallogr., Sect. C: Cryst. Struct. Commun.*, 1988, **44**, 614–616.
20 H. Schumann, P. R. Lee and J. Loebel, *Angew. Chem., Int. Ed. Engl.*, 1989, **28**, 1033–1035.
21 C. C. Quitmann and K. Müller-Buschbaum, *Z. Anorg. Allg. Chem.*, 2005, **631**, 1191–1198.
22 G. B. Deacon, A. Gitlits, B. W. Skelton and A. H. White, *Chem. Commun.*, 1999, 1213–1214.
23 X. Zhou, H. Ma, X. Huang and X. You, *J. Chem. Soc., Chem. Commun.*, 1995, 2483–2484.
24 F. H. Allen, Conquest version: 1.19, 2016, *Acta Crystallogr., Sect. B: Struct. Sci.*, 2002, **58**, 380–388.
25 G. B. Deacon, B. M. Gatehouse, S. Nickel and S. N. Platts, *Aust. J. Chem.*, 1991, **44**, 613–621.
26 K. Müller-Buschbaum, C. C. Quitmann and A. Zurawski, *Monatsh. Chem.*, 2007, **138**, 813.
27 T. Morawitz, F. Zhang, M. Bolte, J. W. Bats, H.-W. Lerner and M. Wagner, *Organometallics*, 2008, **27**, 5067.
28 R. D. Shannon, *Acta Crystallogr., Sect. A: Cryst. Phys., Diffr., Theor. Gen. Crystallogr.*, 1976, **32**, 155–169.
29 N. G. Connelly, T. Damhus, R. M. Hartshorn and A. T. Hutton, *Nomenclature of Inorganic Chemistry*, IUPAC, 2005.

